SC543.16FR

IDENTIFICATION AND INTERPRETATION OF TECTONIC FEATURES FROM ERTS-1 IMAGERY

Southwestern North America and The Red Sea Area

Monem Abdel-Gawad and Linda Tubbesing
Science Center, Rockwell International Corporation
1049 Camino Dos Rios (P.O. Box 1085)
Thousand Oaks, California 91360 U.S.A.

May 5, 1975

Type III Final Report for Period
May 30, 1972 - February 11, 1975

Prepared for

NASA/GODDARD SPACE FLIGHT CENTER
Greenbelt, Maryland 20071

163

SC543.16FR

IDENTIFICATION AND INTERPRETATION OF TECTONIC FEATURES FROM ERTS-1 IMAGERY

Southwestern North America and The Red Sea Area

M. Abdel-Gawad

Monem Abdel-Gawad and Linda Tubbesing
Science Center/Rockwell International Corporation
1049 Camino Dos Rios, P.O. Box 1085
Thousand Oaks, California 91360 U.S.A.

May 5, 1975

Type III Final Report for Period
May 30, 1972 - February 11, 1975

Prepared for

NASA/GODDARD SPACE FLIGHT CENTER
Greenbelt, Maryland 20071

Science Center
Rockwell International

1049 CAMINO DOS RIOS
THOUSAND OAKS CALIF 91360

805/498 4545

REPORT DOCUMENTATION PAGE

READ INSTRUCTIONS BEFORE COMPLETING FORM

1. REPORT NUMBER	2. GOVT ACCESSION NO. / 3. RECIPIENT'S CATALOG NUMBER
4. TITLE (and Subtitle): IDENTIFICATION AND INTERPRETATION OF TECTONIC FEATURES FROM ERTS-1 IMAGERY Southwestern North America and The Red Sea Area	5. TYPE OF REPORT & PERIOD COVERED: Type III Final Report 5/30/72 - 2/11/75 6. PERFORMING ORG. REPORT NUMBER: SC543.16FR
7. AUTHOR(s): Dr. Monem Abdel-Gawad Linda Tubbesing	8. CONTRACT OR GRANT NUMBER(s): NAS5-2167
9. PERFORMING ORGANIZATION NAME AND ADDRESS: Science Center/Rockwell International 1049 Camino Dos Rios, P.O. Box 1085 Thousand Oaks, California 91360	10. PROGRAM ELEMENT, PROJECT, TASK AREA & WORK UNIT NUMBERS
11. CONTROLLING OFFICE NAME AND ADDRESS: NASA/GODDARD Space Flight Center Greenbelt, Maryland 20771	12. REPORT DATE: May 5, 1975 13. NUMBER OF PAGES: 163
14. MONITORING AGENCY NAME & ADDRESS (if different from Controlling Office)	15. SECURITY CLASS. (of this report): Unclassified 15a. DECLASSIFICATION/DOWNGRADING SCHEDULE

16. DISTRIBUTION STATEMENT (of this Report)

Approved for public release; distribution unlimited.

17. DISTRIBUTION STATEMENT (of the abstract entered in Block 20, if different from Report)

PRICES SUBJECT TO CHANGE

18. SUPPLEMENTARY NOTES

19. KEY WORDS (Continue on reverse side if necessary and identify by block number)

ERTS-1 imagery, fault intersection, linears, transverse faults and structures, earthquake epicenters, shear zones, mineralization, rift zones, Basin and Range

20 ABSTRACT (Continue on reverse side if necessary and identify by block number)

ERTS-1 imagery was utilized to study major fault and tectonic lines and their intersections in southwestern North America. A system of transverse shear faults was recognized in the California Coast Ranges, the Sierra Nevada, the Great Basin and Mexico. Transverse linears within the Texas and Parras shears were mapped. They are interpreted as expressions of a major left-lateral shear which predated the San Andreas System, the opening

of the Gulf of California and Basin and Range rift development. Tectonic models for Basin and Range, Coast Ranges, and Texas-Parras shears have been developed. Geological structures and Precambrian metamorphic trendlines of schistosity were studied across the Red Sea rift.

PREFACE

a) Objective:

The objectives in this investigation are aimed at determining the utility of ERTS-1 imagery in the identification and interpretation of tectonic features of the earth's crust. The study includes four main objectives.

1) Determine the feasibility of utilizing ERTS-1 imagery to study the regional structural framework of the Southwestern United States, the Gulf of California, Baja California and Northwestern Mexico in terms of current theories of oceanic and continental crustal plate interactions. Study the nature of fault and tectonic line intersections and possible displacements.

2) Study the relationship between observed structures and the distribution of known mineral deposits and determine whether it is possible to infer any correlation between the present distribution of known mineral districts or individual large deposits with observable structural elements or intersections.

3) Assess the utility of ERTS-1 imagery in providing geomorphic criteria indicating unknown fault zones of recently active movement. When active fault movements are indicated, the relationship to the seismicity of the area will be analyzed and implications discussed.

4) Discuss and examine the utility of ERTS-1 imagery in providing new insights into other applications in the discipline of geology which can be the subject of future investigations or experiments.

b) Scope of Work:

The primary target area (Fig. 1) for this investigation includes the southwestern United States, Baja California, the Gulf of California, and a large part of northwestern Mexico. The approximate geographic coordinates of the corners of this area are:

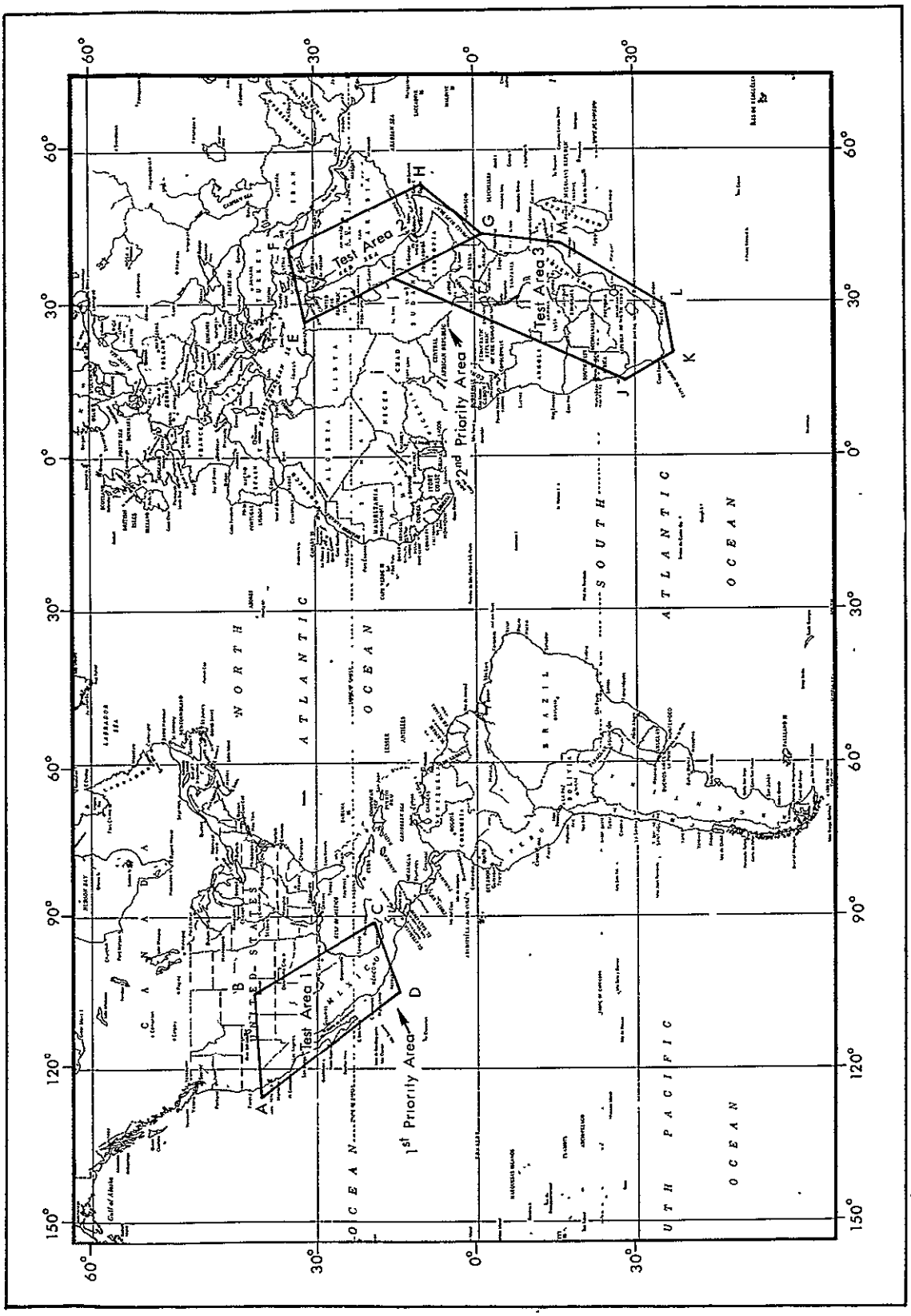

FIGURE 1 INDEX MAP

A.	125° 40' W	38° 50' N
B.	104° 40' W	40° 05' N
C.	91° 25' W	19° 35' N
D.	104° 10' W	15° 00' N

To accomplish the main objectives of the investigation, emphasis was placed in those areas where important tectonic intersections or structures occur. Three major study areas developed.

Area 1) Central and southern California, including the Coast Ranges.

Area 2) Eastern California, and western and central Nevada.

Area 3) Baja California, the Gulf of California, northern Mexico, and the Parras and Texas Shear Zones.

We have studied the geological structures across the Red Sea rift which is considered a part of the greater East African Rift system. The major objective here was to correlate the Precambrian metamorphic tendencies of schistosity in Africa and Arabia.

The bulk of this report describes observations on fault patterns, observations on fault zones suspected to have undergone recent breakage, plots of earthquake epicenters and magnitudes on overlays corresponding to ERTS-1 imagery, and correlations between earthquake epicenters and fault patterns. In central and southern California (Area 1), transverse faults in the coast ranges are discussed and their role in the overall fault pattern and mineral deposition is studied. Preliminary analysis of relationships between faulting, seismicity, and Quaternary volcanic activity are discussed in the Basin and Range rift zone in Eastern California, and western and central Nevada (Area 2). In Area 3 (Baja California and western Mexico) ERTS-1 imagery is used to determine whether or not there exists unique structures on both sides of the Gulf of California which indicate major lateral displacement of Baja California relative to mainland of Mexico. The validity of major transverse fault zones and extensions of submarine faults suggested in some models of plate tectonics is studied, and major shear zones related to the Parras and Texas structural trends in Mexico and southwestern United States are identified with the help of geologic overlays prepared for several ERTS-1 images.

c) Conclusions:

ERTS-1 imagery is providing valuable data on active fault intersections. It appears feasible to identify geomorphic criteria of recent fault movements.

Area 1: In the coast and western Transverse Ranges of California, many criteria of recent fault movements are observable in the imagery. We found that where earthquake epicenter clusters occur, evidence of recent fault movements is generally observed. The opposite is not necessarily true: there are areas where evidence of recent faulting is observed, often along major known faults which are peculiarly devoid of significant seismicity. A tentative conclusion is that the seismicity pattern alone can often be a misleading criteria for potential earthquake hazard. The feasibility of recognizing geomorphic criteria of recent fault movement from ERTS-1 imagery suggests that ERTS imagery should be used to map potentially active faults and utilize this data to develop better criteria for the identification of areas prone to future earthquakes.

Area 2: The seismicity pattern in the Basin and Range zone suggests that the California-Nevada seismic belt which generally trends north-south consists of a series of northeast trending seismic zones arranged en echelon. Earthquake epicenters were plotted on 7 ERTS-1 images covering the Nevada seismic zone of Ryall, Slemmons, and Gedney (1966) and Gumper and Scholz (1971). We plotted known faults on image overlays and then utilized ERTS imagery to identify lineaments and probable fault structures not previously mapped. The inferred structures fall into four classes:

(1) Three relatively major fault zones similar in trend to the Walker Lane and Furnace Creek faults were recognized in central and north central Nevada. These are tentatively named the Black Butte Shear, the Austin Shear, and the Battle Mountain Fault Zone. In addition, we identified many smaller faults of similar northwest-southeast trend. Many faults of this class are suspected to represent strike-slip zones of shear caused by unequal rates of extension in the Basin and

Range province. We suspect that some of these shear zones may have a left-lateral component of movement, that is opposite to the sense of movement on major fault zones such as Walker Lane and Furnace Creek, Las Vegas shear, etc.

(2) North-south to north-northeast faults parallel to the main trend of the Basin and Range structures in Nevada were analyzed. Although faults of this trend have long been known to characterize the main grain of the Basin and Range province, ERTS imagery contributed significantly in identifying many faults of this class which show evidence of Holocene activity. The belt containing the recent faulting coincides generally with areas of seismic activity.

(3) Northeast-southwest faults were recognized trending oblique to the Basin and Range grain. Some of these, e.g., in the Excelsior Mountain area and Slate Ridge area, are suspected to have left-lateral sense of movement. The significance of this observation within the general tectonic framework has not yet been determined.

Area 3: Using ERTS-1 imagery to study major faults in northern Mexico and across the border into the United States, we arrived at the conclusion that the entire southwestern part of North America was subject to large scale left-lateral regmatic shear. From the ages of the rocks most involved in the Parras shear, it is evident that this major deformation took place contemporaneously with folding and thrusting of the Laramide orogeny. Early Tertiary rocks are much less affected. It is believed that the main phase of widespread left-lateral shear preceded the tensional rift faulting of the Basin and Range phase of tectonic development and was essentially older than the right lateral San Andreas type faulting.

A fundamental concept which may help explain many complexities in the tectonic development is beginning to emerge: the southwestern part of North America was torn by massive left-lateral shear of transverse trend (west-northwest) during the compressive

stage of the late Mesozoic and early Cenozoic. This tectonic style has changed into tensional rifting (Basin and Range) and right-lateral shear later in the Cenozoic.

Red Sea Rift

Study of regional metamorphic grain of the Precambrian basement complex across the Red Sea shows that the Arabian-Nubian massif can be divided roughly into three main parts.

The southern part of the massif up to approximately 21° N in Arabia and 19° N in Africa is characterized by regional schistosity trending generally north.

The northern part of the massif from 28° N to 25° N in Arabia and from 26° N to 23° N in Africa is characterized by northwest and west-northwest schistosity.

The middle part of the massif northeast trending schistosity is prevalent.

It is also interesting to note that major shear zones and large faults associated with Precambrian structures also tend to follow the general trend of schistosity and seem to have no apparent relation to the younger faults associated with the development of the rift and which control the fault blocks outlining the Red Sea depression.

A shift of approximately two degrees of latitude seems to exist between the African and the Arabian plates which amounts to a relative northward movement of Arabia some 200 km.

d) Summary and Recommendations:

Area 1: ERTS-1 imagery of the Coast and western Transverse Ranges of California is providing invaluable information on the relationship of active faults and the displacement patterns at their intersections. There is evidence that a major phase of transverse shear faulting has affected the Coast Ranges prior to the last phase of activity on the San Andreas system.

Many west-northwest trending segments of old wrench faults have been identified lodged between throughgoing faults of the San Andreas system. In the geological maps, many of these transverse fault segments are shown incorporated with other faults which rendered their tectonic significance to be largely overlooked.

Information on the existence of these faults as a distinct system in its own right and not as a secondary or conjugate feature of the San Andreas system is consistent with our fault model which explains the development of the fault pattern in southern California. Here, the interaction is more complex.

To state it briefly: ERTS-1 imagery is providing evidence that the San Andreas "fault" has not always been one fault as it appears today and may have been offset into several segments by transverse faults periodically during its history.

We identified from ERTS-1 imagery of the Transverse Ranges, a fault lineament across the Pine Mountains (California) which seems to be quite distinct from the Ozena and Pine Mountain faults. This lineament lines up but does not seem at present to be connected with the middle segment of the San Gabriel fault.

It is speculated that the intervening unfaulted area in the vicinity of Lake Piru is a likely site for a future break. We recommend that this area be included in the network of geophysical measurements of tilt and fault creep.

An apparent correlation was observed between the distribution of mercury deposits in the California Coast Ranges Province and transverse fault zones trending west-northwest oblique to the trend of the San Andreas system. The significance of this correlation and the full extent of its implication on mercury exploration should receive further detailed study.

Plots of earthquake epicenters from the vicinity of San Francisco to Los Angeles were completed and the patterns were analyzed. Preliminary analysis suggests clustering controlled by fault intersections.

A fault lineament was identified in the Colorado Plateau in northern Utah. Near Dragerton, Utah, the lineament shows evidence of recent faulting associated with moderate seismic activity.

Area 2: In Eastern California, and western and central Nevada, it was noted in our study that areas covered by Quaternary and late Tertiary volcanic rocks coincide generally with Quaternary faulting including many suspected recent fault breaks, as well as zones of historic seismic activity.

Three major trends appear in the overall fault pattern for this area.

1) Major northwest-trending shear zones.
2) North-northeast rift faults.
3) Northeast-southwest faults and lineaments.

From this investigation we found that the eastern California-Nevada seismic belt coincides with areas characterized by Holocene (recent) faulting and Quaternary volcanic activity. The distribution of historic earthquakes, Holocene faulting, and Quaternary volcanics suggests a tectonic model based upon the concept that east of the Sierra Nevada lies an active rift belt crossed by several shear zones analogous to rift zones and transform faults on the ocean floor.

A most important result of this investigation which has direct practical applications is the ability to recognize and map fault lines showing evidence of Holocene breakage.

Faults suspected to have undergone movement during the Quaternary Period are indicated by the symbol (R) in overlay maps.

Evidence of recent faulting in a given area can be safely considered to indicate that the area has been subject to earthquake recurrence even though the pattern of historic earthquake data may for statistical considerations not reveal such activity.

We believe that the ability to identify from ERTS imagery areas and specific lines where recent faulting is indicated can be of considerable value to both national and local programs for the evaluation of earthquake hazards and for planning corrective measures to reduce damage and loss of life.

Because the entire western third of the North American continent lies within a belt of crustal deformation, a viable program to inventory potentially active faults in such a vast and rapidly developing area by conventional field and aerial photographic methods is an endeavor of major proportions in cost, manpower availability, and time considerations. The utilization of ERTS imagery to identify and map potentially active faults can significantly reduce the cost and effort of planning detailed field investigations. Although a quantitative estimate is not available at present, ERTS imagery can conceivably reduce the total areas to be examined in detail and the cost by a factor of 100 and probably more.

Area 3: Geological correlation of terrain across the Gulf of California using ERTS-1 imagery revealed significant similarities between Isla Tiburon, Isla Angel de la Guarda and the San Carlos Range in mainland Mexico. These data were used to reconstruct the position of the Baja Peninsula in Middle Tertiary in two different models. In the first model Isla Tiburon, Isla Angel de la Guarda and Baja California were offset northwestward from their initial positions distances on the order of 140 km, 270 km, and 380 km, respectively. After studying this first

model in more detail, it seemed almost impossible that Isla Tiburon had moved very far from its present position. Assuming that Isla Tiburon is locked in its position with the Mexican mainland, a second model was developed. The second model locked Isla Tiburon to the Mexican mainland and Isla Angel de la Guarda to the Baja Peninsula. In this model Baja California and Isla Angel de la Guarda were offset about 230 km NW from their original positions. Although we fixed Isla Angel de la Guarda in its present position with respect to Baja California, it is very probable that a small movement may have taken place. Since its original position is uncertain, we have placed it in a locked position with Baja California for the time being. We have found in the second model that such reconstruction brings the isolated mass of Lower Cenozoic intrusives - now lying southeast of Laguna Salada at the head of the Gulf of California - in juxtaposition with the main cluster of similar intrusives in Sonora. Reconstruction also brings the Tertiary continental deposits of northern Baja California in juxtaposition with the north-south trending belt of Tertiary continental deposits of Sonora, Mexico. This indicates a late Tertiary age for the opening of the Gulf of California.

We utilized ERTS-1 imagery to check the validity of the existence of major transverse fault zones. In the northern part, which was not submerged during the Tertiary age, several transverse faults were verified. In the southern part we observed discontinuous remnants of possible transverse breaks. It is suggested that the old transverse faults are masked by Tertiary and Quaternary volcanic cover and by a blanket of marine sediments of late Tertiary age.

ERTS-imagery shows that high albedo sediments similar to known late Tertiary marine sediments are widespread in the southern and middle part and extend in places to the eastern side of the Peninsula. If our assumption that the high albedo areas are mostly marine sediments is verified by later field work, the

distribution is highly significant. Much of the southern part of Baja California was probably submerged during the late Tertiary and early Quaternary, and at that time appeared as a chain of islands in the Pacific.

ERTS-1 imagery was used to map major faults in northern Mexico and across the border in the United States. We found ample evidence that the Parras and parts of the Texas lineament are belts of major transverse shear faults. In areas outside the supposed limit of the Texas and Parras lineaments, similar linears were also recognized which suggests that shearing deformation has affected a broad area of southwestern North America.

Red Sea Rift

ERTS-1 imagery was used to map and correlate Precambrian metamorphic trendlines of schistosity across the Red Sea rift where those structures could be visually observed. Results of this work corroborate previous work by Abdel-Gawad (1969-1970) on Gemini photographs. Correlation of the metamorphic grain and major shear zones seem to indicate that translational movements across the Red Sea have taken place. While ERTS-1 imagery has provided a considerable amount of new information on the regional Precambrian grain and the location of circular structures many of which are believed to be granitic stocks, the overall reconstruction model for the Red Sea proposed by Abdel-Gawad (1969-1970) remains unchanged.

TABLE OF CONTENTS

TABLE OF CONTENTS (CONT'D)

LIST OF ILLUSTRATIONS

LIST OF ILLUSTRATIONS (CONT'D)

LIST OF ILLUSTRATIONS (CONT'D)

AREA 1

CENTRAL AND SOUTHERN CALIFORNIA

INTRODUCTION

The area studied in this section covers the southern part of the Coast Ranges from San Francisco to the vicinity of Los Angeles, including the western part of the Transverse Ranges (Figure 2).

ERTS-1 scenes covering this area used in this study are:

MSS 1021-18172 and 1075-18173
MSS 1021-18174
MSS 1056-18120
MSS 1037-18064.
MSS 1053-17551
MSS 1022-18223
MSS 1074-18121.

OBSERVATIONS ON FAULT PATTERN

The significant feature we were looking for in the Coast Ranges was evidence for Transverse faults trending west-northwest lodged in blocks between faults of the San Andreas set. Examples of these and other faults are described.

San Francisco-Monterey

MSS 1021-18172; Fault Structures, Fig. 3; Earthquake Epicenters, Fig. 4
MSS 1075-18173

In Figure 3 the major known faults are: San Andreas, Hayward, Calaveras, King City fault, and air photo lineament. In order to avoid crowding, some major known faults are outlined by a solid line. Observed lineaments, believed to be faults which are either not previously mapped or only partially mapped or not sufficiently emphasized in the literature, are indicated by broken lines.

(1) Fault lineament trending NNW parallel to and running approximately between Hayward-Calaveras fault zone and air photo lineament (San Jose map sheet). This lineament which cuts the Diablo Range was first recognized by Lowman (1972).

(2) Fault lineament along western side of Salinas River Valley and eastern side of Sierra de Salinas. Fault trends northwest and appears to extend to Monterey Bay.

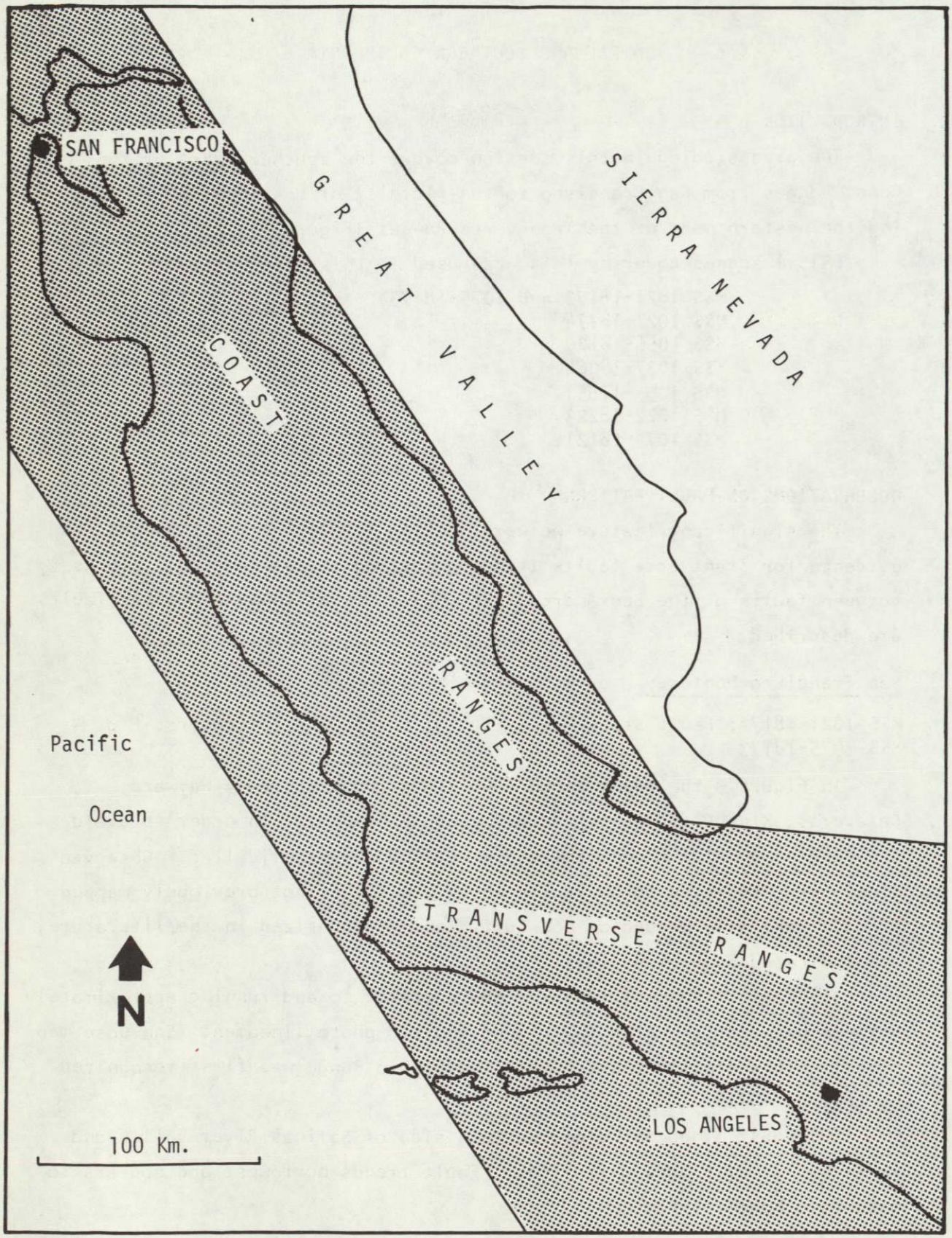

FIGURE 2 Area Studied

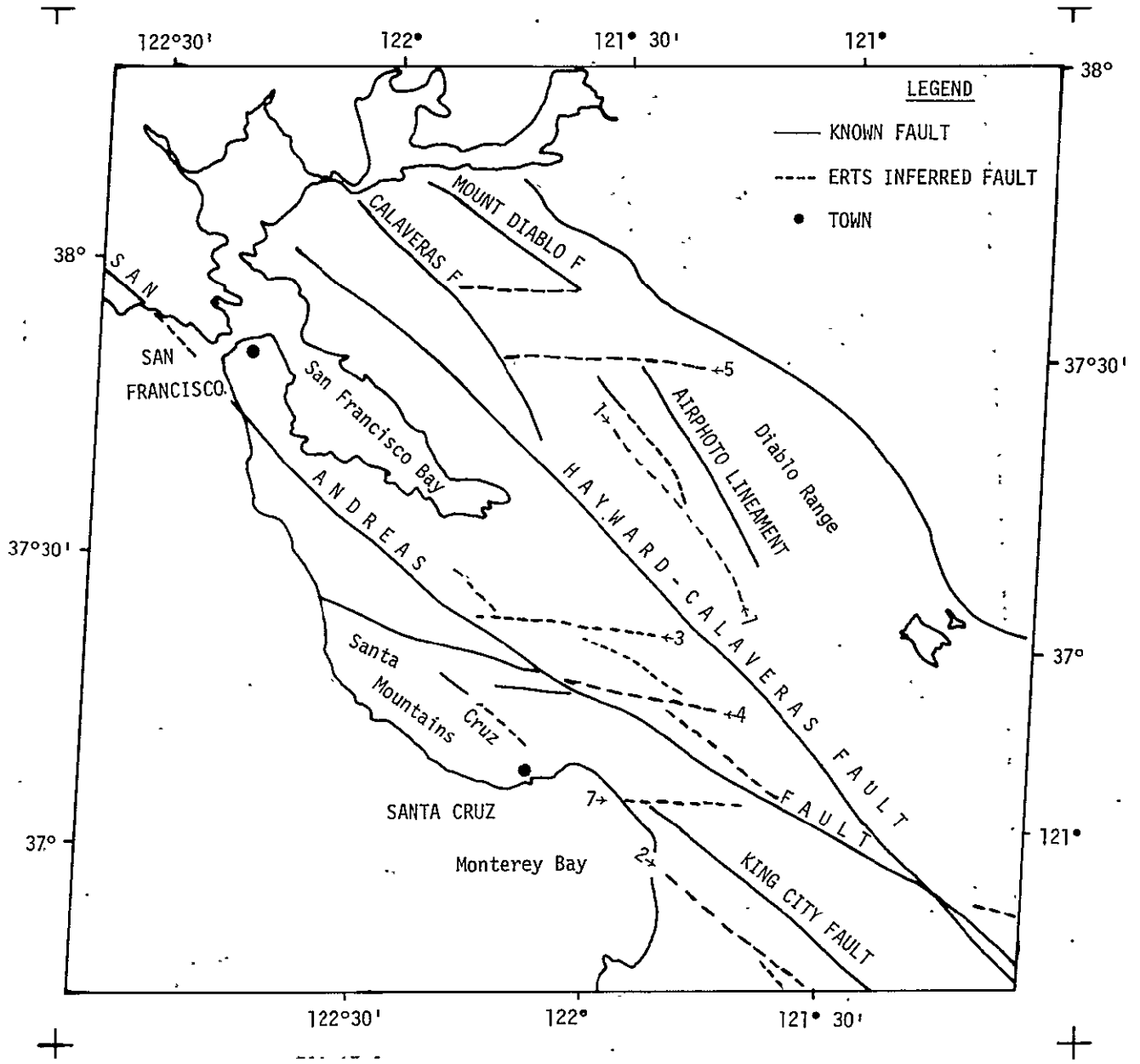

FIGURE 3 Fault Structures on Photograph 1021-18172

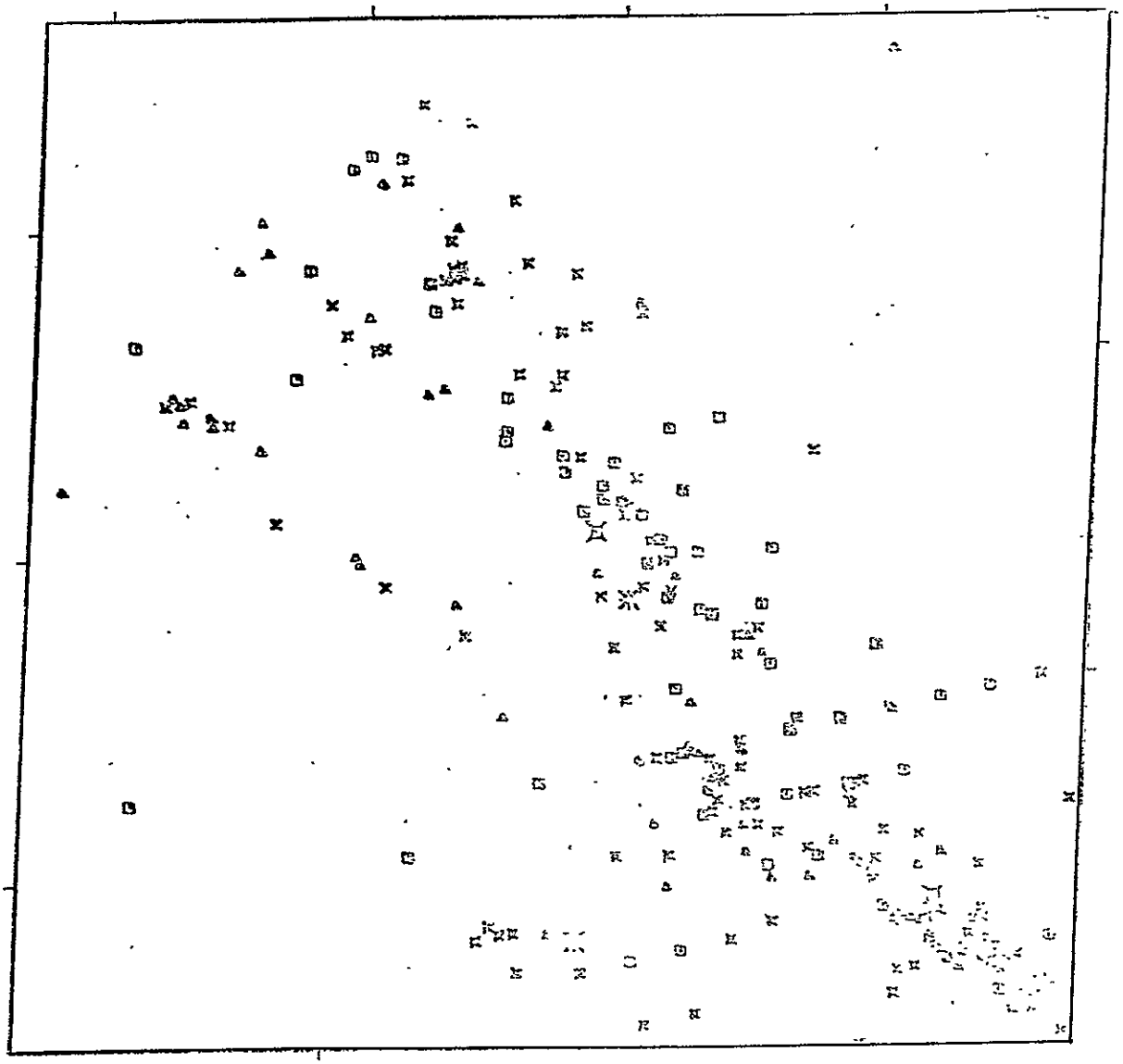

Symbol	Richter Magnitude
⊡	Unknown
□	0 - 4.0
△	4.1 - 4.9
×	5.0 - 5.4
◇	5.5 - 5.9
⊠	6.0 - 6.9
⊗	7.0 - 7.9
⊠	8.0 - 8.4
⊗	> 8.4

FIGURE 4 Earthquake Epicenters on Photograph 1021-18172

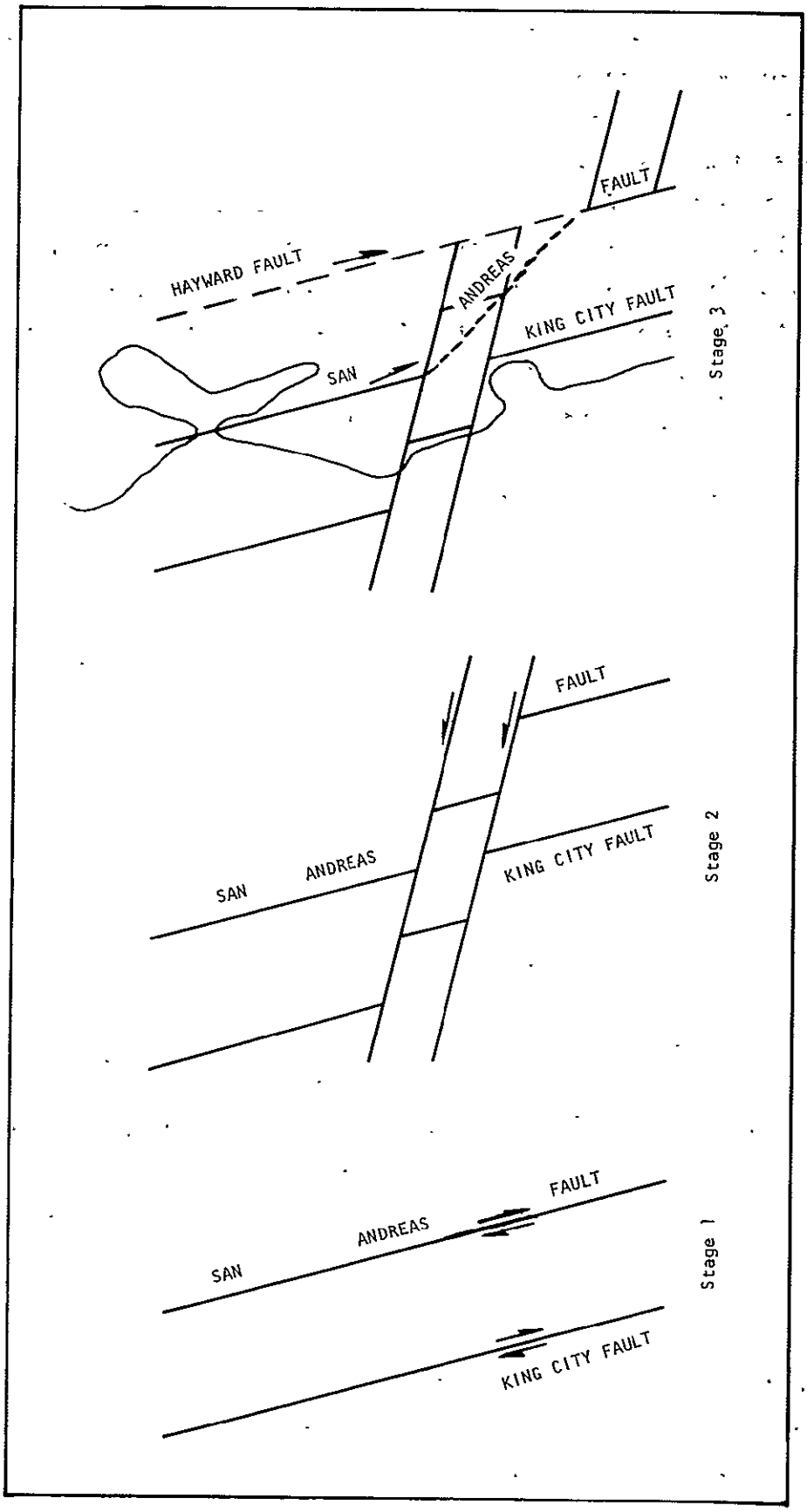

Stage 1 - Ancestors of San Andreas and King City faults
Stage 2 - Development of left-lateral transverse faults offsetting San Andreas ancestor
Stage 3 - Propagation of faulting along Hayward and development of San Andreas short-cut near Monterey Bay

FIGURE 5 Proposed Development of Fault Pattern in San Francisco-Monterey Area
State 1 - Ancestors

Transverse Faults

Although the fault pattern here is dominated by the northwest-trending San Andreas and Hayward-Calaveras, we note the presence of another distinct system of faults trending west-northwest. These faults are relatively short and often occur lodged between throughgoing faults of the San Andreas system. Some of these transverse faults are shown in the geological maps (Atlas of California) incorporated as bends or branches in the San Andreas system. Others have not been previously mapped. But certainly they are represented as secondary features and were not given the emphasis commensurate with their immense significance in shaping the structure of the Coast Ranges. Fault lineaments 3, 4, 5, 6, and 7 are examples of the transverse faults we are referring to (Figure 3).

The effect of the transverse faults on the structure of the Coast Ranges here can be visualized if one for a moment ignores the San Andreas fault to realize that the blocks north of the transverse fault segments are consistently shifted westward relative to the blocks on their southern side. This suggests that the most of the lateral displacement on these faults was left-lateral and had taken place at some time prior to the establishment of the San Andreas along its present trace. One interpretation we considered is illustrated in Figure 5. This interpretation would suggest that the Hayward fault had developed by propagation to surmount a locked structure created by the offset of the San Andreas ancestor by left-lateral transverse faults. The segment of the San Andreas east of Monterey Bay may be considered as another short cut surmounting the locked structures.

Despite the apparent linearity of the San Andreas fault we note that minor bends in the fault may in fact be small offsets at its intersection with the transverse faults. The resultant knickpoints are eventually broken through by fault propagation. If this interpretation is valid, it suggests that the tectonic forces causing the transverse shear may have continued to be active in the Quaternary. The displaced extension of the King City fault which runs under the Salinas Valley would be offshore of San Francisco. As we will show later, there is ample evidence that major transverse shear has predated the initiation of the San Andreas system. However, evidence from the southern California intersection also indicates later recurrence of transverse shear.

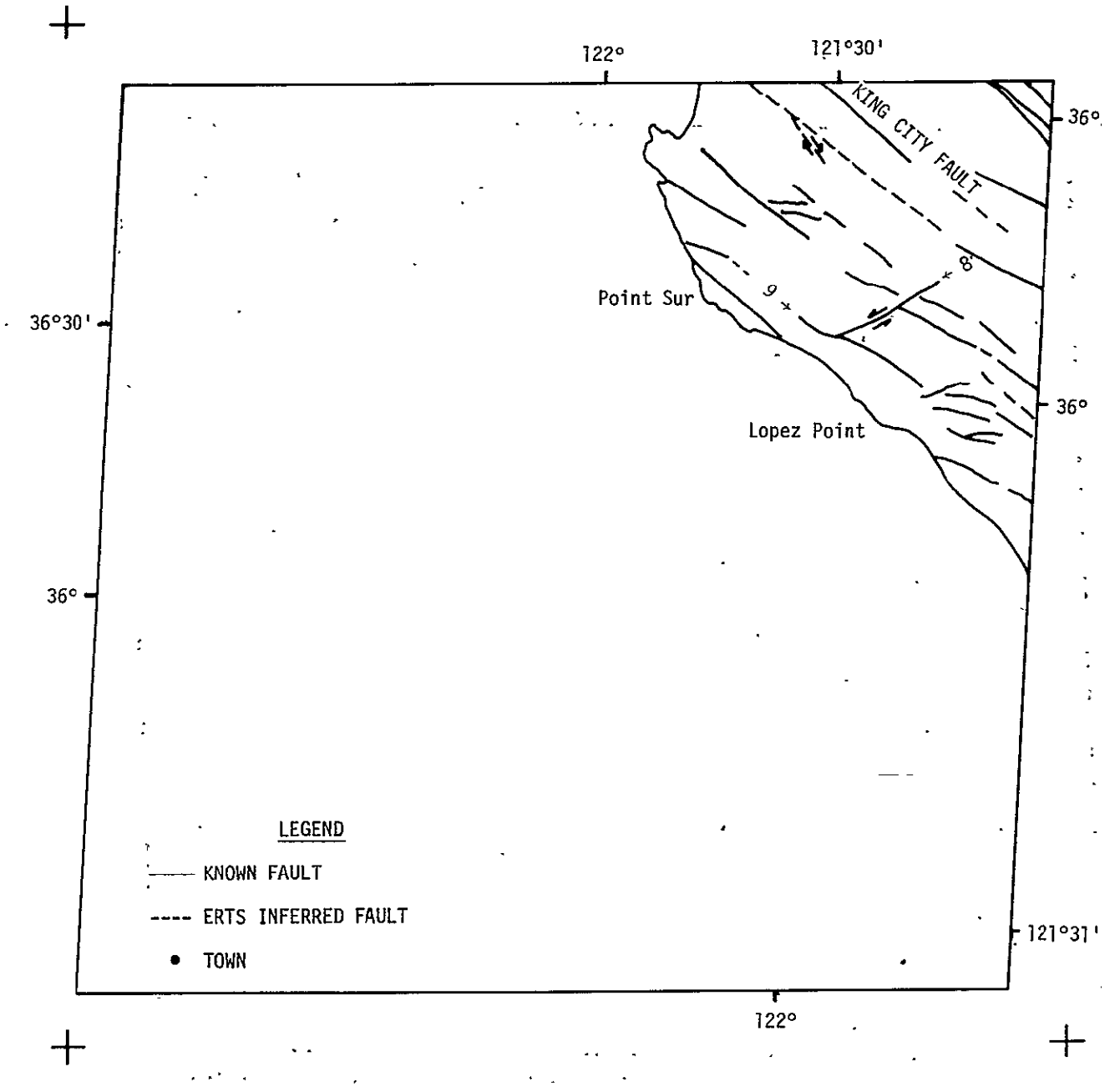

FIGURE 6 - Fault Structures on Photograph 1021-18174

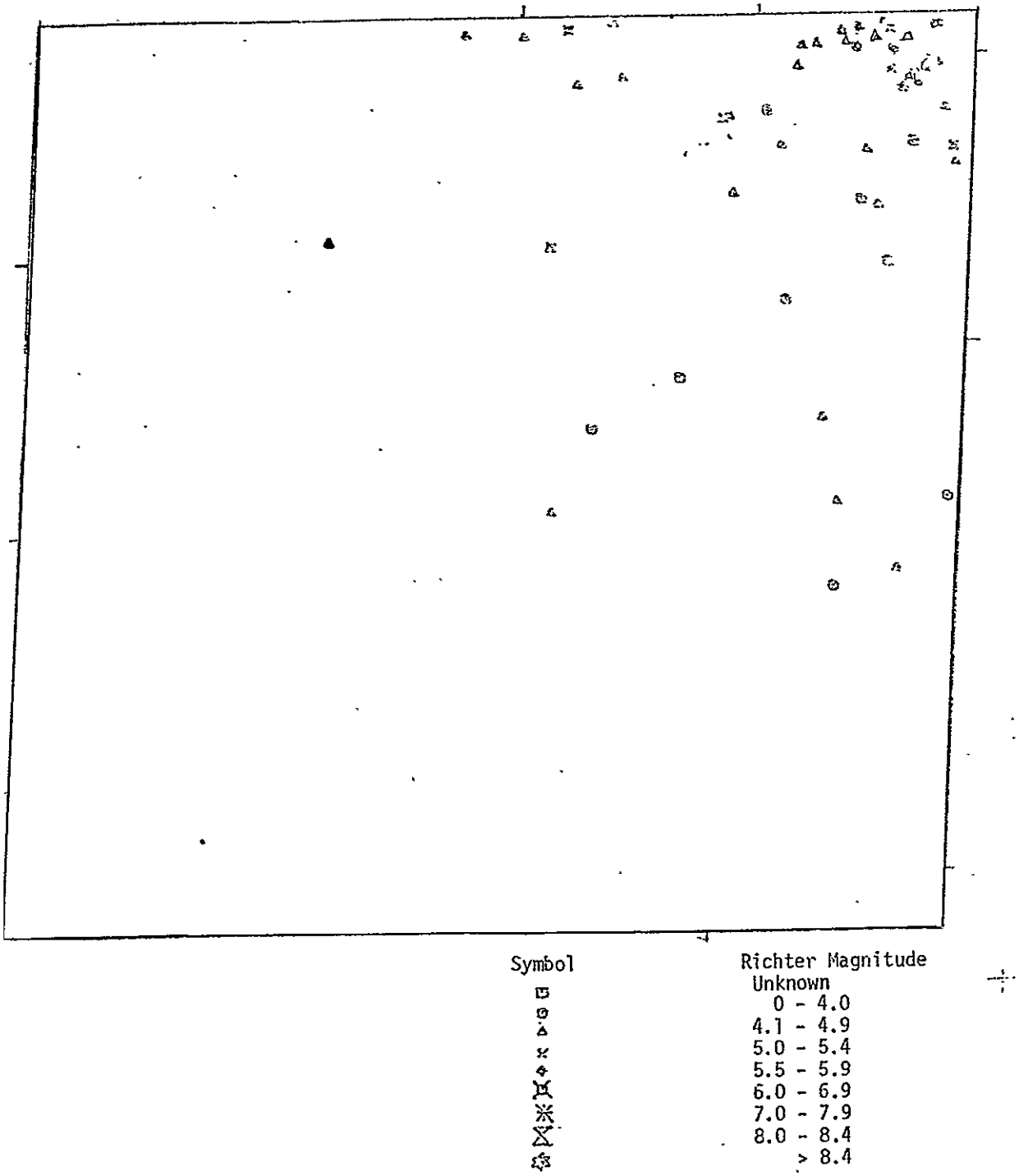

FIGURE 7 Earthquake Epicenters on Photograph 1021-18174

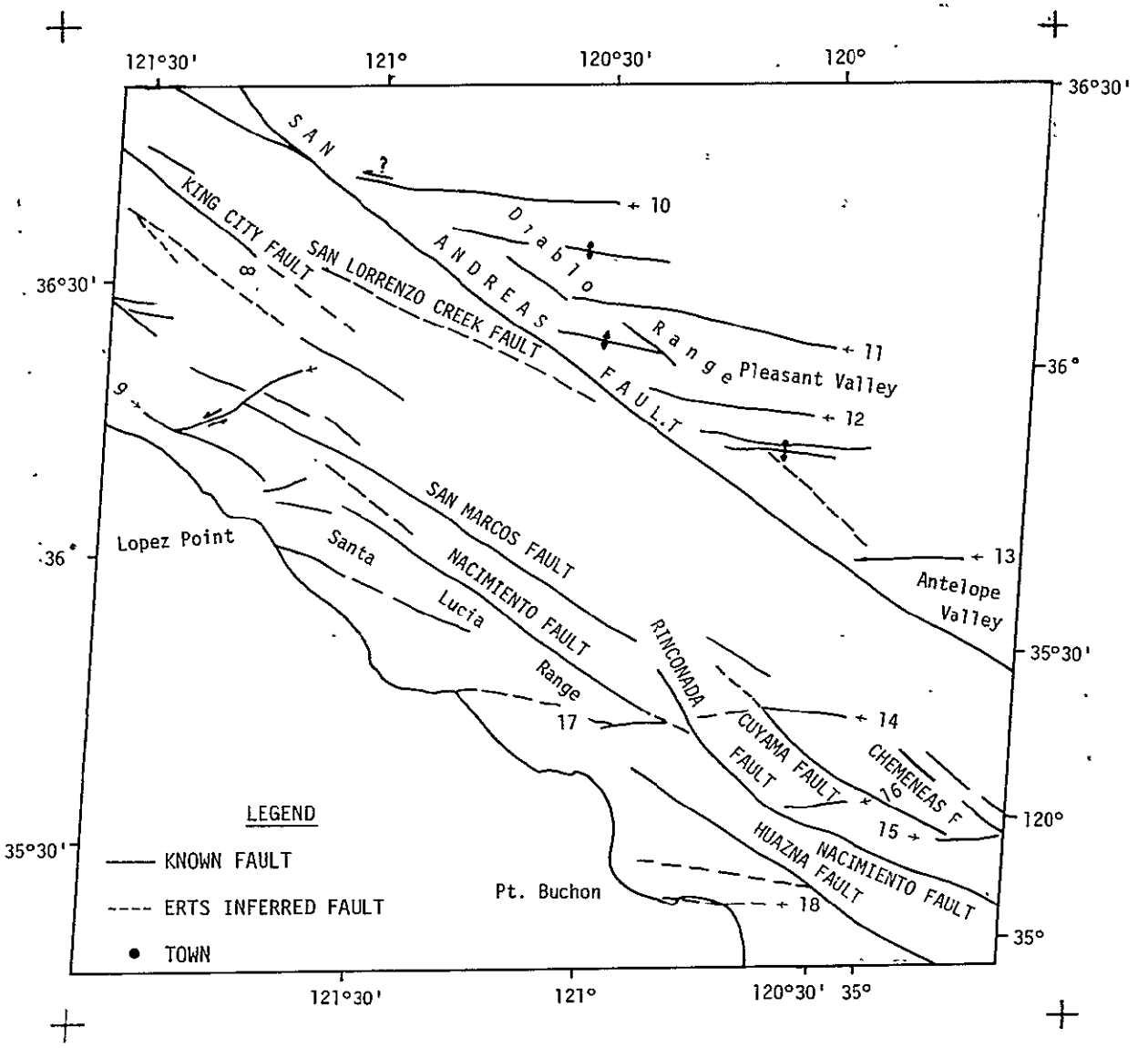

FIGURE 8 Fault Structures on Photograph 1056-18120

ORIGINAL PAGE IS
OF POOR QUALITY

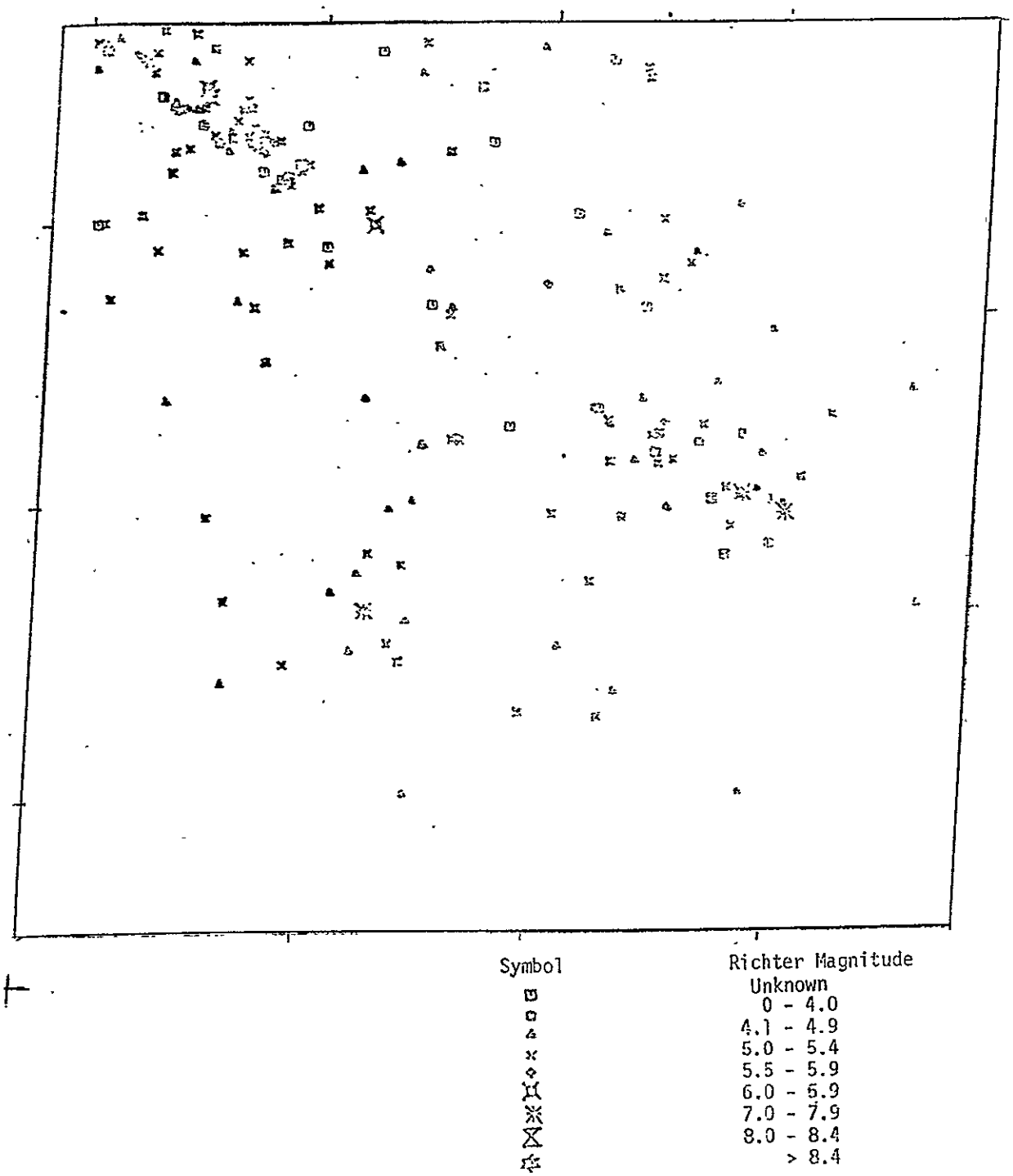

FIGURE 9 Earthquake Epicenters on Photograph 1056-18120

Monterey-Lopez Point

MSS 1021-18174; Fault Structures, Fig. 6; Eqrthquake Epicenters, Fig. 7

The information concerning the relation of Willow Creek fault (8) and Coast Ridge fault (9) (Fig. 6) is not new for it is well displayed in the Santa Cruz geologic map sheet. It is a clear case where ground truth provides strong support to our concept of fault interactions. The Willow Creek fault is a pronounced transverse fault somewhat anomalous in trend and appears to displace the Mesozoic granites and metamorphic rocks of the northern Santa Lucia Range some 15 km in a left-lateral sense. Its effect on the Miocene sedimentary rocks is less certain and would mean that transverse shear has indeed taken place as far north as the Salinas block, and that the faulting took place at least late in the Miocene. The Willow Creek fault is clearly terminated (most probably offset) by the Coast Ridge fault zone (9) on the west and by Salinas Valley fault (2, Fig. 3) on the east. The orientation of the Willow Creek is intriguing since it is similar to the orientation of the Garlock fault and the eastern part of the Big Pine fault some 230 km to the southeast.

Lopez Point to Point Buchon

MSS 1056-18120; Fault Structures, Fig. 8; Earthquake Epicenters, Fig. 9

This photograph which shows the southern part of the Coast Ranges (Santa Lucia Range) and the Inland Diablo Range shows that transverse faults are pervasive. In the Diablo Range several examples are noteworthy:

In Figure 8 faults 10, 11, 12, and 13 are examples. All of these lie along synclinal axes between anticlinal structures. Correlation with geological maps (Santa Cruz, San Luis Obispo sheets) shows that fault contacts occur between the Franciscan metamorphic group and the Upper Cretaceous sedimentary rocks. The Eocene and younger rocks seem to be unfaulted. This would seem to indicate that these transverse faults were active prior to the deposition of the Eocene sediments and that subsequent deformation along these structures largely took place by folding. It is significant however to note that both the Franciscan and the upper Cretaceous rocks appear to be displaced in a left-lateral fashion across these late Mesozoic breaks.

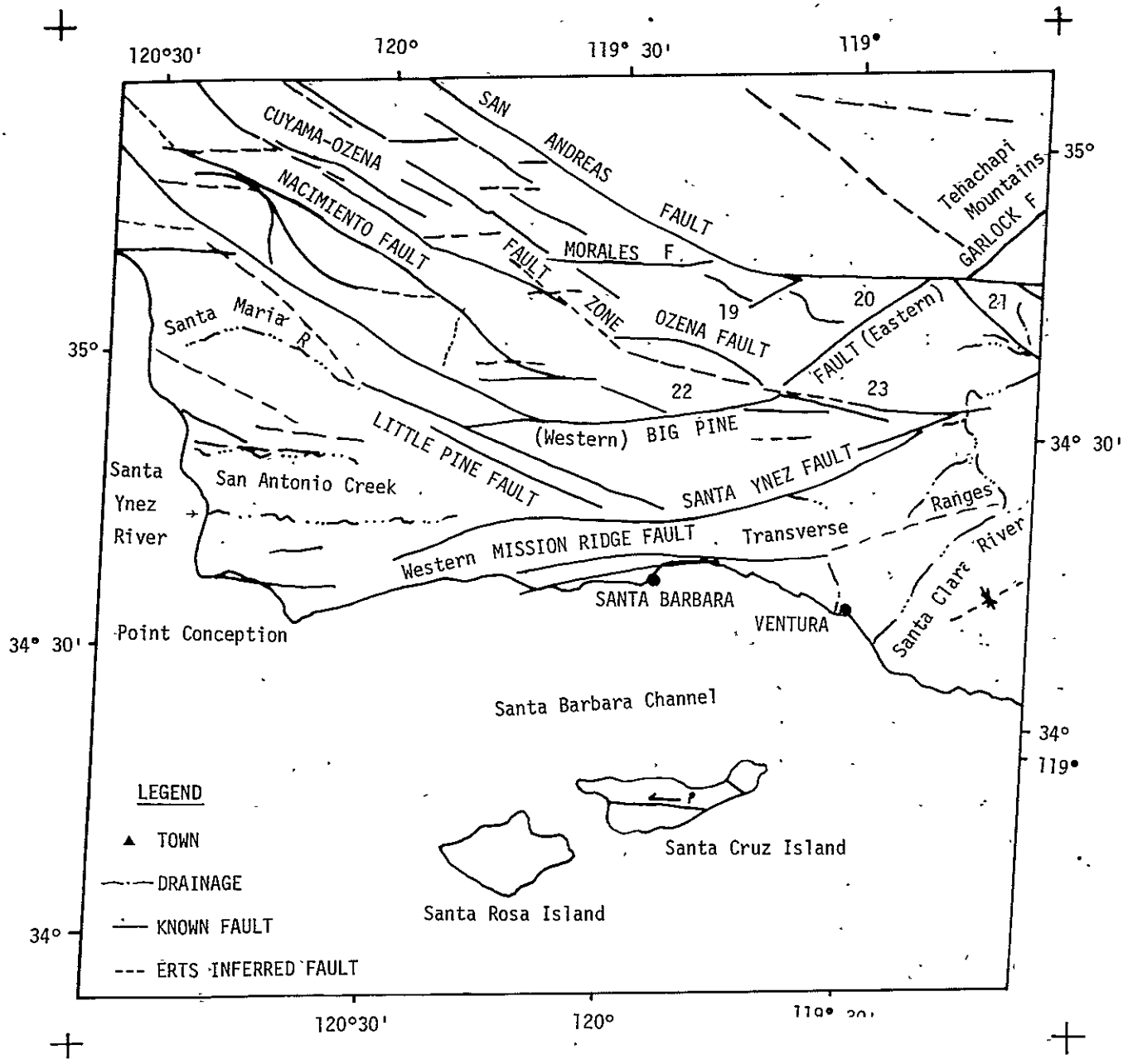

FIGURE 10 Fault Structures on Photograph 1037-18064

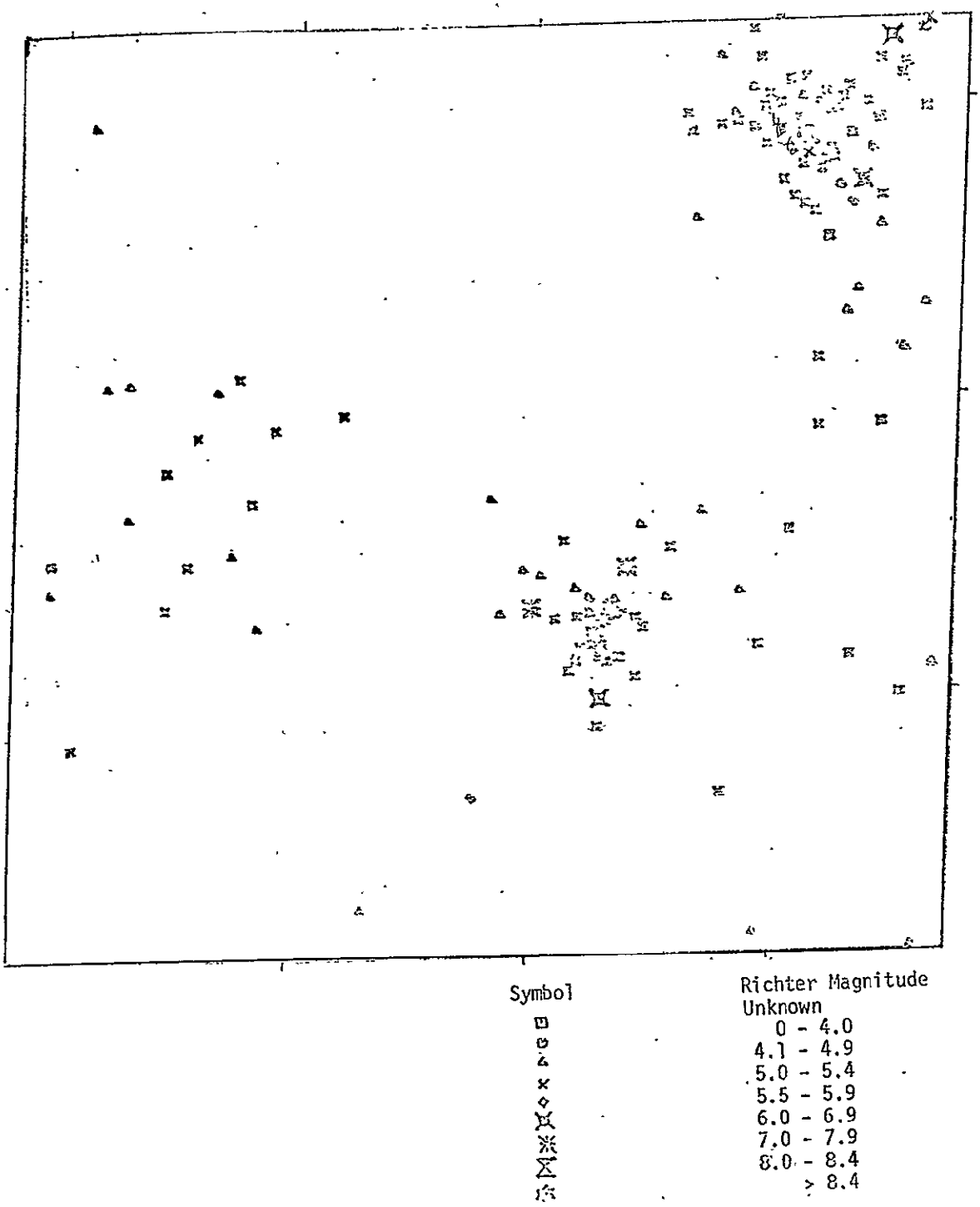

FIGURE 11 Earthquake Epicenters on Photograph 1037-18064

Further west in the Santa Lucia Range several transverse faults are observed lodged between Chimencas, Cuyama, Nacimiento, Huasna, and the coast line. Many of the projections of the coastline in fact appear to be controlled by transverse faults. In the geological maps some of these structures are shown incorporated as bends in faults of the San Andreas system.

Western Transverse Ranges

MSS 1037-18064; Fault Structures, Fig. 10; Earthquake Epicenters, Fig. 11

The presence of major left-lateral wrench faults in the western Transverse Ranges such as Santa Ynez, Big Pine, and Mission Ridge faults are too well known to be emphasized here. The abrupt termination of several faults of the San Andreas forming T-junctions with the Transverse faults is a problem which has been discussed (Abdel-Gawad and Silverstein, 1972). Observations derived from ERTS-1 imagery are relevant. The San Andreas fault along the segment between Morales and Garlock faults across the Tehachapi block appears to have an older trace which is zigzag in shape and seems to have been displaced repeatedly by east-northeast trending faults 19, 20 (Figure 10) which probably are related to the Garlock-eastern Big Pine faults.

If we ignore the Tehachapi segment of the San Andreas fault for a moment, we can visualize how the northern segment of the San Andreas may have been offset left-laterally by the Garlock-eastern Big Pine from its old route along the San Gabriel fault (21). This would suggest that the Tehachapi segment of the San Andreas is a relatively young break.

Hot Springs Lineament

The Ozena fault is shown in the Los Angeles geologic map sheet to be cut off by the Big Pine fault. We recognized from the ERTS-1 image (1037-18064) a lineament (22,23, Figure 10) cutting the Eocene rocks of Sierra Madre Mountains south of Ozena fault. This suspected fault continues across Big Pine fault, cuts across the Eocene rocks of Pine Mountain along Hot Springs Canyon and is intersected by the Santa Ynez fault. This fault lineament is quite pronounced and has a well-defined trace. The lineament

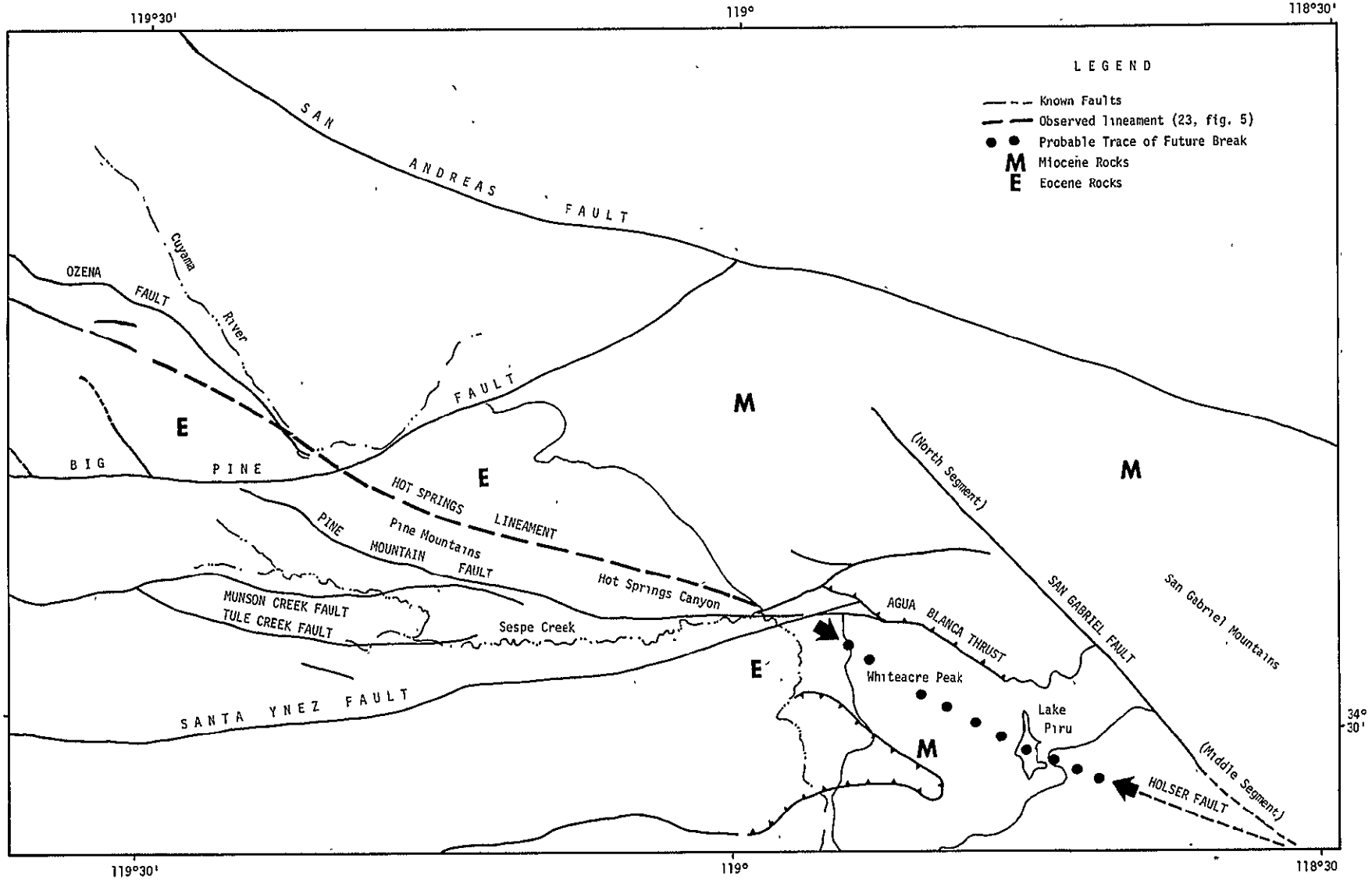

FIGURE 12 Generalized Fault Map of the Hot Springs Lineament

The lineament appears distinct from the Pine Mountain fault which runs approximately parallel to it and some 5-7 km to the south. Our plots of earthquake epicenters on the image show moderate seismicity in the vicinity of this lineament, particularly near its junction with the Santa Ynez fault. Hot springs occur where this fault runs along Hot Springs Canyon. The significance of this lineament goes beyond being one additional fault recognized in ERTS-1 imagery. The lineament lines up with the middle segment of the San Gabriel fault (the segment east of Newhall) and southeastward to the Sierra Madre fault zone. To the northwest it lines up on the Cuyama fault zone. Considering this, the lineament provides a link between the Sierra Madre and the Cuyama fault zones. There appears to be an interruption of this lineament by the Santa Ynez fault. The Middle Upper Miocene rocks exposed west of Lake Piru in the White Acre Peak-Hopper Mountains do not appear to be faulted along the projection of this lineament. If we make the reasonable assumption that major faults tend to straighten their knickpoints caused by transverse offsets, propagation of faulting along this lineament would likely link it with the middle segment of the San Gabriel fault with which it lines up. The two probable routes that are candidates for breakage are along the Agua Blanca thrust and southeastward along Halsey Canyon, that is 15 km northeast of Lake Piru or along a new break in the White Acre Peak area through Lake Piru to the San Gabriel fault.

Although it is hazardous to "predict" where a given fault may break next, it seems justifiable to propose that the Piru Lake area be monitored for evidence of strain buildup.

Figure 12 is a map showing the fault relations discussed.

It is noteworthy that the epicenter of the San Fernando earthquake (February 9, 1970) and the cluster of aftershocks is centered at a point some 40 km to the southeast of Piru Lake and in alignment with the Hot Springs lineament.

EARTHQUAKE EPICENTERS

Figures 4, 7, 9, and 11 are copies of overlays showing computer plots of historic earthquake epicenters which occurred in the period 1934 through 1972 within areas covered by the ERTS-1 images listed below.

ERTS-1 images used for earthquake epicenter plots include:

MSS 1021-18172
MSS 1021-18174
MSS 1056-18120
MSS 1037-18064

Earthquake data was compiled from NOAA Geographic Hypocenter Data File (magnetic tape) January 1961 through December 1971; NOAA Hypocenter Data Cards, January 1972 through August 1972 and California Department of Water Resources Bull. 116-2 (1962).

Because the tick marks on the ERTS-1 images varied in ground accuracies up to 7 km we utilized a computer program to generate longitude and latitude grids which reduced the ground error of the grids to the order of 2 km, a value which is acceptable considering the uncertainties of epicenter determinations in the first place. Using these grids and our computer file of earthquakes, the epicenters were plotted according to the following nine categories of estimated or determined magnitudes: unknown, 0-4.0, 41.-4.9, 5.0-5.4, 5.5-5.9, 6.0-6.9, 7.0-7.9, 8.0-8.4, >8.4.

The purpose for this is to obtain epicenter plots on transparent sheets which can be placed as accurately as possible on the corresponding ERTS-1 image in order to observe any significant relationship between seismic activity and structure.

Considering the importance of the San Andreas fault system as a major seismic zone, selection of this area is obviously justified. From preliminary analysis the following tentative observations are relevant.

PRELIMINARY OBSERVATIONS ON SEISMICITY PATTERNS

There appears to be no strict correlation between observed evidence of recent surface breakage and the distribution of earthquake clusters. It is quite obvious that very straight segments of the San Andreas fault showing evidence of relatively recent breakage are conspicuously quiescent. Examples are the segment between Maricopa and Cholame and the segment between the Garlock intersection and Cajon Pass.

These two observations are not new and were pointed out by Ryall *et al.* (1966), Allen *et al.* (1965), and others.

There are however three observations which to our knowledge are not emphasized sufficiently in the literature.

First, that earthquake clusters characterize regions of complex structure where transverse faults meet or tend to distort the San Andreas system and vice versa.

Second, that the earthquakes tend to cluster where propagation of a fault is likely to occur where it is offset by a crossing fault.

Third, that seismic activity and stress buildup on transverse structures and their distorting effect on the San Andreas system should receive equal attention to that given the San Andreas fault itself.

SOUTHERN CALIFORNIA LINEAMENT

ERTS MSS 1018-18010. We observed a prominent zone of structural and physiographic lineaments extending approximately from San Fernando, Los Angeles County towards the Oxnard area in Ventura County in an east-northeast trend. It was studied in more detail utilizing U-2 color infrared imagery and aerial photographs.

In Ventura County several previously unknown faults within this zone were identified and their traces plotted on large scale maps and 1:60,000 aerial photographs. Field checking at many points in Simi Valley and Simi Hills and in the Conejo Valley showed that some lineaments correspond to fault scarps or fault line scarps. This important fault zone is significant because it trends parallel to and partly coincides with a recent belt of seismicity related to the San Fernando 1971 earthquake reported by J. H. Whitcomb, C. R. Allen, J. D. Garmany, and J. A. Hileman (1973).

Practical Applications

The San Fernando-Oxnard fault zone may prove to be susceptible to seismic activity. To say the least, it should be considered in assessing the seismic hazards in this fast growing area of Ventura County. As a result of our discussions with Ventura County Planning Department, we requested from NASA Ames Research Center more recent U-2 coverage of Ventura County and vicinity. A cooperative effort of detailed fault mapping would be highly beneficial to the County's program of defining seismic hazards.

Specific Information and Application

The national and some states' awareness of a strong need to obtain more comprehensive data on earthquake hazards is now beginning to be felt on the country and city government levels.

Contacts have been made with Ventura County Planning Commission (Victor Husbands, Planning Director) and Kern County Office of Emergency Services Commission (Ray Jackson) for the purpose of making the results of our ERTS studies available to them. Both agencies are starting programs for evaluating earthquake hazards which include as an essential element making an inventory of potentially active faults in their counties.

Lineaments in the alluvium identified in ERTS imagery were of particular interest to Kern County council of governments. According to a letter received from Bradley F. Williams, Principal Planner for Technical Assistance, the information and ERTS imagery which we made available to them "were beneficial in developing regional concepts in their studies relating to a seismic safety plan for Kern County".

We made pertinent data derived from analysis of ERTS imagery available to these counties and hope it will be beneficial in realizing the objectives of their seismic hazards assessment programs.

FRAGMENTATION MODEL FOR TRANSVERSE AND COAST RANGES, CALIFORNIA

The east-west trending Transverse Ranges interrupts the northwest trending structures of the Coast Ranges and the continuity of the Sierra Nevada and the Peninsular Ranges-Baja California intrusive complex. As already discussed, thrusts and left-lateral wrench faults characterize the fault pattern of the Transverse Ranges. Farther north along the Coast Ranges many transverse elements within the northwest trending structural grain are observed. The presence of transverse faults there and the peculiar distribution of granitic and Franciscan basement rocks are two highly significant features.

The middle coast ranges of California from north of San Francisco southward consist of two main classes of basement rocks. The Franciscan group of metasediments with associated ultrabasic intrusives and the granitic intrusives of the Sierra Nevada type. The distribution of these rocks is peculiar in that the granitic rocks mainly form the central Salinia block bound by the San Andreas fault on one side and Nacimiento fault on the other. The Franciscan rocks occupy mainly the block east of the San Andreas fault extending in the Diablo Range and occur also in the Santa Lucia Range west of Nacimiento fault.

The similarity of the granitic rocks of Salinia to those which constitute the bulk of the Sierra Nevada batholith and particularly to the pre-Franciscan metamorphics and intrusives of the Tehachapi Mountains at the southern end of the Sierra Nevada block has been long recognized. King (1959) proposed that the Salinia block could be a sliver cut off from the Sierra Nevada and brought to its present position by lateral movement along the San Andreas fault. King reasoned that the Franciscan rocks probably represented a Mesozoic geosynclinal belt which lay along the western side of the intrusive belt of the proto Sierra Nevada. Taking this concept as a starting point, there are several features of the Coast Ranges which suggest that the Coast Ranges may have been affected by transverse shear prior to the development of the San Andreas fault as defined at present.

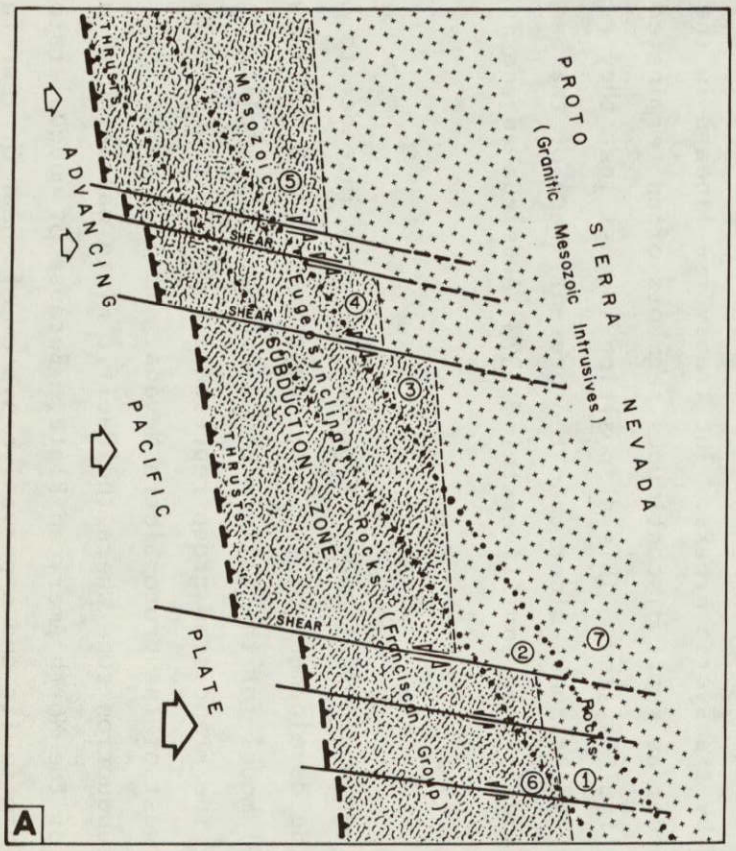

FRAGMENTATION MODEL OF COAST RANGES IN CALIFORNIA

A) TRANSVERSE SHEAR:
EUGEOSYNCLINAL FRANCISCAN SEDIMENTARY BELT LYING WEST OF SIERRA NEVADA INTRUSIVE BELT WAS A ZONE OF SUBDUCTION OF PACIFIC PLATE UNDER NORTH AMERICAN PLATE. TRANSVERSE SHEAR FAULTS DEVELOPED BETWEEN PACIFIC BLOCKS ADVANCING AT UNEQUAL RATES AND EXTENDED INTO INTRUSIVE BELT.

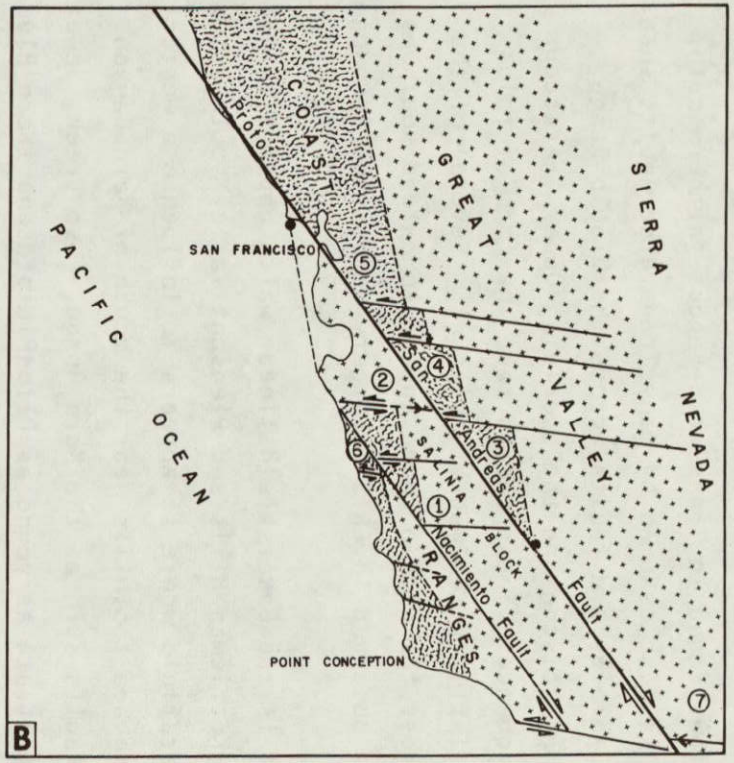

B) SAN ANDREAS SHEAR:
RIGHT-LATERAL SHEAR OF SAN ANDREAS SYSTEM DEVELOPED AS EAST PACIFIC RISE APPROACHED CONTINENTAL MARGIN. EFFECTS OF OLDER LEFT-LATERAL SHEAR AND YOUNGER RIGHT LATERAL DISPLACEMENTS CAUSED COMPLEX JUXTAPOSITION OF GRANITIC AND FRANCISCAN BASEMENT BLOCKS. NOTE DISTRIBUTION OF FRANCISCAN GROUP MAINLY EAST OF SAN ANDREAS AND WEST OF NACIMIENTO FAULTS AND GRANITIC SALINIA BLOCK IN BETWEEN. MODEL SUGGESTS PRESENCE OF TRANSVERSE FAULTS UNDER GREAT VALLEY SEDIMENTS AND EXPLAINS TRANSVERSE FAULTS OBSERVED IN COAST RANGES.

MARINE SEDIMENTARY BLANKET OF UPPER CRETACEOUS AND CENOZOIC ROCKS IS OMITTED. NUMERALS INDICATE CORRESPONDING BLOCKS IN A AND B: e.g. (7) AND (2) REPRESENT PRE-FRANCISCAN SEDIMENTARY AND INTRUSIVE ROCKS IN TEHACHAPI MOUNTAINS AND MONTEREY BAY BLOCK.

FIGURE 13 FRAGMENTATION MODEL OF COAST RANGES IN CALIFORNIA

We note from ERTS-1 imagery that the Coast Ranges, particularly the Franciscan terrain, shows a distinctive structural grain bearing west-northwest oblique to the strike of the San Andreas fault. This trend is similar to that found in Transverse Ranges farther south. The transverse grain is also assumed by many Transverse faults shear zones and thrusts. Examples are faults across the Diablo Range affecting mostly the Franciscan and the overlying Upper Cretaceous marine sedimentary sequence. These faults take the form of folds and flextures in the Tertiary sedimentary blanket. Several of the Transverse faults across the Diablo Range appear to extend southeastward as vague linears observed in ERTS-1 imagery across the San Joaquin Valley.

One such feature is the Bakersfield linear which appears to extend from the vicinity of Kettleman Hills and Pleasant Valley southeastward, passing north of Bakersfield where it appears to influence a westerly swing of the Sierra Nevada foothills near the mouth of Kern Canyon. Transverse trending faults such as the Kern Gorge, Poso Creek, Jewett and Edison, which cut strata as young as Plio-Pleistocene (Kern River formation) (Smith, 1964) may be rejuvenated breaks of the Bakersfield linear. Farther west, the Salinia block and Santa Lucia Range appear to be segmented by transverse breaks. The transverse linears in the Coast Ranges appear as short discontinuous segments often terminated by the San Andreas fault system. This disposition suggest that they represent a system of shear zones older than the present trace of the San Andreas fault (Abdel-Gawad and Silverstein, 1973; Abdel-Gawad and Tubbesing, 1974).

Tectonic Model

The idealized model sketched in Figure 13 is only intended to convey a concept for the development of the Coast Ranges. It is a modification of King's (1959) model for the Salinia block and basically follows his suggestion that the Franciscan group represents a Mesozoic sedimentary belt which lay west of the proto-Sierra Nevada. It is assumed that this belt lay in a subduction zone where the Pacific Plate was being thrust under the edge of the North American Plate. Because of unequal rates of advance, transform faults and a pervasive system of shear or tear faults

develop across the entire belt of plate collision. The deformation may conceivably have extended across the proto-Sierra Nevada complex (Figure 13a).

In the model we assume that the San Andreas fault system developed later, perhaps as a transform fault system, related the advance of the East Pacific rise.

Figure 13b illustrates the disposition of granitic and Franciscan basement blocks after right-lateral displacements took place along the San Andreas and Naciminento faults. Here we note that the older transverse shear faults have been intersected into short discontinuous segments lying east and west and in between the thoroughgoing faults of the San Andreas system. The Salinia granitic block had its origin as part of the Sierra Nevada. For example points 2 and 7 (Figure 13b) were once adjacent (Figure 13a) and represent the pre-Franciscan igneous metamorphic complex exposed in Monterey Bay block and in the southern part of the Sierra Nevada block. The Franciscan group which originally lay west of the proto-Sierra Nevada is now distributed mostly east of the San Andreas fault and west of Nacimiento fault, a configuration remarkably consistent with their actual distribution.

The model provides a possible explanation for the transverse linears observed in ERTS-1 and Skylab imagery across the San Joaquin Valley. The linears may indeed be the surfacial expression of deep-seated basement breaks reflected in the Great Valley sedimentary section as folds. The deep-seated transverse breaks may conceivably have been rejuvenated during the late Cenozoic uplift and westward tilt of the Sierra Nevada.

CORRELATION OF KNOWN MERCURY DEPOSITS WITH TRANSVERSE FAULTS*

There are some 100 mercury deposits in California clustered in 21 districts. Most deposits occur in the California Coast Ranges from Lake County to the north to Santa Barbara County to the south (Davis, 1966).

*In this section we discuss the results of a study of the correlation between transverse faults inferred from ERTS imagery and known mercury deposits in the Coast Ranges of California. This effort is aimed at deposits in the Coast Ranges of California. This effort is aimed at investigating an approach to mineral exploration based upon structural analysis of space imagery data. Under Rockwell International funding a similar and more detailed approach has been applied to a geologically and structurally different region in Nevada for the purpose of identifying specific target areas favorable for base and precious metals exploration, followed by reconnaissance ground truth studies. Because the two different studies indicate the usefulness of space imagery in mineral exploration planning, a separate report on the Rockwell funded effort has been included as a supplement to this contractural report.

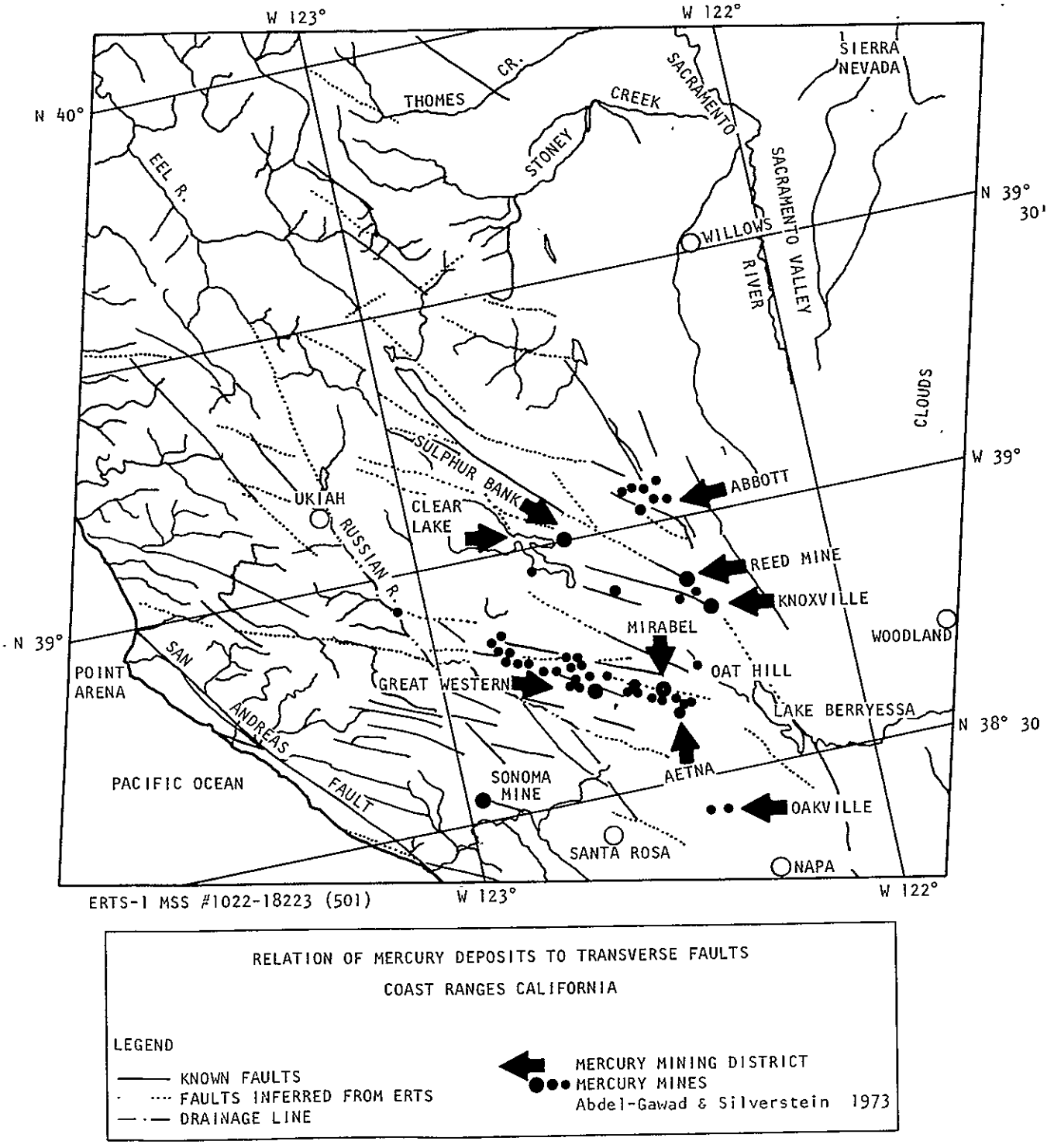

RELATION OF MERCURY DEPOSITS TO TRANSVERSE FAULTS
COAST RANGES CALIFORNIA

LEGEND

——— KNOWN FAULTS
· ···· FAULTS INFERRED FROM ERTS
— · — DRAINAGE LINE

MERCURY MINING DISTRICT
MERCURY MINES
Abdel-Gawad & Silverstein 1973

FIGURE 14 Relation of Mercury Deposits to Transverse Faults Coast Ranges California

Mercury ore has long been known to be deposited in epithermal (low temperature hydrothermal) conditions and is often associated with Tertiary and Quaternary volcanic regions. In California Coast Ranges mercury deposits occur in host rock conditions which are generally similar but the individual deposits have often been described an erratic, with marked differences in character, size, grade, and local structural conditions.

The carbonate-silica rock, an alteration product of serpentine often associated with mercury deposits, is so much more widespread than the ore itself as to be almost useless as an ore guide. In northern California mercury ore is found in the Clear Lake volcanic area (Figure 14, MSS 1022-18223). The Sulphur Bank Mine is a major hot spring-quicksilver deposit (White and Roberson, 1962).

Regionally, there has been little known regarding any specific tectonic or structural element which could be related to the regional distribution of mercury deposits even though many mines are known to occur in highly faulted, sheared, and deformed host rocks of the Franciscan group and the overlying Upper Cretaceous strata.

That transverse faults constitute a distinct tectonic element in the deformation history of the Pacific mountain system of California appears to be economically important in addition to its profound scientific value.

Taken as an example, the distribution of known mercury deposits in the California Coast and Transverse Ranges when plotted on ERTS-1 imagery shows a striking correlation with west-northwest trending shear zones, oblique to the prevalent trend of the San Andreas system.

The most striking correlation is noted in northern California in the Clear Lake and the Great Western mercury districts. Figure 14 shows an overlay map corresponding to ERTS-1 multispectral scanner scene no. 1022-18223. On this map we have plotted identifiable known faults as well as others inferred from ERTS imagery. We have also plotted as approximately as practical the most significant mercury mines as compiled

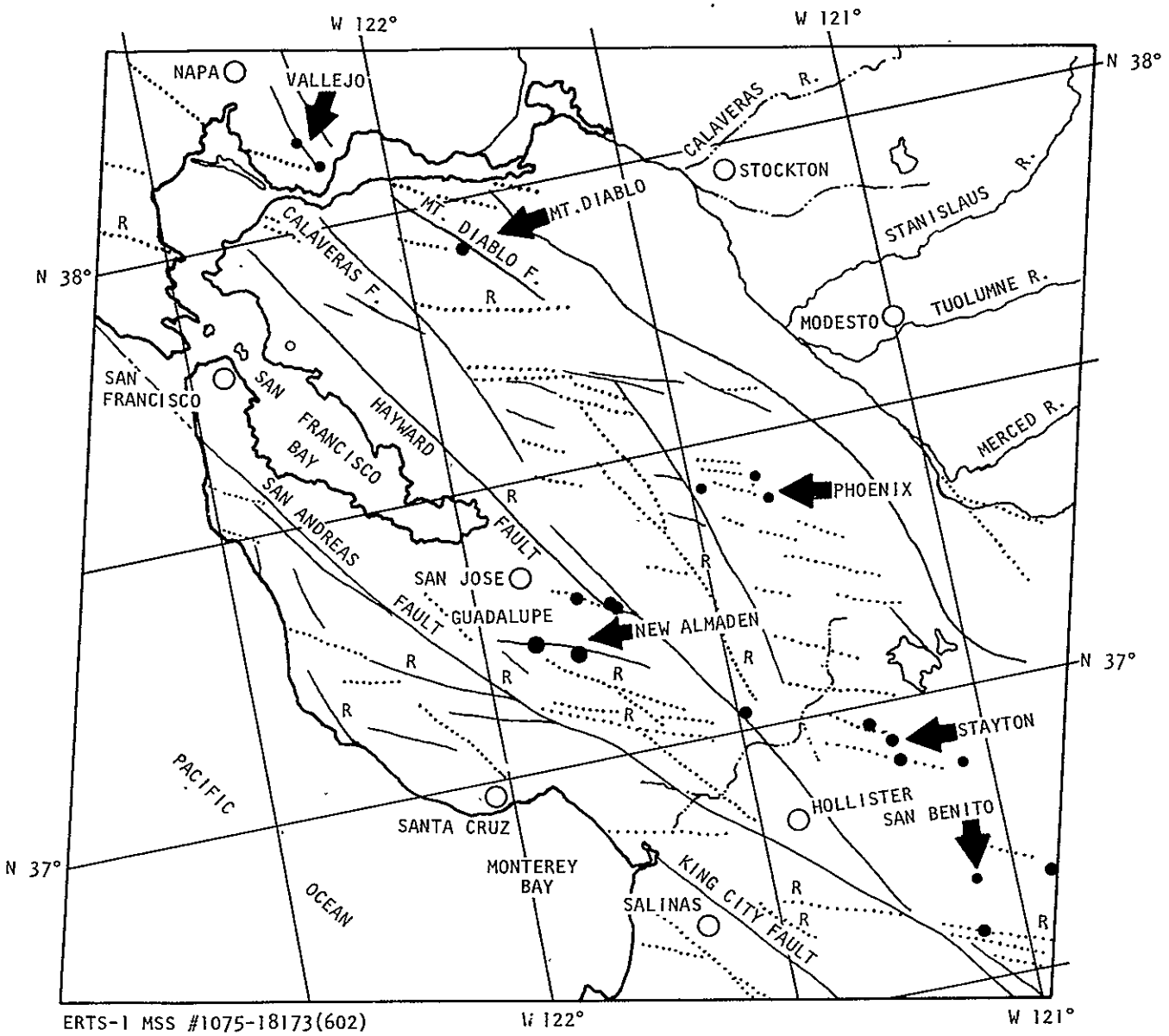

RELATION OF MERCURY DEPOSITS TO TRANSVERSE FAULTS
COAST RANGES CALIFORNIA

LEGEND

- R ..... Fault with evidence of recent movement
- ——— KNOWN FAULTS
- · ····· FAULTS INFERRED FROM ERTS
- —·— DRAINAGE LINE
- MERCURY MINING DISTRICT
- ●●● MERCURY MINES

Abdel-Gawad & Silverstein 1973

FIGURE 15 Relation of Mercury Deposits to Transverse Faults Coast Ranges California

ORIGINAL PAGE IS
OF POOR QUALITY

by Bailey (1962). They are identified by the name of the district and some of the larger mines. The cluster of mercury mines in the Great Western, Aetna, Mirabel, and Oat Hill is the most striking in that it forms a distinct belt trending west-northwest which coincides with a zone of transverse faults. Many of these faults appear on the Santa Rosa Geological Map Sheet, Atlas of California. In this specific case the relationship between mercury deposits and the transverse fault zone is rather evident from the fault pattern on the geological map. This relation, however, is not evident from the geological maps elsewhere in the Coast Ranges, because most of the known transverse faults are incorporated as bends in the northwest-trending faults of the San Andreas set and, therefore, do not stand out as a separate and significant entity. Besides, many transverse fault structures became evident from ERTS-1 imagery.

The relation between mercury occurrences and transverse fault zones is consequently much less apparent from the geological maps than from ERTS-1 imagery farther south in the Coast Ranges. In Figure 15 we have plotted known mercury occurrences together with transverse fault zones inferred from ERTS-1 scene 1075-18173. In this area of the Coast Ranges there are six mercury mining districts including the New Almaden, the first quicksilver mine discovered in North America and one of two most productive in California since 1846.

The New Almaden mine is typical of mercury ore associated with silica-carbonate rock underlain by graywacke, shale, greenstone, and serpentine of the Franciscan Formation. The mine is located on a "northwest trending anticline whose southwest limb is sheared and cinnabar was introduced along narrow northeast trending fractures" (Davis, 1966). Although some transverse faults are shown in the geological map (San Jose sheet) mostly as flextures in the San Andreas fault system, the position of the New Almaden, Guadalupe, and other deposits in distinct relation to transverse fault zones became readily apparent from correlation with ERTS imagery. In the Diablo Range, east of the Hayward fault four mercury districts, Vallejo, Mount Diablo, Phoenix, and Stayton are located on or near transverse fault zones identified from ERTS-1 imagery.

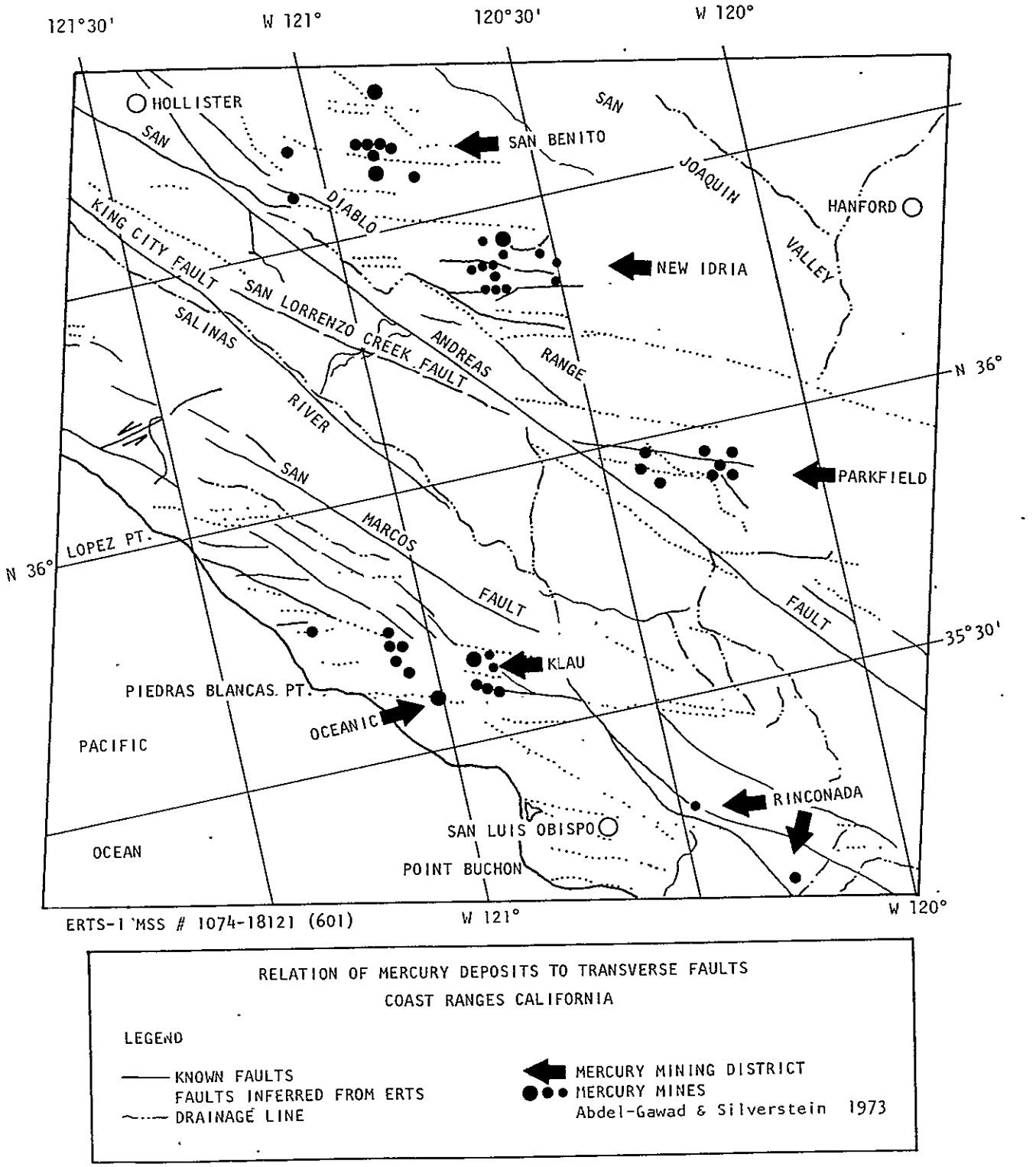

FIGURE 16 RELATION OF MERCURY DEPOSITS TO TRANSVERSE FAULTS COAST RANGES CALIFORNIA

Figure 16 (MSS scene 1074-18121) shows the spatial relation between six mercury districts and transverse structures in the southern part of the Coast Ranges. The New Idria Mining district in San Benito County stands out as including the most productive mercury mine in the United States, which together with the New Almaden mine produced more than half a million flasks of mercury since its discovery in 1853. The New Idria cluster occurs associated with a serpentine mass which intruded through a sequence of shales and sandstones of the Upper Cretaceous Panoche formation and overlying Tertiary sedimentary rocks. Mercury ore has been described (Eckel and Myres, 1946; Davis, 1966; Linn, 1968) as localized under the New Idria thrust fault in altered Upper Cretaceous Panoche formation. A large ore shoot lies at the intersection of the New Idria thrust with a tear fault. We find it significant that the New Idria thrust has a definite transverse trend and may in fact be the surface expression of a transverse shear fault in depth. When we examine the transverse faults in this part of the Coast Ranges, particularly those which cut across the Diablo Range, east of the San Andreas fault and correlate them with the geological maps we find that they are often associated with known folds. Those have been widely regarded as drag folds and secondary faults resulting from primary right-lateral shear on the San Andreas fault. Most of the transverse faults shown on the geological maps cut the Mesozoic Franciscan formation and the overlying Upper Cretaceous sedimentary rocks, with only a few cutting rocks younger than Eocene. ERTS-1 imagery, however, show that a significant number of transverse faults, particularly those occurring along fold flexures on the eastern side of the Diablo Range, persist as distinct lineaments across Tertiary and Quaternary sedimentary rocks of the Great Valley. While the tectonic stresses which produced the transverse shear structures may have been initiated in pre-Tertiary times, the observation of fault lineaments across the blanket of younger rocks in the San Joaquin Valley suggests that transverse shear has either persisted during the deposition of Tertiary and Quaternary rocks or has been reactivated during the late Tertiary uplift of the Sierra Nevada.

Figure 17 corresponds to ERTS-1 scene 1037-18064 and shows the complex interaction of the Transverse Ranges and characteristic left-lateral wrench

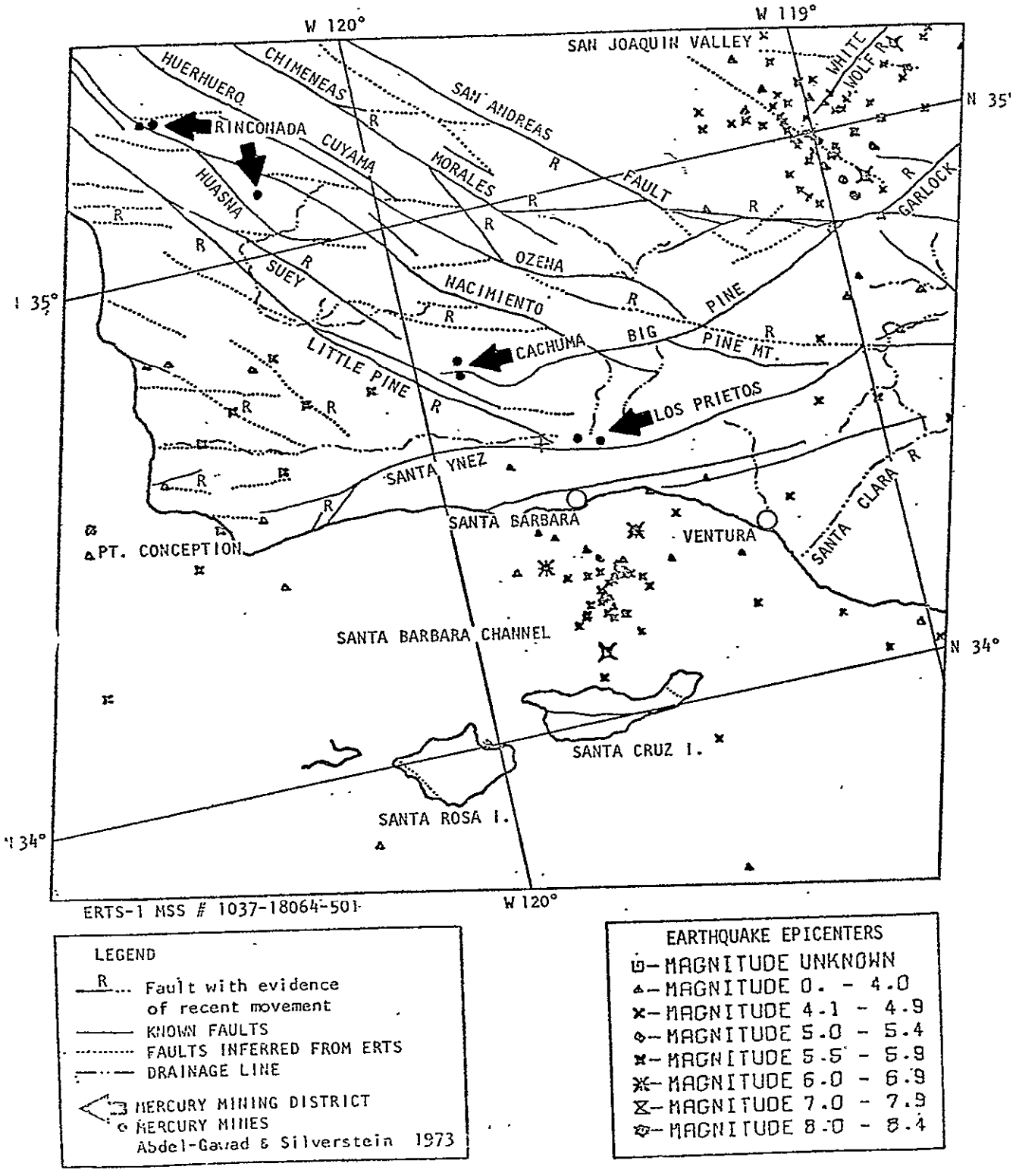

FIGURE 17 ERTS-1 MSS #1037-18064-501

faults with the Coast Ranges and the San Andreas fault set. The three mercury districts, Rinconada, Cachuma, and Los Prietos indicate a relation to transverse structures. Although the Sunbird open pit mine (Los Prietos district) in Santa Barbara County has become among the large producers in the late 1960's (Mitko, F. C., 1968), it may appear surprising the mercury deposits were not found in greater abundance within the Transverse Ranges. The widespread presence of a thick blanket of Tertiary marine sedimentary rocks in this province probably accounts for the apparent scarcity of mercury deposits on the surface but there is no reason to discount the likelihood of more extensive occurrences in depth.

DISPLACEMENT OF SAN GABRIEL, SAN BERNARDINO, AND SAN JACINTO MOUNTAINS

ERTS-1 imagery shows that the southern segment of the San Gabriel fault which controls the west fork of the San Gabriel River in the San Gabriel Mountain block is strikingly similar to the Mill Creek fault in the San Bernardino Mountains. We have also noted the similarity of the Sierra Madre thrust zone of the San Gabriel Mountains to the Banning thrust of the San Bernardino Mountains. These and other physiographic similarities suggest that the southern San Gabriel fault was once continuous with the Mill Creek fault. Similarly the Sierra Madre fault zone probably continued eastward along the Banning fault zone.

When the San Bernardino Mountain block is theoretically moved to the northwest along the San Jacinto fault so that the Mill Creek fault is aligned with the southern part of the San Gabriel fault, it was found that the four transverse fault segments become aligned with the Pinto fault on the east and with the Raymond-Santa Monica Malibu fault zone on the west. The reconstruction thus identifies a continuous zone of transverse faulting extending from the Colorado River Desert to the Pacific. Considering that the Pinto fault on one end and the Malibu fault on the other are both characterized by left-lateral strike-slip movement it seems likely that the entire fault zone was once a continuous left-lateral shear. For future reference we shall refer to this fault as the Anacapa shear since it probably extends to the Anacapa, Santa Cruz, and Santa Rosa Islands in the Santa Barbara Channel. A 50 km left-lateral

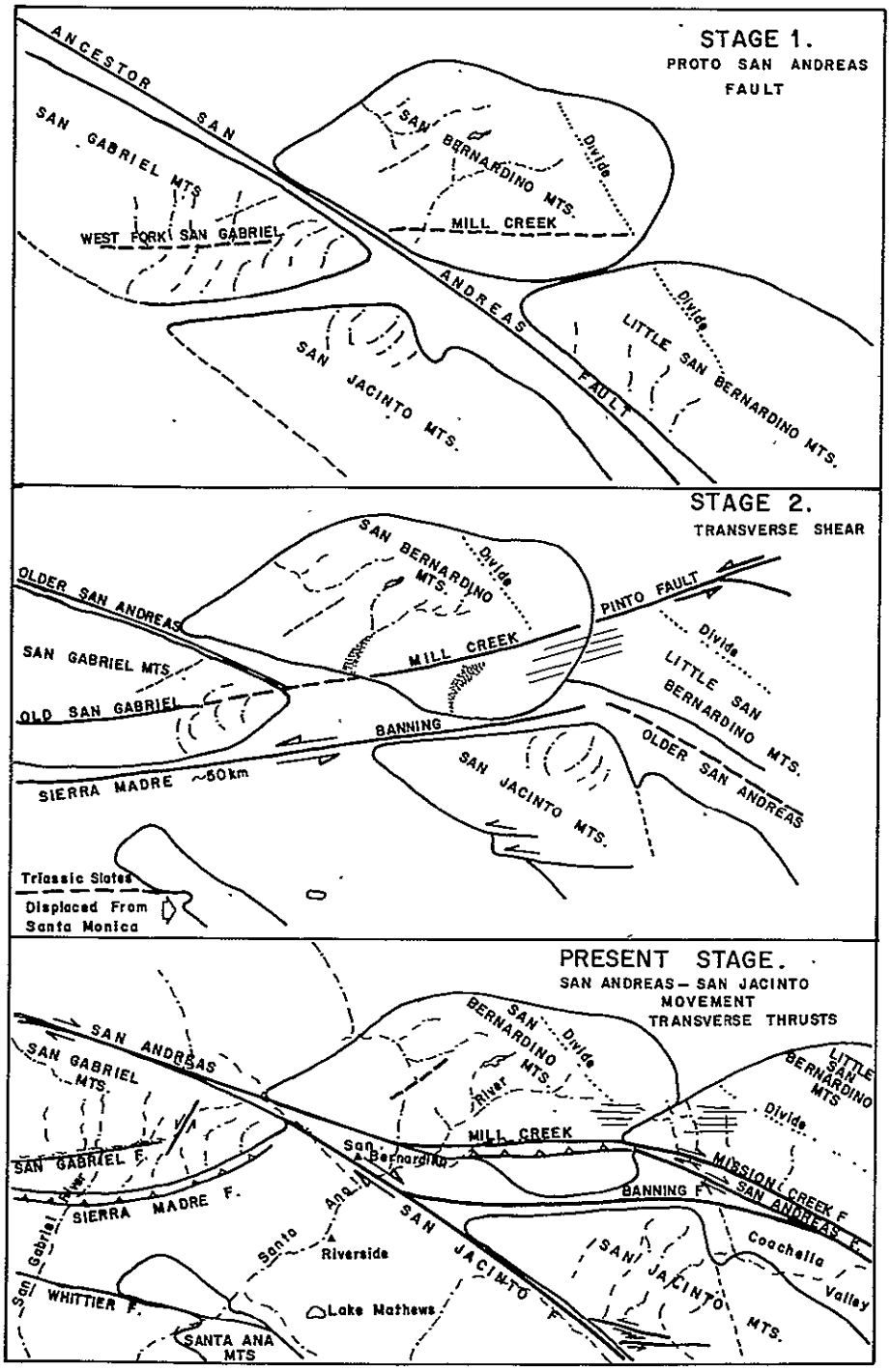

RECONSTRUCTION MODEL OF SAN GABRIEL, SAN BERNARDINO, AND SAN JACINTO MTS., SOUTHERN CALIFORNIA... MSS 1053-17551

LEGEND

—— KNOWN FAULT ▲ TOWN

--- ERTS INFERRED FAULT —·— DRAINAGE

FIGURE 18 RECONSTRUCTION MODEL OF SAN GABRIEL, SAN BERNARDINO, AND SAN JACINTO MTS., SOUTHERN CALIFORNIA ... MSS 1053-17551

movement has taken place on the Anacapa shear. Reconstruction based upon this figure would bring the Triassic Bedford Canyon formation of the Santa Ana Mountains in juxtaposition with the strikingly similar Santa Monica slate in the Santa Monica Mountains.

This analysis suggests that the tectonic history of the Transverse Ranges has been characterized by episodes of left-lateral shear on transverse faults and right-lateral shear on the San Andreas fault system. This conclusion is consistent with the fault model we developed for southern California. Based upon these key structural similarities, we developed a three-stage reconstruction model which explains the lateral displacement history of the mountain blocks (Figure 18).

In following sections we present evidence that a major system of left-lateral transverse shear along the Texas and Parras belts developed in late Mesozoic predating the initiation of the San Andreas fault system. We also argue that transverse shear has been an important element in late Cenozoic Basin and Range rifting. The association of transverse shear both with compressional and tensional tectonic periods is a fundamental thesis in this investigation.

PAGE INTENTIONALLY BLANK

AREA 2

EASTERN CALIFORNIA AND WESTERN AND CENTRAL NEVADA

INTRODUCTION

The area discussed in this section is largely within the Basin and Range province east of the Sierra Nevada. It includes the northern Mojave Desert, Owens and Panamint Valleys and extends northward covering western and central Nevada (Figure 19).

ERTS-1 scenes covering this study area are:

MSS 1019-18050
MSS 1054-17594
MSS 1055-18053
MSS 1018-17592
MSS 1018-18001
MSS 1018-18003
MSS 1018-18055.

FAULTS, SEISMICITY, AND YOUNGER VOLCANIC ZONES

The tectonic style in this area suggests a close relationship between faulting, seismic activity and the distribution of Quaternary to late Tertiary volcanic rocks.

For this reason, we plotted on overlays the following data:

a) Known faults derived from published maps and geologic reports drawn in solid lines.

b) Suspected faults or lineaments inferred from ERTS-1 imagery and believed to be significant for the objectives of the investigation. Many of the inferred structures need to be checked and studied in the field in detail. Their identification on the overlays serves to pinpoint their suspected trace and will serve to guide interested agencies and field geologists. Faults or lineaments suspected to have been active in the Holocene on the basis of photogeomorphologic evidence are indicated by the symbol (R).

c) Areas of known or suspected Quaternary volcanic exposures are shown for comparison (Figure 27).

A preliminary description of significant observations for each ERTS-1 scene follows:

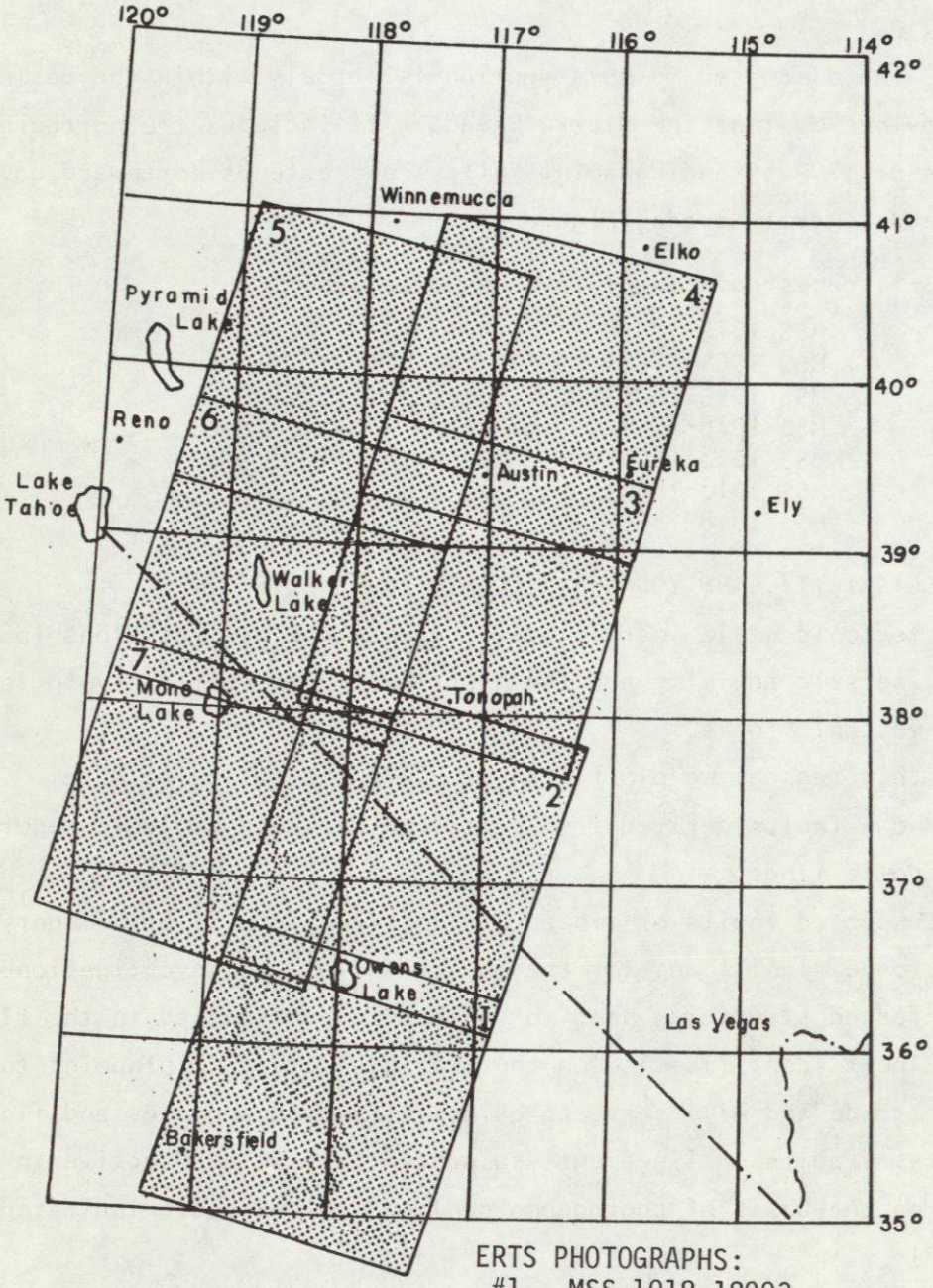

ERTS PHOTOGRAPHS:
#1 - MSS 1018-18003
#2 - MSS 1018-18001
#3 - MSS 1054-17594
#4 - MSS 1018-17592
#5 - MSS 1019-18050
#6 - MSS 1055-18053
#7 - MSS 1055-18055

FIGURE 19 MAP OF AREA STUDIED

TRANSVERSE FAULTS AND LINEARS, SOUTHERN SIERRA NEVADA, CALIFORNIA
OBSERVED IN ERTS-1 MSS 1018-18003

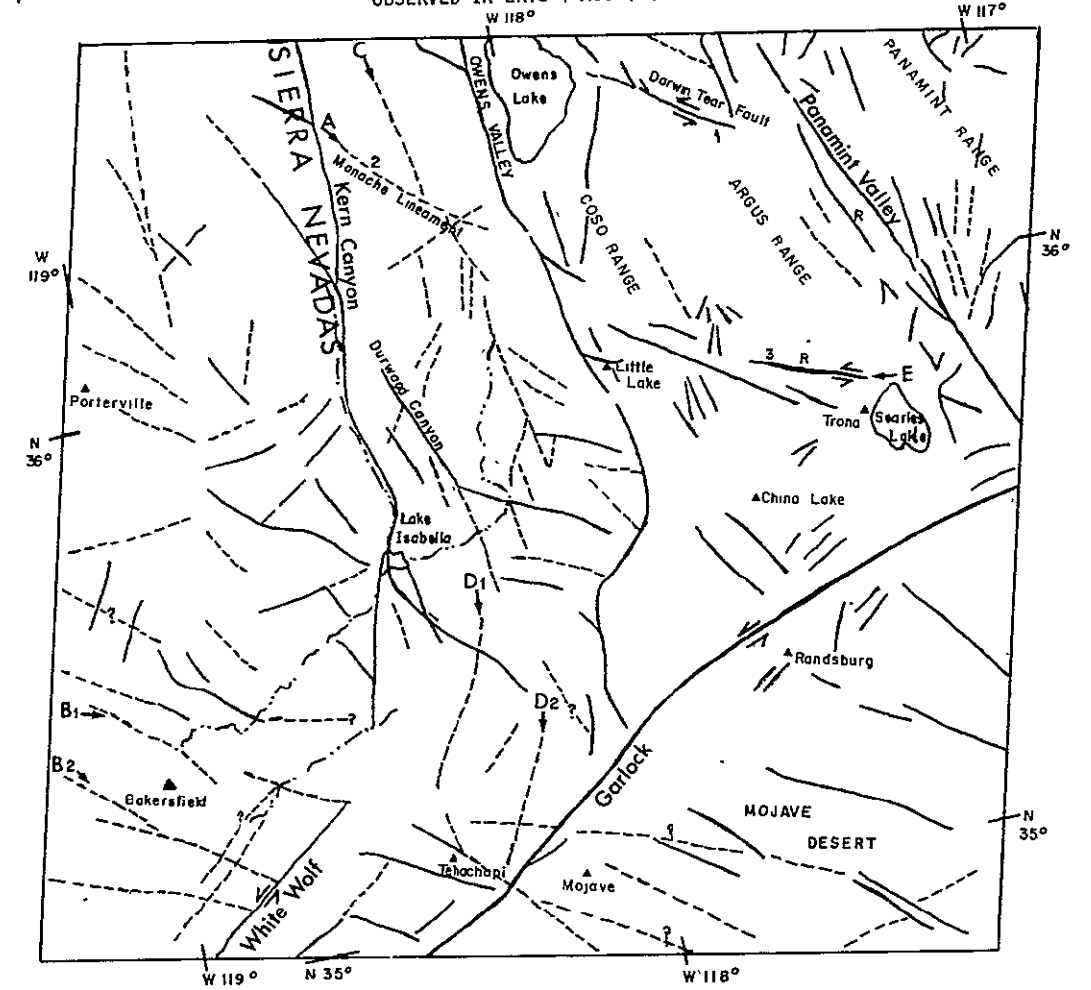

LEGEND

- ▲ TOWN
- —— KNOWN FAULT
- ---- INFERRED FAULT OR LINEAMENT FROM ERTS IMAGERY
- —·— DRAINAGE

LINEAMENTS OR FAULTS:

- A - NW-SE EXTENSION OF MONACHE LINEAMENT ACROSS THE SIERRA NEVADA
- B_1, B_2 - WNW UNDER SAN JOAQUIN VALLEY
- C - WITHIN SIERRA BLOCK, PARALLEL TO EASTERN ESCARPMENT
- D_1, D_2 - PARALLEL TO SOUTHERN SEGMENT OF KERN RIVER FAULT
- E - KNOWN FAULT WITH INFERRED LEFT LATERAL OFFSET OF 2-3 km
- 1,2,3 - WNW FAULTS

FIGURE 20a

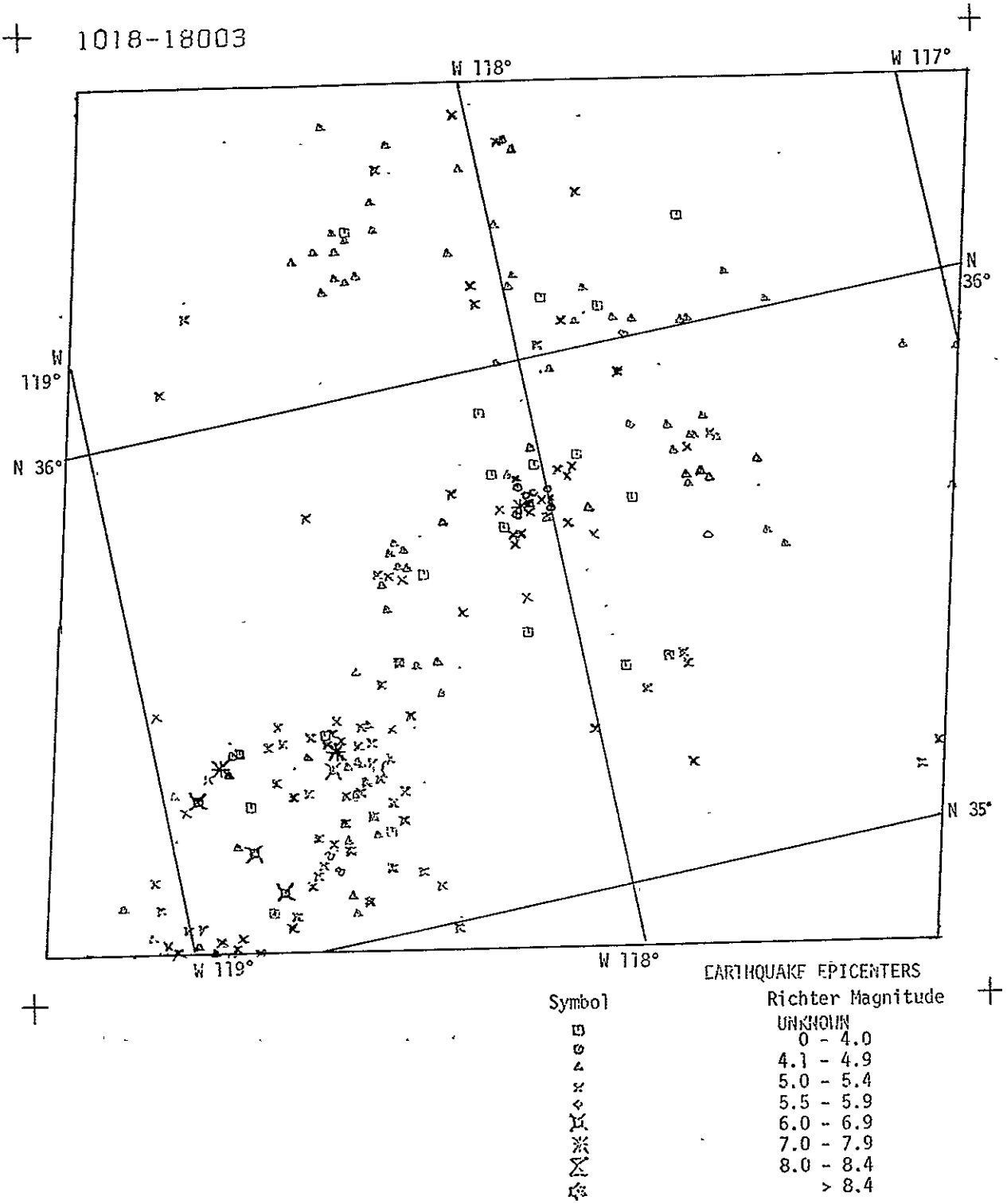

FIGURE 20b Earthquake Epicenters Plotted on Photograph MSS 1018-18003

Southern Sierra Nevada

Reference: MSS 1018-18003; overlays: Figures 20a, 20b

The scene shows the southern part of the Sierra Nevada Mountains. The main known fault zones are: the Owens Valley fault zone running along the eastern scarp of the range, Panamint Valley fault, Kern River fault, Garlock and White Wolf faults. Other significant faults are identified by a key number.

The known faults in this area have the following general trends:

- North-south to NNW-SSE, e.g., Kern River, Owens, Panamint.
- Northeast-southwest, e.g., Garlock, White Wolf.
- West-northwest: Known examples occur in the Mojave desert. The fault east of Owens Lake (1 Figure 20a) is a left-lateral strike-slip fault (Mayo, 1947).

In Figure 20a we recognized in ERTS-1 imagery many possible faults belonging to all three major systems which do not appear in the geological maps (Geologic Atlas of California); Bakersfield, Trona, Death Valley, and Fresno sheets.

Most of the suspected faults occur in Kern and Tulare counties. Several west-northwest trending lineaments appear to cut across the southern end of the Sierra Nevada and Tehachapi Mountains almost at right angles to the Garlock and White Wolf faults. Although the Garlock fault stands out as a very prominent feature in ERTS imagery, the active White Wolf is no more prominent than west-northwest lineaments referred to. Because known faults of the same trend occur in this area, their existence should be checked in the field. They may be particularly significant because they appear to extend northwestward under the San Joaquin Valley in the vicinity of Bakersfield, California. The area east and south of Bakersfield is seismically active and lies at the intersection of three major fault systems. The Kern River fault, Garlock and White Wolf and the west-northwest system which parallels the San Andreas fault in its middle segment.

Another important fault which we refer to here as the Monache lineament trends west-northwest and cuts obliquely across the Owens Valley

extending from Searles Lake to south of Owens Lake. Several faults of this zone east of the Sierra Nevada have been previously known. ERTS imagery, however, shows that it is a continuous fault zone extending across the eastern side of the Sierra Nevada to the Kern River fault (2, Figure 20a). This fault zone is probably older than the main eastern fault scarp of the Sierra Nevada because the latter cuts boldly across it.

The Monache Fault zone is significant for several reasons:

a) It marks a possible continuation of an important fault zone across the faulted eastern scarp of the Sierra Nevada.

b) It marks a significant altitude difference of the Sierra Nevada blocks north and south of it. This significant altitude difference causes the block directly west of Owens Lake to show higher albedo and lighter vegetative cover in the color prints than the block directly southwest of lineament.

c) It is associated with several Tertiary volcanic centers and hot springs.

d) This fault may belong to the transverse tectonic element observed pervasively throughout California. It is significant that this transverse element persists outside the Transverse Ranges where it has been traditionally recognized.

It may be appropriate to refer to our previous reports (Abdel-Gawad and Silverstein, 1971, 1973) on manifestations of the transverse tectonic element within the Coast Ranges of California.

The seismicity pattern suggests that earthquakes tend to cluster near intersections of transverse fault zones with the other more widely recognized fault systems.

Prominent faults such as Garlock, Kern River and Panamint Valley faults are not particularly associated with earthquakes except near certain fault intersections.

East of the Sierra Nevada, earthquake epicenters tend to cluster near Quaternary and late Tertiary volcanic areas.

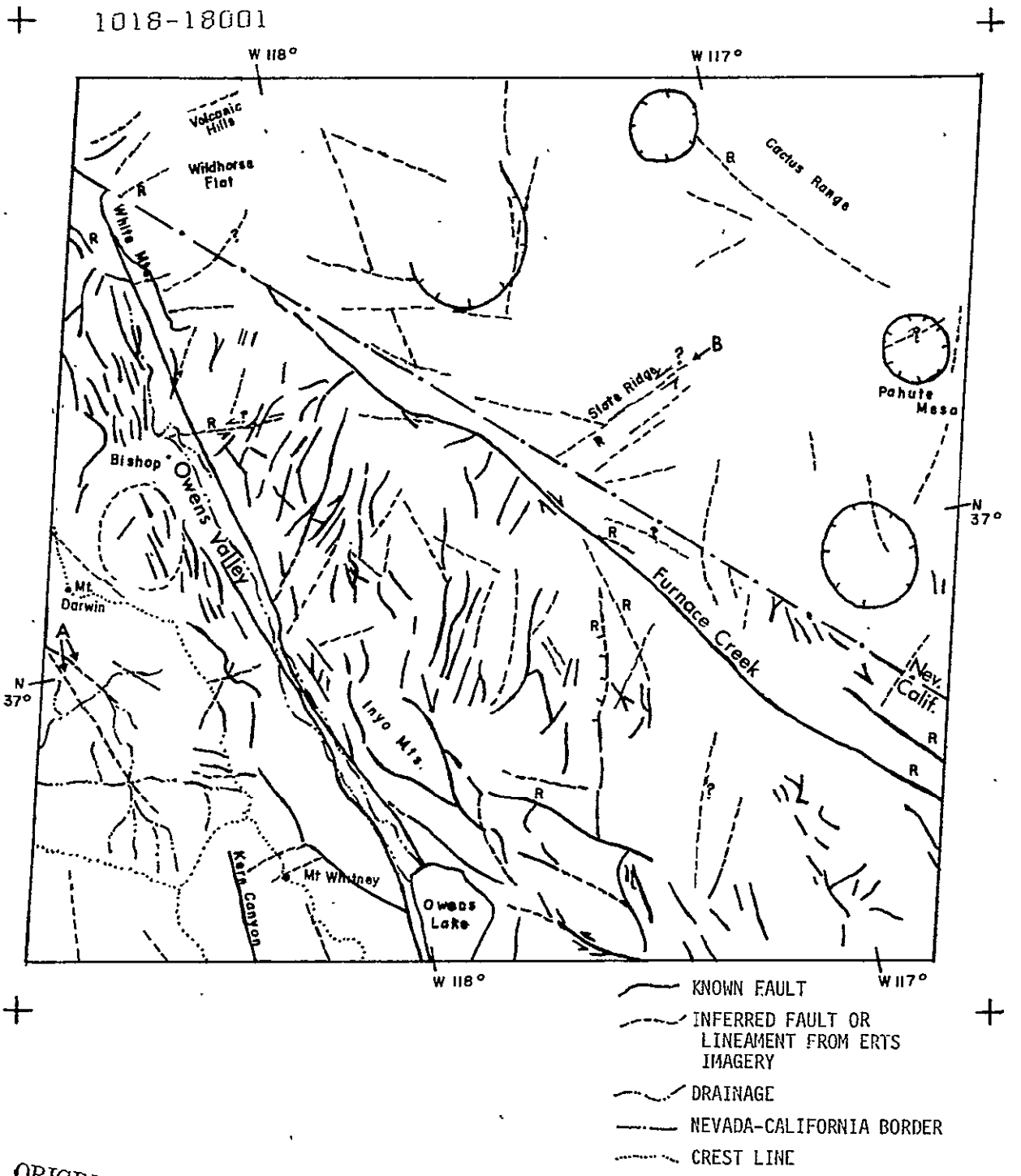

FIGURE 21a FAULT STRUCTURES ON PHOTO MSS 1018-18001

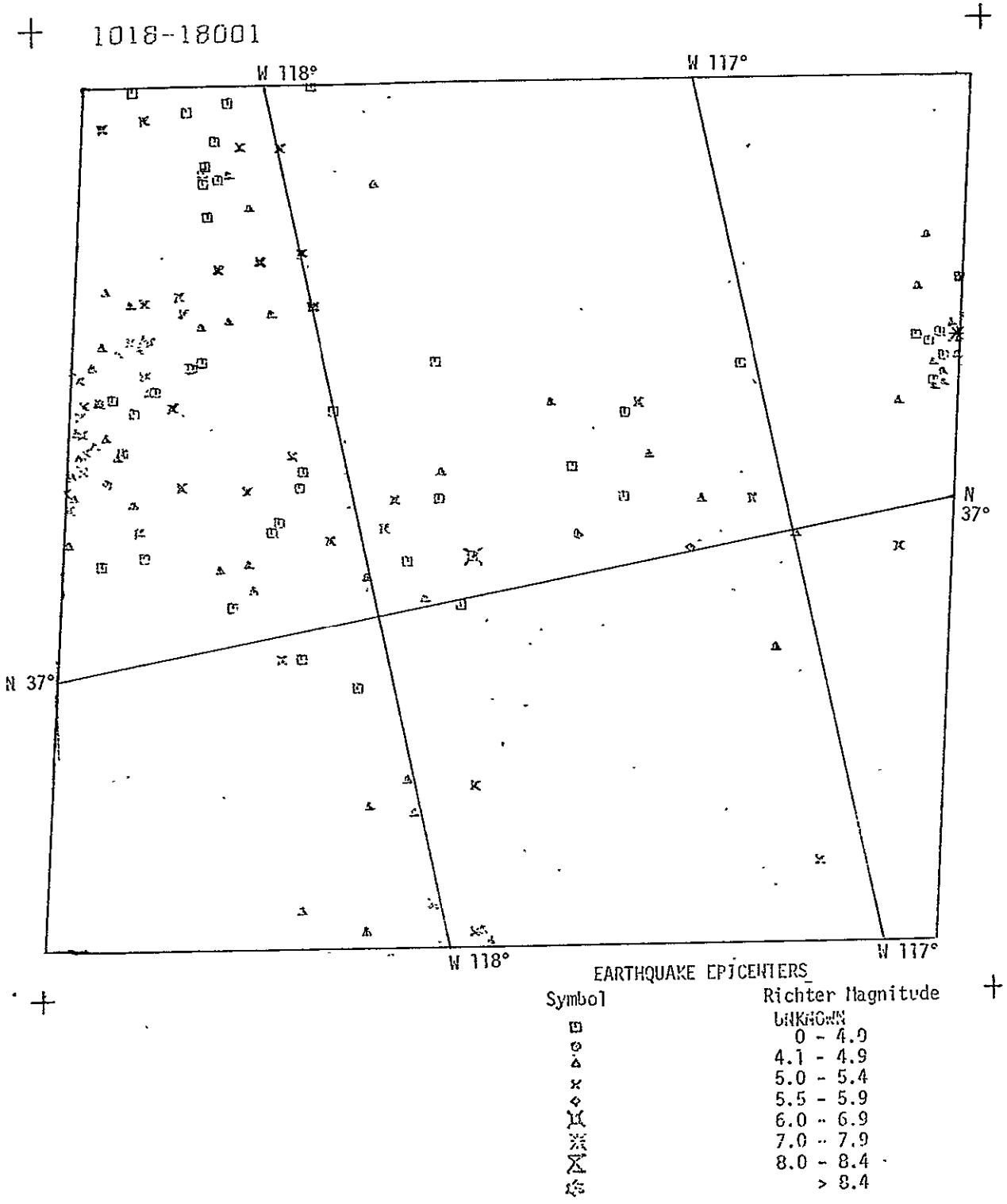

FIGURE 21b EARTHQUAKE EPICENTERS PLOTTED ON PHOTOGRAPH MSS 1018-18001

New major features inferred in Figure 20a:

A. Northwest-southeast extension of the Monache fault lineament across the Sierra Nevada.

B1,B2. West-northwest fault (?) zones across San Joaquin Valley which belong to the Bakersfield lineament. These appear to continue southeastward beyond White Wolf and perhaps beyond Garlock fault, as well as, into the Mojave Desert.

C. Fault (?) lineament within Sierra block and parallel to its eastern escarpment.

D1,D2. Fault (?) lineaments parallel to southern segment of the Kern River fault.

E. Known fault; left-lateral offset of 2-3 km is inferred.

Inyo and White Mountains, California

MSS 1018-18001; overlays: Figures 21a and 21b

The scene shows part of the Sierra Nevada Crest, Owens Valley between Bishop, California and Owens Lake, Inyo and White Mountains, bounded on the northeast by the Furnace Creek fault running adjacent and parallel to the California-Nevada state line and across the border part of the Basin and Range Province in Nevada.

The two major known fault zones are: The Owens Valley fault marks the eastern side of the Sierra Nevada block and has been reported to be a combination normal and strike-slip right-lateral fault with a total lateral displacement of 25 km or less (Hamilton and Myers, 1966). The Furnace Creek fault is generally considered a north-westward continuation of the Death Valley fault. Together the Furnace Creek-Death Valley faults have been reported to be major strike-slip faults with a cumulative displacement amounting to some 80-100 km (Hamilton and Myers, 1966).

Between these two major breaks the White and Inyo Mountain block is broken by a system of north-south to NNE-SSW mostly normal faults with an evidently tensional tectonic style, as indicated by the many grabens and horsts within the Inyo-White Mountain block.

The area across the state line in Nevada has evidently not been mapped in detail comparable to that in California. We utilized ERTS imagery to identify many linear features which will contribute to a better understanding of the tectonic style in Nevada in more detail.

Known faults and probable faults derived from analysis of ERTS imagery are shown in Figure 21a.

Epicenters of historic earthquakes corresponding to Fig. 21a are plotted in Figure 21b.

The following observations are significant:

a) Sharp physiographic lineaments are observed within the Sierra Nevada block west of the crestline (A, Figure 21a). These lineaments are not shown on the Fresno and Mariposa sheets, Geologic Atlas of California. They trend northwest-southeast parallel to the Furnace Creek fault and appear more clearly on other ERTS images not masked by clouds (see for example, MSS 1055-18055).

The lineaments do correspond, however, to contacts between the Mesozoic granitic intrusives and a Jurassic-Triasic metavolcanic belt. The linearity of this feature suggests a fault contact and should be field checked.

b) Geomorphologic evidence of recent faulting can be inferred along many fault traces belonging to at least three fault systems. Examples are indicated by the symbol R in Figure 21a.

A northwest-southeast system includes the Furnace Creek fault, the Owens Valley fault and the Cactus Range fault. A north-south fault system encompasses many smaller faults between the Furnace Creek and Owens Valley faults, a fault running east of Fish Lake Valley and two cutting through the Cottonwood Mountains. A third system is a northeast-southwest fault system including, for example, arrow B (Figure 21a).

c) It is noted that while some seismicity appears to be associated with the Furnace Creek fault zone and many segments of the fault zone show evidence of recent breakage, the most seismically active sites are the Pahute Mesa Caldera, Wildhorse Flat and Owens Valley, areas of subsidence due to tension with extensive development of Quaternary and late Tertiary volcanics.

Mono Lake, Sierra Nevada, Owens Valley

MSS 1055-18055; overlays: Figures 22a and 22b

This scene covers the area from Mono Lake in the north to Mt. Whitney and the Kings River in the south. It shows the Sierra Nevada Range and the San Joaquin Valley to the west, and the Owens Valley to the east.

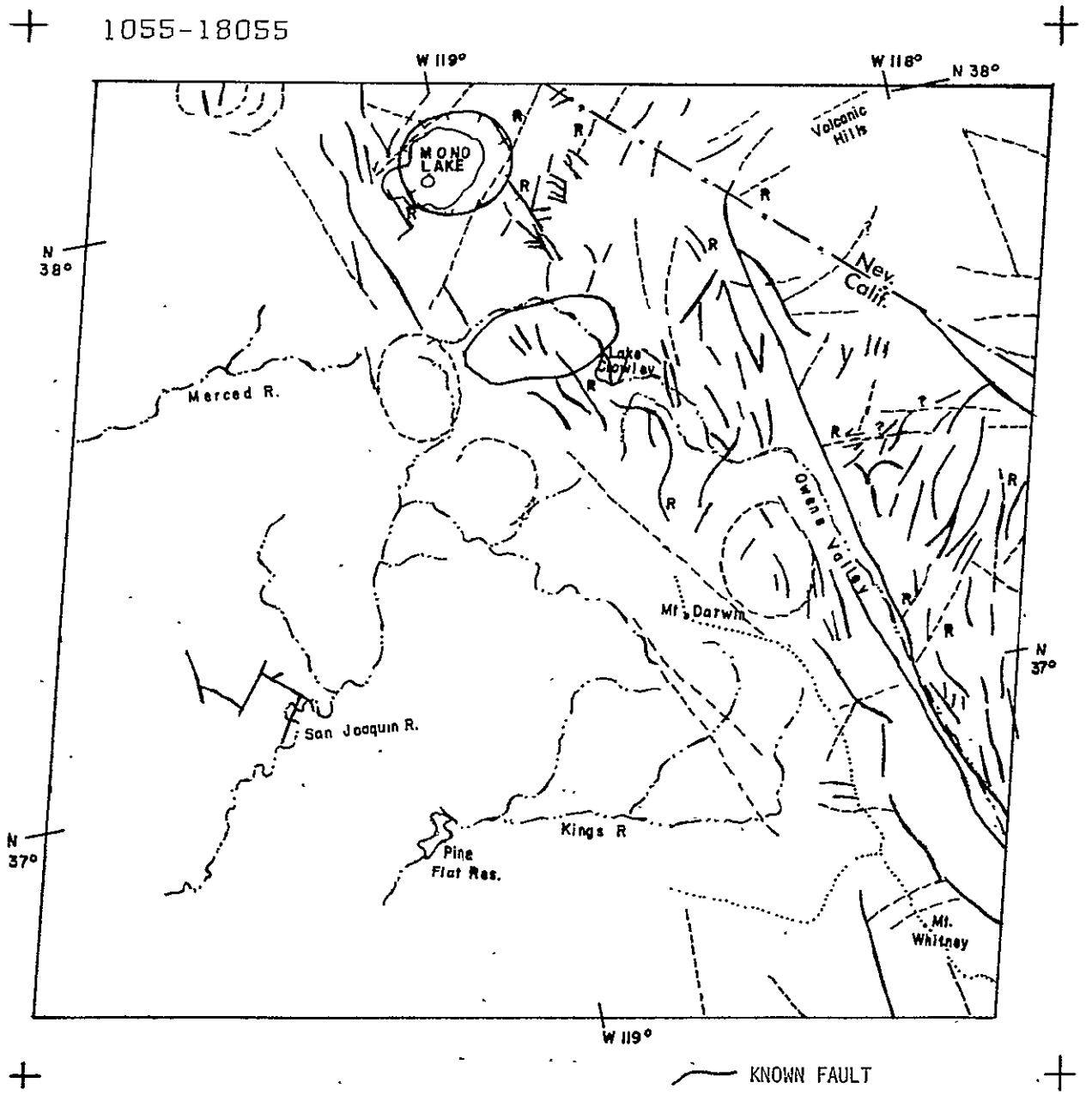

FIGURE 22a FAULT STRUCTURES ON PHOTO MSS 1055-18055

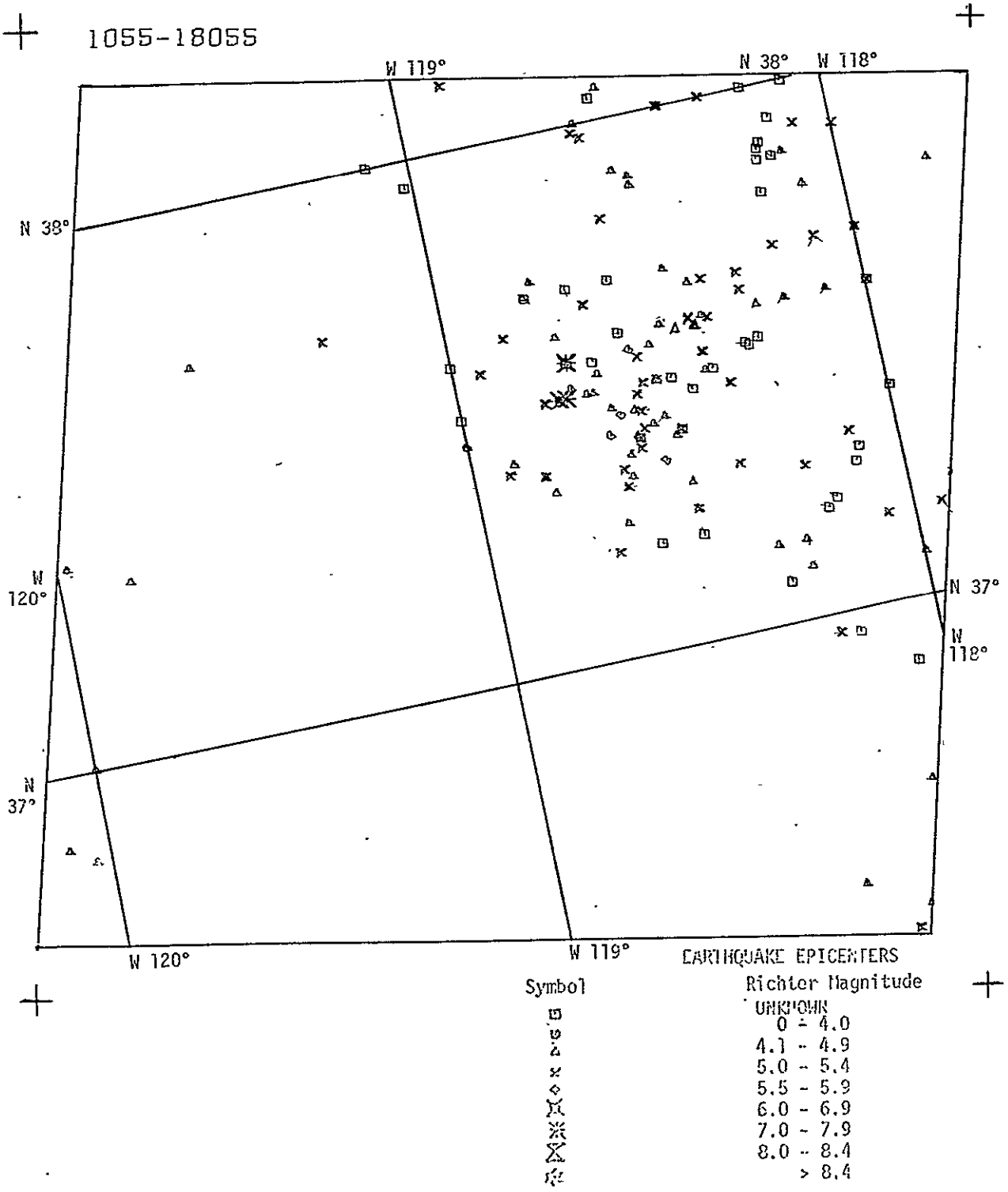

FIGURE 22b EARTHQUAKE EPICENTERS PLOTTED ON PHOTOGRAPH MSS 1055-18055

LINEARS ALONG WALKER LANE FAULT ZONE, WESTERN NEVADA
OBSERVED IN ERTS-1 MSS-1055-18053

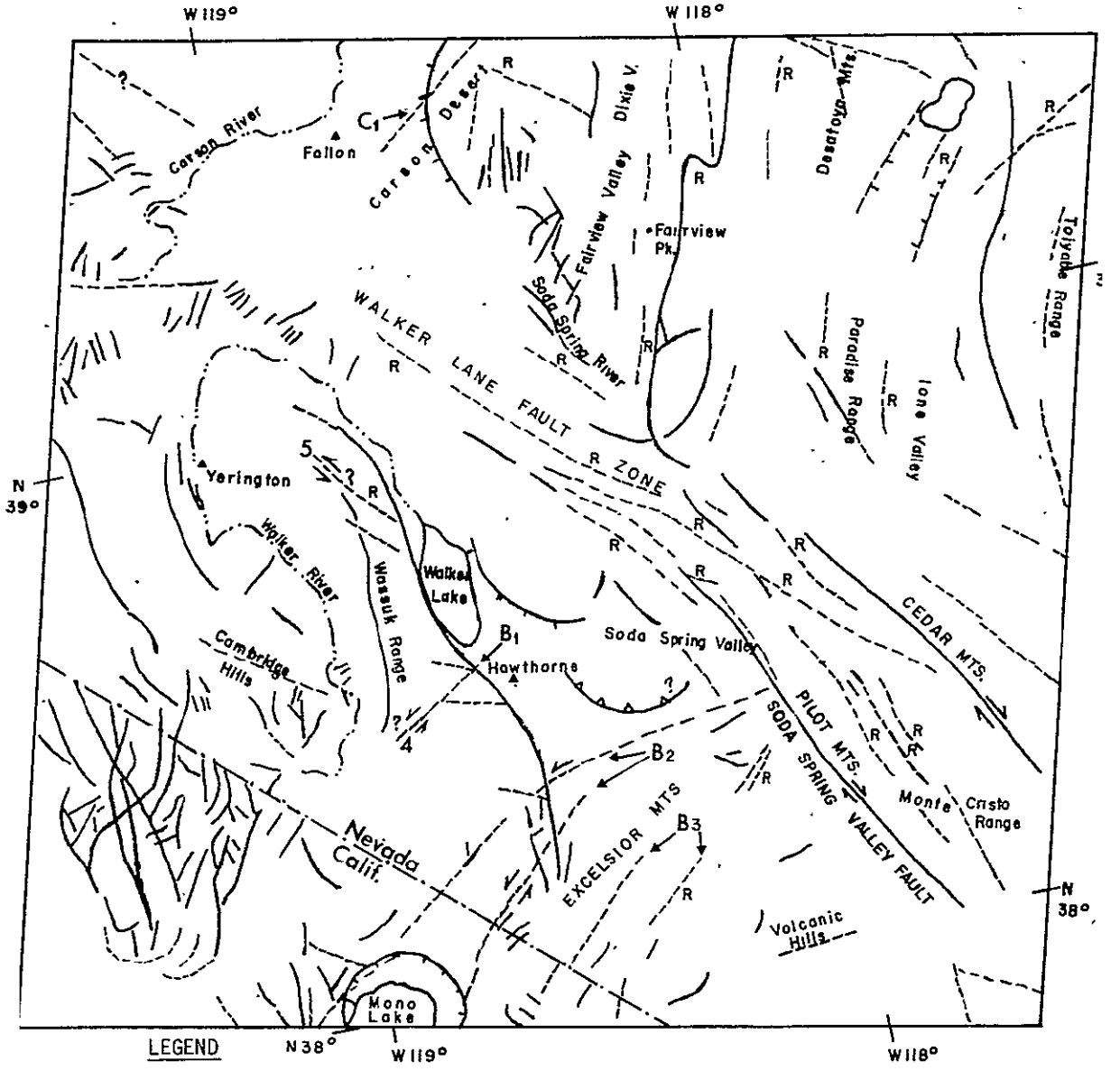

FIGURE 23a

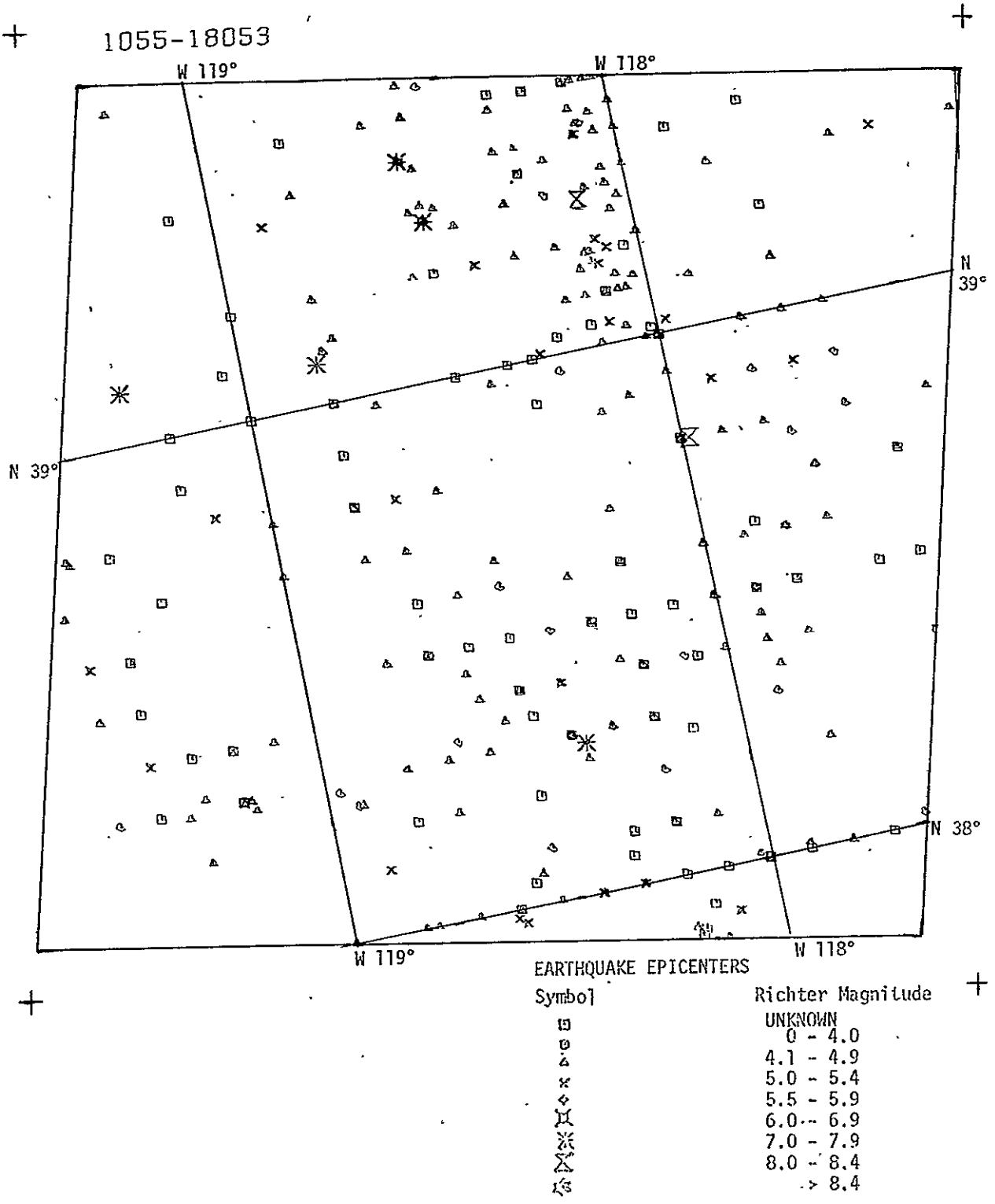

FIGURE 23b EARTHQUAKE EPICENTERS PLOTTED ON PHOTOGRAPH MSS 1055-18053

Known faults and the faults or lineaments inferred from ERTS imagery are shown in Figure 22a.

Four main fault systems can be recognized in this scene (Figure 22a):

1) North-northwest trending faults are represented by the Owens Valley fault. Sharp northwest-southeast physiographic lineaments can be seen within the Sierra Nevada block west of the crestline. They appear to run parallel to the Furnace Creek fault.

2) The northeast-southwest faults include several showing evidence of Holocene breakage located east of Mono Lake.

3) Some of the east-west faults, such as those located east of the Owens Valley, suggest fairly recent left-lateral offsets. However, there is relatively very little seismic activity which could be related directly to these faults.

4) Several circular features are observed east of the headwaters of the Merced River and the San Joaquin River, east of Mount Darwin, and west of Mono Lake.

Historic earthquake epicenters for Figure 22a are shown in Figure 22b.

Seismic activity is concentrated on the eastern side of the Sierras with an almost complete void of earthquake activity on the western side. The heaviest concentration of earthquakes is in the area between Lake Crowley, the Owens Valley, and the California-Nevada border. Here the cluster shows a strong northeast trend.

Mono-Walker Lakes, Carson River, Nevada

MSS 1055-18053; overlays: Figures 23a and 23b

This scene is particularly important because it shows one of the most seismically active areas in the western United States and includes a large part of the Walker Lane, "a zone separating ranges where trend is mostly northward, northeast of the fault from ranges where dominant trend is northwestward, southwest of the fault" (Hamilton and Myers, 1966, p. 531). According to Gianella and Callaghan, 1934, numerous small rifts and fissures formed during a 1932 earthquake show an echelon pattern of right-lateral displacement.

Several pre-Tertiary structures and statigraphic units have been offset about 20 km right-laterally within the zone (Nielsen, 1965). The

Cedar Mountain fault, the Soda Spring Valley fault and other major known faults shown in Figure 23a are taken from King, 1969.

ERTS-1 imagery shows the Walker Lane zone as a definite major fault zone characterized by well-recognized fault traces, many of which appear to be quite young as evidenced by lineaments in the alluvium and stream interruptions and deflections. Examples of fault traces suspected of recent breakage are indicated by the symbol R in Figure 23a.

Recent breakage occurs along at least three fault systems: Northwest-southeast parallel to the Walker Lane shear, north-south to NNE-SSW parallel to the Basin Range Nevada trend, and NE-SW. The latter system particularly characterizes the Tertiary volcanic area north and east of Mono Lake.

The area lies within the Ventura-Winnemucca seismic belt of Ryall, Slemmons and Gedney, 1966, and was the site of several major earthquakes of magnitude 6.0 and above, Figure 23b.

Correlation of Figures 23a and 23b suggest that while several major shocks occurred on or near the Walker Lane fault zone, the general pattern of the seismicity appears to be more related to the meriodional trend of Basin and Range faults, such as the sharp north-south faults observed in the Fairview-Dixie Valley area.

These lines of evidence suggest that at present Basin and Range tensional tectonism is most active here.

Evidence of pervasive recent faulting along both north-south tensional lines and a northwest-southeast shear line strongly suggest that the two tectonic elements are contemporaneously active and are genetically related. A tectonic model relating the fault and seismicity patterns is illustrated in Figures 29 and 30.

The ENE trend of the Excelsior Mountains is anomalous to the general NNW or NW trend of other ranges in that area and projects perpendicular to the Pilot and Cedar Mountains. This unusual trend was pointed out by Gilbert *et al.* (1968) who recognized that the fault pattern forms a structural knee in the area between the White Mountains and Mono Lake. In their study of microseismicity of the Nevada seismic zone, Gumper and Scholz (1971, p. 1421) found a similar bend as the seismic zone is displaced eastward from Owens Valley to Cedar Valley. Microearthquakes tend to cluster north of the Excelsior Mountains.

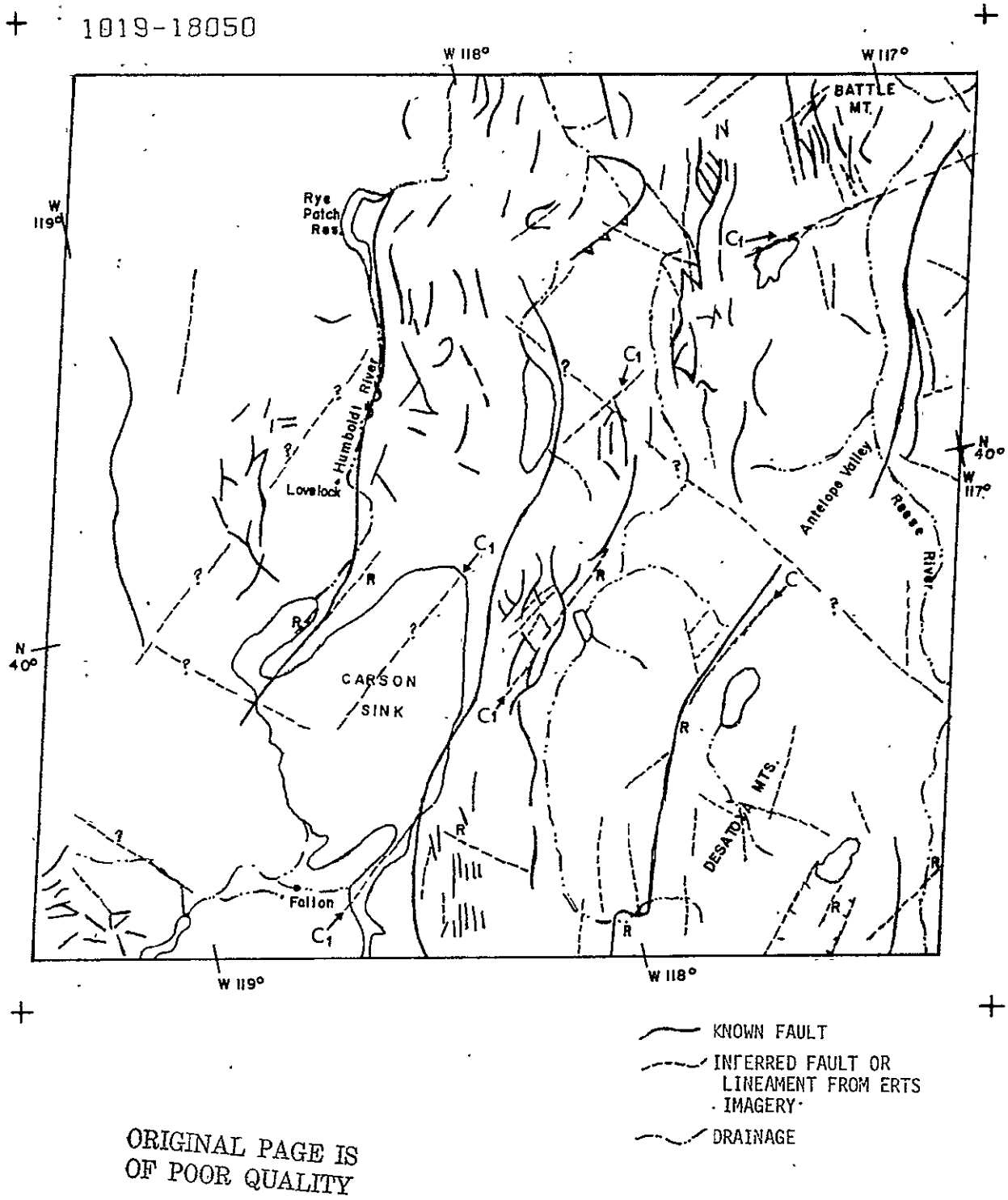

ORIGINAL PAGE IS
OF POOR QUALITY

FIGURE 24a FAULT STRUCTURES ON PHOTO MSS 1019-18050

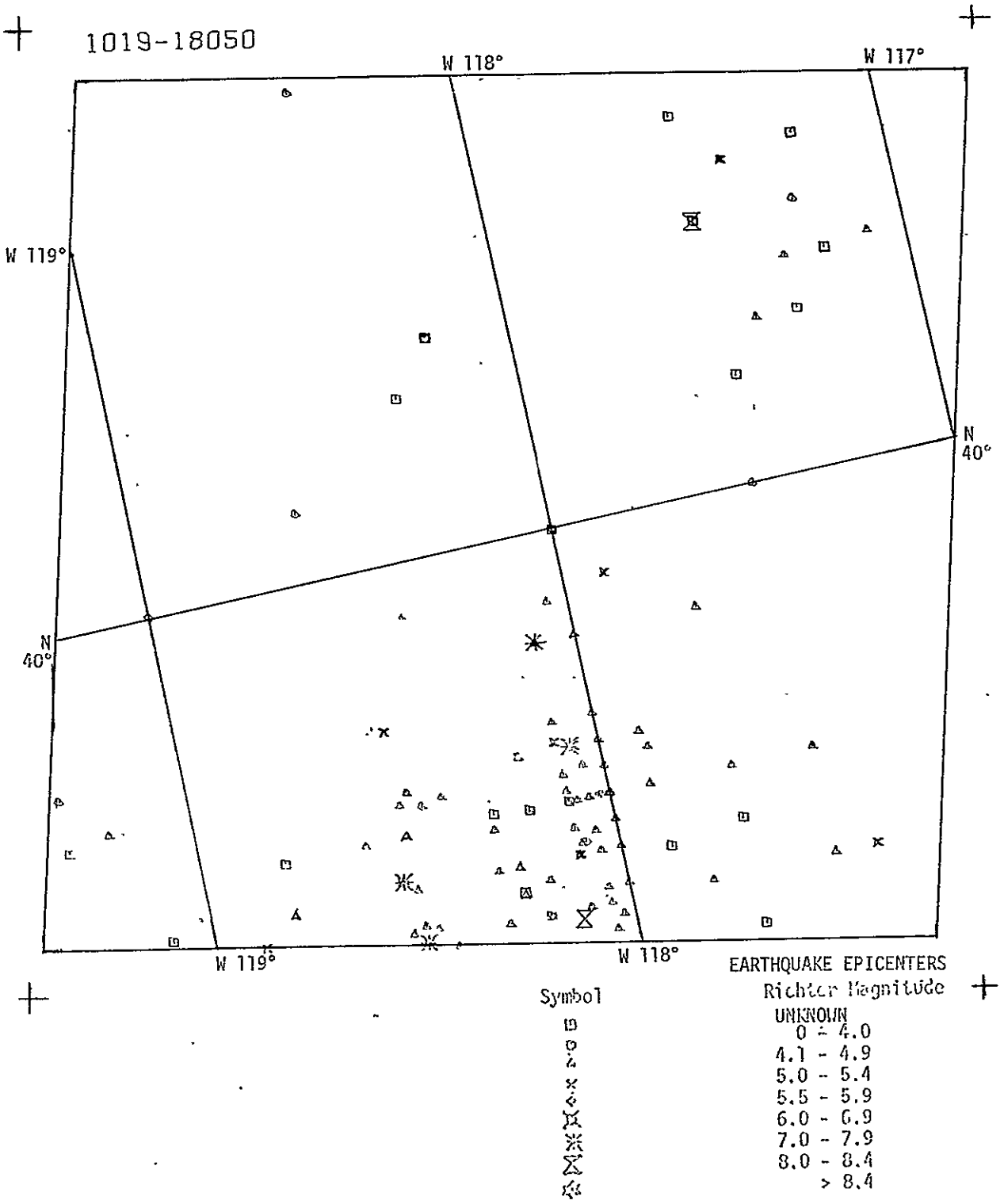

FIGURE 24b Earthquake Epicenters Plotted on Photograph MSS 1019-18050

When they examined the microearthquakes between Mono Lake and Pilot Mountains in detail, their fault plane solutions indicate predominantly "strike-slip" faulting with the two nodal planes striking N 11° E and N 86° E.

Considering the work of Gilbert *et al.* (1968) and the N 65° E trending scarp forward after the 1934 Excelsior Mountain earthquake (Callaghan and Gianella, 1935), they assumed the N 86° E nodal plane to be the fault plane and their fault plane solution suggested left-lateral faulting consistent with observations by Gilbert *et al.* (1968) in the area east of Mono Lake.

The ENE faults observed in ERTS imagery range from N 60° E and N 70° E consistent with field observations of Gilbert *et al.* (1968) and Callaghan and Gianella (1935).

Carson Sink, Nevada

Reference: MSS 1019-18050; overlays: Figures 24a and 24b

Figure 24a shows a plot of known faults (Webb & Wilson, 1962 and King, 1969) and some lineaments and faults inferred from the ERTS-1 image. The quality of the available images in this particular area did not allow more detailed analysis. However, the northeast trending lines marked C_1 (Figure 24a) seem to belong to an important fault system extending from the vicinity of Fallon to Carlin, Nevada. This system is discussed later in the text in the section on the northeast-southwest lineaments.

The area shows the continuation of the Ventura-Winnemucca seismic belt.

Figure 24b is a plot of earthquake epicenters.

Figure 27 also shows the distribution of Quaternary volcanic rocks which seem to generally follow the California-Nevada seismic zone.

Central Nevada

Reference: MSS-1054-17594; overlays: Figures 25a and 25b

The scene shows three known tectonic elements:

1) North-northeast trending Basins and Ranges and the large normal faults mainly responsible for the present physiography.

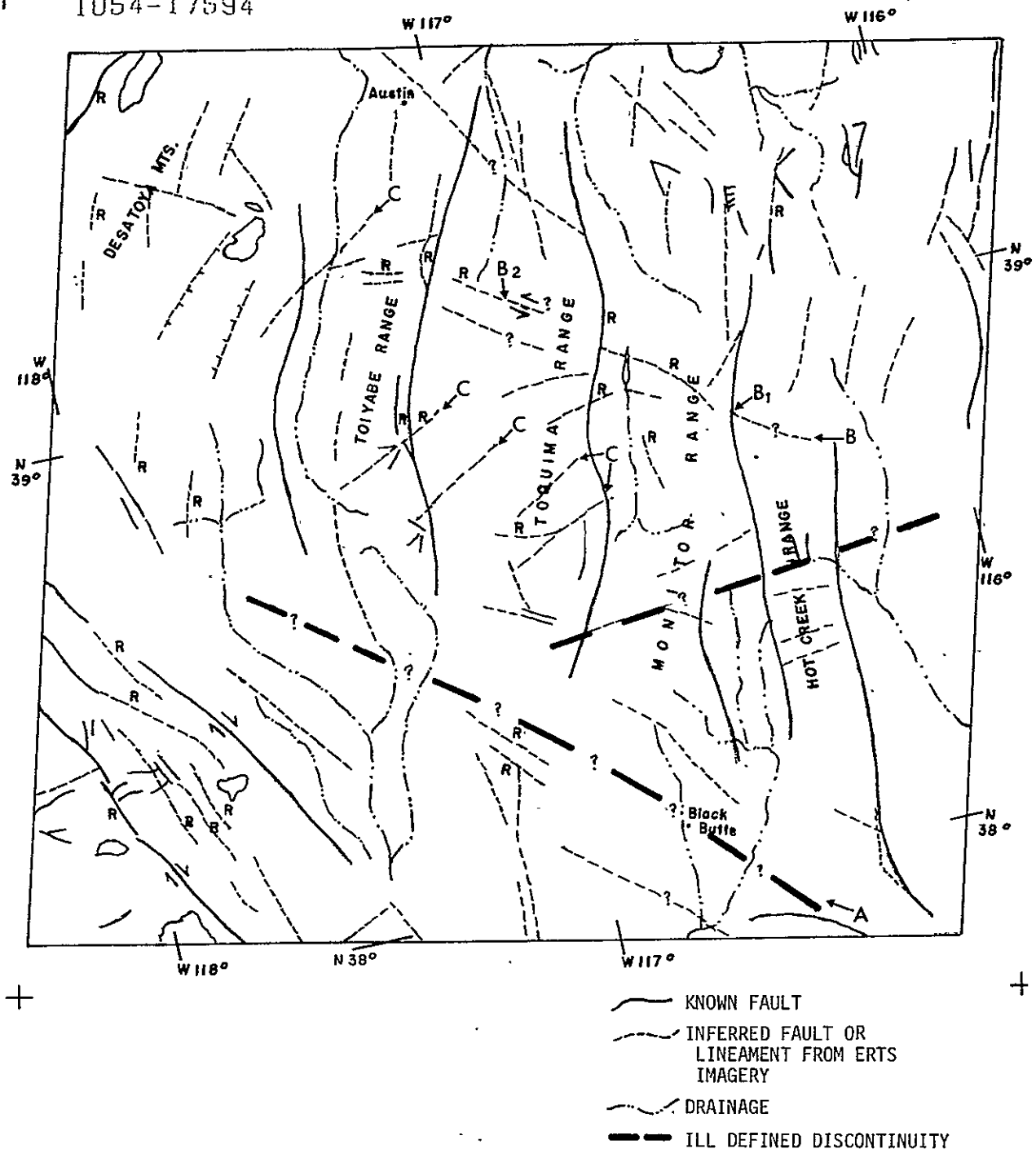

FIGURE 25a FAULT STRUCTURES ON PHOTO MSS 1054-17594

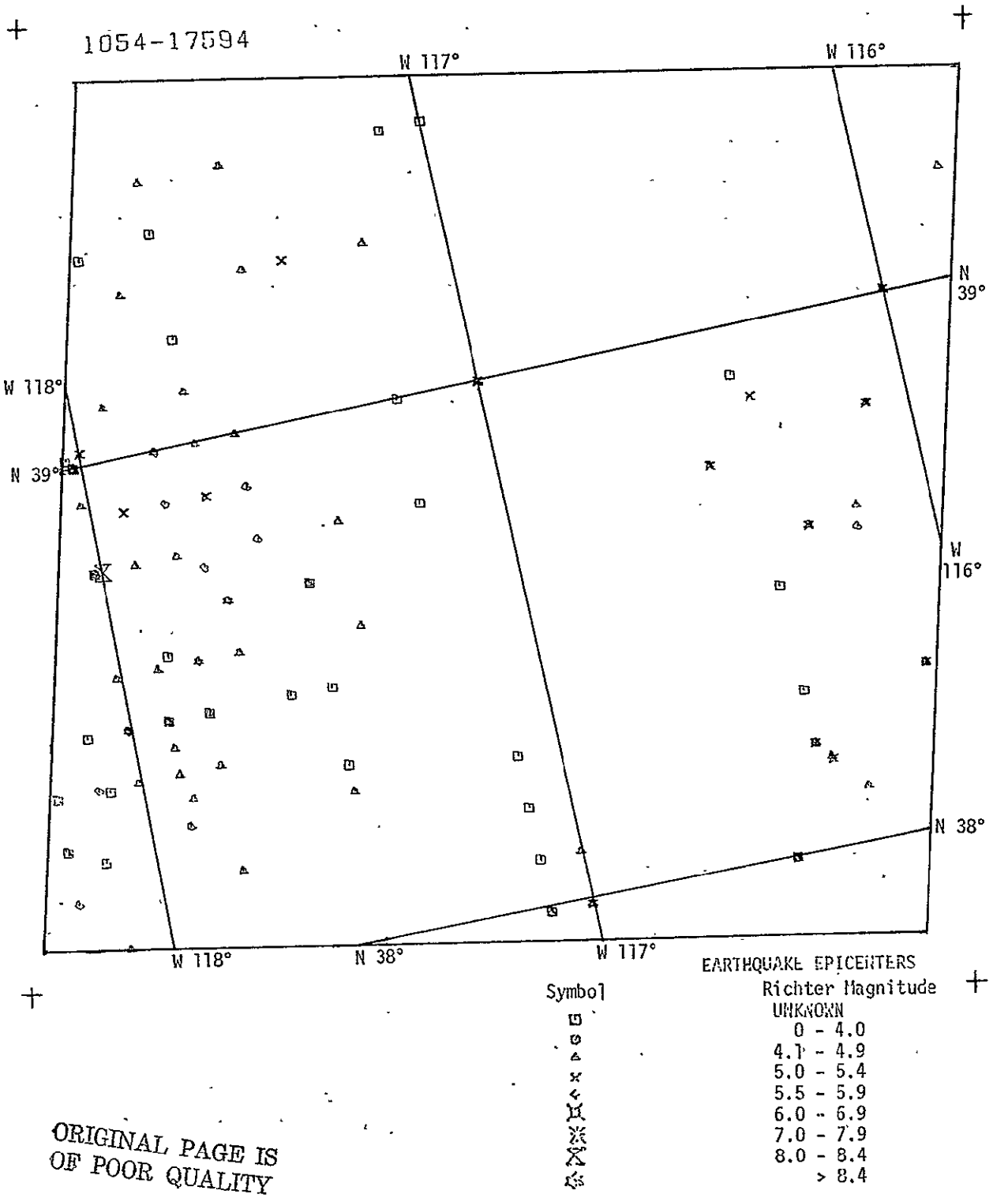

FIGURE 25b Earthquake Epicenters Plotted on Photograph MSS 1054-17594

2) The scene lies within the Antler Orogenic Belt, a major Paleozoic uplift separating a miogeosyncline on the east and an eugeosyncline on the west.

3) The continuity of the north-south trending structures is interrupted by the Walker Lane fault zone.

Additional observations derived from the ERTS scene are:

a) An ill-defined structural discontinuity (arrow A, Figure 25a) running north-west somewhat parallel to the Walker Lane fault zone. The nature of this discontinuity is not known but may be related or part of the Walker Lane fault system.

b) Faults showing evidence of recent breakage cut the Toiyabe, Toquima, Monitor and Hot Creek Ranges and intervening valleys. These young faults trend NNE-SSW, NE-SW and northwest-southeast.

c) The ERTS image shows a probably very young fault zone cutting across several ranges and valleys almost at right angle to the Basin and Range trend. An almost continuous zone of sharp lineaments extends from across Hot Creek Range on the southeast to the Toiyabe Range and probably extends farther northwest towards Desatoya Mountains (B, Figure 25a).

The sharpness and linearity of the fault strands particularly evident across the alluvium of the basins suggest a very young age. Minor lateral offsets in some range fronts across the fault strands, e.g., at B1 and B2, suggest an incipient left-lateral fault zone.

d) Northeast trending faults (C, Figure 25a) of the Carlin-Fallon fault system are discussed later in the text.

e) Seismic activity (Figure 25b) is relatively mild east of the Toiyabe Range but the seismicity pattern maintains a preferred north-south to NNE-SSW trend.

West of the Toiyabe Range of approximately longitude 117° 30' seismicity is considerably higher.

None of the individual major faults or observed lineaments in particular appear to have a clear relationship to the distribution of earthquakes.

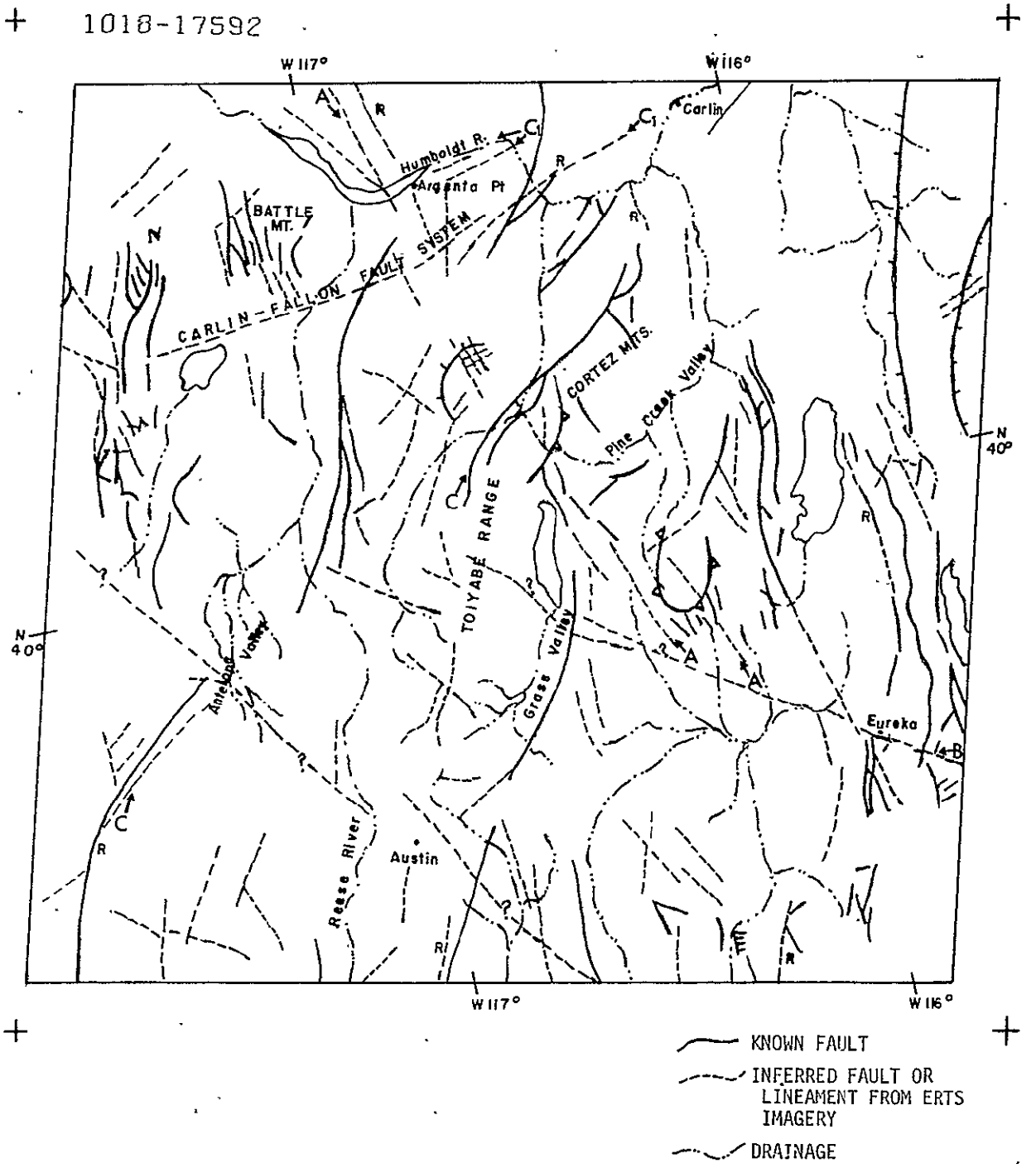

FIGURE 26a FAULT STRUCTURES ON PHOTO MSS 1018-17592 .

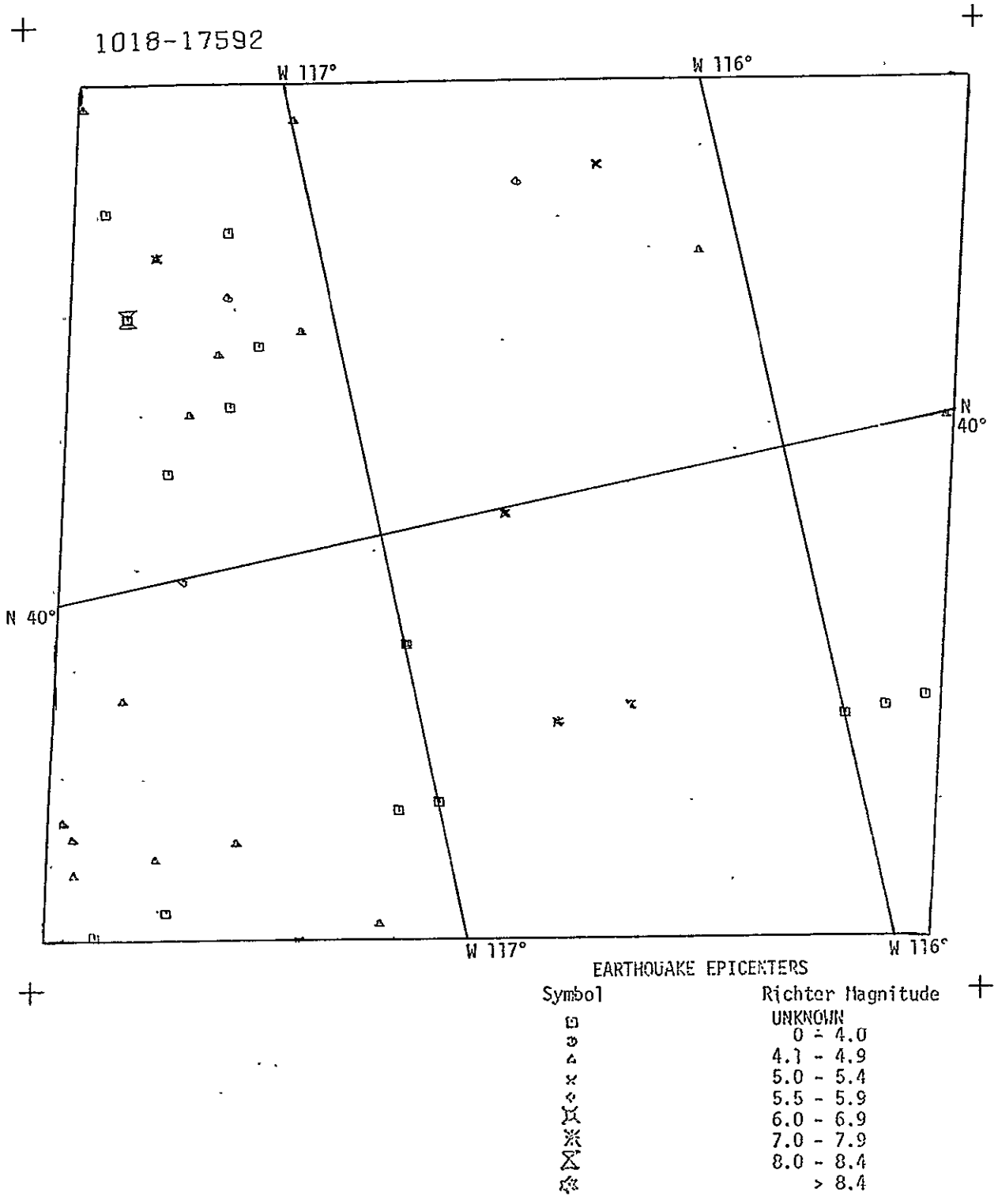

FIGURE 26b. Earthquake Epicenters Plotted on Photograph MSS 1018-17592

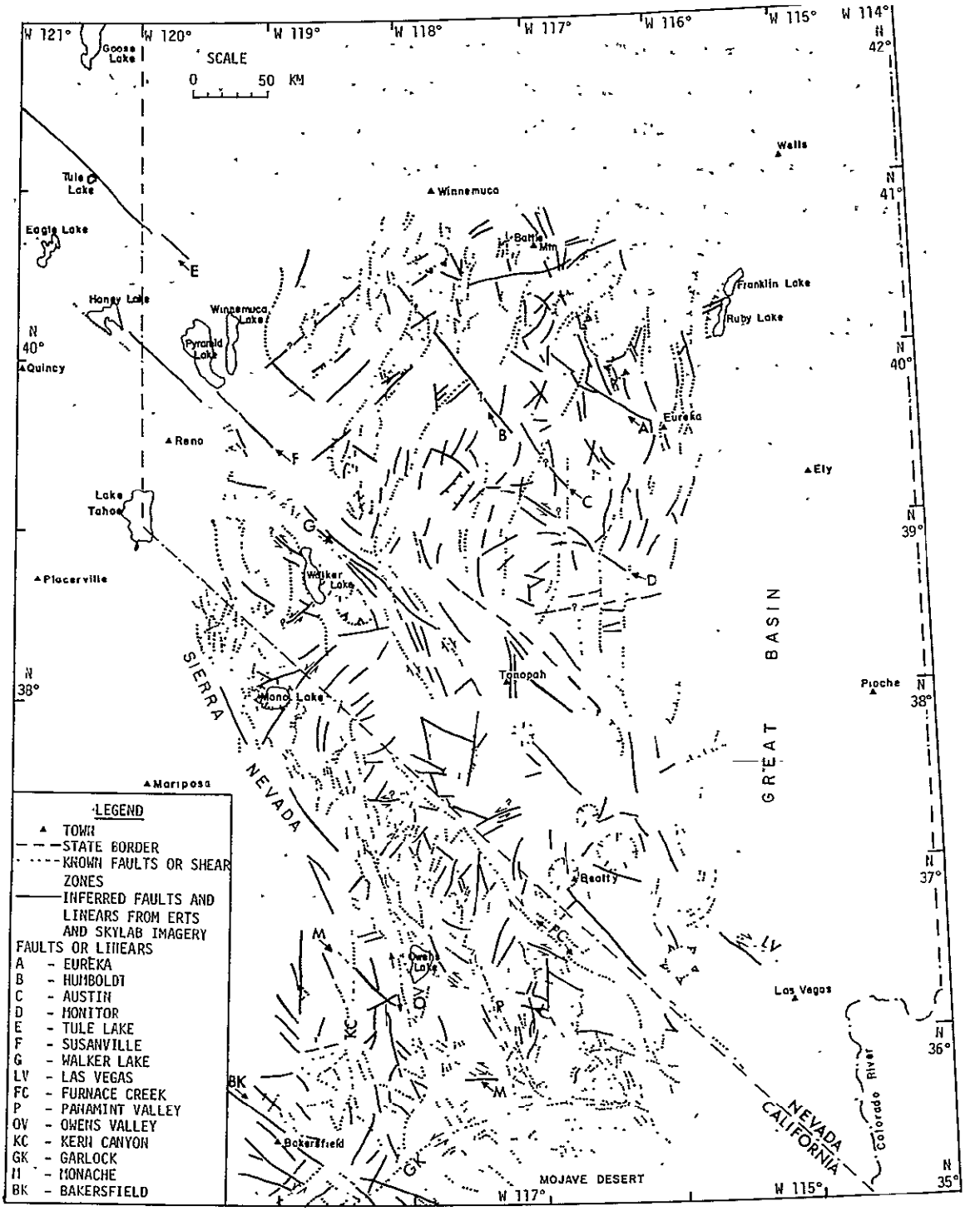

FIGURE 27 FAULTS AND LINEARS IN WESTERN GREAT BASIN INFERRED FROM ERTS AND SKYLAB IMAGERY

East-Central Nevada

Reference: MSS 1018-17592 (Color Composite); overlays: Figures 26a and 26b

The scene shows part of the Humboldt River near Carlin and Battle Mountain in the north, Eureka Mining district, and Austin, Nevada. Most of the scene lies within the Antler Orogenic Belt.

One major feature recognized in the ERTS image is a prominent en echelon fault zone trending north-northwest from the vicinity of Eureka and crosses the Humboldt River near Argenta point without any visible effect on the river valley. Strands of the fault zone cut the Quaternary volcanics north of the river (arrows A, Figure 26a).

The second fault structure is more subtle and extends from near Eureka, Nevada west-northwestward and across Grass Valley and the north end of the Toiyabe Range. Although this structure practically has little or no physiographic expression, lineaments and tonal and color differences in the alluvium are notable. Where it cuts the ranges, structural discontinuities are often observed. Near Eureka the lineament corresponds to the well known Ruby Hill normal fault which displaces the Eureka mineralized zone and has in fact delayed mining development for many years (Nolan and Hunt, 1968).

From the ERTS-1 symposium abstracts Rowan and Wetlaufer (1973, p. 46) mentioned that they recognized northeast and northwest trending lineaments in northeast Nevada. We are not certain whether the features referred to here are the same or are related to Rowan and Wetlaufer's lineaments.

What we wish to emphasize here is that the seismicity in this region is relatively mild except near Battle Mountain where a major earthquake of magnitude above 6.0 shows in Figure 26b.

This area however represents the northernmost limit of the California-Nevada seismic belt.

TECTONIC ANALYSIS

Figure 27 is a preliminary map showing the fault pattern in part of the Basin and Range province east of the Sierra Nevada. The map which covers southeastern California and western Nevada contains a combination of published data* and inferred lineaments and faults derived from ERTS-1

*References to fault maps used include Webb and Wilson, 1962; King, 1969; Matthews and Burnett, 1963; and Hill, Lao, Moore, and Wolfe, 1964; and others.

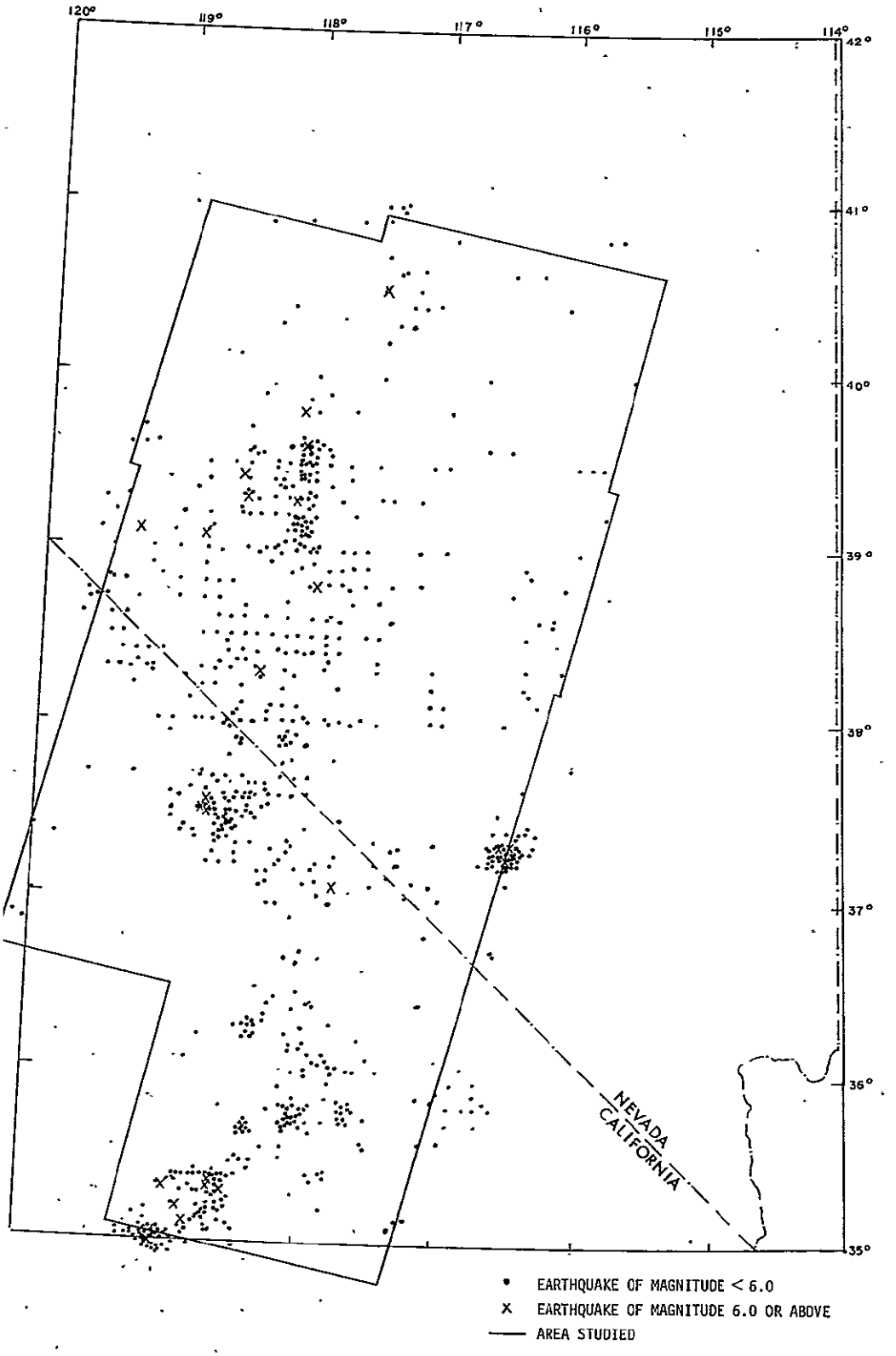

FIGURE 28 SEISMICITY MAP OF AREA STUDIED

imagery. The latter class of data is by its very nature tentative until verified by field methods. During the course of this study, it was noted that areas covered by Quaternary and late Tertiary volcanic rocks coincide generally with Quaternary faulting including many suspected recent fault breaks, as well as zones of historic seismic activity. In order to avoid crowding we have omitted from Figure 27 known exposures of the younger volcanics.

Figure 28 shows the epicenters of historic earthquakes for the same area plotted at the same scale as Figure 27. Here, however, we have shown only two classes of earthquakes: those under magnitude 6 are represented by dots and the major shocks above 6.0 by the symbol X.

The fault pattern has three essential elements:

Major Northwest-Trending Shear Zones

Previously known shear zones of this class are prominent in ERTS imagery. These are: Las Vegas shear (right-lateral), Furnace Creek (right lateral), Death Valley (right-lateral), and Walker Lane (right-lateral). In addition, analysis of ERTS-imagery suggests the presence of other incipient shear zones in central Nevada (e.g., A B C & D, Figure 27) of the same trend. The sense of lateral motion indicated by the symbols are tentative and need field confirmation.

It should be noted, however, that while the major known shear zones are right-lateral, there are several suggesting an opposite or left-lateral sense of motion. Some of these have been reported in the literature; Mayo (1947, Figure 20a) for example, identified the Darwin fault (#1) east of Owens Lake as left-lateral. Examples of known and suspected left-lateral shear faults of northwest trend are: #1 Figure 20a, #5 Figure 23a
#3 Figure 20a, Arrow B, Figure 26a.

The presence of left-lateral shear faults in the Basin and Range Province, if indeed confirmed, would be highly significant because it has been often stated in the literature that a general right-lateral shear exists in the western United States (e.g., Hamilton, 1966). While there is abundant evidence for regmatic right-lateral shear, the existence of

FRAGMENTATION MODEL OF BASIN AND RANGE BLOCKS
SHEAR FAULTS DEVELOP ACROSS FAULT BLOCKS PULLED
APART ALONG RIFT BASINS

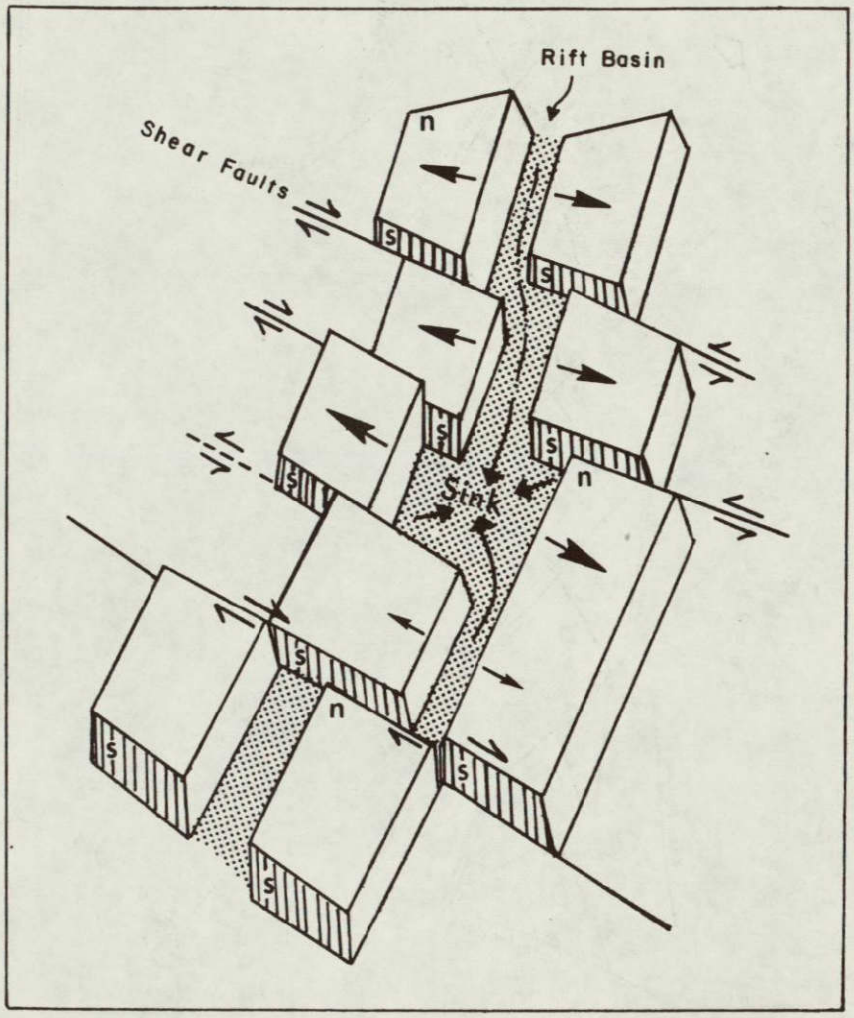

FIGURE 29

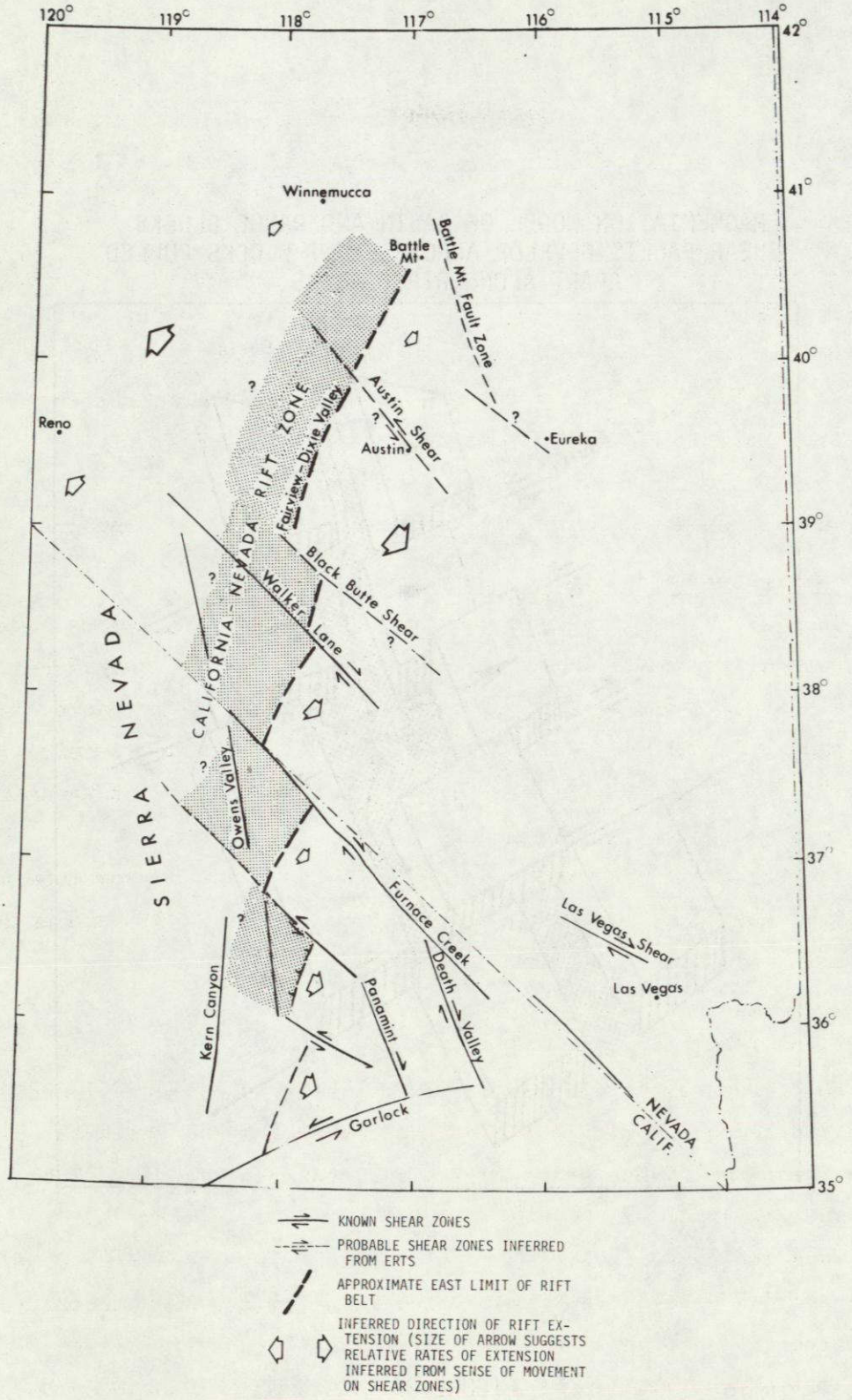

FIGURE 30 INTERPRETIVE DIAGRAM SHOWING A RIFT AND TRANSFORM FAULT MODEL FOR THE CALIFORNIA-NEVADA RIFT BELT

left-handed motion on certain fault zones has to be accomodated within a general tectonic model for the development of Basin and Range structures.

Figure 29 illustrates that both right and left-handed shear can develop when various segments of a rift split apart at unequal rates.

It became clear from our analysis of ERTS imagery that the shear zones in the Basin and Range Province are not continuous but are arranged en echelon. On the northwest they start in the volcanic rift area directly east of the Sierra Nevada block and appear to die out or change into flextures associated with thrusts toward the southeast.

Observation from ERTS imagery indicate that the northwest-trending shear zones have been active in the Holocene.

North-Northeast Rift Faults

The north trending Basin and Range structures in Nevada have long been recognized as features of regional tension. The interfaces between mountain blocks and adjacent basins are often marked by normal faults. ERTS imagery contributed abundant evidence of Holocene (recent) faulting along Basin and Range faults within the California-Nevada seismic belt (Figures 27 and 28).

The pattern of seismicity revealed from this investigation (Figure 28) agrees generally with earlier work by Ryal *et al.* (1966) and Gumper and Scholz (1971).

However, there are several observations of significant detail which merit attention:

While the California-Nevada seismic belt has a general northerly trend, we recognize within the belt where earthquake epicenter plots show higher density. These segments are also characterized by shocks of higher magnitude (>6).

When the seismic belt is examined from south to north, we discern a pattern of en echelon segments of denser seismicity and recent faulting which trending northeast and becoming offset across major shear zones. This pattern is illustrated in Figure 30.

When we consider the general fault pattern and particularly areas of Holocene faulting, together with the offset nature of highly seismic

segments and the distribution of Quaternary volcanics, we find that they fit a tectonic style reminescent of tension rifts and transform faults observed in areas of spreading centers on the ocean floors. The geological record indicates that the Sierra Nevada block was part of a huge Tertiary uplift which included a considerable part of Nevada. In late Tertiary time the eastern part of the uplift collapsed and produced the present Basin and Range physiography (Lindgren 1911; Christensen, 1966). When we consider the observations made in this investigation together with ideas advanced by Thompson (1960, 1964), Cook (1965), Hamilton and Myers (1965), and others, it seems certain that the California-Nevada seismic belt represents the site of an actively opening rift characterized by interrelated features of lateral extension, differential shear, volcanicity and seismic activity.

Minor Transverse Structures

The north-northeast trending Basin and Range blocks are cross-cut by second order faults belonging to two prevailing trends: northwest and northeast. These faults are limited in length cutting obliquely across an individual valley, some extend across one or both ranges bounding the valley. Some extend across several basins and ranges often terminating a range or otherwise coincide with oroflexes and bends. The shape of many valley floors and the location of sinks (lowest areas in valleys where drainage from all directions converge) appear to be controlled by these transverse structures. The physiographic pattern is consistent with a tectonic style for the development of Basin and Range structures illustrated in Figures 29 and 30.

Northeast-Southwest Lineaments

Significant northeast trending faults are observed in the Basin and Range province of Nevada. Examples can be seen in the Slate Ridge area (arrow B, Figure 21a). Other examples cut across the Monitor, Toquima, Toiyabe, and other ranges in Central Nevada (arrows C, Figure 25a).

Among the prominent northeast trending faults that are observed in Northeast Nevada [arrows C_2 and C_1, Figures 23a and 26a), a large northeast trending system is observed in the area between Carlin and Fallon (arrows

C_1, Figures 23a, 24a, and 26a). This zone extends from Carlin and Battle Mountain, Nevada, southwest towards the Carson Sink area (Figure 24a), and then heads in the direction of Fallon, Nevada (Figure 23a). The following physiographic features appear to be strongly influenced by the Carlin-Fallon Fault System: the east fork of the Humboldt River, the Humboldt River Valley between Elko and Carlin, Nevada, Boulder Valley, Cortez Mts., the north part of Dixie Valley, West Humboldt Range, and the Carson Sink. Near Fallon, Nevada (Figure 23a), the relationship between the Carlin-Fallon System and the northwest extension of the Walker Lane Fault Zone is uncertain. However, in Figure 23a we note that across the Walker Lane Fault Zone a prominent zone of northeast-southwest faulting passes between Walker Lake and Mono Lake. Faults of this zone cut across the Wassuk Range, which lies west of Walker Lake, Nevada (arrows B_1, B_2, and B_3, Figure 23a) and they appear to control the trend of the Excelsior Mts., northeast of Mono Lake, as well as, the down-faulted block containing Mono Lake (arrows B_2 and B_3, Figure 23a).

The widespread occurrence of this class of faults and their relatively young age, as inferred from their continuation across the alluvium of the valleys and sharpness of physiographic lineaments associated with them, suggest a regional rather than local character.

Viewed within the framework of the Basin and Range tectonics, of northwest extension of Nevada, the northeast trending faults would represent rift or tension zones characterized by vertical fault displacements.

This class of faults, however, has two puzzling characteristics: First, a left-lateral strike-slip component appears to be associated with many of these faults (arrow B, Figure 21a, and arrows B_1 and B_2, Figure 23a).

Second, their trend is oblique to the prevailing northerly grain of Basin and Range rift structures.

The full meaning of these puzzling characteristics is not yet fully clear and will be subject of further analysis.

PAGE INTENTIONALLY BLANK

AREA 3

BAJA CALIFORNIA, GULF OF CALIFORNIA, NORTHERN MEXICO, AND PARRAS AND TEXAS SHEAR ZONES

ERTS COVERAGE USED

Gulf of California

MSS 1070-17502	MSS 1029-17231	MSS 1045-17115
MSS 1052-17495	MSS 1028-17183	MSS 1062-17063
MSS 1069-17443	MSS 1068-17385	MSS 1079-17015
MSS 1068-17394	MSS 1067-17335	MSS 1079-17012
MSS 1068-17391	MSS 1067-17333	MSS 1078=16565
MSS 1067-17342	MSS 1066-17281	MSS 1078-16563
MSS 1049-17340	MSS 1029-17225	MSS 1078-16560
MSS 1030-17292	MSS 1028-17174	MSS 1078-16554
MSS 1048-17290	MSS 1028-17171	MSS 1077-16511
MSS 1030-17285	MSS 1027-17120	MSS 1080-17071
MSS 1066-17283	MSS 1068-17382	MSS 1032-17384
		MSS 1065-17222

Mexican Interior

MSS 1078-16542	MSS o038-16321	MSS o075-16380
MSS 1078-16533	MSS 1042-16541	MSS 1078-16540
MSS 1078-16551	MSS 1060-16550	MSS 1079-16592
MSS 1079-17003	MSS 1078-16545	MSS 1079-17001
MSS 1062-17045	MSS 1062-17051	MSS 1045-17110
MSS 1045-17104	MSS 1049-16364	MSS 1028-17162
MSS 1058-16433	MSS 1028-17160	MSS 1039-16370
MSS 1065-17213	MSS 1047-17220	MSS 1059-16492
MSS 1059-16483	MSS 1039-16373	MSS 1039-16375
MSS 1058-16431	MSS 1077-16490	

An index map of the study area is seen in Figure 31.

SIGNIFICANT RESULTS

1. Correlation Across the Gulf of California

MSS 1049-17340, MSS 1029-17225 and MSS 1066-17281

A strong geologic similarity between Isla Tiburon, Isla Angel de la Guarda in the Gulf of California and the San Carlos Range in mainland Mexico was observed.

The Tertiary volcanic rocks which cover those areas show a distinctive north trending grain or rill-like texture. This geomorphologic characteristic is probably due to intrinsic structural similarities and the volcanic rocks enhanced by similar conditions of erosion.

Along the length of Baja California and the eastern side of the Gulf of California, this particular rill texture appears to be unique to the

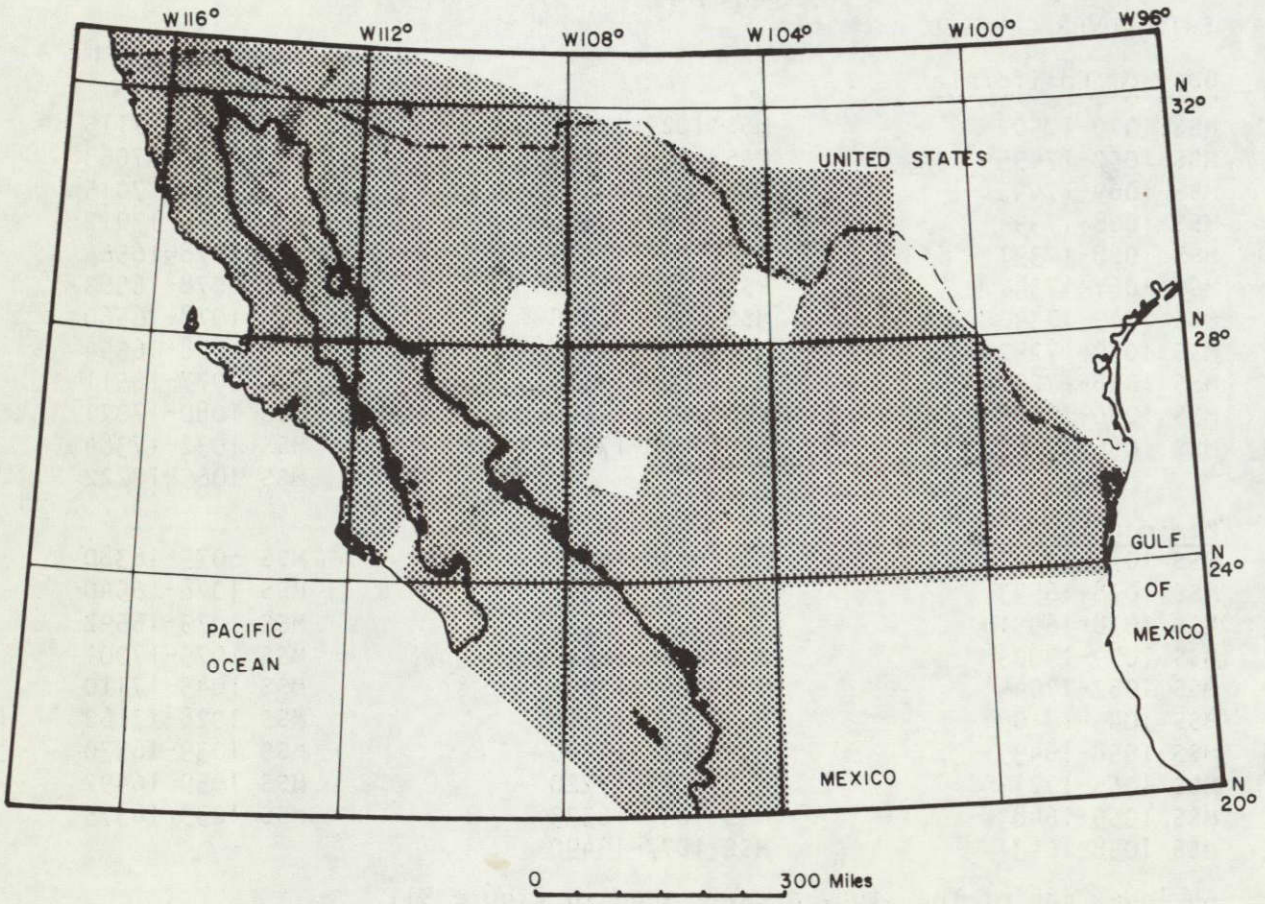

Area studied in the investigation.

FIGURE 31 INDEX MAP

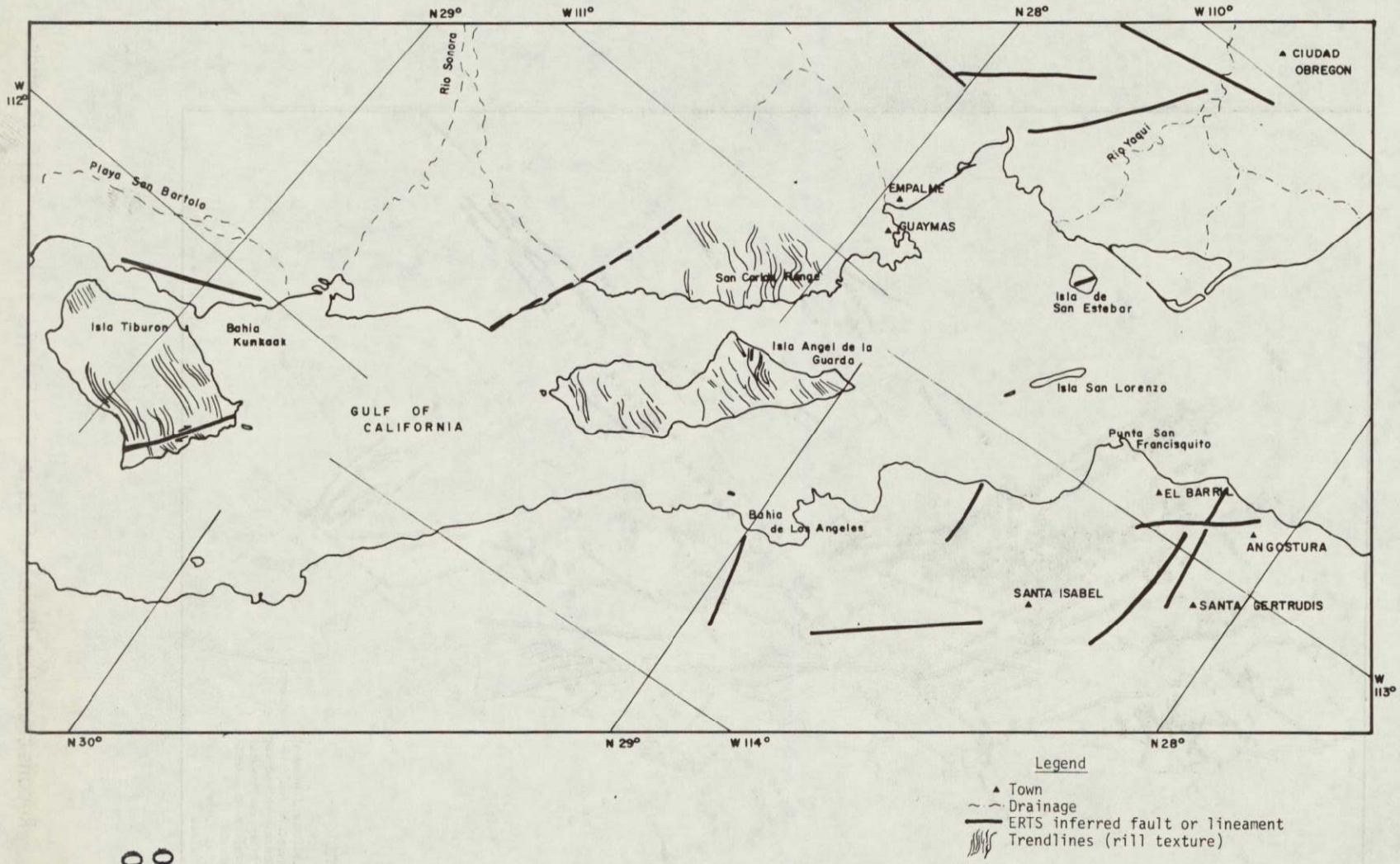

FIGURE 32 Reconstruction Model Showing Similarity of Rill Texture between Isla Angel de la Guarda and the San Carlos Range. (The offset of Baja California and Isla Angel de la Guarda is about 230 km SE of their present positions.)

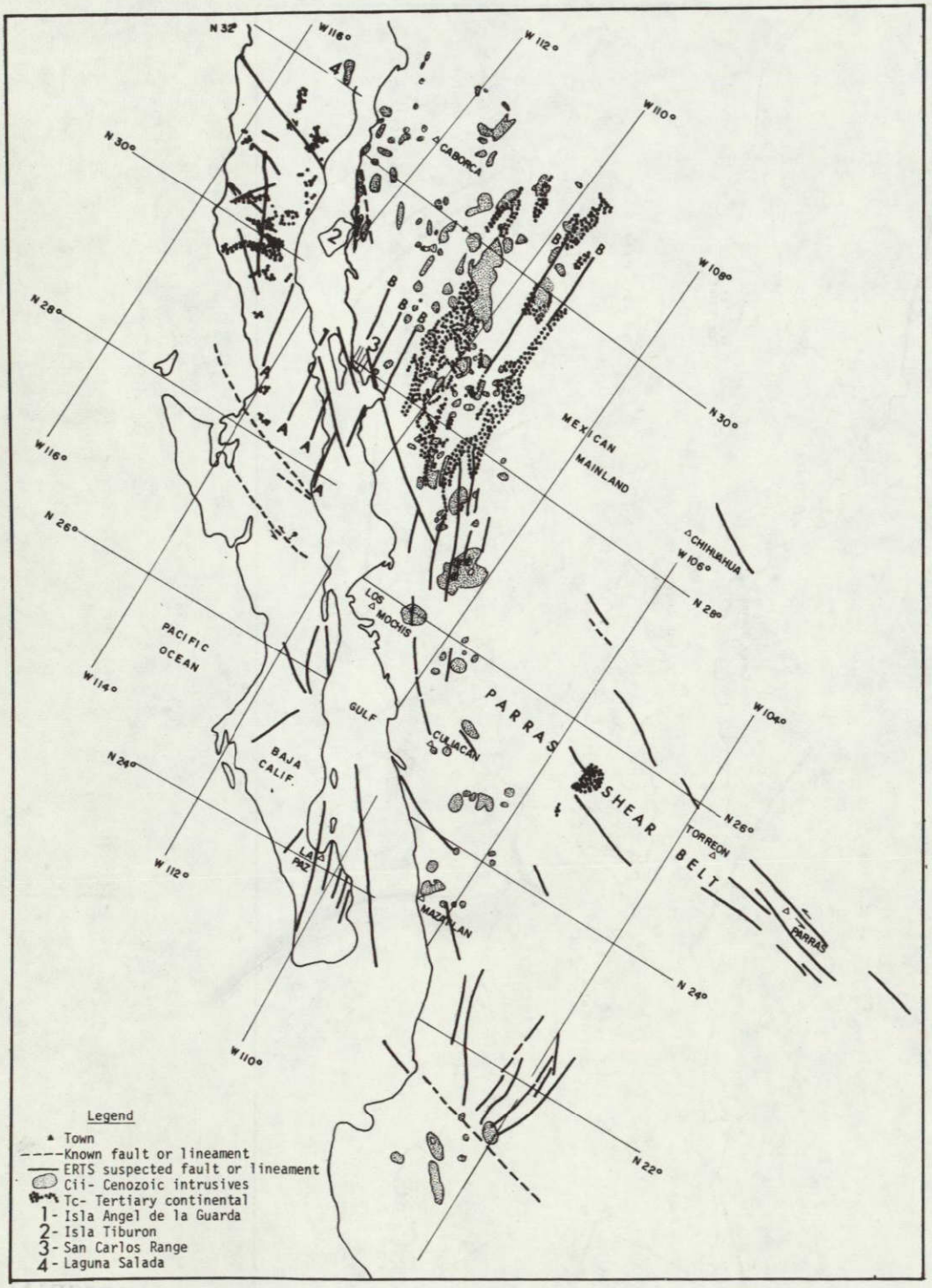

FIGURE 33 Reconstruction Model of Baja California and the Gulf Islands.

three areas (Fig. 32). The remarkable similarity of the terrain suggests that the three blocks were once adjacent. Isla Tiburon appears from ERTS imagery to be locked in its present position with the Mexican mainland. Isla Angel de la Guarda has most probably been displaced. The block now forming the island of Isla Angel de la Guarda within the Gulf was probably situated somewhere to the southeast as part of the Mexican mainland near latitude 28°N.

Assuming that Baja California has moved northwestward relative to the mainland the ERTS data were used to reconstruct a working model showing the initial position of the blocks prior to the displacement (Fig. 33).

Significantly, the reconstruction brings the prominent north-south trending fault belt of middle Baja California (A, Fig. 33) in continuity with an equally prominent fault belt in Sonora, Mexico (B, Figure 33).

We have also plotted in Figure 33 the distribution of the early Cenozoic intrusives and the Tertiary continental deposits from the Geological Map of Mexico (de Cserna, 1961). Reconstruction also brings t : the isolated mass of early Cenozoic intrusive rocks now on the eastern side of Laguna Salada (Baja California Block) in juxtaposition with the similar intrusives in Sonora. Tertiary continental sediments form a north-south trending belt in Sonora. Reconstruction brings this belt in a position of continuity with similar exposures in Isla Angel de la Guarda and within Baja California (Figure 33).

2. Identification and Verification of Major Faults in Baja California

Several major faults have been known in Baja California. Other faults and lineaments have been conjectured.

The occurrence and nature of transverse faults across Baja California, particularly any strike-slip breaks, are of critical importance in tectonic models. One model considers that in the process of separation and displacement Baja California may have undergone some telescoping. Depending upon the model and the sense of movement on transverse faults telescoping could have resulted in considerable stretching of the Peninsula or its shortening. Displacement of Baja California as one rigid block without significant telescoping has also been suggested. This underlies the importance of identifying major transverse faults and their relation to faults within the Gulf and in mainland Mexico.

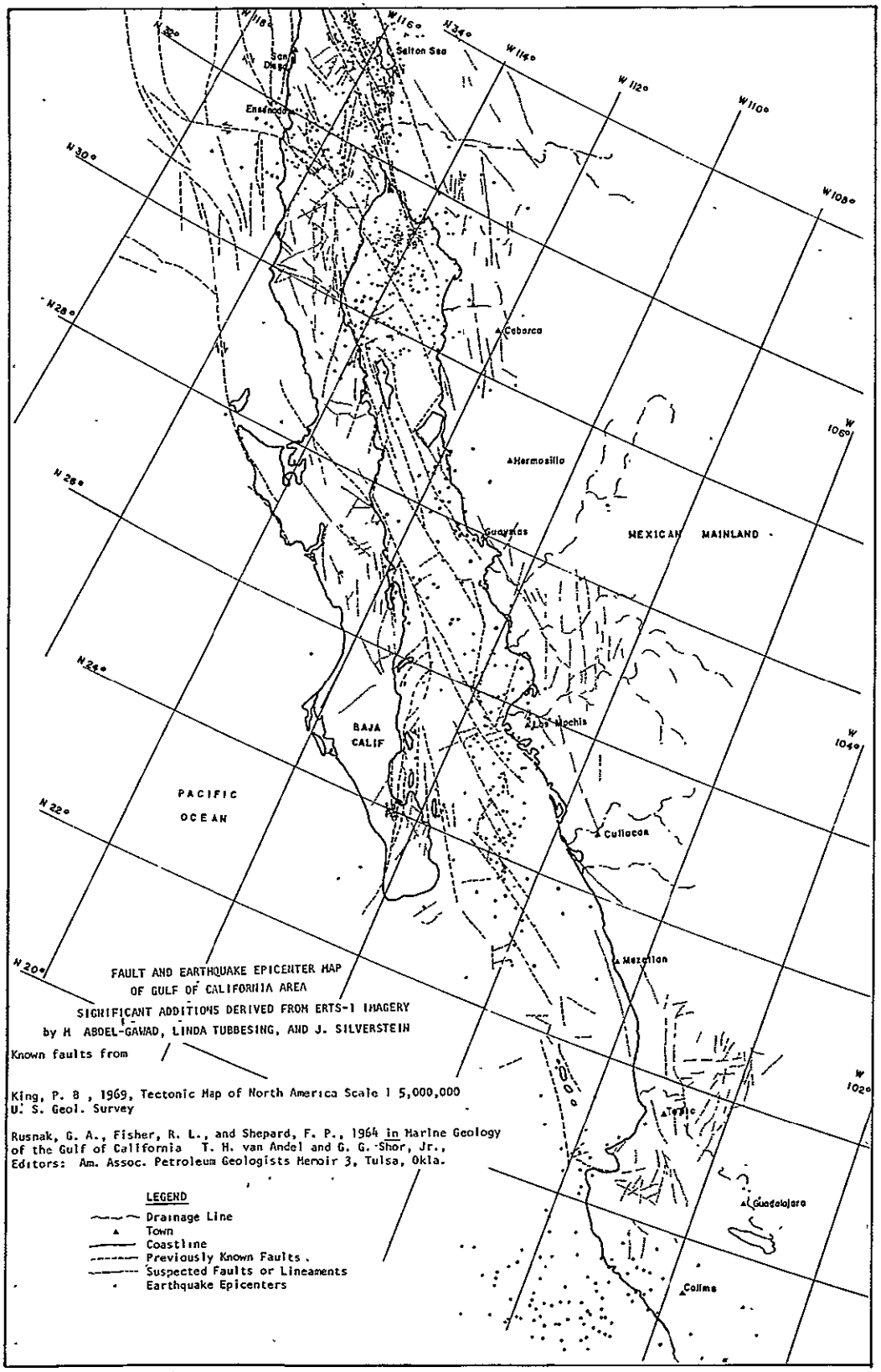

ORIGINAL PAGE IS
OF POOR QUALITY

FIGURE 34

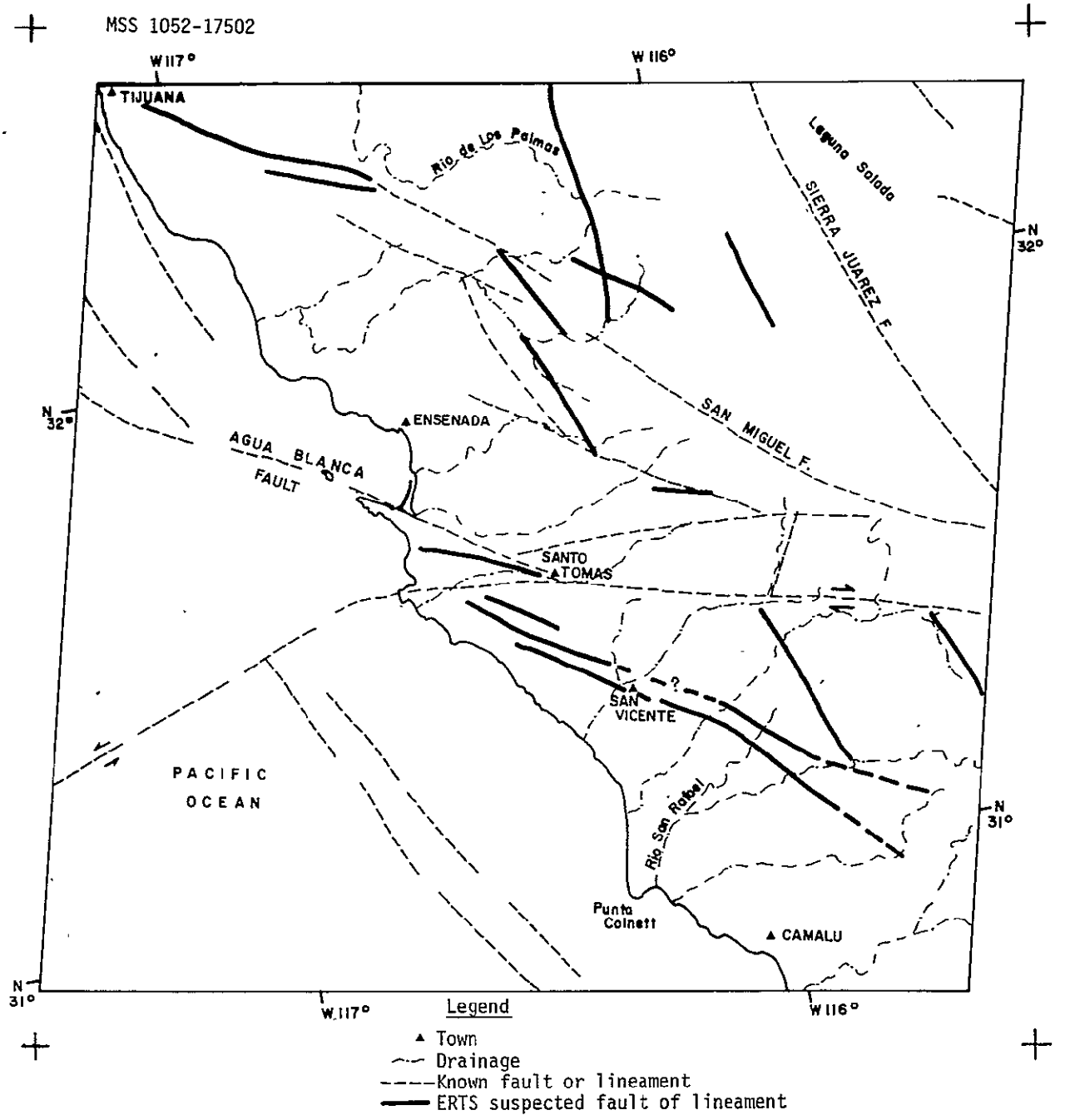

FIGURE 35 SIGNIFICANT FAULTS IN NORTHERN BAJA CALIFORNIA
MSS 1052-17502

In Figure 34 we plotted the major faults in Baja California differentiating the following classes:

- Major known faults or lineaments proposed or conjectured in the literature.
- Faults or lineaments inferred in our ERTS investigation.

A discussion of significant details follows.

NORTHERN BAJA CALIFORNIA

In the northern part of Baja California, which was not covered by ocean water since the Mesozoic, several transverse shear zones similar to Agua Blanca were identified in areas not covered by volcanic rock. Faults previously known or conjectured were verified or questioned.

MSS 1052-17502

This ERTS image covers an area from Tijuana, Mexico, south past Ensenada to Punta Colnett (Fig. 35). Several major transverse faults cutting across Baja California are evident. The Agua Blanca fault is clearly visible in the ERTS imagery as it boldly cuts through several mountain ranges. An ERTS inferred transverse fault is observed south of the Agua Blanca fault 20 to 30 km in a NW direction. This fault zone meets the Agua Blanca fault near Santo Tomas. A possible right-laterial movement is observed in this zone.

The Sierra Juarez fault zone is inferred by the structure of the mountains and basin area trending in a NNW direction.

The San Miguel fault, also recognizable in the ERTS photo, was mapped by Rusnak, Fisher, and Shepard, 1964. It extends northwestward into a fault zone recognized by King (1969). ERTS image 1052-17502 suggests that the fault zone extends to the Pacific, passing near Tijuana, Mexico. This Tijuana-San Miguel fault zone is a major one and is characterized by major earthquakes. In continuity and physiographic expression, this fault is not consistent. It is bold and clearly recognizable in places, but vague in others. Seismic activity (as seen in Figure 34) is mainly concentrated in the block north of the Agua Blanca fault. Although large earthquakes have occurred near large faults, mostly trending NW-SE, the earthquake pattern at large appears to trend NE-SW. Large shocks occur

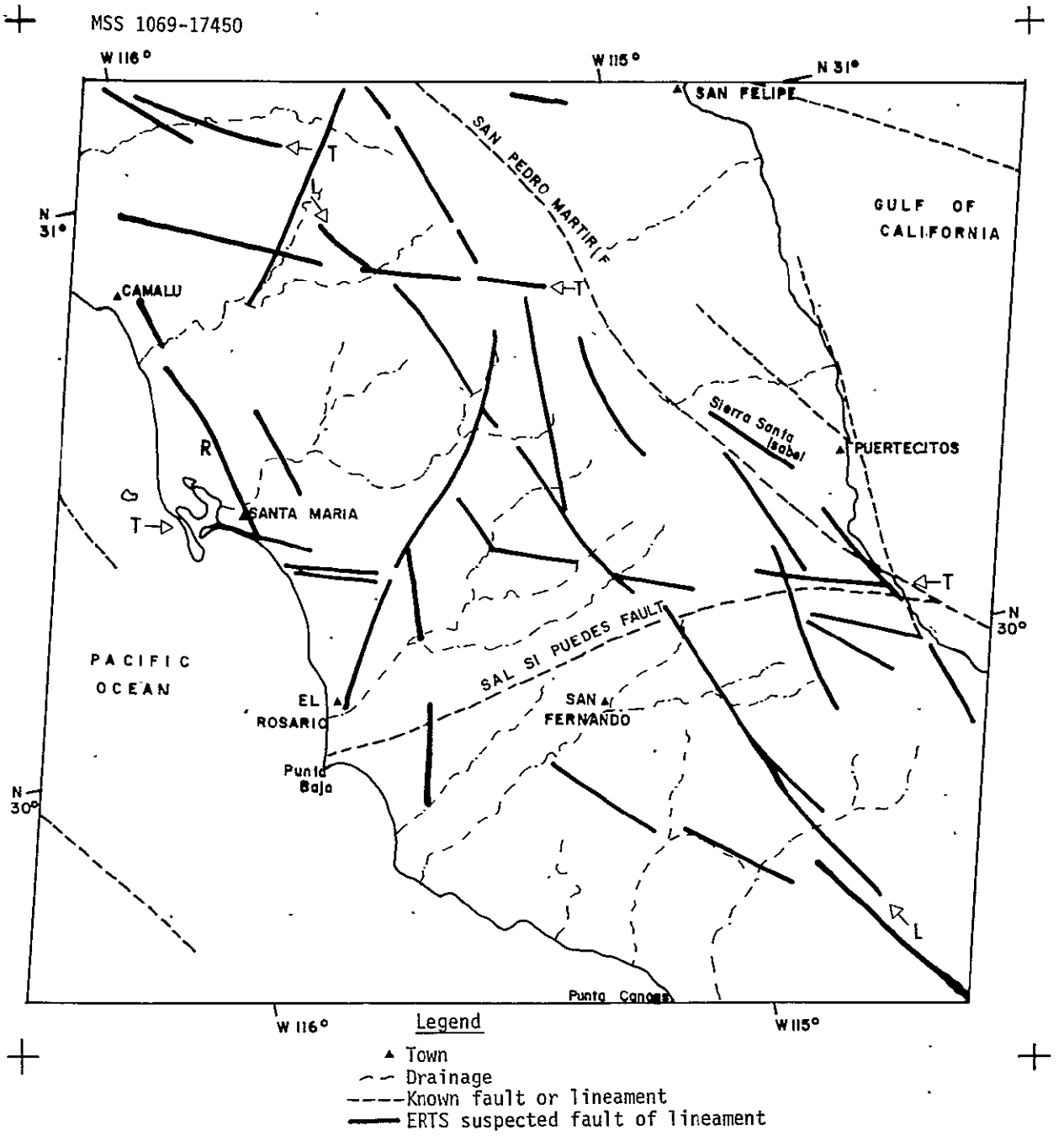

FIGURE 36 SIGNIFICANT FAULTS IN NORTHERN BAJA CALIFORNIA

MSS 1069-17450

near the boundaries of the block (i.e. near faults). Tijuana, Ensenada, and Santo Tomas, Mexico lie in highly seismic zones, being on projections of major active faults.

MSS 1069-17450

The area covered by this ERTS photo includes the area south of the Agua Blanca fault, including the Santo Domingo River, Santa Maria, El Rosario, and Punta Cancas (Fig. 36). There is no evidence of any transverse fault cutting across the entire width of Baja California. There is evidence against the existence of Sal Si Puedes fault suggested by Rusnak *et al.* (1946, plates 2 and 3). There are several other ERTS inferred faults, lineaments, and geological structures crossing perpendicular to the Sal Si Puedes fault that would seem to question its existence. Its surface expression is not clearly visible in the ERTS imagery. The San Pedro Martir fault trending NW is vaguely visible as it controls the long valley between the two ranges, Sierra San Pedro and Sierra Santa Isabel. There are several discontinuous transverse lineaments trending west-north-west; one extends from the area of Isla Miramar to Santa Maria (T). We also recognized: a major lineament trending northwest, running along the axis of Baja California and parallel to the San Pedro Martir fault (L); a probable young fault (R) running parallel to the western coast just north of Santa Maria; and several other faults trending north and northeast.

ERTS-1 imagery fails to show conclusive evidence that the transverse faults are associated with major lateral displacements which is an essential criteria if tectonic telescoping has taken place. The knee shape of Baja California here does not appear to be influenced by wrench faulting.

SOUTHERN BAJA CALIFORNIA

In the southern part of Baja California only segments of transverse faults are observed. It is probable that late Tertiary and Quaternary volcanism and the submergence of the southern part have acted to cover large segments of major faults. The observation of several segments of transverse faults here is consistent with Baja California being broken into several major blocks which moved differentially as a result of the spreading of the Gulf of California. Definitive proof is however lacking.

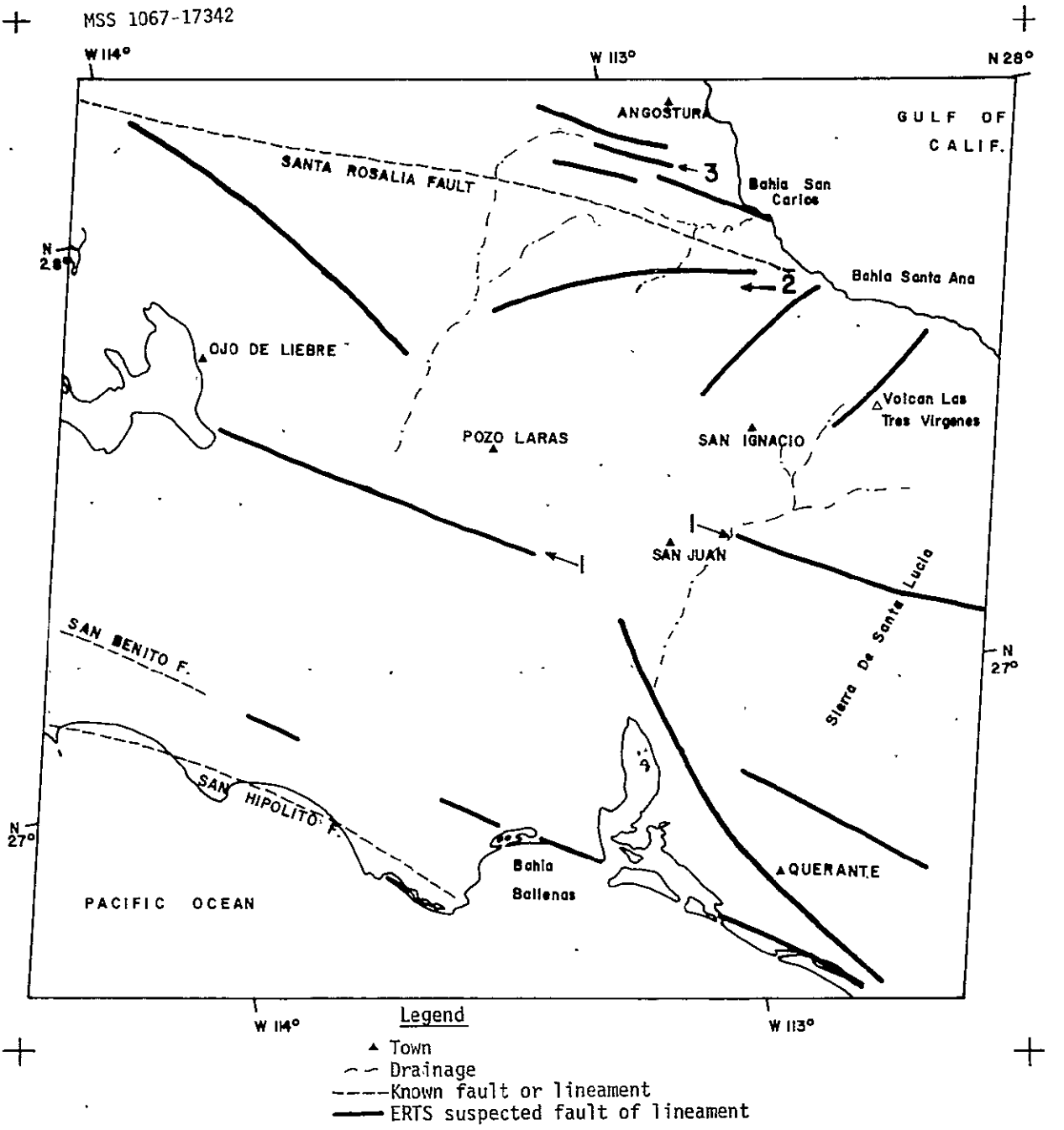

FIGURE 37 MSS 1067-17342 SIGNIFICANT FAULTS IN SOUTHERN BAJA CALIFORNIA

MSS 1067-17342

This ERTS image covers the areas of Ojo de Liebre, Punta Abreojos, San Ignacio, Santa Rosalia, and Bahia San Carlos (Fig. 37). Previously known faults or conjectured faults in this area include the Santa Rosalia fault which, for instance, shows no surface expression in ERTS as it extends through the alluvium SW of the mountains. In this area, near Santo Domingo, ERTS inferred lineaments run obliquely in a NNW direction to the Santa Rosalia fault. The eastern half of the fault runs through the mountains west of Bahia San Carlos. Although the actual fault trace is extremely vague several other ERTS inferred lineaments close by trend in the same direction, parallel to the known fault and are clearly seen. There are also other lineaments trending EW and NE. The San Benito-Cedros-Tortuga fault is also very poor in surface expression. Trending NW, its path runs just south of the Sierra Placeres, and then extends into the valley alluvium. Its existence is not verified by ERTS imagery anywhere along its conjectured path. Oblique to its position several other ERTS lineaments trend NNE, but mostly NNW through the Sierra Placeres. The San Hipolito fault is mainly an offshore fault crossing the land only twice. In both these areas, Quaternary alluvium is found, which suggests why the fault cannot be clearly seen. Even though the fault may be covered up by this alluvium, there appears to be similar NW trending lineaments in the area.

Several ERTS inferred northwest trending lineaments can be seen in this photo. One extends from Ojo de Liebre to San Juan, and another goes through the range Sierra de Santa Lucia, south of Santa Rosalia (1). North of the Santa Rosalia fault, several other northwest lineaments cross the mountains just west of the Bahia San Carlos (3). Near the Gulf, where the Santa Rosalia fault extends into the Bahia Santa Ana, a westward trending lineament intersects the Santa Rosalia fault and extends into the Coastal ranges (2). There is also a possible extension of the San Benito fault down past Bahia Ballenas. The transverse faults in this ERTS photo are pre-Quaternary masked by Quaternary volcanics, Pleistocene marine sediments, and alluvium.

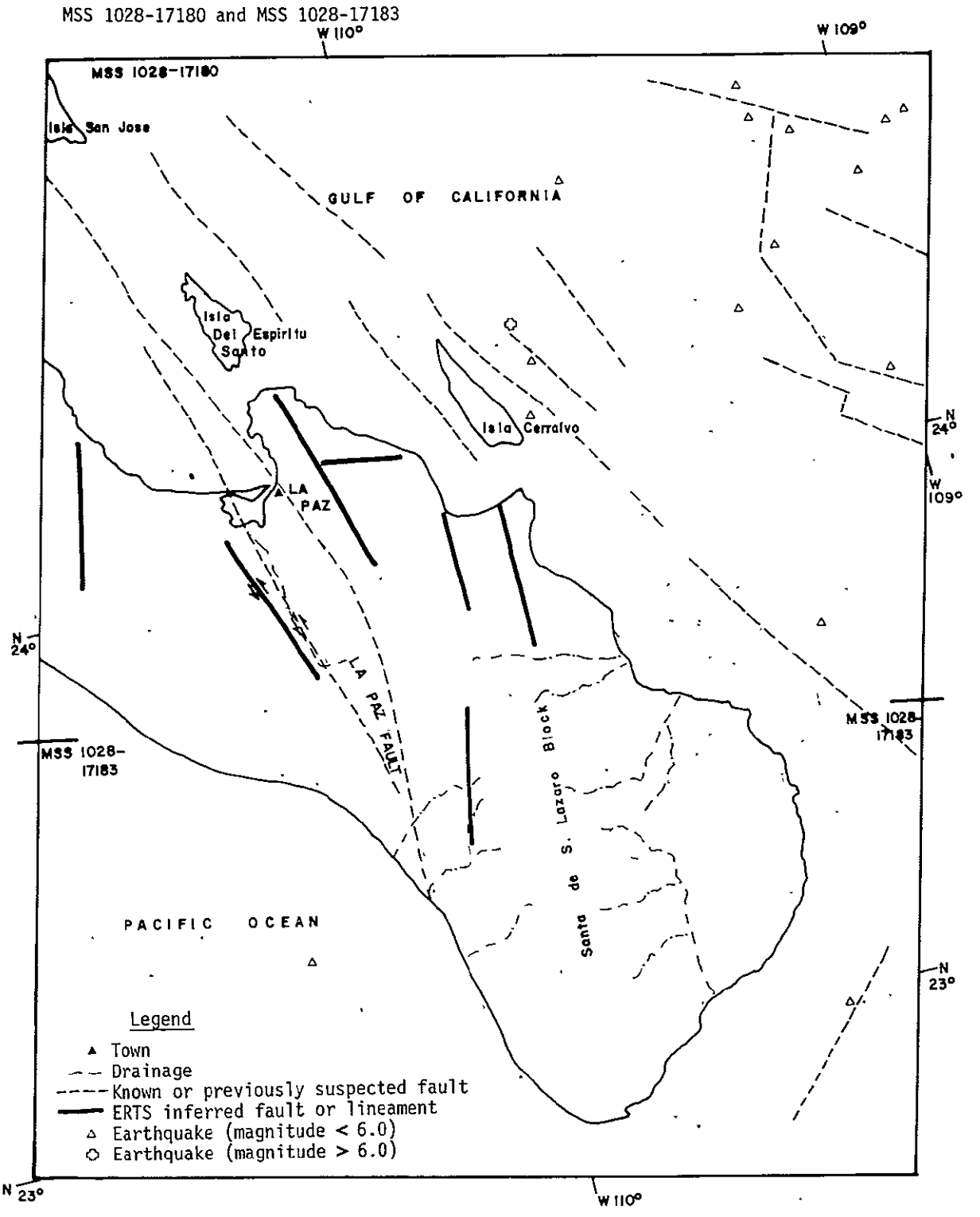

FIGURE 38 MSS 1028-17180 and MSS 1028-17183

FAULTS AND SEISMIC ACTIVITY OF SOUTHERN BAJA CALIFORNIA

MSS 1028-17290

The towns of Santa Rosalia, La Purisima, and Conejo are included in this ERTS photo. This part is covered by Tertiary and Quaternary volcanics. Faults are trending NW, but none appear to be recently active. Several lineaments are observed, generally parallel to the peninsula. If they are faults, they are either old, covered by volcanics, or have not moved for some time. The area generally gives the impression of stability except for the abundance of very well defined Quaternary volcanics. No transverse faults of unquestionable nature are observed.

MSS 1028-17180 and MSS 1028-17183

These images cover the southernmost tip of Baja California from La Paz south to the tip (Fig. 38). Most of the major faults have been mapped, but a few additional faults are inferred from the imagery. The only major fault in this area that extends onto the land is the La Paz fault that trends approximately NNW. It is clearly visible in the ERTS image 1028-17180 and can also be inferred in 1028-17183. ERTS imagery suggests a possible left lateral movement on the fault. Another lineament or fault can be seen just west of the La Paz fault about 5 km. It also trends NW with a possible left lateral movement. Viewing Figs. 38 and 34 the significant observations are:

1. Many of the N-S trending faults show evidence of recent activity. Yet the record of historic earthquakes on the land area can be misleading. From the geologic record the entire southern part of Baja California is susceptible to major shocks and recurrence of fault movement. It is evident from the disruption of drainage lines and fault traces cutting the alluvium and particularly the extent of headward erosion of streams flowing west from the eastward tilted Santa de S. Lazaro block. This indicates the recency of fault breakage and tilt. However, this is hardly evident from the available seismic record.

2. The earthquake pattern forms a belt trending north within the Gulf of California significantly oblique to the major suboceanic faults which trend NW.

3. The distribution of major earthquakes (greater than 6.0 magnitude) show alignments along two definite lines. The first trends N-S from Isla Cerrelvo towards Topolobampo on the Mexican mainland. The second line trends N-W approximately aligned with a major suboceanic fault.

4. In the southern part of Baja California the N-S fault pattern is decidedly different from the northwest trends of suboceanic faults. The latter do not appear to extend into the peninsula..

MSS 1029-17231

This image of Baja California coast near Tripui shows an interesting fault and quake comparison. A seismic zone occurs east of Isla de Carmen (Fig. 34). The major quakes are lined up along a NW trend within the gulf while the lesser earthquakes cluster in a NE trend. Most of the earthquakes occur NE of the faults, known or inferred, under the Gulf.

SEISMICITY

After earthquakes were plotted for each ERTS photo, a large mosaic was made and a seismicity pattern appeared (Fig. 34). From the Gulf head down to the Pacific Ocean west of Colima, the heaviest earthquake activity occurs in the Gulf of California. Northwestward from the Gulf head the earthquakes occur inland, forming a large cluster from Ensenada to the Salton Sea. South of the Agua Blanca fault, Baja California has very minimal seismic activity. This is also the case with the NW Mexican mainland. Four main areas appear to be clustered with earthquakes.

1. Inland, between the Agua Blanca fault zone and the Salton Sea area.
2. In the Gulf, west of Caborca, between latitude N30° and N32°.
3. In the Gulf between latitude N24° and N28°, but heaviest between N24° and N26°.
4. West of Colima in the Pacific Ocean.

BAJA CALIFORNIA MAPPING ERRORS

Mapping errors were found in Baja California and in the coastal islands off mainland Mexico. When comparing the ERTS imagery with the United States Air Force Operational Navigation Charts, the following results were obtained:

MSS 1032-17393

The outline of Baja California (taken from the ONC map) was best fitted to the actual ERTS image coastline. The coastlines showed definite mapping errors. Northwest of Santa Maria and Punta Final the coastlines

from ERTS and the ONC map fit. Isla San Luis was mapped approximately 2 km to the west of its ERTS location. From Punta Final SE to Bahia de Los Angeles, the mapped coast is as much as 2.5 km to the SW of the photo coastline. Isla Angel de La Guarda is mapped 2 km to the west of the ERTS image, and Isla Smith is off about 1 km, also to the west. Southeast of Bahia De Los Angeles the land once again fits the ONC mapped coast. On the western side, between Santa Maria and Punta Maria, and south along Bahia Santa Rosalia, the map shows the coast approximately 1 to 1.5 km north of the photo coastline.

MSS 1066-17283

Using the mainland of Mexico (near Guaymas), Isla San Marcos, and the San Bruno coastline for the best fit, while comparing the ERTS coast to the ONC mapped coast, the following information was obtained: The most dramatic error is Isla Tortuga which is mapped 9 to 9.5 km to the west of its photo location. The coastline from Bahia Santa Ana, through Santa Rosalia, to just NW of San Bruno, is about 2 km, south of the ERTS image coast. Punta Concepcion and Punta Teresa are mapped 1.5 to 2 km to the north of the photo. It is notable that with no amount of shifting will the two mapped coastlines produce a perfect fit.

MSS 1043-17014

This ERTS photo shows the size of the four islands, Isla San Juanito, Isla Maria Madre, Isla Maria Magdalena, and Isla Maria Cleofas, to be much smaller than the ONC map depicts them. Using the coastline of Mexico, near Tuxpan, as a perfect fit between the ONC map and the ERTS imagery, the errors in the mapped islands are as follows:

Isla San Juanito: ONC map shows it located about 5 km north of its ERTS location.

Isla Maria Madre: ONC map shows the northern and southern coasts to be approximately 2 km larger in both directions.

Isla Maria Magdalena: The mapped western tip is 5 km to the SW of the photo, and the eastern tip is 2 km to the NE of the ERTS location.

Isla Maria Cleofas: ONC map shows 2.5 km more of eastern coast that is approximately 2 km wider in a north-south direction.

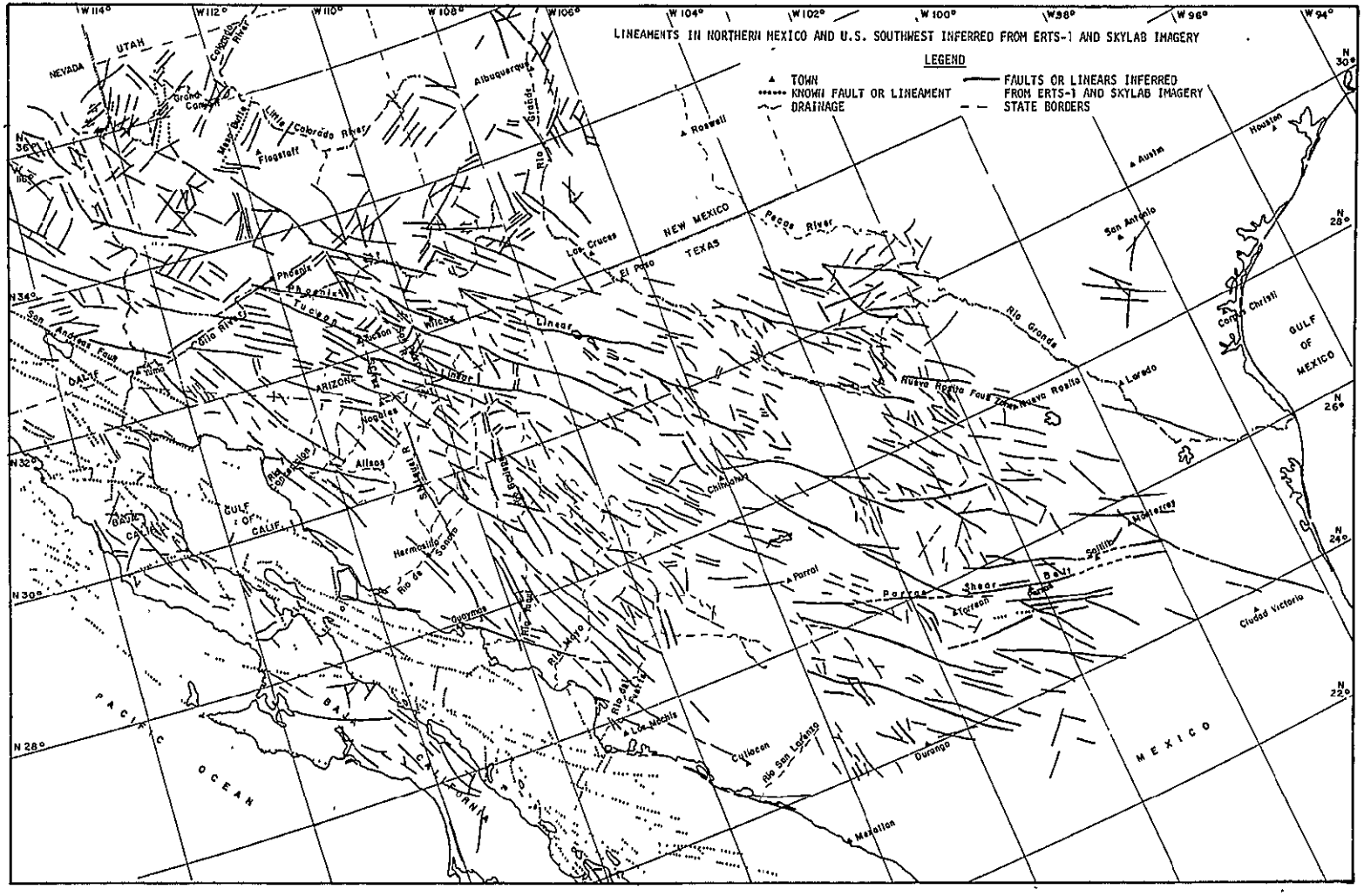

FIGURE 39 LINEAMENTS IN NORTHERN MEXICO AND U.S. SOUTHWEST INFERRED FROM ERTS-1 AND SKYLAB IMAGERY

TRANSVERSE FAULTS AND SHEAR ZONES IN NORTHERN MEXICO

ERTS-1 imagery provides evidence suggesting that the southwestern part of North America was deformed by a major system of left-lateral transverse shear which predated the development of the Gulf of California, the San Andreas fault system, and Basin and Range fragmentation. The widespread shearing deformation of the western part of North America is related with its interaction with Pacific Plate movements.

A major system of transverse faults related to the Texas and Parras lineaments has been recognized. We mapped outstanding strands of this system within an extensive area north of 24°N in Mexico and across the international U.S.-Mexico border (Figure 39).

The Texas lineament was defined by Schmitt (1966) as a transverse structural zone trending N 75°W from the edge of the Gulf of Mexico to the Santa Rosa Island, California. The Texas zone coincides with a "hiatus" in the topography and with chaotic structural blocks and may represent the roots of a major worn-down mountain range. One of the most prominent features of Figure 39 is the Phoenix-Nueva Rosita Belt. This belt lies within the Texas zone and, in our opinion, represents an essentially continuous fault belt which extends more than 2,000 km. from the eastern Mojave and Eastern Transverse Ranges in California across the Colorado River through Phoenix, Arizona, and across the international border through Chihuahua and perfectly aligns with the Nueva Rosita Fault zone in Mexico. On the west, the belt is interrupted by the San Andreas fault system and is probably offset by it and continues along the Western Transverse Ranges of California. On the east, the belt becomes unrecognizable in the late Tertiary and Quaternary sedimentary belt of the Gulf of Mexico. The Phoenix-Nueva Rosita linear is the most remarkable feature in the Texas zone and could very well be a major strand in the Texas shear.

One of the most outstanding element of the system of faults and lineaments in Figure 39 is a left-lateral shear zone trending N70°W extending from south of Monterrey, Mexico through Saltillo, Parras, Torreon, and Parrel. Recognizing that mapping linears can be somewhat subjective, the writers interpreted the imagery independently. We further intentionally studied the imagery at random in order to minimize any tendency to extend a given linear from one frame to the next.

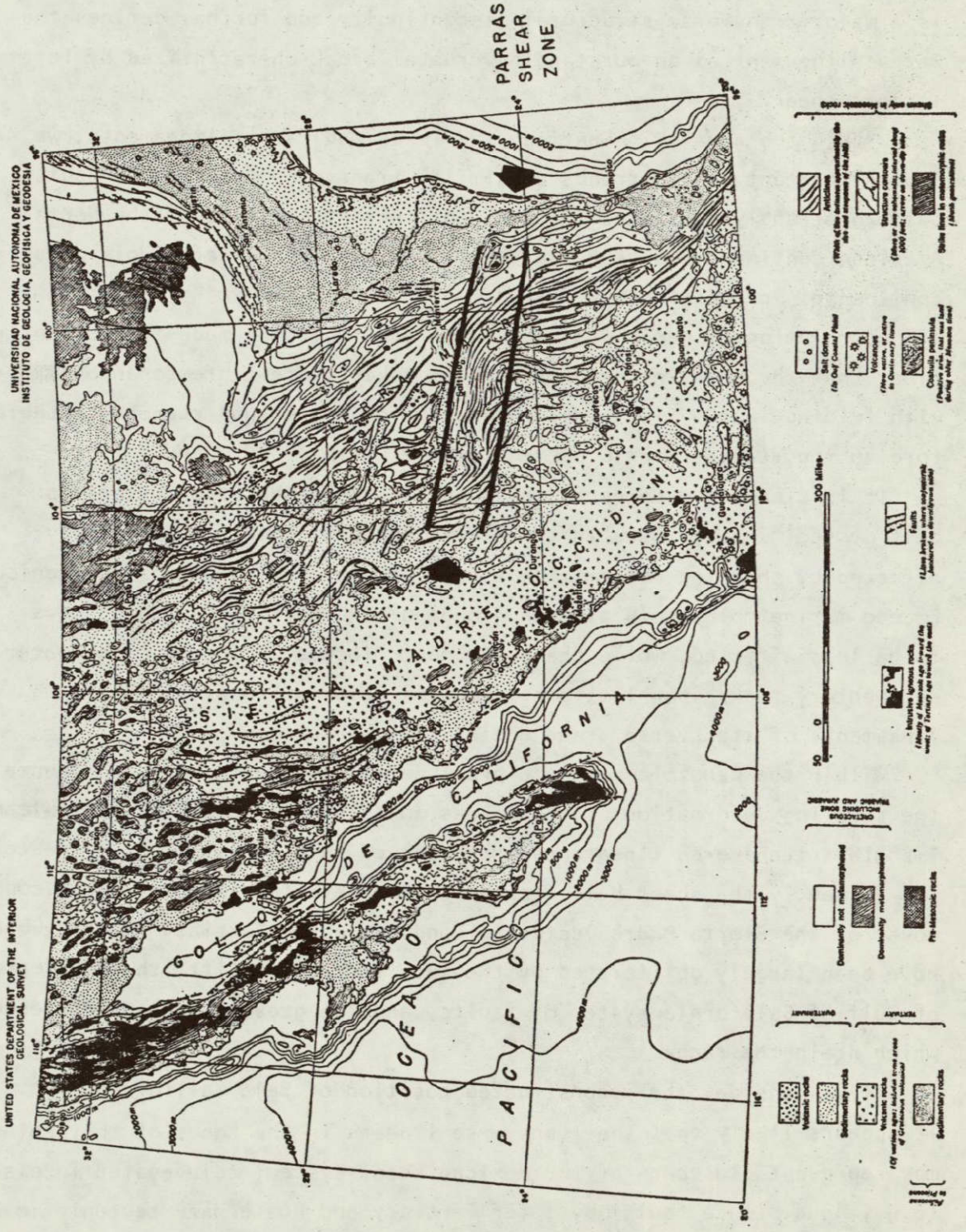

FIGURE 40 Parras Shear Zone

The existence of the "Parras Lineament" has been suggested in the literature (e.g. Schmitt, 1966). Our work confirms that this lineament is a major transverse structural discontinuity and further defines the Parras lineament as an outstanding crustal break characterized by left-lateral shear.

Within the area lying between the Texas and Parras lineaments, we found important fault strands of similar transverse trend. The fault pattern strongly indicates that the entire southern part of the North American continent has been subject to an enormous shear couple of sub-continental proportions.

Correlation of geological maps with our fault map made it abundantly clear that the shearing deformation has taken place contemporaneously with folding in the Sierra Madre Oriental of Mexico and represents therefore an important tectonic element of the Laramide "Orogeny."

It is clear from comparing Figures 39 and 40 that the Cretaceous belt of sedimentary rocks in the Sierra Madre Oriental is profoundly affected by shearing deformation as well as folding. The post-orogenic Eocene marine molasse (Claiborne group) of the Gulf of Mexico appears to be less affected, while the Gulf Coast Miocene, Pliocene, and Quaternary sedimentary rocks show little evidence of deformation although some lineaments of transverse trend could still be detected.

Within the Cenozoic volcanic province of the Sierra Madre Occidental the shearing deformation of the Parras zone is not readily evident although important transverse lineaments are observed in places.

Evidently the shear belt lies buried beneath the immense volcanic cover of the Sierra Madre Occidental and any early Tertiary fault strands have been largely obliterated by the late Tertiary uplift, the development of Gulf of California system of faults, and the great system of canyons which drain the range.

If we consider the reconstructed position of Baja California (Fig. 33), it appears likely that the transverse linears in the zones of the peninsula may represent old scars of the Mexican shear system, rejuvenated in places (e.g., Agua Blanca fault) by later Tertiary and Quaternary tectonic movements which brought about the opening of the Gulf of California.

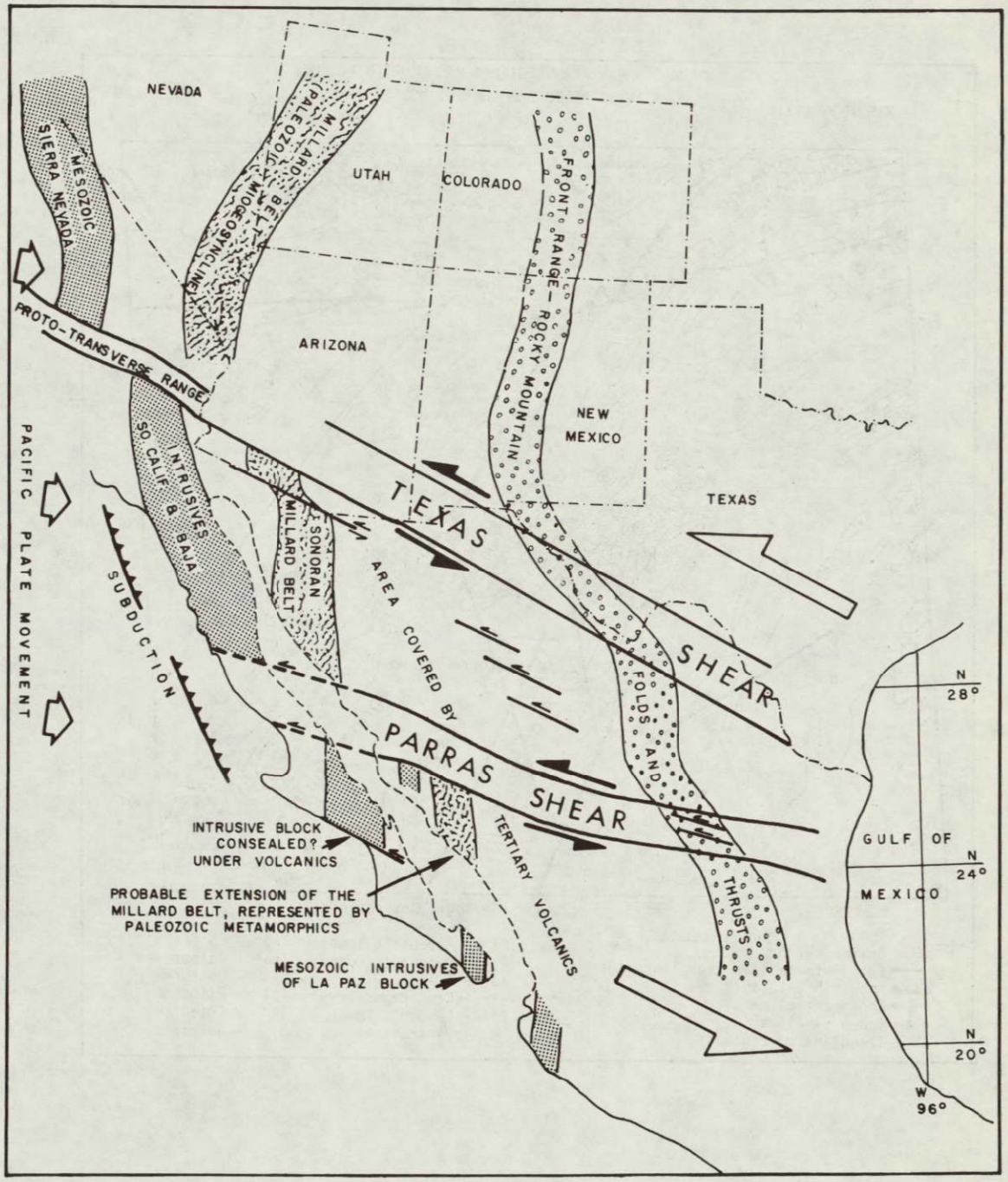

FIGURE 41 Tectonic Model Showing Effect of Parras and Texas Shears on Major Orogenic Belts Prior to Basin and Range Fragmentation

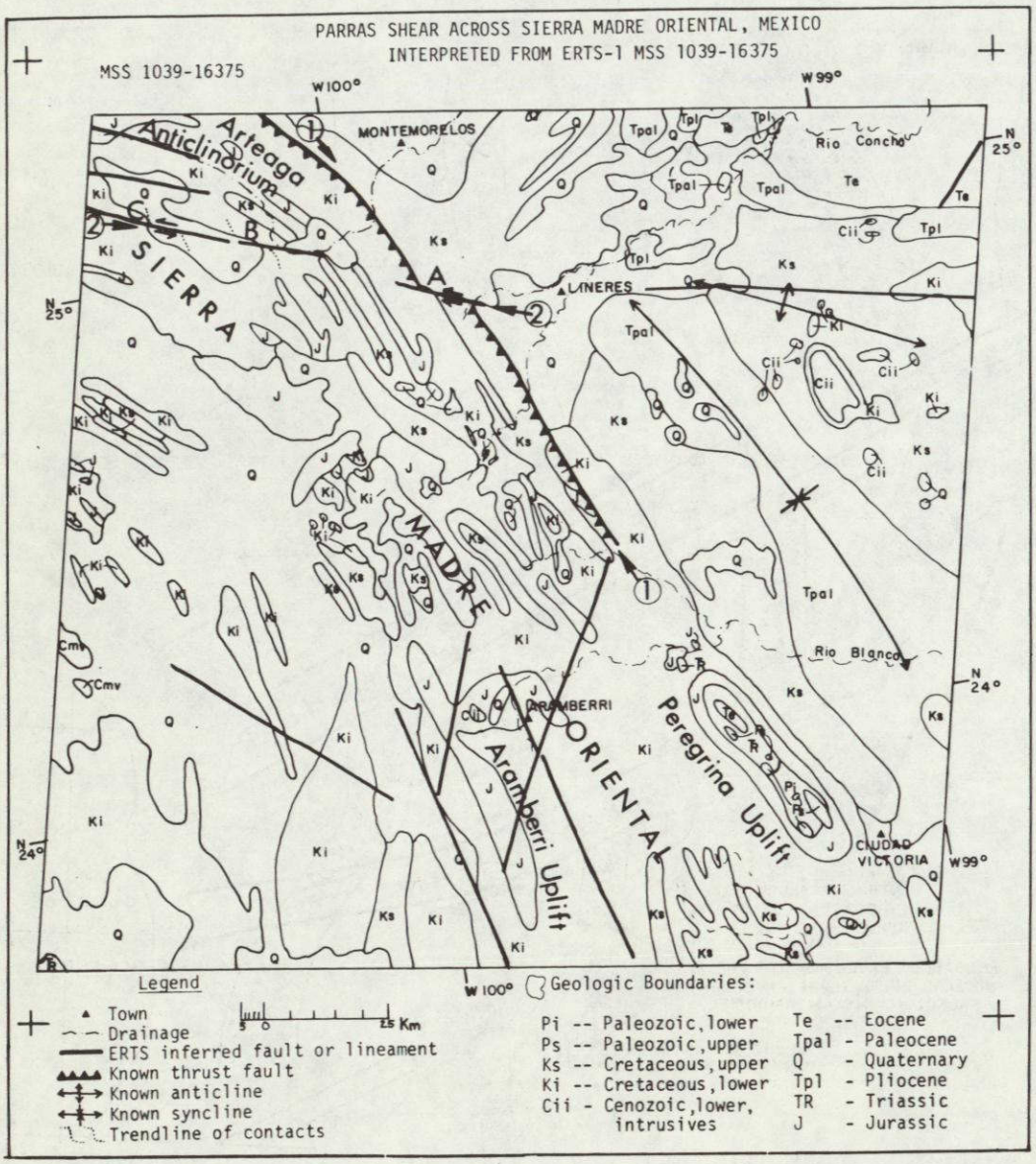

FIGURE 42 PARRAS SHEAR ACROSS SIERRA MADRE ORIENTAL, MEXICO
INTERPRETED FROM ERTS-1 MSS 1039-16375

A proposed tectonic model illustrating the effect of Texas and Parras shears on major orogenic belts is shown in Figure 41. Of particular significance is the position of the Millard Belt described by Kay (1951). This Paleozoic miogeosynclinal sedimentary belt is exposed in southern and eastern Nevada and western Utah. The southern end abruptly ends in southeastern California. The southern extension of the Millard belt had remained beyond the Texas shear which has remained an enigma for a long time until the remarkable similarity of the Paleozoic rocks exposed in western Sonora, Mexico was pointed out by King (1969). The position of the two segments of the Millard Belt leaves very little doubt that the Texas lineament coincides with a major sinistral shear.

We reason that the left-handed Parras shear has probably caused a second major offset of the Millard Belt. The offset extension most likely occurs in the vicinity of Culliacan, Mexico. Indeed the Geological Map of Mexico shows a relatively small exposure of Paleozoic metamorphic rocks along Rio San Lorenzo (near Long. W106°45' Lat. N24°40'). Since the area is now largely covered by the Sierra Madre Occidental volcanic rocks, the older Paleozoic rocks would crop out only in erosional windows.

Left-Lateral Shear Features Along Parras Belt

We have selected three examples within the folded Sierra-Madre Oriental and the Plateau Central to show the effect of the Parras shear and structures indicating its left-lateral nature.

Figure 42 (MSS 1039-16375) shows the Sierra Madre Oriental with its complexly folded Mesozoic marine sedimentary rocks. The three systems of faults discernible here trend north-northwest, northeast, and west-northwest

The eastern front of the range, Fault 1-1, is a thrust shown in part in the Tectonic Map of North America (King, 1969) and discussed elsewhere by Kellum (1930).

The transverse fault (2-2, Fig. 42) quite clearly displaces the eastern front of the Range and the thrust fault approximately 10 km near point A. Farther northwest at points B and C similar displacements of the lower Cretaceous, Upper Cretaceous, and Jurassic strata are observed. Between points A and B the continuity of the tear fault (2-2) is uncertain and is evidently due to the complex relationship between thrust and wrench faulting.

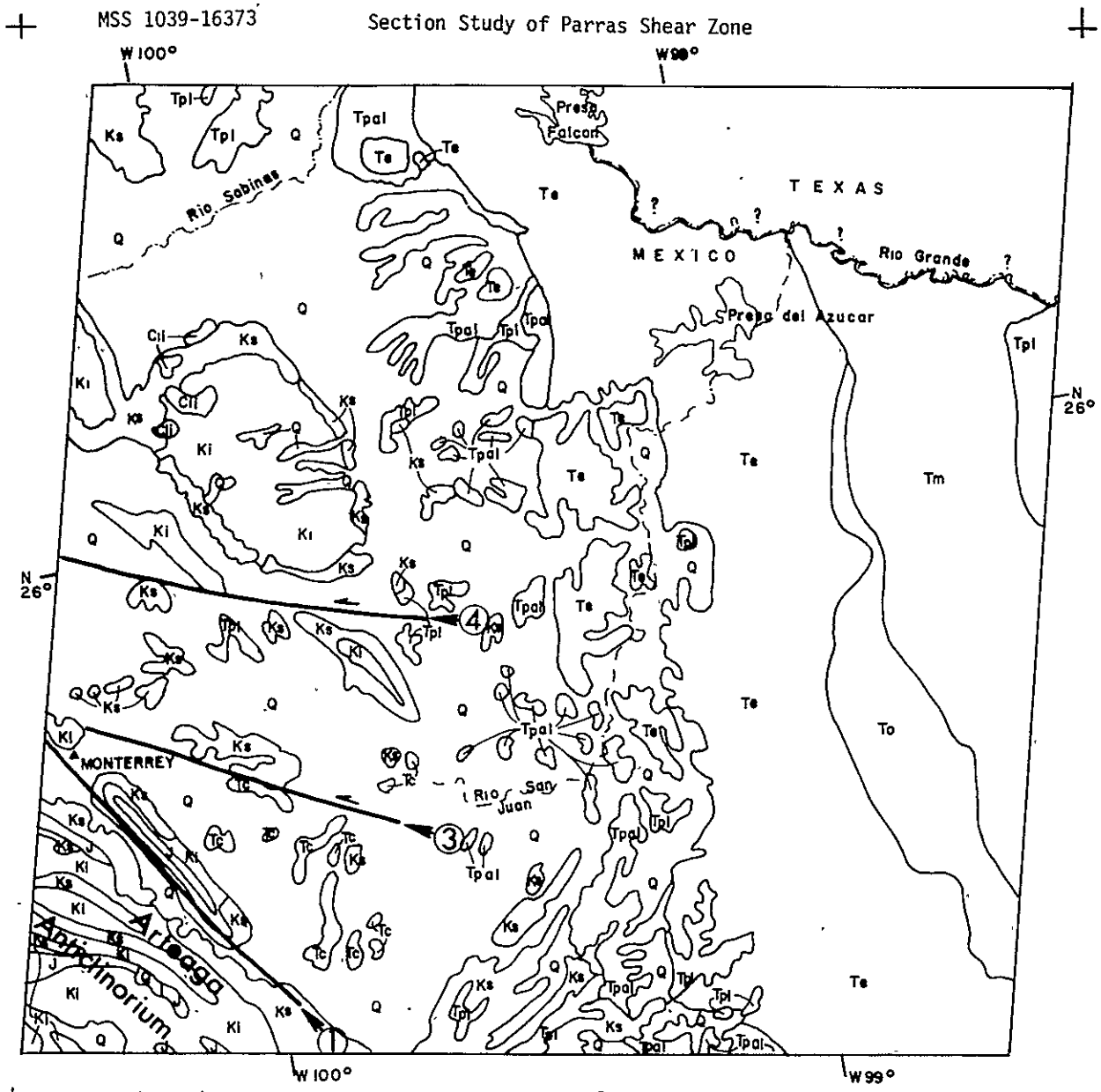

Legend

- ▲ Town
- ERTS inferred fault or lineament
- ~·~ Drainage

Geologic Boundaries:

Ks- Cretaceous superior	Q- Quaternary
Ki- Cretaceous inferior	Tpl- Pliocene
Tm- Miocene	To- Oligocene
Te- Eocene	J- Jurassic
Tpal- Paleocene	
Tc- Tertiary continental	
Cii- Cenozoic inferior, intrusives	

FIGURE 43 MSS 1039-16373 SECTION STUDY OF PARRAS SHEAR ZONE

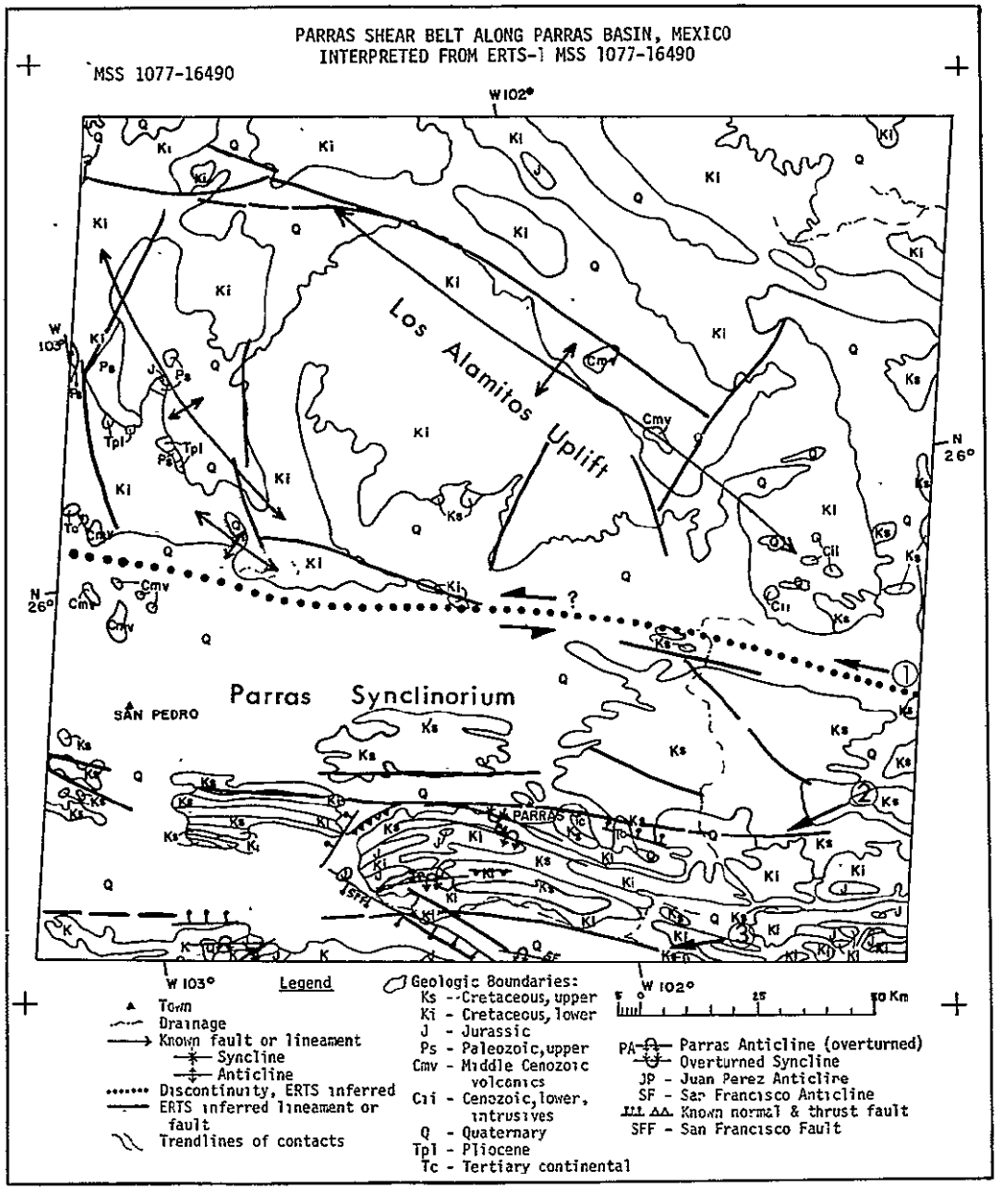

FIGURE 44 PARRAS SHEAR BELT ALONG PARRAS BASIN, MEXICO INTERPRETED FROM ERTS-1 MSS 1077-16490

These types of faults often merge or change from recognizable breaks into flextures and tight folds.

Directly north (Fig. 43, MS1039-16373) of the Arteaga anticlinoram a major zone of transverse shearing is evident. The transverse lineaments 3 and 4 (Fig. 43) are associated with profound flextures in the structural contours and isopach lines (King 1969). Towards the east little or no surface expression of the lineaments is detected across the Tertiary formations (Tpal, Te, To, Tm) which indicates an active pre-Tertiary age. Farther west a great east-west trending structure discontinuity passes through the Parras Synclinorium (1, Fig. 44, MSS 1077-16490). The tightly folded Cretaceous strata forming the south rim of the Parras Syclinorium are cut by large strike faults trending east-west (2, 3 Fig. 44). The regional orientation of the Los Alamitos uplift (anticline) axis and the two anticlines west of it trend oblique to the Parras Fault Zone at an angle consistent with left-lateral shear along the Parras belt. It is evident, however, that the Parras fault belt is not a single throughgoing surface break. It is rather a broad region where profound crustal breaks in depth are expressed in the sedimentary section above the form of regional flextures and tight folds passing in places into an echelon and discontinuous wrench faults and thrusts. We found from studying some 50 ERTS scenes that east-west and west-northwest trending breaks are pervasive in northern Mexico and across the border in the U.S. The breaks are particularly profound along the Parras and the Texas belts.

Projection of Parras Shear Across Sierra Madre Occidental

The Sierra Madre Occidental lies on the western side of Miuland, Mexico. This range is covered by an immense volume of volcanic rocks generally considered of middle Cenozoic age. The huge canyons which drain the range into the Gulf of California have deep gorges and rather youthful geomorphologic features attesting to the relatively recent uplift of the range.

We studied all ERTS-1 scenes of this range between latitudes 20° and 31°N in order to determine whether the range shows any features which could be related to the Parras or other transverse shear structures.

We found that the prevailing fracture pattern consists mainly of two systems: a north-south and northwest-southeast, parallel to the Gulf of California. No major transverse breaks were identified with certainty. In places shown in Figure 33 there are some lineaments of transverse trend. They are generally observed in the eastern and western flanks of the range. It is evident, however, that if the Parras Shear ever affected that area, the evidence for its presence must lie in older rocks underneath the volcanic cover. We must assume therefore that the Parras Shear either terminated east of the Sierra Madre Oriental or more likely it has ceased to be an active feature since the middle Cenozoic volcanics were emplaced.

As mentioned in our discussion of Baja California, reconstruction of the peninsula brings the transverse faults in the middle part of the peninsula in alignment with the westward projection of the Parras Shear. This apparent alignment may be merely coincidental, but may conceivably be an expression of the Parras belt continuity across the site of the Gulf prior to its inception.

PAGE INTENTIONALLY BLANK

RED SEA RIFT

Previous work by Abdel-Gawad (1969) on Gemini photographs has indicated significant geologic correlations suggesting some 150 km offset across the northern part of the Red Sea rift. In this study we utilized ERTS-1 imagery to determine further correlations across the entire length of the Red Sea.

ERTS-1 scenes selected for analysis of the Red Sea rift:

MSS 1071-07374	MSS 1065-07055	MSS 1053-07392
MSS 1052-07322	MSS 1065-07061	MSS 1105-07284
MSS 1068-07205	MSS 1045-06545	MSS 1105-07290
MSS 1068-07212	MSS 1045-06551	MSS 1105-07293
MSS 1068-07214	MSS 1045-06554	MSS 1068-07230
MSS 1049 07160	MSS 1063-06560	MSS 1068-07232
MSS 1048-07102	MSS 1073-07491	MSS 1067-07174
MSS 1048-07104	MSS 1072-07435	MSS 1068-07235
MSS 1067-07162	MSS 1071-07383	MSS 1049-07181
MSS 1068-07221	MSS 1054-07442	MSS 1101-07074
MSS 1065-07052	MSS 1071-07390	MSS 1048-07125
MSS 1067-07165	MSS 1054-07451	MSS 1048-07131
MSS 1048-07111	MSS 1052-07334	MSS 1101-07080
MSS 1048-07113	MSS 1052-07331	MSS 1100-07022

Information derived from 42 ERTS images was compiled on a base map at 1:2,000,000 scale. A reduced copy is shown in Fig. 45. We placed emphasis on comparing regional geological structures, such as metamorphic trendlines, major faults and linears across the rift. The following observations identify seven areas where possible correlations or continuations appear to exist (Fig. 46).

Area 1

Looking from south to north, the first large area of interest is in Saudi Arabia from approximately N17°30' to N20°, and in Africa from about N15°30' to N17°30'. Both areas are characterized by north-northwest and northwest trendlines. Major faults and lineaments trend east to west-northwest.

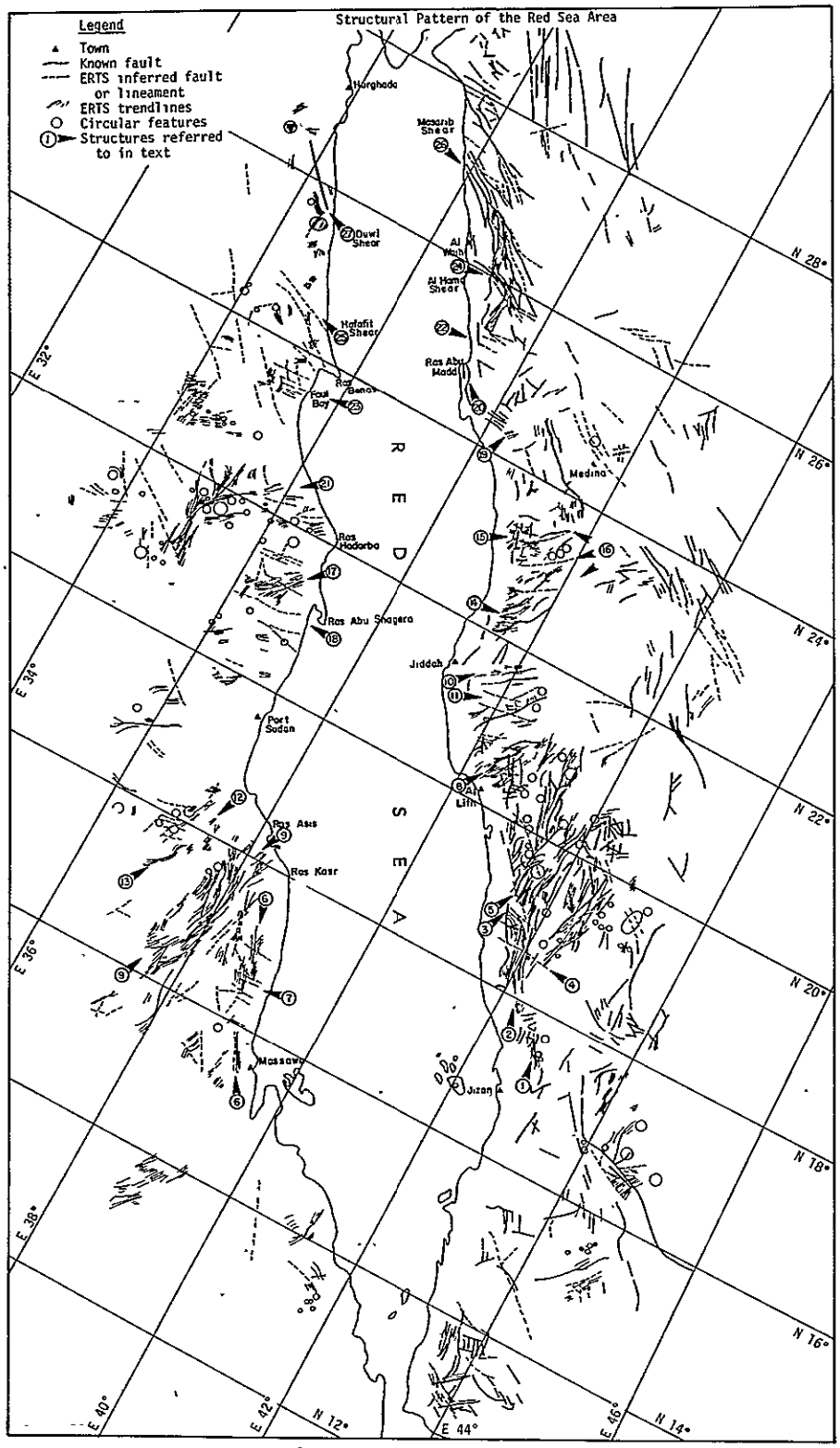

ORIGINAL PAGE IS
OF POOR QUALITY

FIGURE 45 STRUCTURAL PATTERN OF THE RED SEA AREA

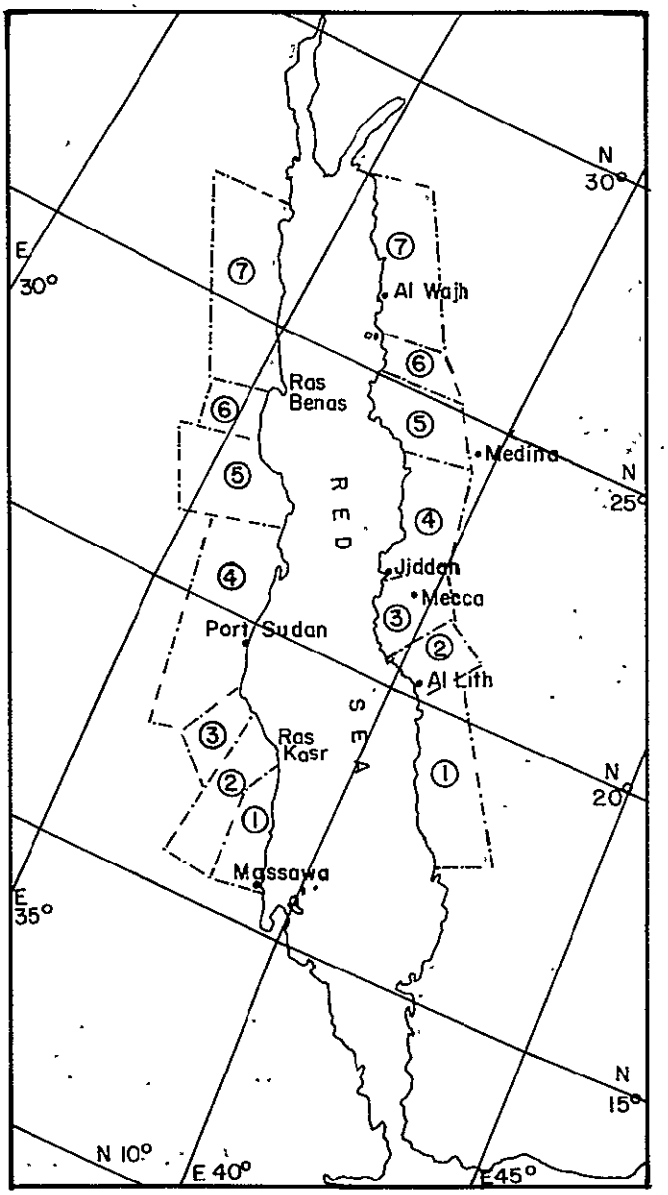

ORIGINAL PAGE IS
OF POOR QUALITY

Figure 46:
RED SEA INDEX MAP
(Areas studied in report
referred to by number)

MSS 1065-07055

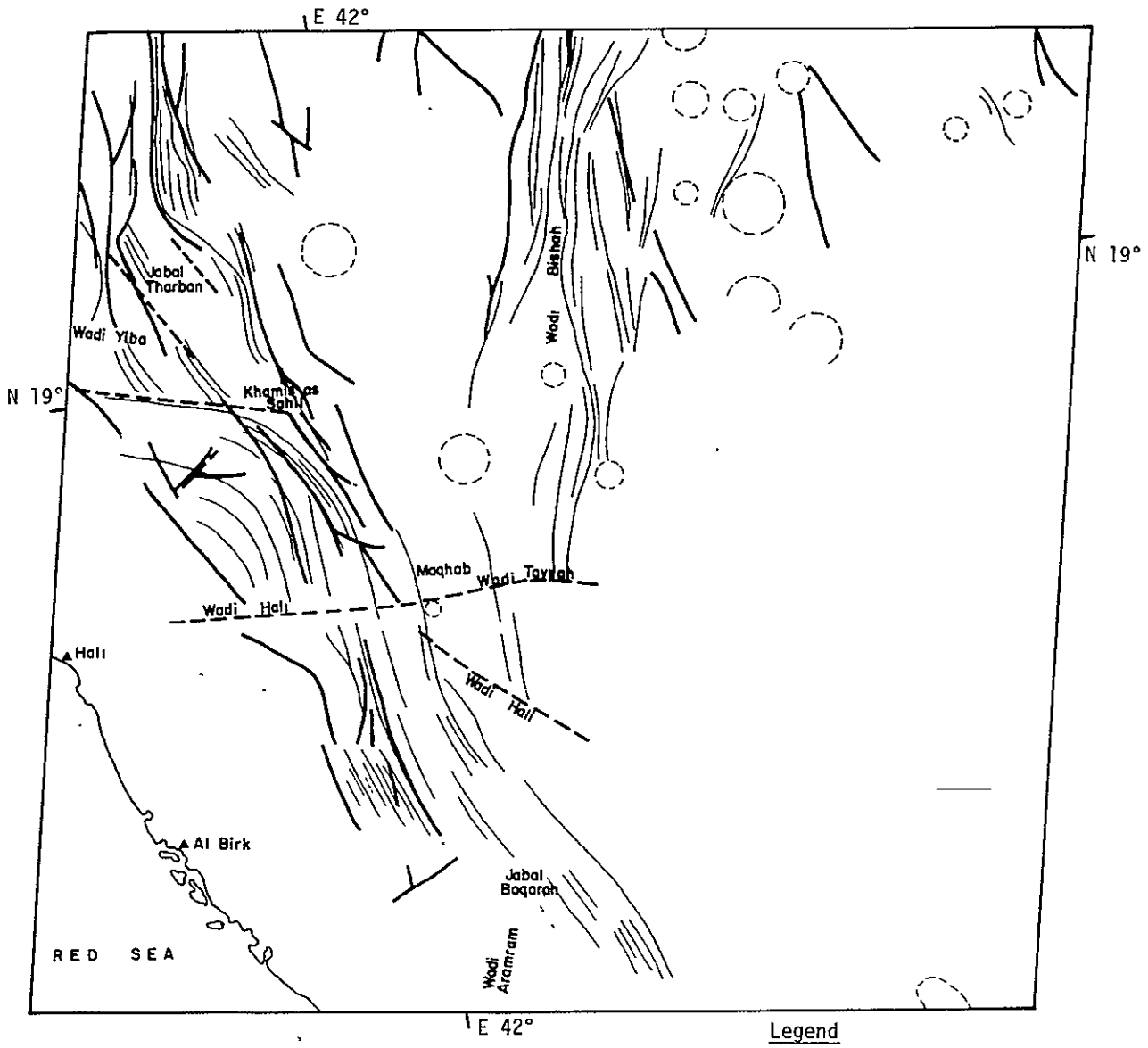

MSS 1065-07055 FIGURE 47 FAULTS, LINEAMENTS AND TRENDLINES IN SAUDI ARABIA

In Saudi Arabia from about N17°30' to N17°45' and E42°50' to E42°40' regional schistosity trendlines bear to the northwest (Arrow 1; Fig. 45) from Wadi Qissi through Harub, Al Haqu to Jabal Fidnayn and the tributaries of Wadi Baysh (MSS 1065-07061). Those trendlines are observed in chlorite and sericite schists, greenstones, slates, and phyllites. The metamorphic rocks are intruded by granitic stocks and plugs. In that particular area the known faults trend mostly northeast with some trending north-south. North-northwest to northwest schistosity trends continue from N17°50' to N18°30', E42°20' to E42° (Arrow 2, Fig. 45) and pass through Jabal al Hammah, Wadi Jandalah, Jabal Baqarah, Jabal al Haylah, Wadi Tayyah, Maqhab and Wadi Majzuah (MSS 1065-07055, Fig. 47). Known faults trend north-northwest to north-south in that area. From about N18°30' to N19° and E41°50'to E41°40' the regional schistosity bends to a north-south direction and then bears northwest near Wadi Hali and Wadi Baqarah (Arrow 3, Fig. 45). At that point the trendlines swing back to a north-northwest direction towards Jabal Baqaratayn and Jabal Tharban. Although mainly observed in chlorite and sercite schists, the trendlines can be discerned in gneissic terrain, amphibolites, green schists, marbles and quartzites. Here the known faults bear north-northwest while faults or lineaments observed in ERTS imagery strike east-west, north-northwest and west-northwest. In MSS 1065-07055 (Fig. 47) and MSS 1048-07113 a large east-west fault runs from about N18°35' to N18°40' and E41°40' to E42°20' (Arrow 4, Fig. 45) and a west-northwest fault or lineament is noted at the trendline bend near Kahamis as Sahil from about N18°50' to N19° and E41°30' (Arrow 3, Fig. 45). North of this area the regional schistosity trends north from about N19° to N20° and E41°30' to E41°30' (Arrow 5, Fig. 45) in the area of Gabal Tharban and Wadi Yiba to Az Zafir, and are generally observed in terrain covered by quartz-feldspar schists and schistose greenstone. Faults in the area predominantly trend north-south with some trending northwest and northeast. Continuing in a northwest direction, trendlines and faults can be seen from about N19°20'

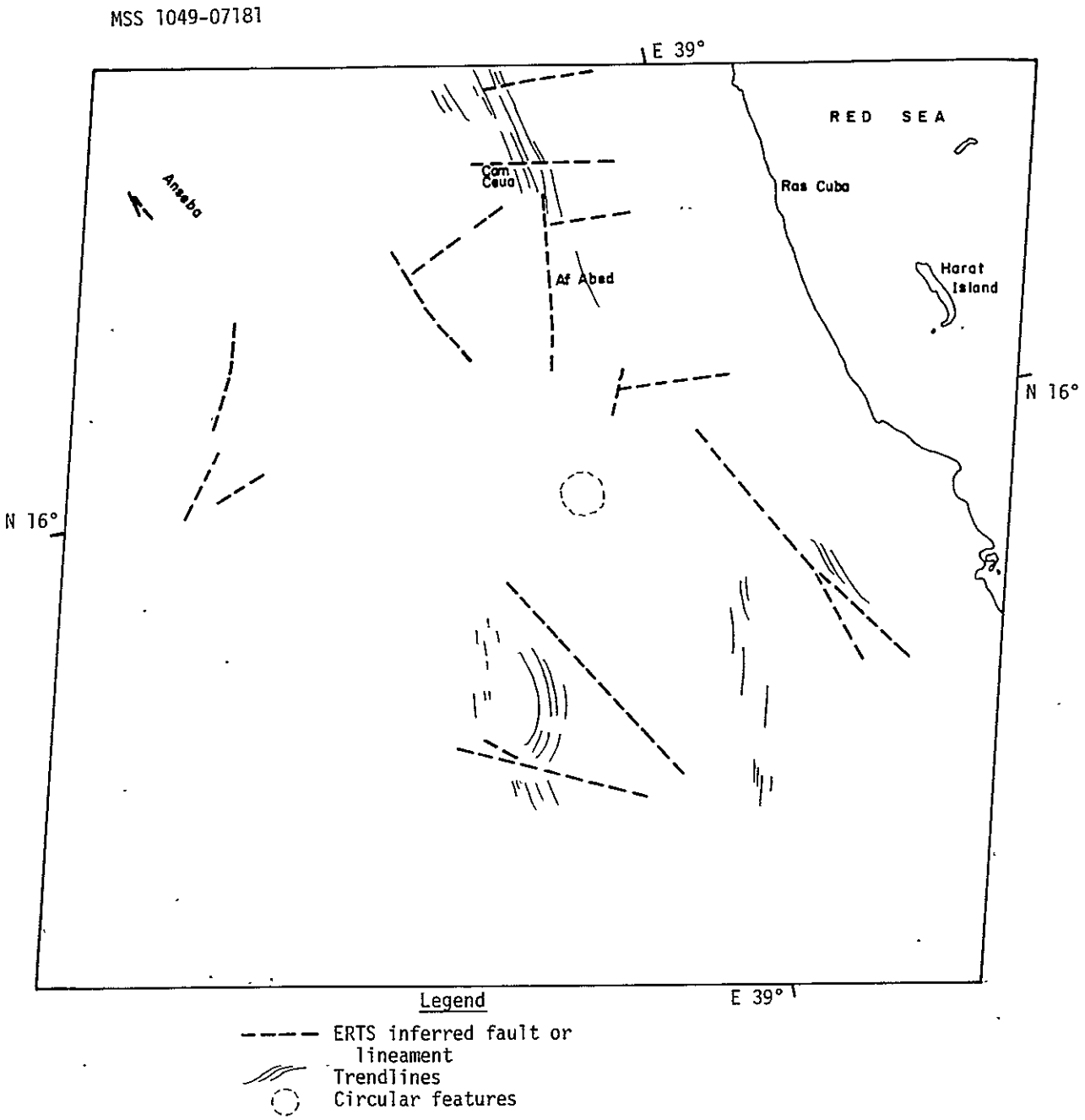

FIGURE 48 Faults, Lineaments and Trendlines in Ethiopia

to N20°10' and E41°20' to E40°50' in the areas of Wadi Nawan, Jibal Naknirah, and Wadi Ilyab (MSS 1048-07111) mostly in greenschist terrain.

On the African side a comparably large area in Eritrea has similar trendline characteristics to the Saudi Arabian side described above (MSS 1049-07181 (Fig. 48), MSS 1067-07174 and MSS 1068-07232). Schistosity trendlines bearing north-northwest are observed from about N15°30' to N17°30' and E39°20' to E38°20', northwest of Massawa through Af Abed, Cam Ceua, Mt. Abot, Ab Anrafa, Jabal Sabda and Jabal Auada (Arrows Fig. 45). These correspond to the Ethiopian Metamorphic Belt. There are north-northwest faults or lineaments in the region. Particularly significant are many Mediterranean or east trending faults (Arrow 7, Fig. 45). Of those, six rather prominent are located near: 1) N17°, 2) N16°43', 3) N16°40', 4) N16°30', 5) N16°20', and 6) N16°05'. A northwest trending fault is observed from about N16°45' to N16°50' and E38°50' to E38°30'.

Area 2

A zone of corresponding geological structures, previously described by Abdel-Gawad (1970) utilizing Gemini and Apollo photographs, is clearly recognized in the ERTS imagery. Regional Precambrian metamorphic trendlines near Ras Kasr (Sudan and northern Ethiopia), N18°, and near Al Lith (Saudi Arabia), N20°, appear to be comparable and indicate a possible offset of some 225 km across the Red Sea. In Saudi Arabia from Al Lith at N20°10' to N21° (Arrow 8, Fig. 45) is a zone characterized by north-northeast to northeast trending Precambrian grain that pass through Jabal Qunah, Wadi Dhudiyah to Umm Al Mahdam (MSS 1048-07111 and MSS 1067-07165). Several faults also trend north-northeast while others strike northwest and northeast. The regional grain is predominantly within the Wadi Lith series, a metamorphic complex of metadiorite, meta-gabbro, amphibolite, and schist.

On the African side very similar north-northeast trendlines and faults can be seen in a band from Ras Asis and Ras Kasr at about N18° to approximately N16°, E37°30' (Arrow 9, Fig. 45) passing through Jabal Hamoyet, Mt. Scirab, Saalla, and Karkabal (MSS 1068-07232, MSS 1068-07235 and MSS 1068-07230).

Area 3

In Saudi Arabia the north-northeast and northeast grain is also observed between Jabal Sita and Harrat ad Damm (MSS 1067-07162). Northeast trendlines and a northeast fault are observed generally in andesite, diabase, greenstone and andesite porphyry. More northeast trendlines are located between Jabal Hubayniyah and Hikhh generally in granite, granitic gneiss, amphibolite schist, greenstone, keratophyre, sericite schist, some marble and quartzite. In the area of Wadi Dayqah and Wadi Majarish east-northeast trendlines border a large northeast fault. Further north to Wadi Fatima is a prominent zone of northeast trendlines (Arrow 10, Fig. 45). Three major known northeast faults cross the area and numerous ERTS inferred structures can also be seen. Along Wadi Naman and Wadi Abyad two ERTS faults or lineaments are noted trending west-southwest, almost east-west (Arrows 11, Fig. 45). Minor northwest trendlines and faults can also be seen.

In Sudan north-northeast to north-south trendlines southwest of Trinkitat (Arrow 12, Fig. 45) are located in the areas of Jabal Shaba, Jabal Meiz, and just south of Erkowit and east of the Ashat River (MSS 1068-07230). A longer, more continuous zone of northeast trendlines extend from N17°20' to N17°50' and E36°45' to E37°15' through Jabal Waharba, Aswit, and Anneib (MSS 1068-07232)(Arrow 13, Fig. 45). The trendlines then bear north-south to Jabal Shaba Katar. Between N17°40' to N18°15' and E36°40' to E36°40' is an area where east-northeast and northeast faults or lineaments prevail (MSS 1106-07293). Several circular structures are also observed in the faulted area.

Area 4

A fourth segment of correlations across the Red Sea is located between N22° and N24° in Saudi Arabia and between N19° and N21°30' in Africa. In Saudi Arabia both the Precambrian grain and faults trend generally northeast to north-northeast. The following are specific examples: from about N22° to N22°40' and E39°30' to E39°40' (Arrow 14, Fig. 45) a distinct zone extends from Umm al Milh through Wadi Murarim, Wadi Marrakh, Julaylah, to

Al Biar (MSS 1067-07162 and MSS 1068-07214). Here, the northeast grain is particularly evident in areas covered by sericite and chlorite schist. Near Wadi Nuwaybah (N23°, E39°20') both the trendlines of the metamorphics and a major known fault strike northeast (MSS 1068-07214). From that point north through Wadi Najah to Umm al Birak the trendlines are relatively short and discontinuous (Arrow 15, Fig. 45). In this area they are predominantly observed in chlorite and sericite schists, interbedded with quartzites and slates. Several known faults crossing this area trend east-northeast and north-northwest. Three large faults or lineaments trending northeast were noted in ERTS imagery (Arrows 16, Fig. 45). Two of those follow major mountain breaks; one along Wadi al Akhal and the second through Wadi Thimrah and Wadi Sitarah. The third is seen very close to two known faults from Wadi Yatamah to Bir Mubayrik.

In Sudan, a general northeast grain characterizes the region between N19° to N21°30' and E35° to E37°30'. Although several areas were obscured by clouds, we noted that the following areas are characterized by northeast trending Precambrian grain: a) a zone running through Jabal Abadab and Jabal Lagag (N18°45' to N19°10' and E35°30' to E36°20')(MSS 1105-07293); b) near N19°15' to N19°20' and E36°10' to E35°50'; c) near Jabal Kaiai and Jabal Nakwat (N20°, E36°40'), Jabal Hadalaweiti (N21°15', E37°), Jabal Mishallieh (N20°20', E36°10') and Jabal Hadarabab (N20°40', E36°40')(MSS 1105-07290); d) from about N21° to N21°30' and E36°30' to E36°40' (Arrow 17, Fig. 45) a band extends from Jabal Tagoti and Bir Lolignet to north of Jabal Hagiri (MSS 1105-07284).

Between N20°30' and N21°30' several east-striking Mediterranean faults cut boldly across the mountains (Arrow 18, Fig. 45). Other faults bear slightly east-northeast, west-northwest and northwest. Five of the more prominant Mediterranean faults are located near Jabal Hagiri, Bis Lolignet, Jabal Erba, Jabal Eirawe, and Jabal Arit. It is interesting to note that the Mediterranean structures (e.g., near Jabal Arit, N21°30') are analogous to those in Saudi Arabia near N23°20' to N23°30' (MSS 1068-07214).

Area 5

The fifth segment of comparison across the Red Sea is located between N22° and N23° in Africa, and between N24° and N25° in Saudi Arabia. The Precambrian metamorphic rocks in this segment have regional schistosity bearing northeast on both sides of the Red Sea. In Saudi Arabia near Suq Suwayq (N24°20', E38°20')(Arrow 19, Fig. 45) a northeast trending fault and Precambrian grain extend across granitic and gneissic terrain and in greenstones, andesite, diabase, and slates; from N24°10' to N24°20' and E38°30 to E38°40' in sericite and chlorite schist. This region is also characterized by east trending faults from about N24°20' to N24°40' and E38° to E38°10', and northwest faults further inland. From N24°25' to N24°50 and E37°15' to E37°35' near Ra's Abu Madd and Jabal Hjinah there is a well known northwest trending Red Sea fault (Arrow 20, Fig. 45). Similar trends are seen in Egypt near Foul Bay.

In Sudan northeast trending schistosity and faults extend from about Ras Hadarba and Aidhab inland through Jabal Shindodai and near Wadi Diib (N22°, E36°10')(MSS 1052-07334), and are observed in a more complete zone from N22°30' to N21°50' and E35°20' to E36°20', and from N21°30' to N21°50' and E35°20' to E35°40' (Arrow 21, Fig. 45). ERTS imagery show four northeast faults or lineaments not shown on the geological maps (Brown, G. F., and Jackson, R. O., 1963) of this area along with many circular features that appear similar to the granitic intrusives in Saudi Arabia. This area in particular bears remarkable similarity to the corresponding segment in Saudi Arabia. Further north there appears another trendline zone from about N22°35' to N22°40' and E34°20' to E35°, bearing in a east-northeast direction with some east-west trends (MSS 1071-07390).

Area 6

The sixth area to compare extends from N23° to N24° in Egypt, and from N25° to N25°30' in Saudi Arabia. The most prominent characteristic of both sides in this segment is a series of east-west trending faults. From about N25° to N25°30' in Saudi Arabia three faults appear along Wadi al Ghumayr,

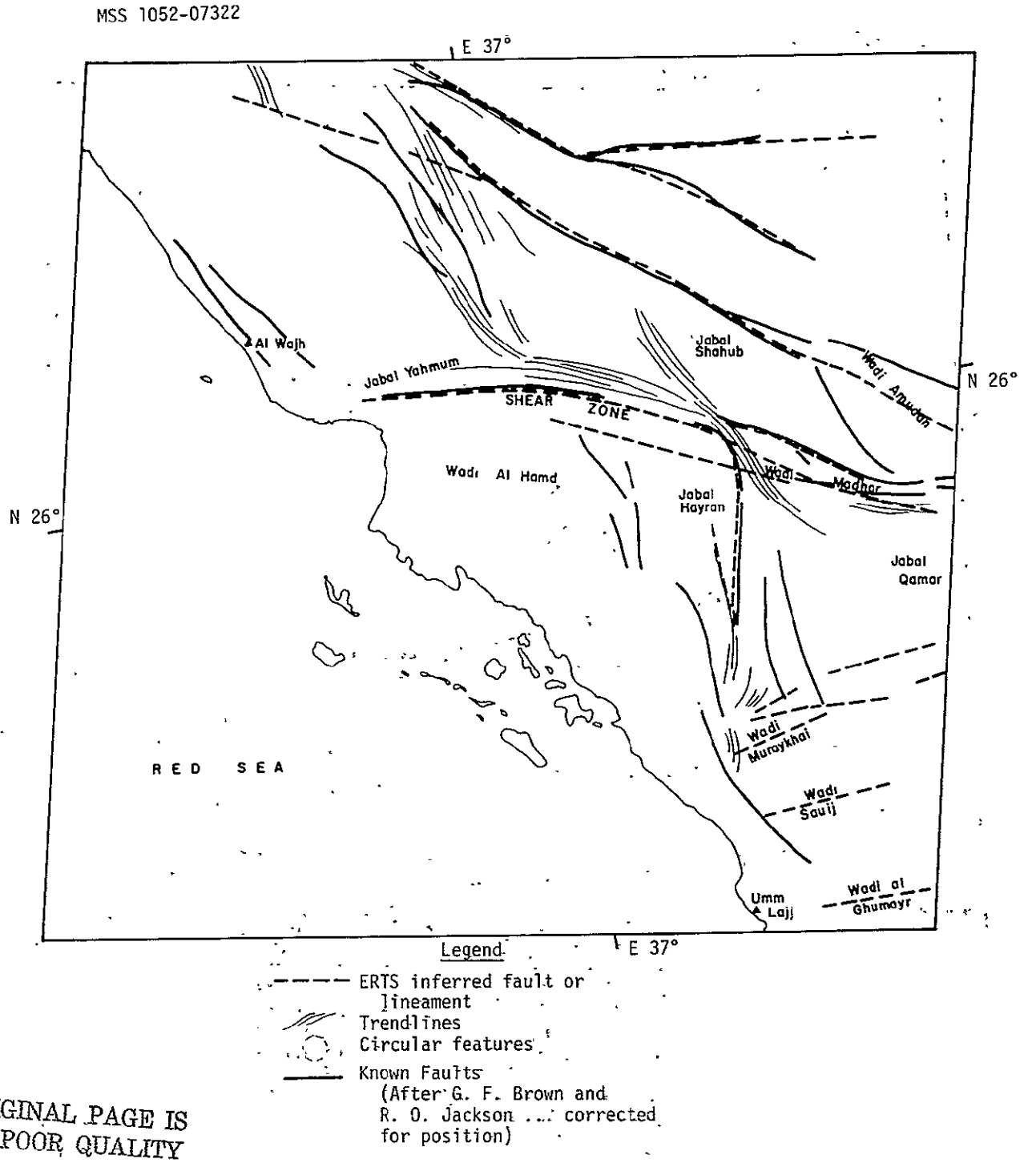

FIGURE 49 Faults, Lineaments and Trendlines of Al Hamd Shear Zone

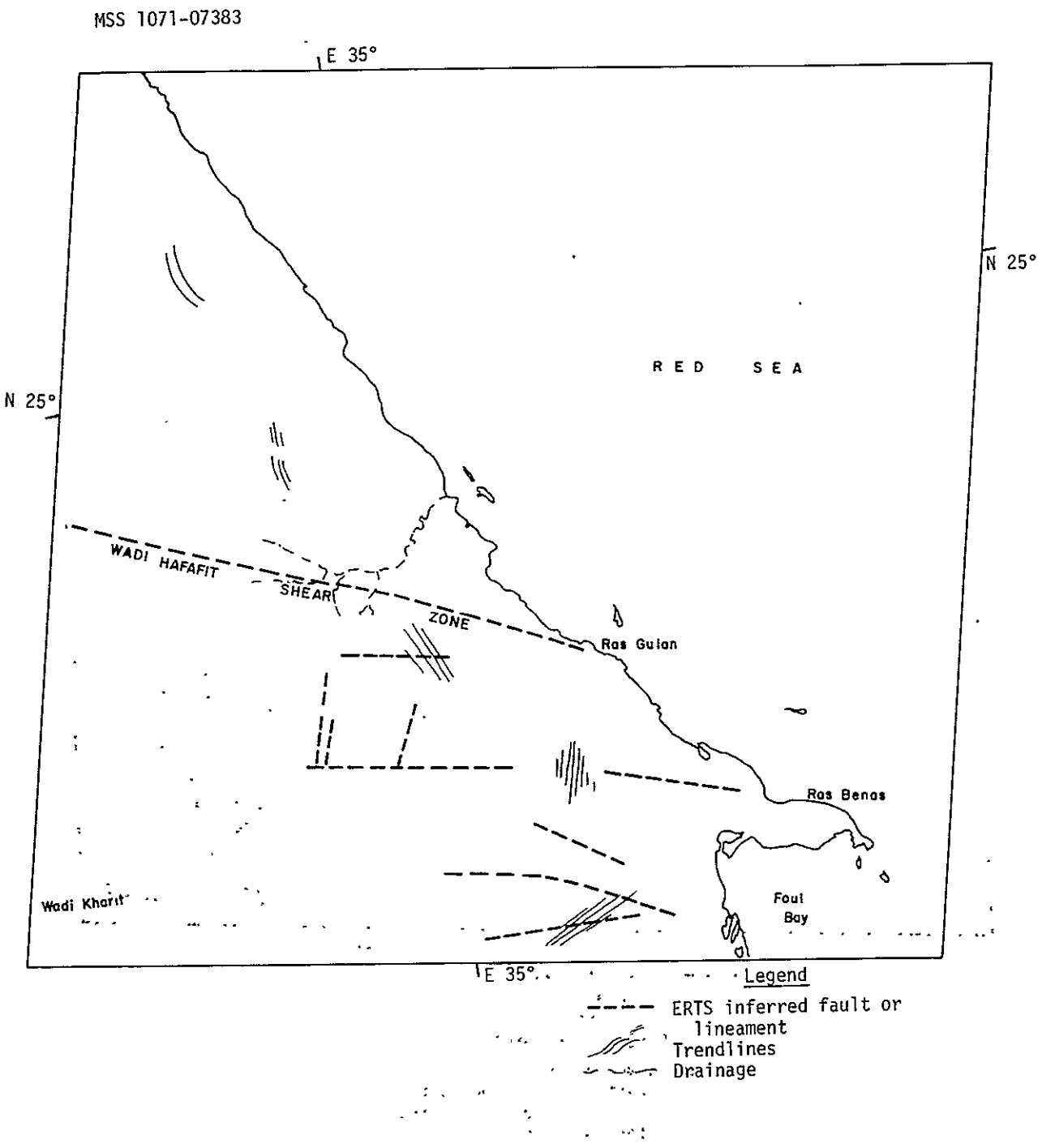

FIGURE 50 FAULTS, LINEAMENTS AND TRENDLINES OF WADI HAFAFIT SHEAR ZONE MSS 1071-07383

Wadi Sauij, and Wadi Muraykhai (MSS 1052-07233)(Arrow 22, Fig. 45). In Egypt from about N23°25' to N23°45' (Arrow 23, Fig. 45) many east-west faults can be seen in the vicinity of Jabal Umm Akra (MSS 1071-07390). A lineament trending northwest is located between N23°10' to N23°45' and E34°30' to 35°30'.

Area 7

The seventh segment, in the northern Red Sea, contains two pairs of displaced shear zones described by Abdel-Gawad (1969-1970). In Saudi Arabia a major west-northwest shear zone extends from Wadi Al Hamd to Wadi Al Batha (N25°45', E38°, mostly in sericite and chlorite schist (MSS 1052-07322)(Arrow 24, Fig. 45 and Fig. 49). In Egypt a similar structure extends from Ras Gulan to Wadi Hafafit (MSS 1071-07383)(Arrow 25, Fig. 45 and Fig. 50).

Further north, two shear zones, Abu Masarib in Saudi Arabia (Arrow 26, Fig. 45) and Gebel Duwi in Egypt (Arrow 27, Fig. 45), appear to be two displaced segments of a once continuous structure (Abdel-Gawad, 1969-1970). Abu Masarib shear zone is very prominent (MSS 1071-07374).

In Egypt, much of the area crossed by Gebel Duwi shear zone is largely obscured by clouds in the ERTS-1 imagery available during this study. The fault zone is, however, well documented in the literature (Abdel-Gawad, 1969, Youssef 1968) and is observed in clear areas of the ERTS image (MSS 1072-07435).

Conclusions

Study of regional metamorphic grain of the Precambrian basement complex across the Red Sea shows that the Arabian-Nubian massif can be divided roughly into three main parts.

The southern part of the massif up to approximately 21°N in Arabia and 19°N in Africa is characterized by regional schistosity trending generally north.

The northern part of the massif from 28°N to 25°N in Arabia and from 26°N to 23°N in Africa is characterized by northwest and west-northwest schistosity.

In the middle part of the massif, northeast trending schistosity is prevalent.

It is also interesting to note that major shear zones and large faults associated with Precambrian structures also tend to follow the general trend of schistosity and seem to have no apparent relation to the younger faults associated with the development of the rift and which control the fault blocks outlining the Red Sea depression.

A shift of approximately two degrees of latitude seems to exist between the African and the Arabian plates, which amounts to a relative northward movement of Arabia some 200 km.

TECHNIQUES EMPLOYED

Bulk Data Evaluation

Standard light tables and projectors were used for bulk data evaluation.

Generation of Fine Geographic Grids

A Science Center computer program together with geographic coordinates on NASA-supplied formats was used to generate a complete geographic grid on an overlay. Computer flexibility of plotting coordinates to any desired grid increment allows quick and accurate location of all important features observed.

Outline and Annotation of Physiography and Geology

Annotated outline maps showing physiography and geology were made on overlays using topographic maps as the basic reference. Outlines of physiography, drainage, and major geologic units serve to speed interpretive processes.

Plotting of Major and Medium Mineral Occurrences

Correlation of mineral deposit clusters with structure requires reasonably accurate plotting of these occurrences on the imagery. This was done when necessary on overlays using both computer and graphic methods.

Plots of Earthquake Epicenters

In selected areas the location of epicenters of moderate and strong earthquakes (> 4 on the Richter scale) can be plotted on overlays corresponding to the geometry of the imagery. Plotting epicenters of various magnitudes by computer (within respective zones of accuracy) allows better assessment of their distribution with relation to observed structures.

Geological Photointerpretation

The visual photogeologic interpretive technique was employed using the criteria of color, tonal differences, texture, pattern. Both color composite and black and white prints were utilized for the photointerpretation. Positive color transparencies were used for projection of scenes and for detailed studies under the binocular microscope.

Literature Survey

During the interpretation investigations, correlations were established with published field data (geologic, topographic, structural, and tectonic maps, mineral distribution maps, epicenter or strain release maps, maps of active faults, geological reports, journal articles, etc.).

Selective Emphasis

A study of this nature has to be selective in emphasis. Certain areas of features judged to be of particular importance economically or to be critical to a scientific principle of hypothesis were probed in more detail. The principal target area (the south-western part of North America) received the greater emphasis. Correlation with the Red Sea and African rift system will be a long-range scientific objective.

Correlation with Other Spacecraft Imagery

As a result of previous Rockwell geological interpretation of Gemini and Apollo photographs of both target areas, a significant amount of background data directly related to this investigation has been accumulated. We applied this experience in correlating ERTS imagery to Gemini, Apollo, and Skylab imagery.

Aircraft Data of Test Sites/Aerial Photographs

For confirmation or documentation certain observations required close examination of geological features in greater detail and higher ground resolution. In such cases, use was made of available NASA test site aircraft data and other aerial photographic data of adjacent areas.

Field Trips

Field observations were made in California and Nevada to examine the surface expressions of certain linears and suspected faults.

PHOTO-INTERPRETATION INSTRUMENTS AND REPRODUCTIVE EQUIPMENT

Standard photographic reproduction techniques were used as necessary, and enlargements were made of specific areas. The following is a partial list of equipment used:

Bausch and Lamb Zoom Transfer Scope
Light Tables
30 mm and 70 mm slide projectors
Sketchmaster
Mirror Stereoscope
Binocular microscope
Magnifiers
Griscombe Microfilm Reader 4317
3M Film AC 400 Microfilm reader printer (16mm and 35mm)
Thermofax 3M Filmac 100 reader printer
Simon Omega D2 enlarger w/Rodenstock Omegaron 135mm F 4.5 lens
Time-o-lite 8 x 10 contact printer
Kenro vertical '24' copy camera
Fotorite model DD1437 film and paper processor
AGA-Gevaert copyproof CP 38 Processor
Polaroid MP-3 land camera multipurpose industrial view camera
w/ Rodenstock F4.5 75mm lens

The computer equipment consists of a CDC 6600 computer with a CALCOMP digital incremental plotter and CI 120 graphic display device. The 6600 is a 315,000 60 bit word machine was mainly used to plot earthquake epicenters on imagery overlays.

REFERENCES

Abdel-Gawad, M., and Silverstein, J., Earthquake Epicenters and Fault Intersections in Central and Southern California, Type II Progress Report for Period June-November 1972, prepared for NASA Goddard Space Flight Center, Greenbelt, Maryland, 1972.

Abdel-Gawad, M., and Silverstein, J., ERTS Applications in Earthquake Research and Mineral Exploration in California, Symposium on Significant Results Obtained from the Earth Resources Technology Satellite-1, V. I, A, NASA Washington, D.C., pp. 443-449, 1973.

Abdel-Gawad, M., Geological Structures of the Red Sea Area Inferred from Satellite Pictures. In "Hot Brines and Recent Heavy Metal Deposits in the Red Sea Area" (Degens, E. T., and Ross, D. A., eds.), Chap. 5, New York: Springer-Verlag; also Am. Geophys. Un. Trans. (Abstr.) 49, 1, p. 192, 1969.

Abdel-Gawad, M., Identification and Interpretation of Tectonic Features from ERTS-1 Imagery - Type I Progress Report for period July 31 to September 30, 1972, p. 2.

Abdel-Gawad, M., Interpretation of Satellite Photographs of the Red Sea and Gulf of Aden, Phi. Trans. Royal Soc., London, A, 267, pp. 23-40, 1970.

Abdel-Gawad, Monem and Silverstein, Joel, The Fault Pattern of Southern California - A Model for Its Development (Abstract), Geological Society of America 1972 Annual Meeting, Minneapolis, Minnesota, November 13, 1972.

Abdel-Gawad, M., The Gulf of Suez: A Brief Review of Stratigraphy and Structure, Phil. Trans. Royal Soc., London, A, 267, pp. 41-48, 1970.

Allen, C. R., St. Amard, P., Richter, C. F., and Nordquist, J. M.: Relationship between seismicity and geologic structure in the southern California region: Bull. Seism. Soc. Am., V. 55 (1965), pp.753-797.

Andel, Tjeerd H. van and George G. Shor, Jr., "A Symposium on Marine Geology of the Gulf of California", Scripps Institution of Oceanography, Univ. of Calif., The American Association of Petroleum Geologists, Tulsa, Oklahoma, 1964, pp. 66-67, Plate 2 and Plate 3, by Rusnak, Fisher, and Shephard.

Bailey, E. H., Mercury in the United States-United States Geol. Survey Mineral Invest. Res. Map MR30, 1962.

Bailey, E. H. and Everhart, D. L., Geology of quicksilver deposits of the New Almaden district: U. S. Geol. Survey Prof. Paper 360, 1964, pp. 206.

Bailey, E. H. and Smith, R. M., Mercury - its occurrence and economic trends: United States Geol. Survey Circ. 496, 1964, pp. 1-11.

Brown, Glen F., and Jackson, Roy O., Geology of the Kingdom of Saudi Arabia; NW Hijaz, Southern Hijaz, Tihamat Ash Sham, and Asir Quadrangles, U.S. Geological Survey and Arabian American Oil Company, Scale 1:500,000, 1963.

California Department of H_2O Resources Bulletin 116-2 Crustal Strain and Fault Movement Investigation - Faults and Earthquake Epicenters in California - January 1934 - December 1961.

Callaghan, E. and V. P. Gianella, The Earthquake of January 30, 1934 at Excelsior Mtns., Nevada, Bull. Seism. Soc. An. 25, 1935, pp. 161-168.

Christensen, M. N., Late Cenozoic Crustal Movements in the Sierra Nevada of California: Geol. Soc. America Bull., V. 77, 1966, pp. 163-182.

Cook, Kenneth L., Rift System in the Basin and Range Province in the World Rift System. Geol. Survey of Canada Paper 66-14, 1965, pp. 246-279.

Cserna, Zoltan de, "Tectonic Map of Mexico, The Geological Society of America", 1961.

Davis, F. F., Mercury in Mineral Commodities of California: Calif. Div. Mines and Geology Bull. 176, 1957, pp. 341-356.

Davis, F. F., Mercury in Mineral Resources of California, Calif. Div. of Mines and Geology Bulletin 191, 1966, pp. 247-254.

Eardley, A. J., Structural Geology of North America, New York, Harper and Row Publishers Inc., second edition, 1962, pp. 743.

Eckel, E. B. and Myres, W. B., Quick silver deposits of the New Idria district, San Benito and Fresno Counties, California: Calif. Div. Mines Report 42, 1946, pp. 81-124.

Gianella, V. P. and E. Callaghan, The Earthquake of December 20, 1932 at Cedar Mt., Nevada and Its Bearing on the Genesis of Basin and Range Structure, J. Geol. 42, 1934, pp. 1-22.

Goddard, Edwin N., "Geologic Map of North America", North American Geologic Map Committee, USGS, Washington, D.C., 1965.

Gumper, Frank J. and Christopher Scholz, Microseismicity and Tectonics of the Nevada Seismic Zone: Bull. Seism. Soc. Am. 61, 5, 1971, pp. 1413-1432.

Hamilton, Warren and Myers, B., Cenozoic Tectonics of the Western United States in the World Rift System: Geol. Survey Canada Paper 66-14, 1965, pp. 291-306.

Hamilton, Warren and W. Bradley Myers, Cenozoic Tectonics of the Western United States: Reviews of Geophysics, V. 4, 4, 1966, pp. 509-549.

Hill, D. M., C. Lao, V. A. Moore, and J. E. Wolfe, Earthquake Epicenter and Fault Map of California (Central and Southern Area), California State Dept. of Water Resources - Crustal Strain and Fault Movement Investigation Bulletin No. 116-2, 1964, January.

Kellum, L. B., "Similarity of Surface Geology in Front Range of Sierra Madre Oriental to Subsurface in Mexican South Fields", Am. Assoc. Petroleum Geologists Bull., V14, 1931, pp. 73-91.

Kellum, L. B., "Geologic History of Northern Mexico and Its Bearing on Petroleum Exploration", Am. Assoc. Petroleum Geologists Bull., V28, 1944, pp. 301-376.

King Phillip B., "Tectonic Map of North America", U.S. Geological Survey, Washington, D.C., 1969.

King, Philip, Tectonic Map of North America. U.S. Geological Survey, Scale - 1:5,000,000, 1969.

Lindgren, W., The Tertiary Gravels of the Sierra Nevada of California: U.S. Geol. Survey Prof. Paper 73, 1911, pp. 198.

Linn, R. K., New Idria Mining District in (John D. Ridge, editor) Ore Deposits of the United States, 1933-1967 - The Graton-Sales Volume, The Am. Ins. Mining, Metal. and Petrol. Engineers, New York, V. 3, 1968, pp. 1623-1649.

Lobeck, A. K., "Physiographic Diagram of North America", The Geographical Press, Hammond Inc., Maplewood, New Jersey, 1948.

Matthews and John L. Burnett, Geological Map of California, Division of Mines and Geology and USGS, Scale - 1:250,000, Olaf P. Jenkins Edition, 1965.

Mayo, Evans B., Structure Plan of the Southern Sierra Nevada, Calif.: Bull. Geological Society of America, Vol. 38, 1947, pp. 495-504.

Mitko, F. C., The Mineral Industry of California in Minerals Yearbook, V. 3, U.S. Dept. of Interior Bureau of Mines, 1968, pp. 127-158.

Neilsen, R. L., Right Lateral Strike Slip Faulting in the Walker Lane, West-Central Nevada: Bull. Geol. Soc. Amer., V. 76, 1965, pp. 1301-1308.

NOAA Geographic Hypocenter Data File (Magnetic Tape), January 1961 through December 1971.

NOAA Hypocenter Data Cards, January 1972 through August 1972.

Nolan, T. B. and R. N. Hunt, The Eureka Mining District, Nevada, in Ore Deposits of the United States, 1933-1937: The Graton-Sales Volume, V. 1, Chapter 48, 1968, pp. 966-991.

Rowan, Lawrence C. and Pamela Wetlaufer, Structural Geologic and Radiometric Analysis of ERTS-1 Images of Nevada and California: Abstract, Paper G20, Symposium on Significant Results Obtained from ERTS-1, March 5-9, 1973, sponsored by NASA/Goddard Space Flight Center, Greenbelt, Maryland, 1973, p. 46.

Rusnak, G. A., R. I. Fisher, and F. P. Shepard, "Bathymetry and Fauls of Gulf of California," Abstract in ... "A Symposium on Marine Geology of the Gulf of California," Andel, T. H. and G. Shor, Jr., Scripps Inst. of Oceanography, Univ. of Calif., The Amer. Association of Petroleum Geologists, Tulsa, Okla., 1964, pp. 59-75.

Ryall, A., Slemmons, D. B., and Gedney, L. D., Seismicity, tectonism, and surface faulting in the western United States during historic time: Bull. Seism. Soc. America, V. 56, 5, 1966, pp. 1105-1135.

Salas, ing, Guillermo P., "Carta Geologica de La Republica Mexicana," Comite de la Carta Geologica de Mexico, 1968.

Shoemaker, E. M., Structural features of southeastern Utah and adjacent parts of Colorado, New Mexico, and Arizona: Guidebook to the Geology of Utah, No. 9, Utah Geol. Soc., 1954, pp. 48-69.

Stose, G. W. and Ljungstedt, O. A. (compilers), Geologic Map of the United States, scale 1:2,500,000 (1960).

Thompson, G. A., Problem of Late Cenozoic Structure of the Basin and Ranges: Intern. Geol. Congress XXI Session, Part XVIII, 1960, pp. 62-68.

Thompson, George A., The Rift System of the Western United States in the World Rift System: Geol. Survey of Canada Paper 66-14, 1965, pp. 280-289.

Webb, B. and R. V. Wilson, Progress Geologic Map of Nevada (Map 16), Nevada Bureau of Mines, University of Nevada, Reno, Scale 1:500,000, July 1962.

Whitcomb, J. H., Allen, C. R., Garmany, J. D., and Hileman, J. A., San Fernando Earthquake Series, 1971: Focal Mechanisms and Tectonics", Reviews of Geophysics and Space Physics, Vol. 11, No. 3, 1973, pp. 693-730.

White, D. E. and Roberson, C. E. Sulphur Bank, California, a major hot-spring quicksilver deposit: in Petrologic Studies: A volume in honor of A. F. Buddington: The Geological Society of America, 1962, pp. 397-428.

Whitton, C. A., The Dixie Valley Fairview Peak, Nevada earthquake of December 16, 1954, Geodetic Measurements: Bull. Seism. Soc. Am. 47, 1957, pp. 321-325.

Youssef, M. I., Structural Pattern of Egypt and Its Interpretation, American Association of Petroleum Geologists Bulletin, 52, 4, 1968, pp. 601-614.

APPENDIX

MINERAL TARGET AREAS IN NEVADA FROM GEOLOGICAL ANALYSIS OF ERTS-1 IMAGERY

Monem Abdel-Gawad
and
Linda Tubbesing

A report describing results of related company IR&D supported work.

SCTR- 75-1

MINERAL TARGET AREAS IN NEVADA FROM GEOLOGICAL ANALYSIS OF ERTS-1 IMAGERY

Monem Abdel-Gawad
and
Linda Tubbesing

February 1975

Distribution

Science Center

Executive File
Library (4)
Patent Section

Group Leader
Author (75)

A. H. Muir, Jr.
R. M. Housley

Other

C. J. Meechan, 001, 805, C55

Goddard Space Flight Center
Greenbelt, Maryland 20071

PREFACE

Over the past four years, the Rockwell International Science Center has been pursuing research on the applications of space photography in the discipline of geology. In addition to the Rockwell International supported effort, the Science Center has been under contract to NASA Goddard Space Flight Center (ERTS-1 Contract #NAS5-21767) and Johnson Space Center (Skylab Contract #NAS2-7523) to perform investigations related to the identification and interpretation of regional geological structures from space imagery and to attempt to correlate known mineral deposits with these observed geological structures. As part of the Rockwell funded application of this technology, the Science Center has carried out an IR&D project for establishing the feasibility of utilizing space imagery to locate favorable target areas for future mineral exploration. The space imagery used in this study were taken by the NASA Resources Technology Satellite ERTS-1. This report presents a summary of the results of the IR&D project.

PAGE INTENTIONALLY BLANK

ABSTRACT

Geological analysis of ERTS-1 scene MSS 1053-17540 suggests that certain known mineral districts in east-central Nevada frequently occur near faults or at faults or lineament intersections and areas of complex deformation and flexures. Seventeen (17) areas of analogous characteristics were identified as favorable targets for mineral exploration. During reconnaissance field trips we visited eleven areas. In three areas we found evidence of mining and/or prospecting not known before the field trips. In four areas we observed favorable structural and alteration features which call for more detailed field studies. In one of the four areas limonitic iron oxide samples were found in the regolith of a brecciated dolomite ridge. This area contains quartz veins, granitic and volcanic rocks and lies near the intersection of two linear fault structures identified in the ERTS imagery. Semiquantitative spectrographic analysis of selected portions of the samples showed abnormal contents of arsenic, molybdenum, copper, lead, zinc, and silver. These limonitic samples found were not in situ and further field studies are required to assess their source and significance.

PAGE INTENTIONALLY BLANK

INTRODUCTION

One of the objectives of our research project funded by Rockwell International Science Center (CFY 1974) was to investigate the application of space imagery for identifying targets for mineral exploration and to carry out field studies in order to check our observations in the field. This special report describes significant results obtained from analysis of an ERTS Scene No. 1053-17540 over east-central Nevada.

BACKGROUND

Research on the utilization of space imagery as a tool for mineral exploration is based on the assumption that sites of hydrothermal mineral concentrations may have characteristics which can either be directly observed in the imagery or more likely to be indirectly derived from a combination of geological indicators. The assumption is generally valid because mineral deposits do not occur at random and are often associated with ore guides. Although each mineral district has some unique characteristics, occurrences in a given metallogenic province often have in common distinctive similarities in their modes of occurrence such as a favorable host rock, type of structural control, the mineral assemblage and alteration features. Global factors, which control the distribution and type of metallogenic provinces, are caused by deep seated tectonic and magmatic processes within the earth's crust and are reflected in an intimate relation between metallogenic and petrographic provinces. On

a regional scale, many geologists have presented persuasive arguments that clusters of mineral deposits tend to occur at the intersections of tectonic belts. An example is the porphry coppèr districts in southern Arizona which lie at the intersection of Jerome and Texas tectonic belts. Individual lineaments and their intersections have also been noted to control the location of mineral districts and even an individual large mine. On the local scale of an individual mine detailed geological studies have frequently revealed that ore bodies are structurally controlled. In cases, the ore body may occur along a specific structure such as a shear zone, a fault, a breccia pipe, etc.

If these structures could be identified, satellite imagery could be utilized in mineral exploration. It has become very well known that linear structures such as faults, fractures and shear zones are among the most prominent features observed in satellite imagery and are the easiest to map. It is also true that some "lineaments" recognized by researchers are subtle and are not recognized by all. Subjectivity of interpretation no doubt complicates lineament analysis of imagery and detracts from the basic validity of this potentially useful approach.

Area of Investigation

One area selected for this study is in the Basin and Range province in east-central Nevada. The space imagery used is ERTS-1 Scene No. 1053-17540 (Fig. 1).

Selection of this particular scene for detailed study was based upon several geological factors:

1. From regional stratigraphic considerations, the area lies mainly in the eastern Nevada province which is underlain largely by Precambrian metamorphic and sedimentary rocks and particularly by Paleozoic carbonate rocks in contradistinction to the western province characterized by Paleozoic and Mesozoic clastic rocks (Nolan 1943, 1962). The significance of this distinction is that the carbonate strata particularly the dolomites of Cambrian age have been known to be favorable host rocks for emplacement of mineral deposits where intruded by the Laramide granitic stocks.

2. Most of this area lies east of the leading edge of the Roberts Mountain thrust which brought the western clastic Paleozoic section on top of the carbonate section (Fig. 3). Farther west, within the domain of this major thrust many mineral deposits probably occur concealed beneath the upper clastic plate; several major mineral districts occur in erosional windows where the carbonate section is uncovered.

3. Although large areas have not been geologically mapped in detail, many Laramite granitic intrusives are known to occur.

4. Besides the carbonates as favorable host rocks, Tertiary acidic volcanic tuffs and rhyolites which are known to be good host rocks for precious metals are widespread and are exposed in many places from beneath the generally barren volcanic flows.

5. The area lies within the eastern Nevada metallogenic province characterized by major lead and zinc deposits with associated gold and silver. The western province is known for gold and silver, tungsten, antimony, mercury and iron. Two northwest-trending mineral belts or

metallogenic lineaments cross the area: Ely, Battle Mountain-Eureka. The Lovelock-Austin and Fallon-Manhattan belts may also project southeastward (Figs. 3 and 4).

6. The scene includes three major mining districts: Eureka, Mount Hamilton, and Ruth: major producers of silver, gold, lead, zinc, copper and molybdenum. In addition, many smaller mining districts and individual mines are present.

Analysis of the structural pattern in relation to those known occurrences was made in order to gain some insights which may help us identify structurally analogous areas.

Approach

The basic approach in conducting this investigation was to: 1) analyze the structural pattern inferred from the imagery in relation to known mineral districts and relevant geological data, and 2) apply this analysis in identifying favorable sites for detailed mineral exploration in the field. In order to attain our objectives we performed the following tasks:

1. Assembled and plotted on overlays relevant data from the literature. These included: a) Basic geographic and geomorphologic data. b) The locations of known mineral districts classified by type and relative size of production, as well as many individual mines. c) Major structural elements, lineaments or mineral belts published in the literature. d) Basic geological information on the distribution of major time-stratigraphic or rock units.

2. Identified and mapped significant structures which include: a) Linears such as inferred faults, shear zones or fractures. b) Structural trends showing bends, flextures, oroclines, discontinuities.

3. Analyzed all pertinent data in relation to the distribution of known mineral districts.

4. Identified candidate targets for exploration on the basis of a) Location within the structural pattern such as intersections, flexures, re-entrants and areas of complex deformation. b) Areas showing color and textured characteristics similar to those observed in known mining districts.

5. Identified priorities for field checking mainly on the basis of easy access from major transportation routes and probable presence of favorable host rocks.

6. Carried out reconnaissance field observations for obtaining ground truth data.

PROGRESS

The area selected for this investigation covered approximately 26,000 km^2 in the Basin and Range province of east-central Nevada (Fig. 1).

In order to apply the concept that analogous metallogenic districts often show similarities in their structural settings, we plotted known mineral districts on imagery overlays showing the elements produced and their relative size of production. Figure 2 shows the known mineral

districts and occurrences in relation to geological structures inferred from ERTS-1 imagery. Figure 3 and 4 show the axes or trends of major mineral belts which cross or project into the area taken from Roberts (1964). The leading edge of the Robert Mt. thrust was also approximately located. The mineral belts suggested by Roberts are: Ely, Battle Mt.-Eureka, Lovelock-Austin and Fallon-Manhattan, all trending northwest and Pioche which trends east-west.

The ERTS-1 image was analyzed to identify and map significant structural lineaments, fault zones, fracture lines and major flexures or structural bends. Figures 2 and 5 show the structural pattern corresponding to Fig. 1.

Some of our lineaments appear to coincide with or are parallel to the Battle Mountain-Eureka and Pioche mineral belts. The structural expressions of Ely, Lovelock-Austin, and Fallon-Manhattan mineral belts are either vague or absent. However, we noted that many mineral deposits tend to occur along faults or lineaments and particularly at their intersections (Fig. 2). Examples of these are the Eureka mining district which was a major producer of silver, gold, lead, zinc and copper. This district lies at the intersection of north and northwest and northeast trending fault systems and a structural flexure. The Ruth district, which is a major producer of copper, silver, gold, molybdenum, lead and zinc, lies at a structural flexure where north and northwest trending fault zones converge. Mount Hamilton district is known mainly for silver and gold production together with tungsten, molybdenum and copper. This district appears to be controlled by north and northwest fault systems.

From observations on the structural control of known mining areas, as well as color, tonal and textural characteristics which reflect rock properties, we have identified a number of target areas judged to be favorable for exploration.

Study of the target areas on geological maps resulted in the selection of 17 high priority targets for ground truth field investigation. The high priority target areas (Fig. 5) were selected mainly on the basis of the presence of rocks of geochemical composition favorable for mineralization. Examples of these are Paleozoic dolomites, limestones and Tertiary rhyolitic intrusives, flows and tuffs.

SUMMARY OF FIELD OBSERVATIONS

During reconnaissance field trips we visited 11 sites. In all sites we were able to identify the structural and lithologic features observed in the imagery. Table 1 lists a summary of the most pertinent field observations. Sites 17, 18, and 19 were found to have mining areas not known to us before the field trips. Sites 4, 23, 25, and 32 show favorable structural and alteration features which call for more detailed field studies.

AREA OF LIMONITIC IRON OXIDE

Area No. 4 lies in the Hot Creek Range, Morey Peak Quadrangle, Nye County, Nevada. Since available topographic maps show that section corners have not been established in much of that quadrangle, the precise location within section corners has not yet been established.

Table I. Summary of Field Observations

Sites	Field Structures	Country Rocks	Evidence of Mineralization
1	NW trending fault	Volcanic tuffs	Limonitic alteration, placer magnetite
2	ENE fractures	Tertiary volcanics	None
4	N-S and NE fault intersection	Dolomite, granite quartz veins, volcanic rocks	Gossan samples found in float
17	NW topographic linears	Tertiary volcanics	Hematitic alteration old mining areas
18	NE fracture zone	Tuffs, volcanic flows	Alteration, prospecting pits
19	Extremely deformed rocks	White tuffs, Paleozoic rocks	Prospecting pits, mining in vicinity
22	Subtle, uncertain	Paleozoic rocks	None
23	Highly deformed	Quartzites, dolomite basalt	Secondary copper minerals in basalt
24	NE anticline	Intrusive granites, dolomite, quartz veins	None visible
25	NE fracture zone	Tertiary volcanics	Widespread rock alteration
32	NW, NE faults	Volcanic tuffs	Alteration, pyrite in green tuffs

During reconnaissance field work within target area No. 4 (Fig. 5), limonitic iron oxide samples were found in the regolith of a dolomite ridge. The area lies at the intersection of a northeast-trending fault zone with a north-trending regional fault zone which aligns with the Eureka mining district. The latter zone is approximately parallel to the leading edge of the Roberts Mountain thrust. The country rock consists of dolomite, a favorable host rock for sulfide mineralization, cut by quartz veins and intrusive granite. We have not located any of this limonitic material in situ and further detailed field work and geophysical measurements are needed to establish the source of the float and its economic significance.

Table 2, columns 2, 3, and 4 show semiquantitative emission spectroscopic analyses of representative material scraped from three distinctively different color regions in these limonitic samples. A large number of semiquantitative x-ray fluorescence analyses done in our scanning electron microscope showed that in addition to the major elements, potassium at about the one percent level and arsenic at less than one percent were generally distributed through these samples. On a scale varying from centimeters to micrometers no significant local concentrations of important elements could be found.

Gray dolomite samples collected from the regolith and a brecciated outcrop are veined with calcite. Spectroscopic analysis of white, fluorescent encrustations shows trace amounts of lead, copper, and silver, Table 2, column 5.

Table 2. Semiquantitative Analysis* of Samples Found in Hot Creek Range, Nevada

	Red	Yellow-Orange	Black	White	Best
Fe-	55.%	56.%	65.%	0.57%	35.%
Si-	5.4	5.5	2.3	2.1	4.0
Aℓ-	1.3	1.1	0.36	0.50	4.4
As-	0.74	0.76	0.69	-	17.
Ca-	3.5	1.7	0.33	29.	2.6
B-	0.016	ND<0.003----------		TR<0.005	0.22
Sb-	-	ND<0.05----------		-	0.95
Mg-	0.22	0.49	0.22	6.1	0.40
Mn-	0.042	0.20	0.14	0.013	0.12
Pb-	0.091	TR<0.02----------		0.016	0.63
Mo-	0.082	0.086	0.034	-	0.28
V-	0.0051	0.0063	0.0034	-	0.0090
Cu-	0.017	0.027	0.023	0.00041	0.18
Ag-	0.0010	TR<0.0002----------		TR<0.002	0.0045
Zn-	0.064	0.26	0.073	-	0.86
Ti-	0.085	0.027	0.0096	0.027	0.049
Ni-	0.0026	0.0038	0.0016	TR<0.002	0.017
K-	-	ND<0.50----------		-	TR<0.50
Cr-	TR<0.0005	0.0058	TR<0.002	0.00075	TR<0.002
Other Elements		nil	nil		nil

*Pacific Spectrochemical Laboratory, Inc., Los Angeles, California

Our first spectroscopic analysis of red limonitic material showed concentrations of arsenic, antimony, lead, and zinc much higher than a subsequent analysis of similar material taken for verification. These initial results are listed in Table 2, column 6. Flakes from all identifiable red areas in the remaining samples have been examined in the scanning electron microscope. No region with arsenic, lead, or zinc concentrations approaching those in column 6 could be found. Therefore, it is certain that even if that analysis is correct, it can represent only a very small fraction of the material in the samples.

Available evidence seems consistent with the possibility that these samples are a gossan derived from the weathering of a massive sulfide vein, although other possible modes of origin certainly cannot be ruled out without additional work.

SUMMARY AND CONCLUSIONS

Geologic and structural analysis of an ERTS-1 scene in east-central Nevada in relation to known mineral districts resulted in the selection of 17 target areas for mineral exploration. During reconnaissance field observations three areas were found to show evidence of mining and prospecting not known before these areas were visited. Four areas showed structural as well as alteration features which appear to be favorable for detailed geological and geophysical exploration. In one area in the Hot Creek Range we found limonitic iron oxide samples in the regolith of a dolomite ridge containing abnormal contents of several economic elements. These limonitic samples found were not *in situ*, and further field exploration is needed to assess their source and significance.

REFERENCES

Nolan, T. B., 1943, The Basin and Range Province in Utah, Nevada and California; U.S. Geol. Survey Prof. Paper 197-D, pp. 141-196.

Nolan, T. B., 1962, The Eureka Mining District, Nevada; U.S. Geol. Survey Prof. Paper 406, p. 78.

Roberts, R. J., 1964, Economic Geology in Mineral and Water Resources of Nevada; Nevada Bureau of Mines Bull. 65, pp. 39-45.

Figure 1 - ERTS-1 Scene MSS 1053-17540, Band 5.

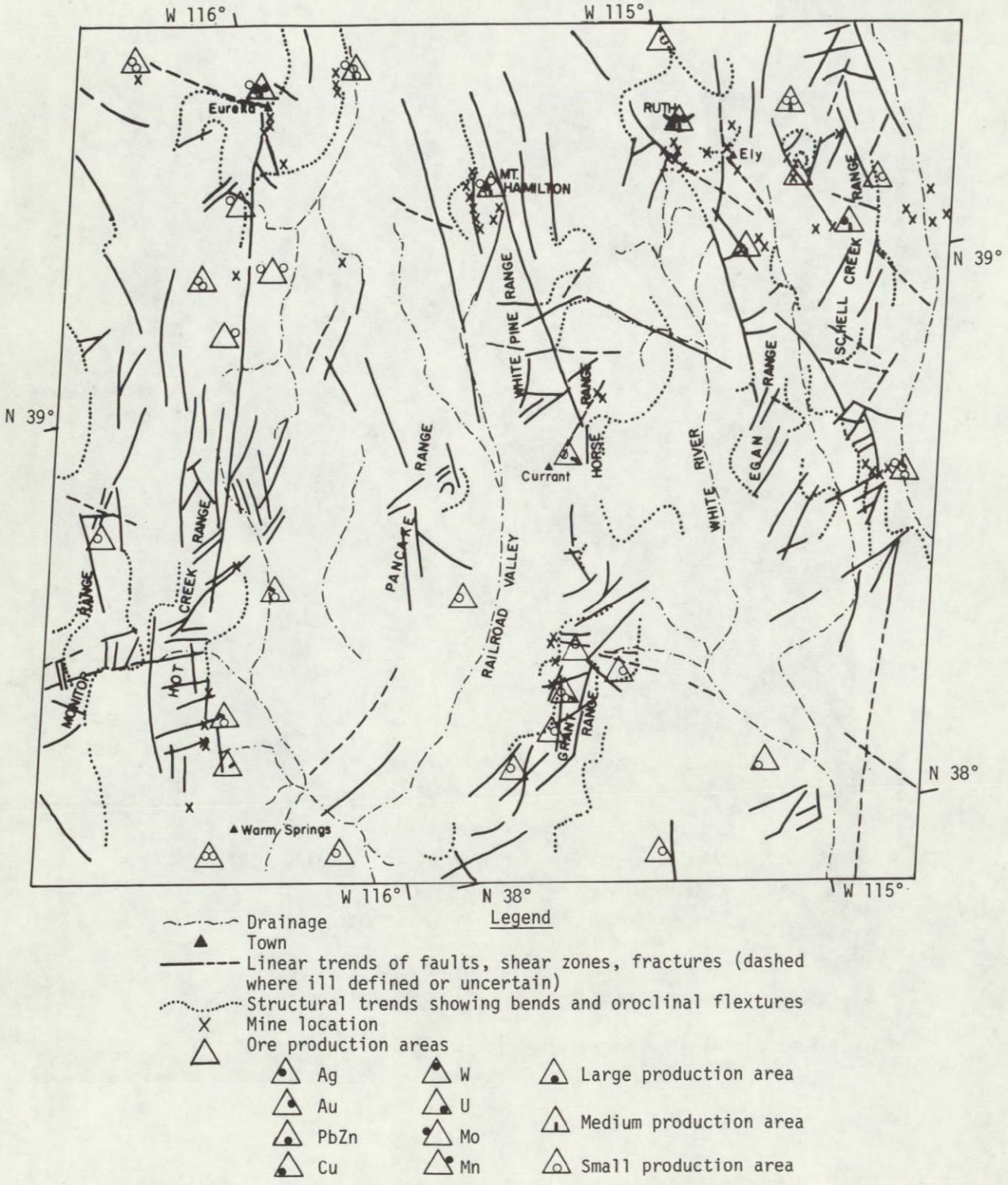

Figure 2 - Structures Inferred from ERTS-1 Imagery and Mineral Districts

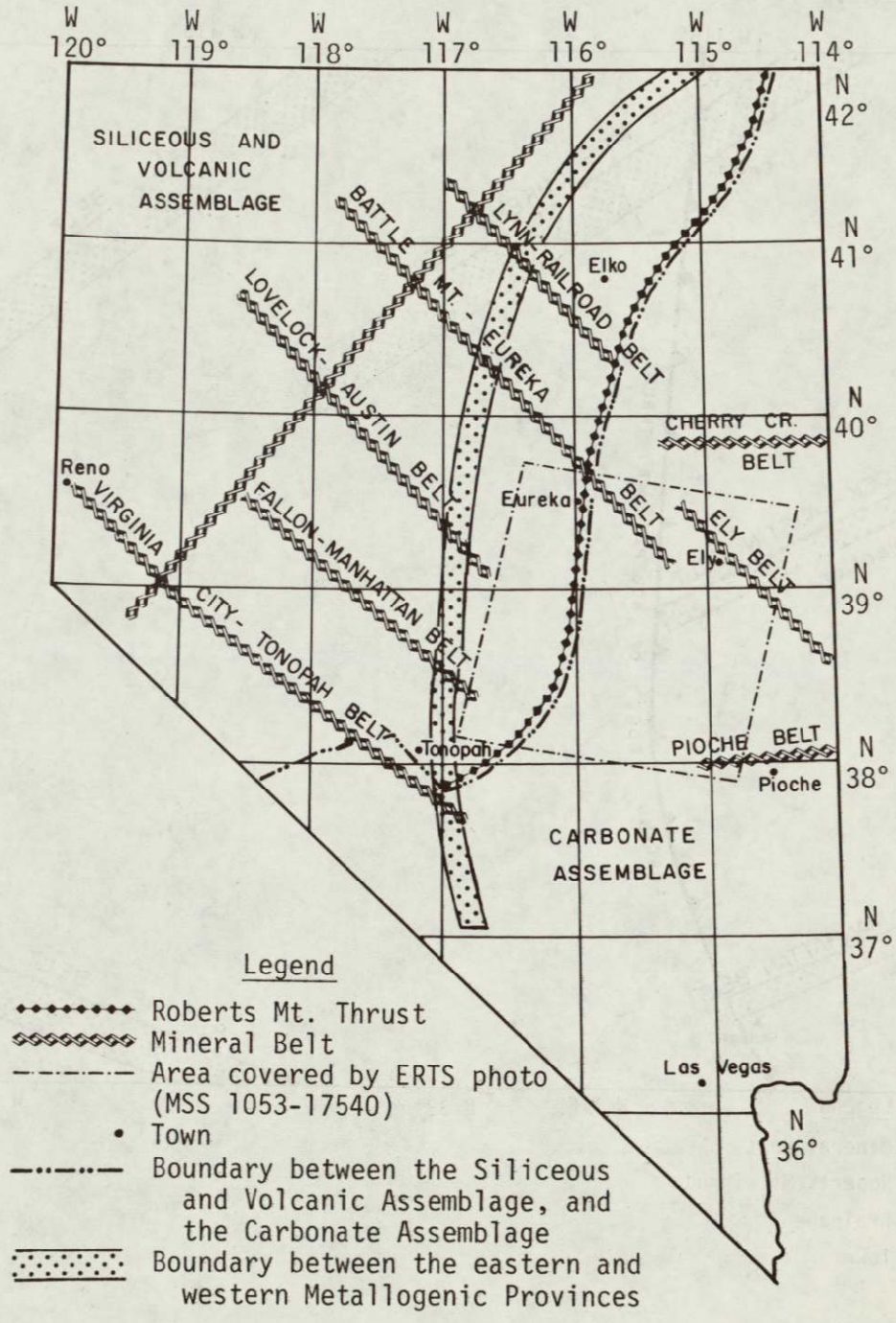

Figure 3 - Mineral Belts of Nevada (After: R. J. Roberts, 1964)

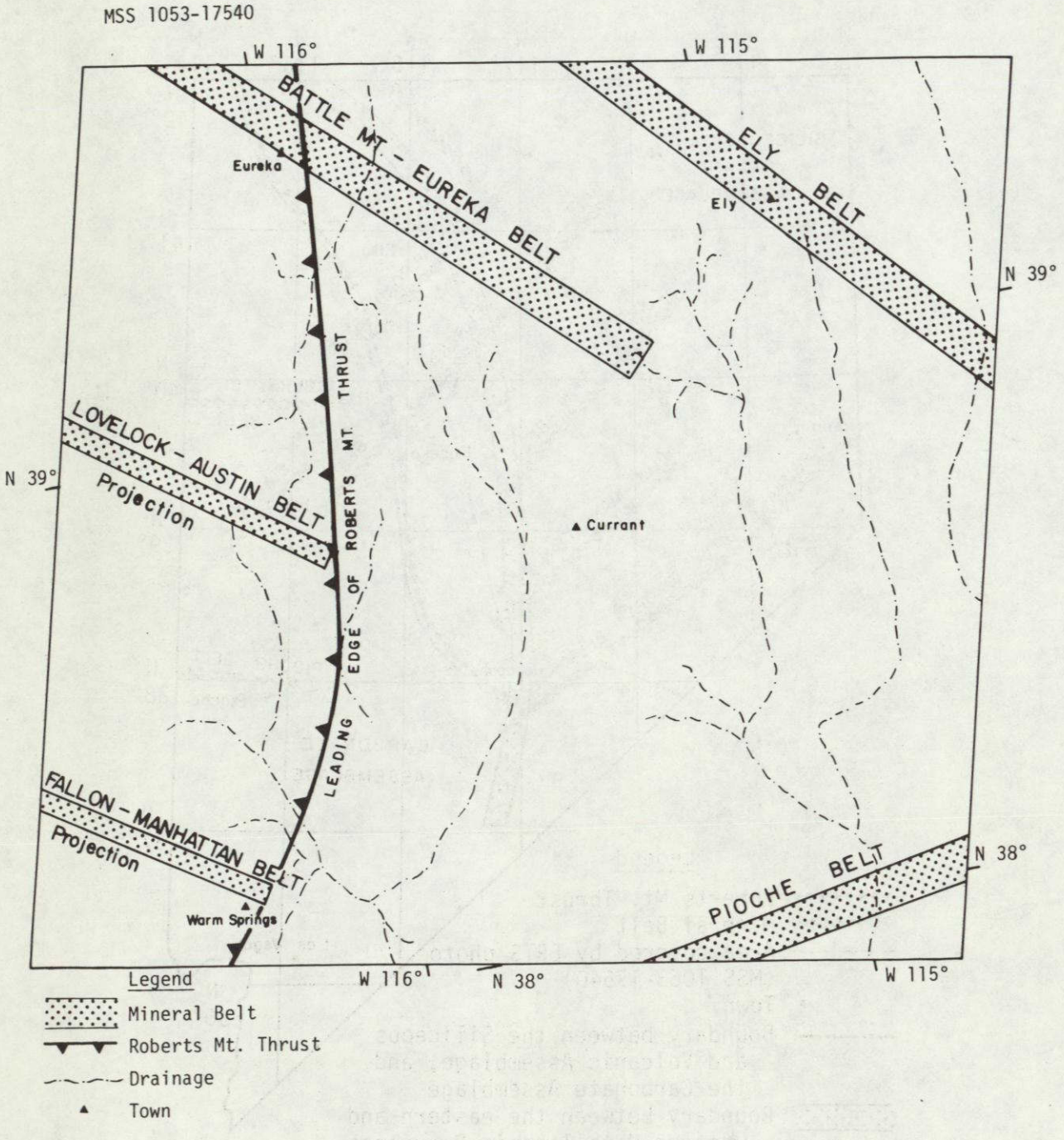

Figure 4 - Mineral Belts Projected on ERTS-1 Scene MSS 1053-17540

ORIGINAL PAGE IS
OF POOR QUALITY

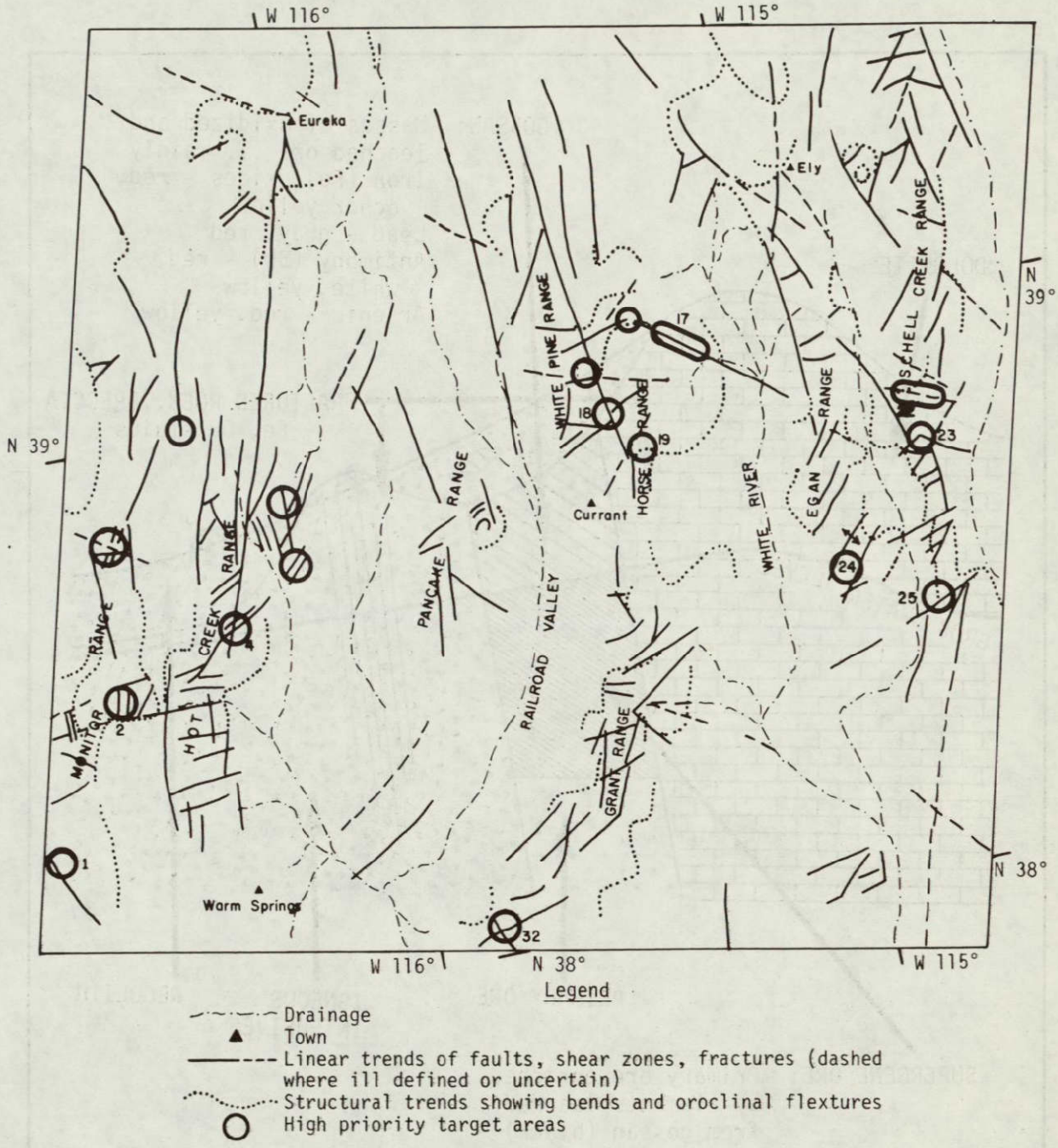

Figure 5 - High Priority Targets Identified on ERTS-1 Imagery Scene MSS 1053-17540

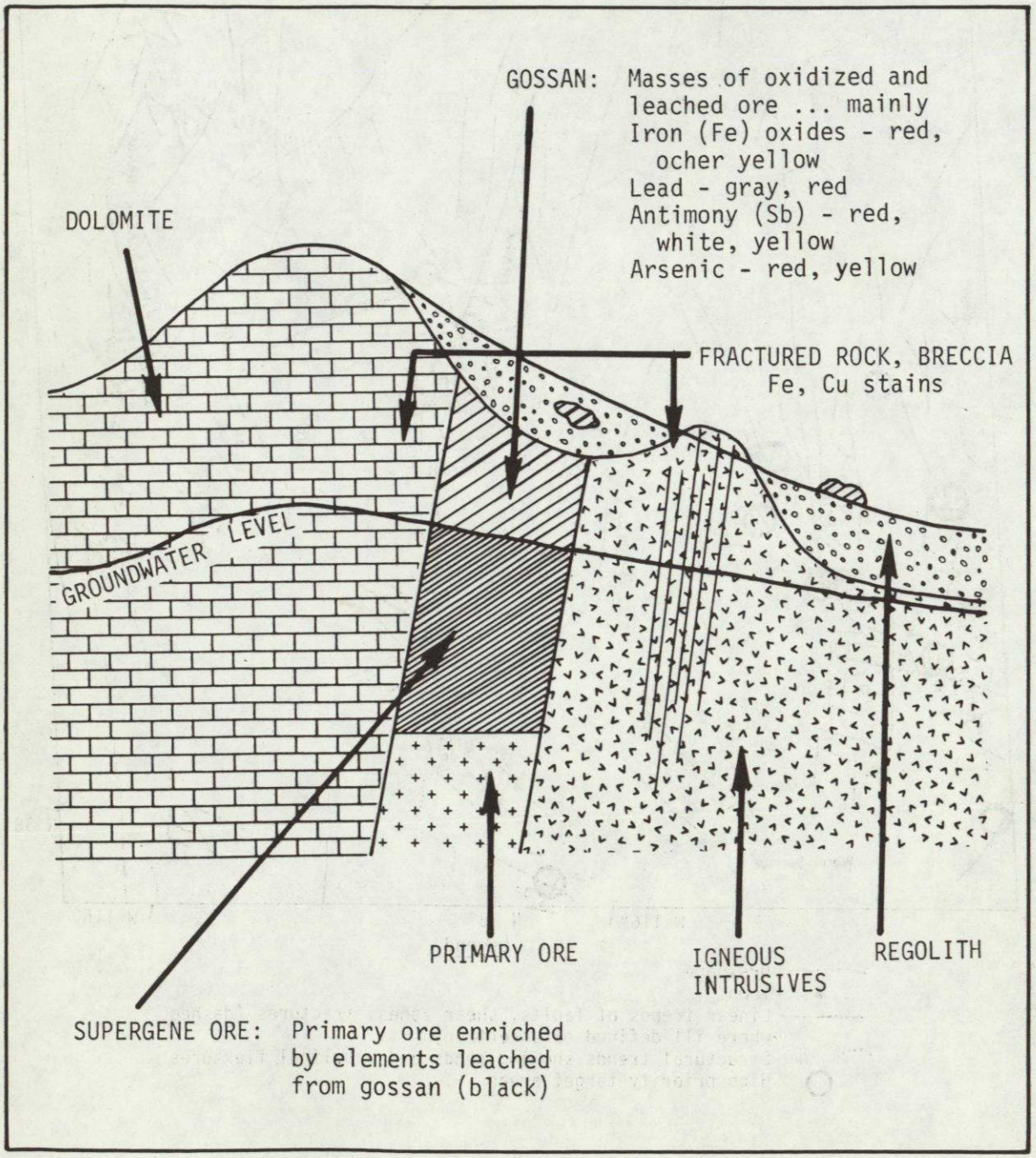

Figure 6 - Hypothetical Cross-Section of Vein Type Deposit.

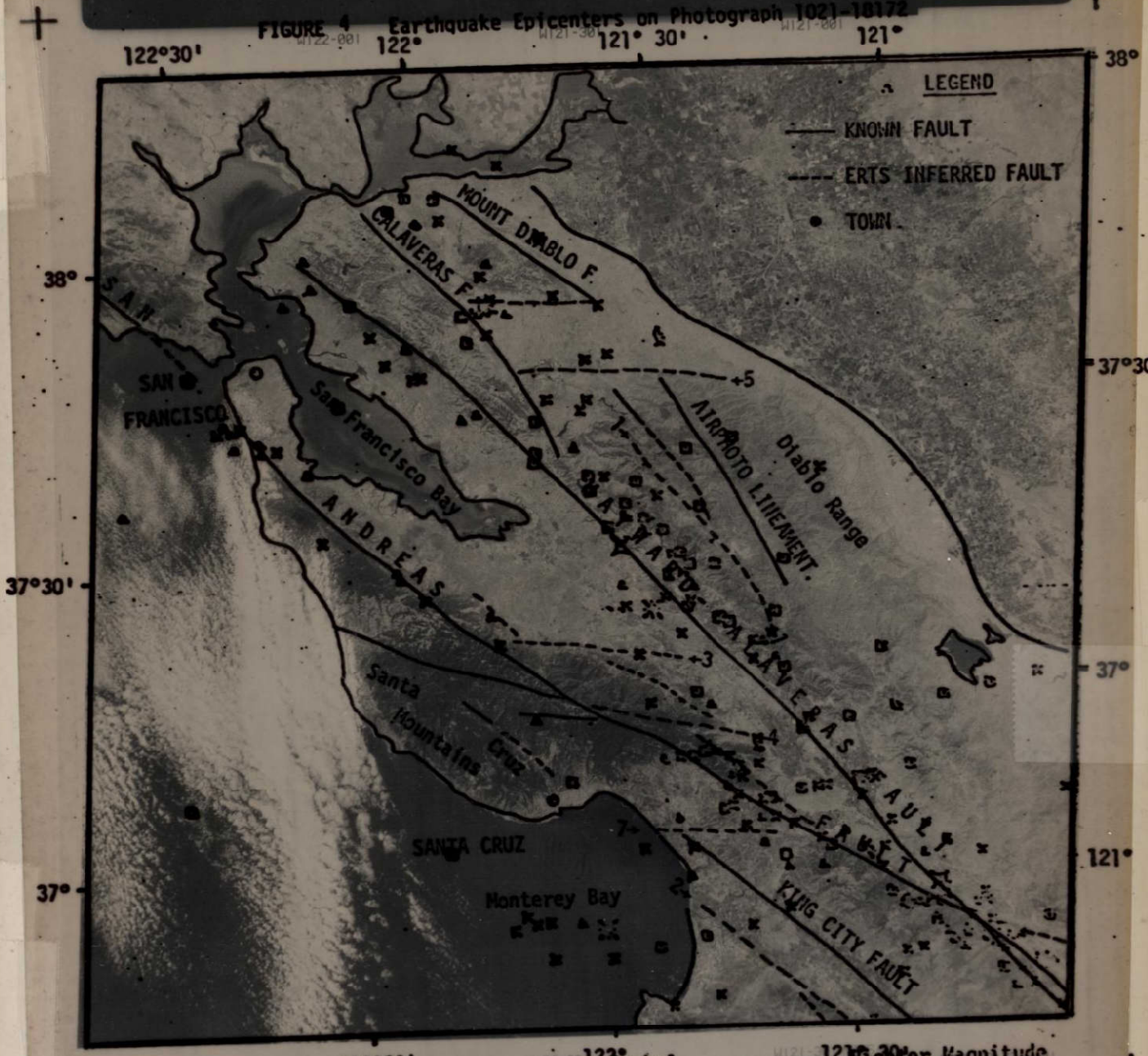

FIGURE 4 Earthquake Epicenters on Photograph 1021-18172

FIGURE 3 Fault Structures on Photograph 1021-18102

FIGURE 6 Fault Structures on Photograph 1021-18174

FIGURE 7 Earthquake Epicenters on Photograph 1021-18174

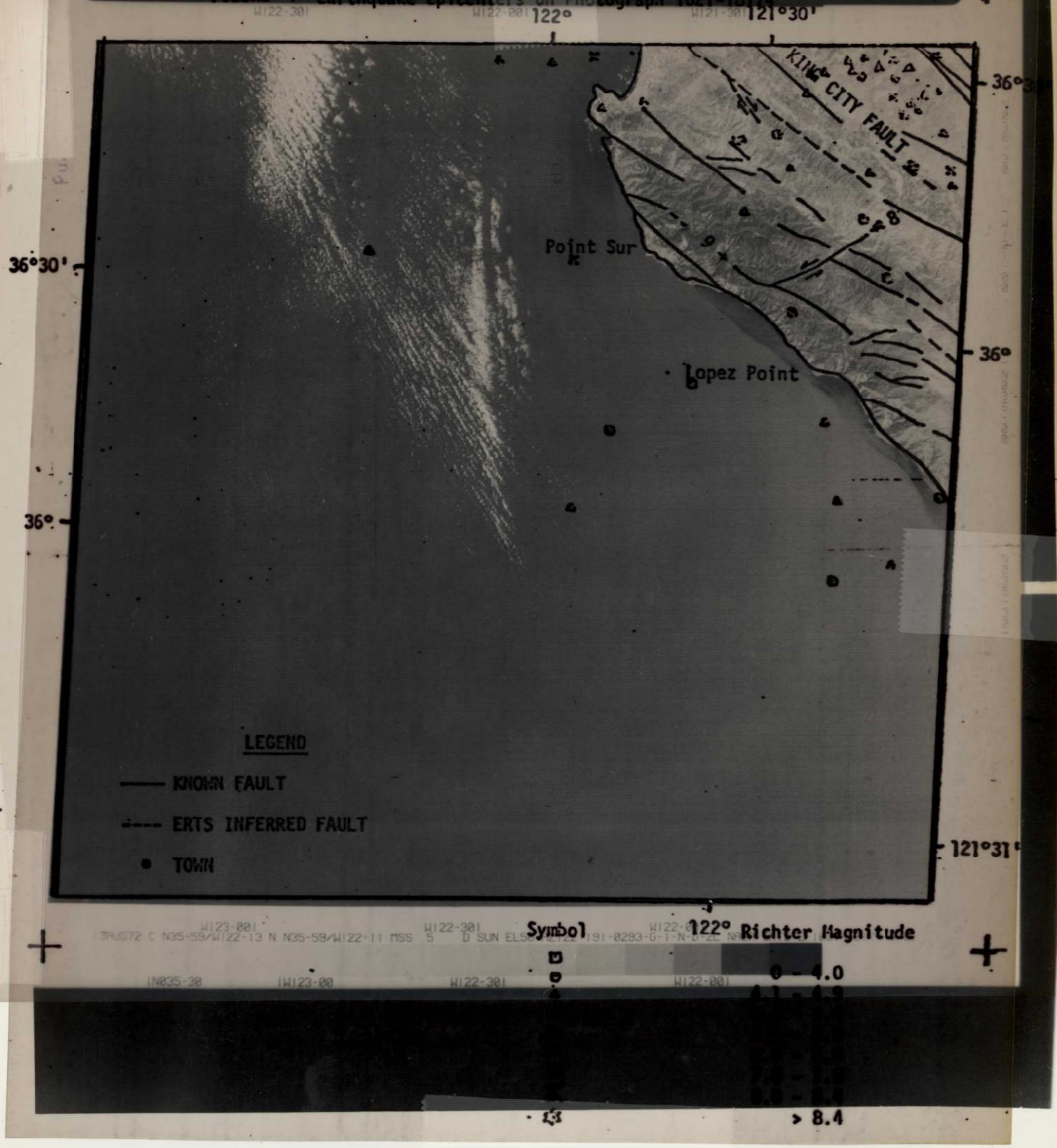

A-26

FIGURE 8 Faults Structures on Photograph 1056-18120

FIGURE 9 Earthquake Epicenters on Photograph 1056-18120

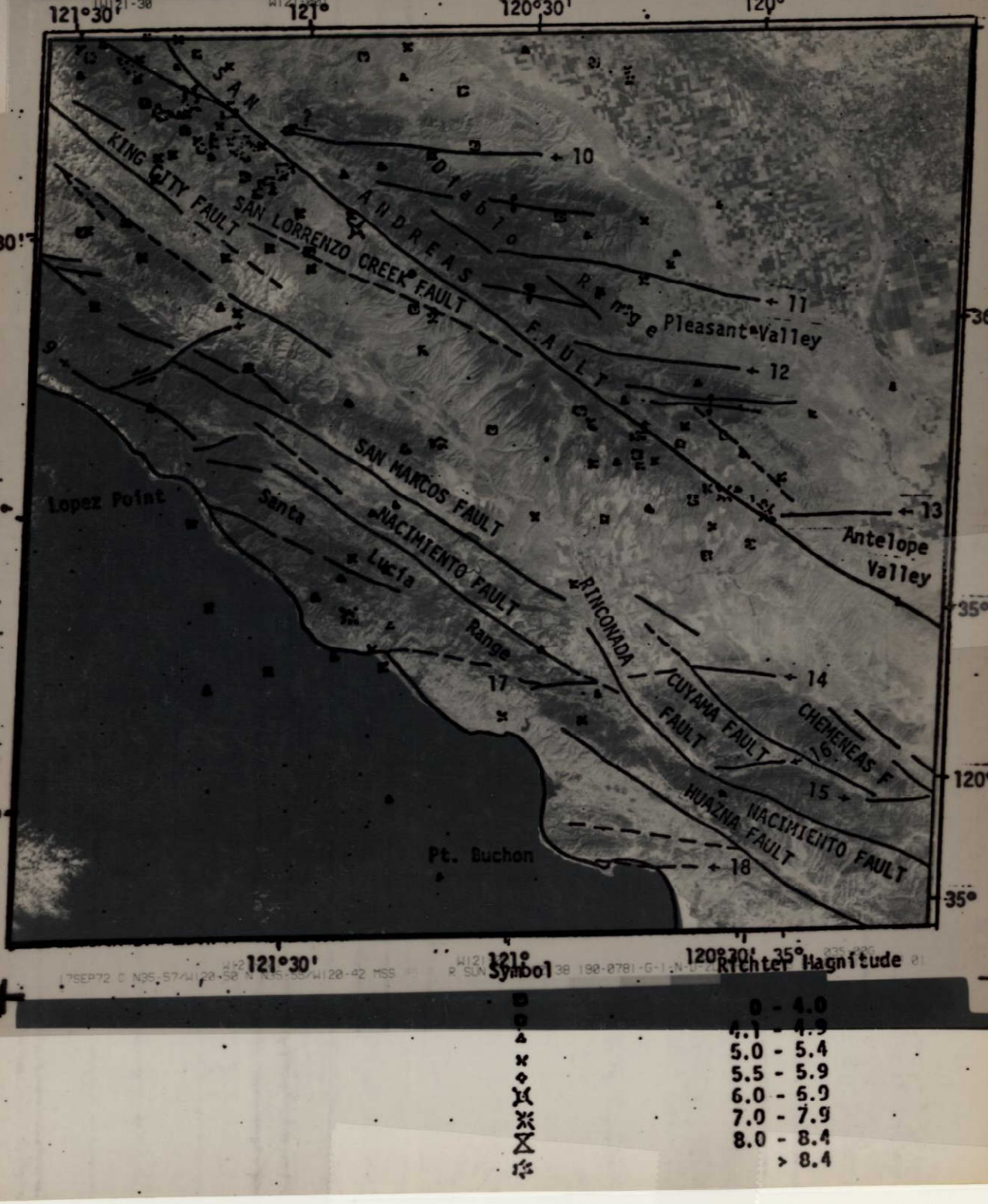

A-27

Figure 10 Fault Structures on Photograph 1037-18064

FIGURE 11 Earthquake Epicenters on Photograph 1037-18064

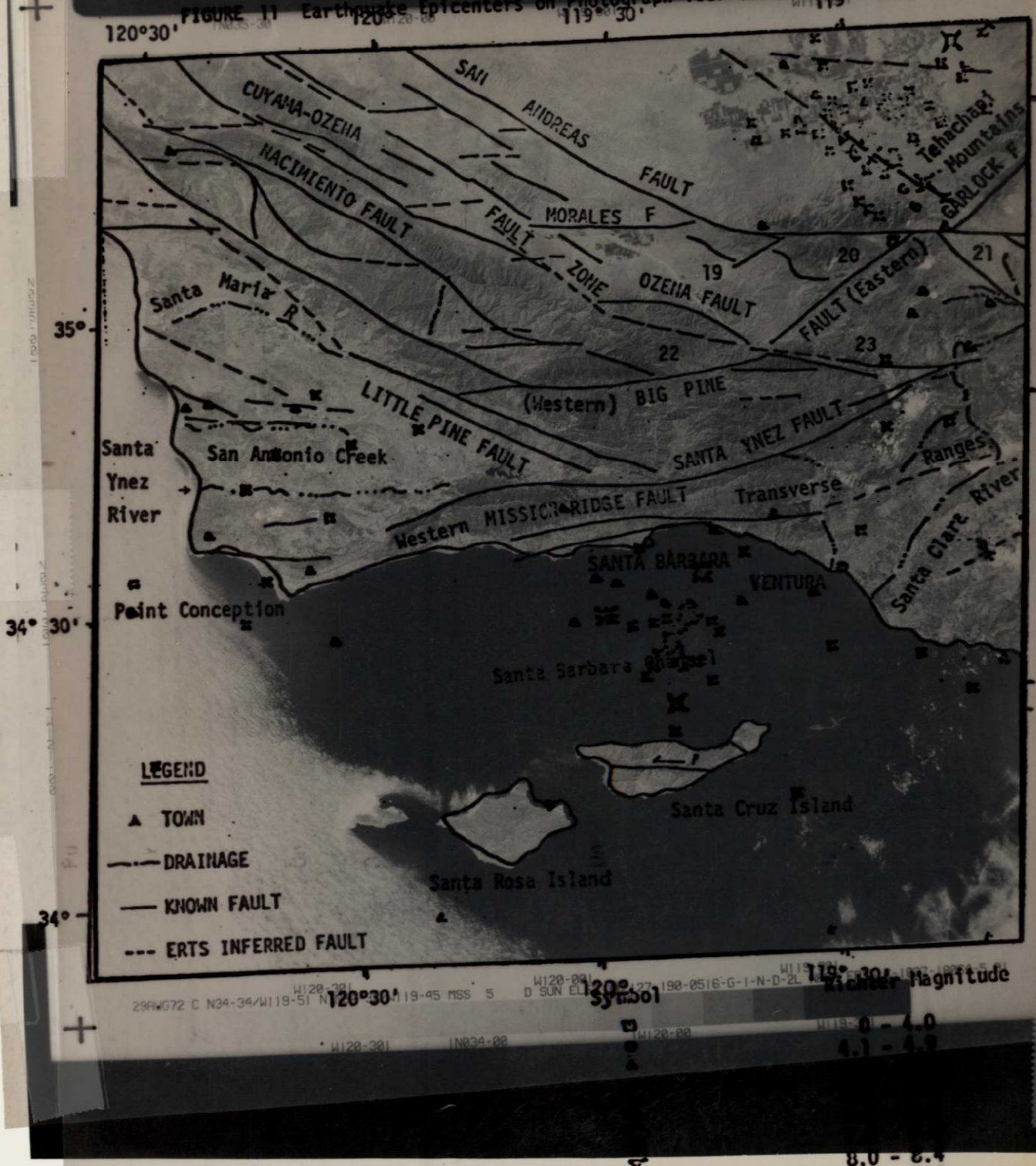

A-28

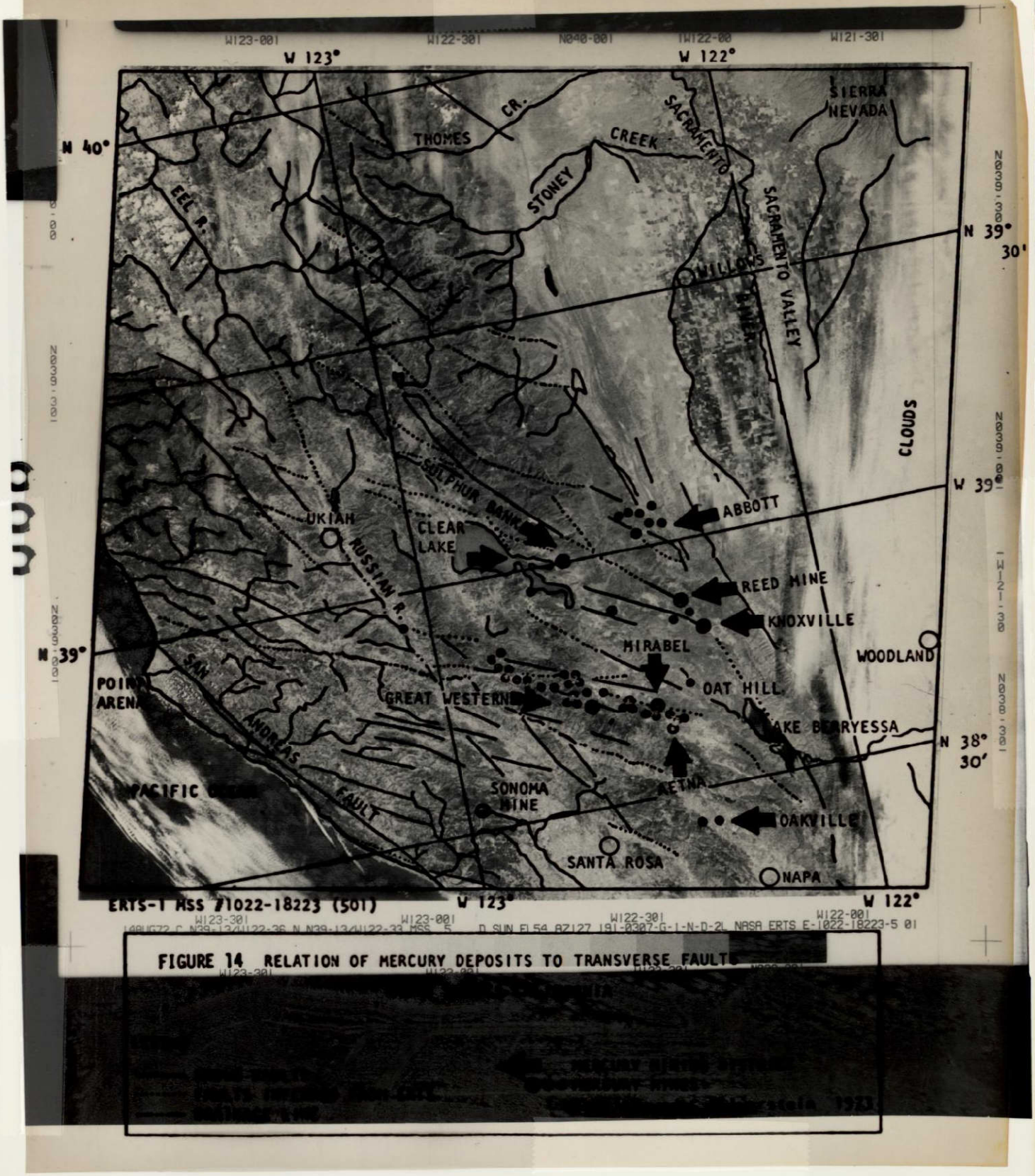

FIGURE 14 RELATION OF MERCURY DEPOSITS TO TRANSVERSE FAULTS

A-29

ERTS-1 MSS #1075-18173(602)
060CT72 C N37-29/W121-44 N N37-27/W121-38 MSS 5 D SUN EL41 AZ146 190-1046-G-1-N-D-2L NASA ERTS E-1075-18173-5 02

FIGURE 15 RELATION OF MERCURY DEPOSITS TO TRANSVERSE F

...Silverstein 1973

A-30

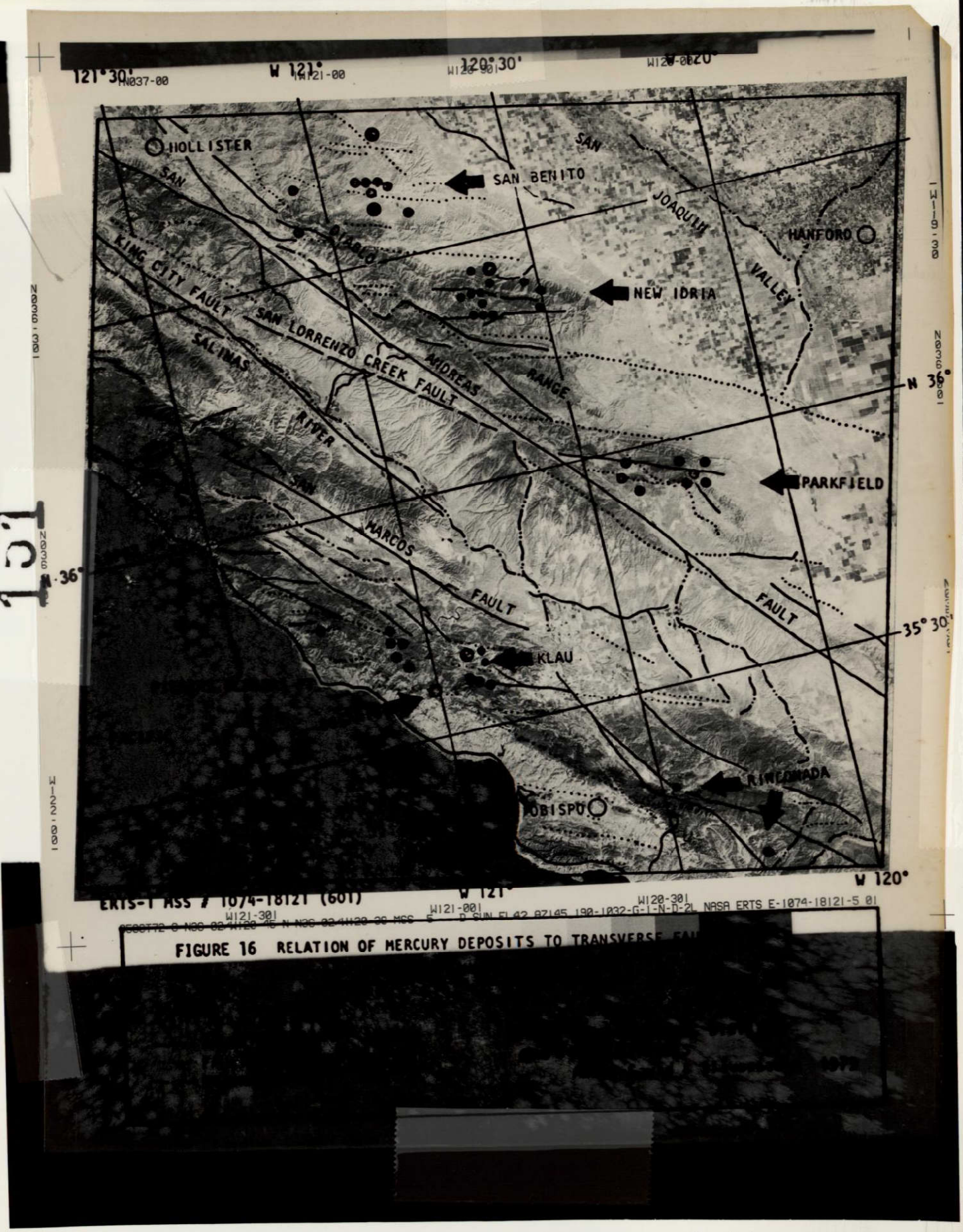

ERTS-1 MSS # 1074-18121 (601)

FIGURE 16 RELATION OF MERCURY DEPOSITS TO TRANSVERSE FAU

A-31

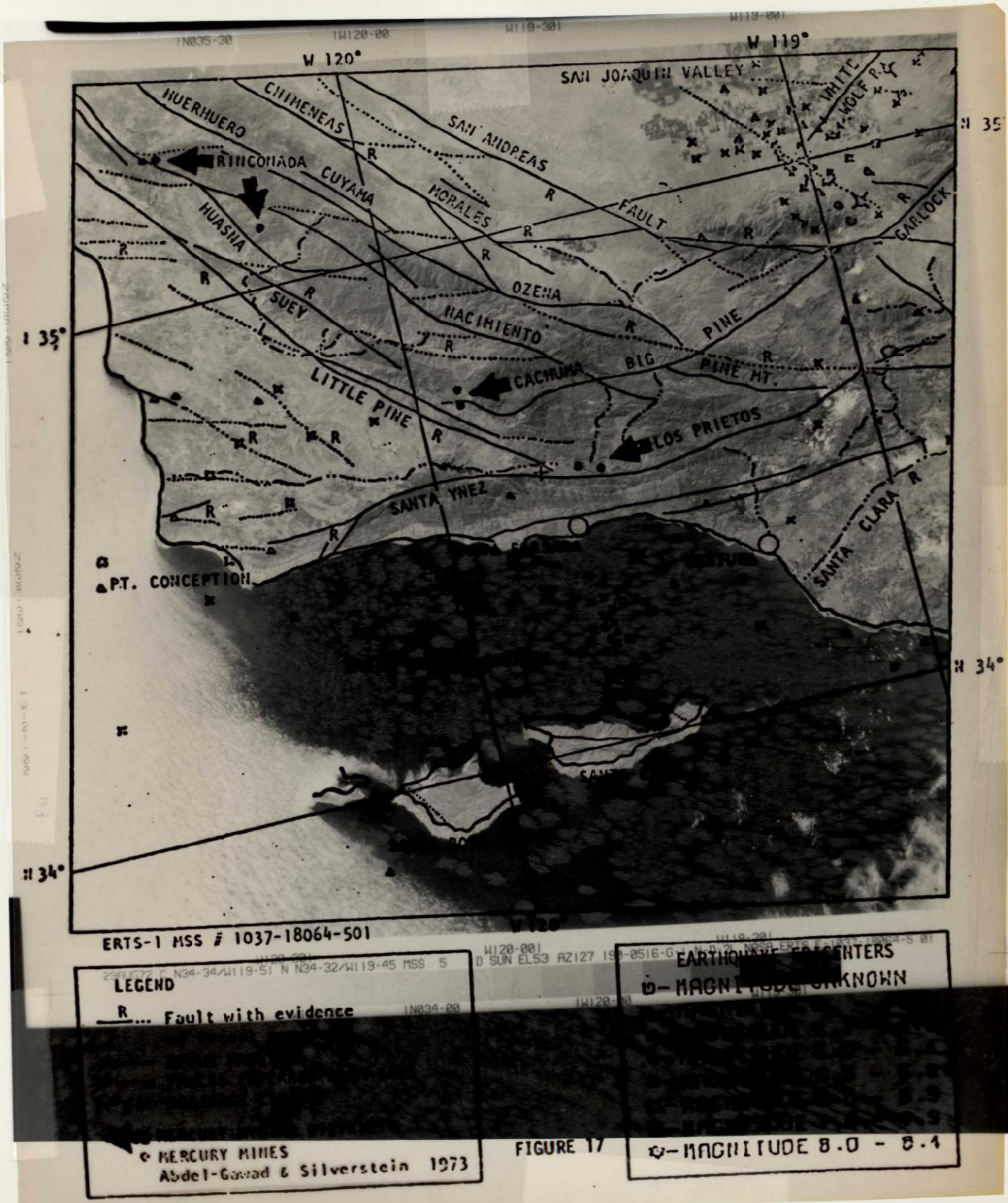

FIGURE 17

A-32

FIGURE 20a

TRANSVERSE FAULTS AND LINEARS, SOUTHERN SIERRA NEVADA, CALIFORNIA

OBSERVED IN ERTS-1 MSS 1018-18003

LEGEND

- TOWN
- KNOWN FAULT
- INFERRED FAULT OR LINEAMENT FROM ERTS IMAGERY
- DRAINAGE

LINEAMENTS OR FAULTS:

- A - NW-SE EXTENSION OF MOHACHE LINEAMENT ACROSS THE SIERRA NEVADA
- B_1, B_2 - WNW UNDER SAN JOAQUIN VALLEY
- C - WITHIN SIERRA BLOCK, PARALLEL TO EASTERN ESCARPMENT
- D_1, D_2 - PARALLEL TO SOUTHERN SEGMENT OF KERN RIVER FAULT
- E - KNOWN FAULT WITH INFERRED LEFT LATERAL OFFSET OF 2-3 km
- 1,2,3 - WNW FAULTS

EARTHQUAKE EPICENTERS

Richter Magnitude

- 6 - 4.0
- 4.1 - 4.9
- 5.0 - 5.9
- 6.0 - 6.9
- 7.0 - 7.9
- 8.0 - 8.4
- > 8.4

FIGURE 20b - Earthquake Epicenters Plotted on Photograph MSS 1018-18003

FIGURE 21b - Earthquake Epicenters Plotted on Photograph MSS 1018-18001

1055-18055

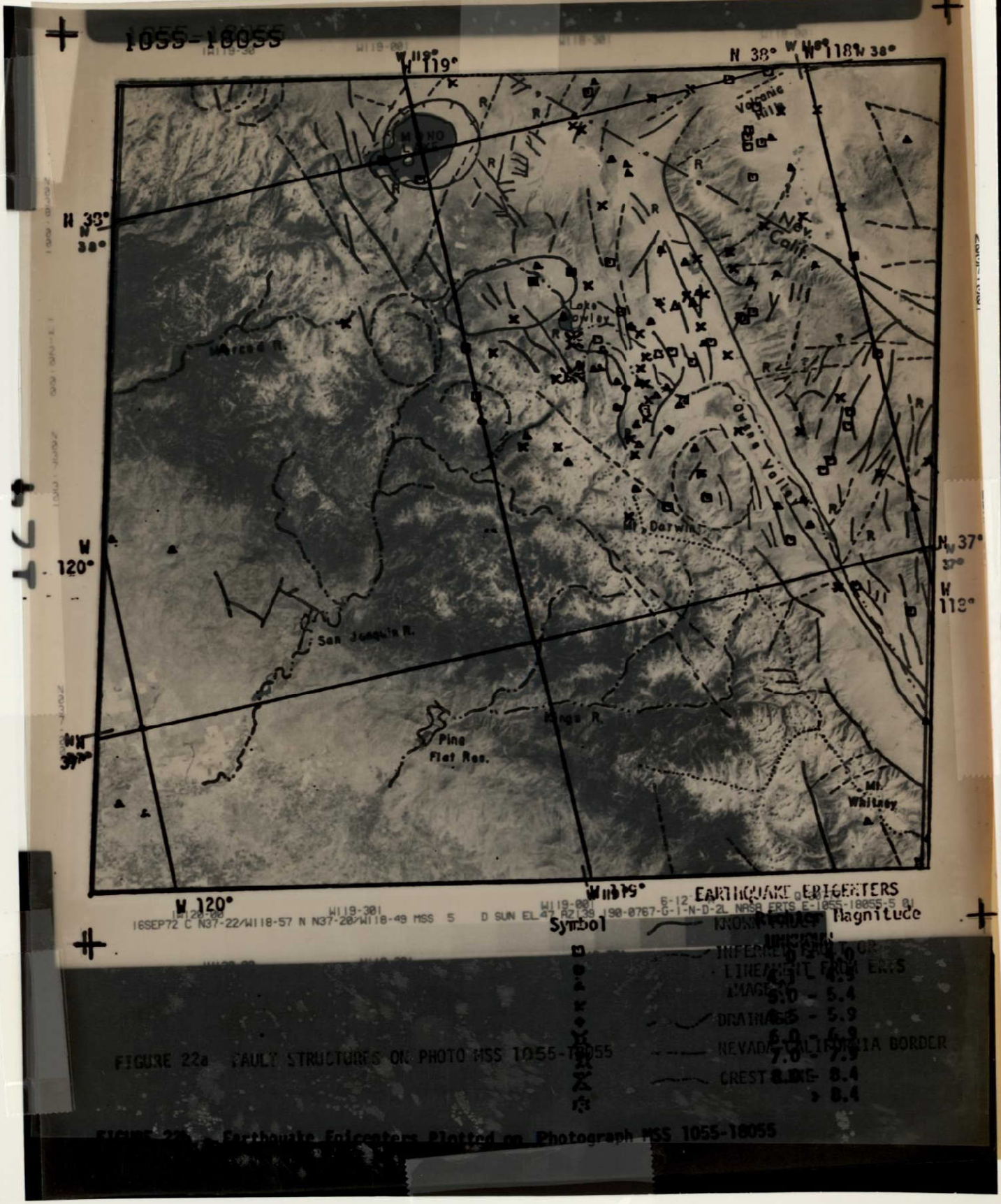

FIGURE 22a FAULT STRUCTURES ON PHOTO MSS 1055-18055

FIGURE 22b Earthquake Epicenters Plotted on Photograph MSS 1055-18055

A-35

FIGURE 23a

LINEARS ALONG WALKER LANE FAULT ZONE, WESTERN NEVADA

1055-18053

OBSERVED IN ERTS-1 MSS-1055-18053

LEGEND

EARTHQUAKE EPICENTERS

▲	TOWN	R = LINEAR WITH INFERRED RECENT FAULT MOVEMENT	
———	KNOWN FAULT	B = NORTHEAST LINEARS WITH INFERRED SINISTRAL FAULT MOVEMENT	Symbol / Magnitude
– – – –	INFERRED FAULT OR LINEARS FROM ERTS IMAGERY	——— NEVADA-CALIFORNIA BORDER	3.0 - 4.0 4.1 - 4.9 5.0 - 5.4 5.5 - 5.9 6.0 - 6.9 7.0 - 7.9 8.0 - 8.4
———	DRAINAGE		

Plotted on Photograph

A-36

FIGURE 24a FAULT STRUCTURES ON PHOTO MSS 1019-18050

FIGURE 24b - Earthquake Epicenters Plotted on Photograph MSS 1019-18050

A37

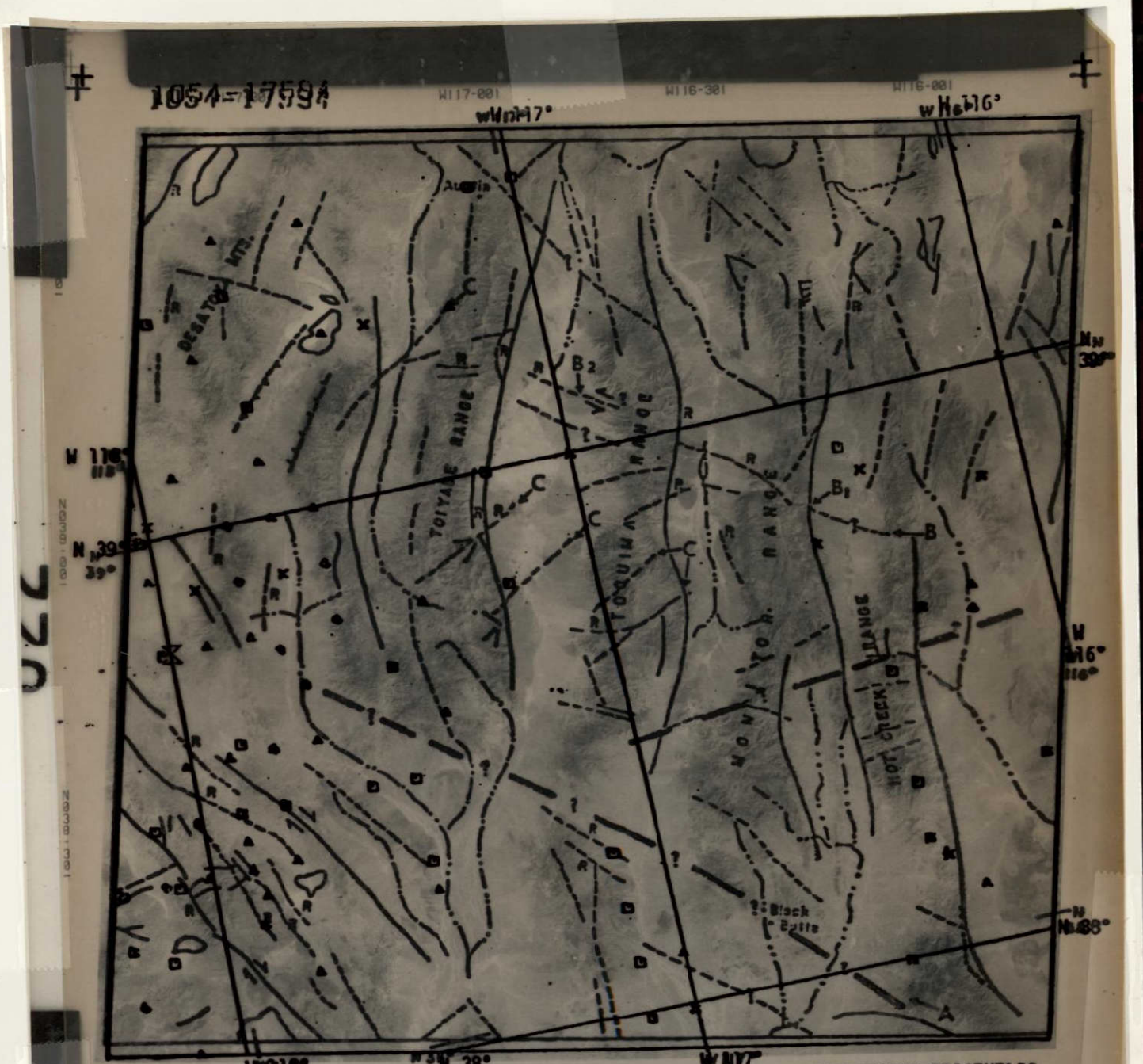

FIGURE 25a FAULT STRUCTURES ON PHOTO MSS 1054-17594

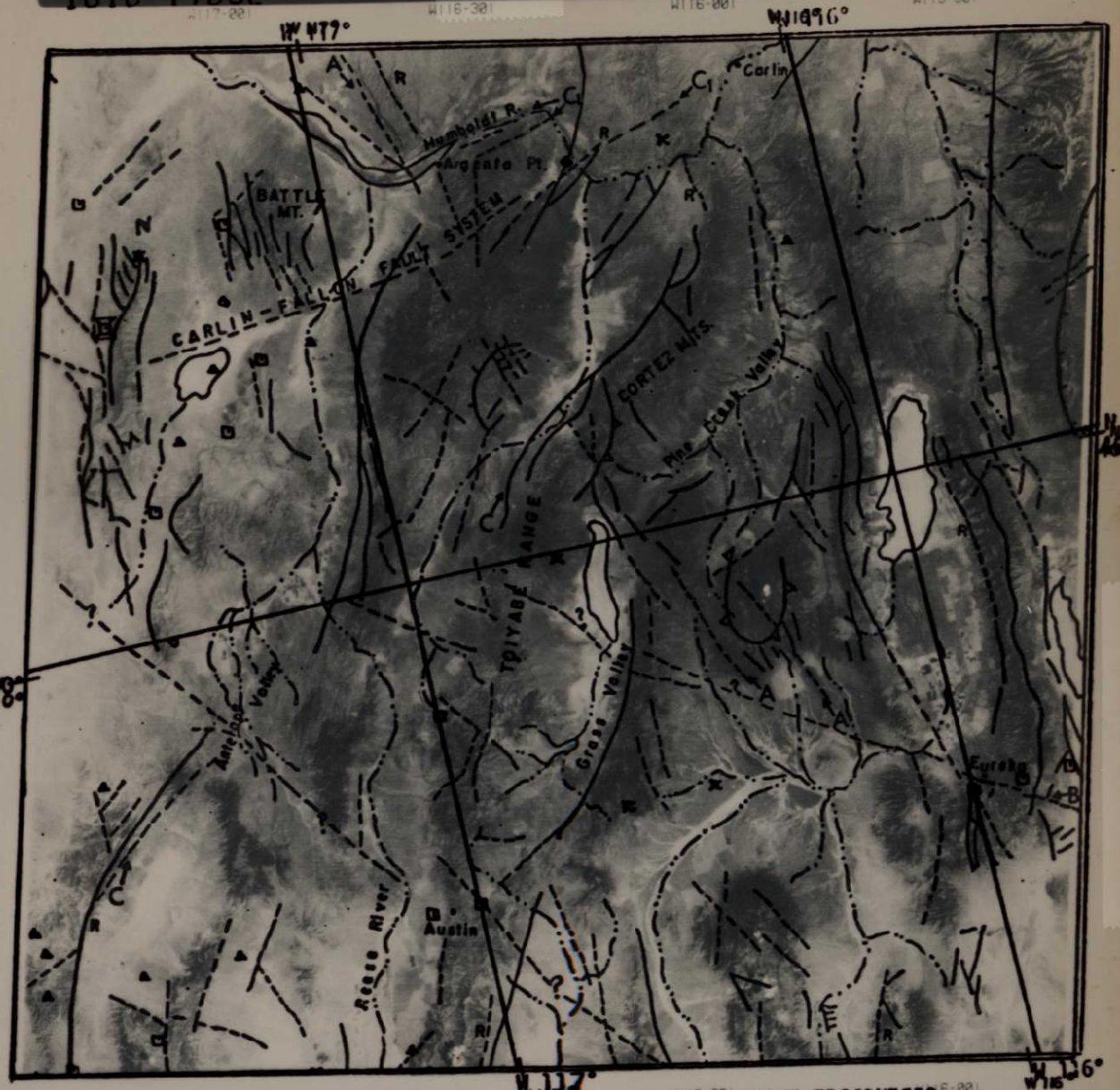

FIGURE 26a FAULT STRUCTURES ON PHOTO MSS 1018-17592

FIGURE 26b Earthquake Epicenters Plotted on Photograph MSS 1018-17592

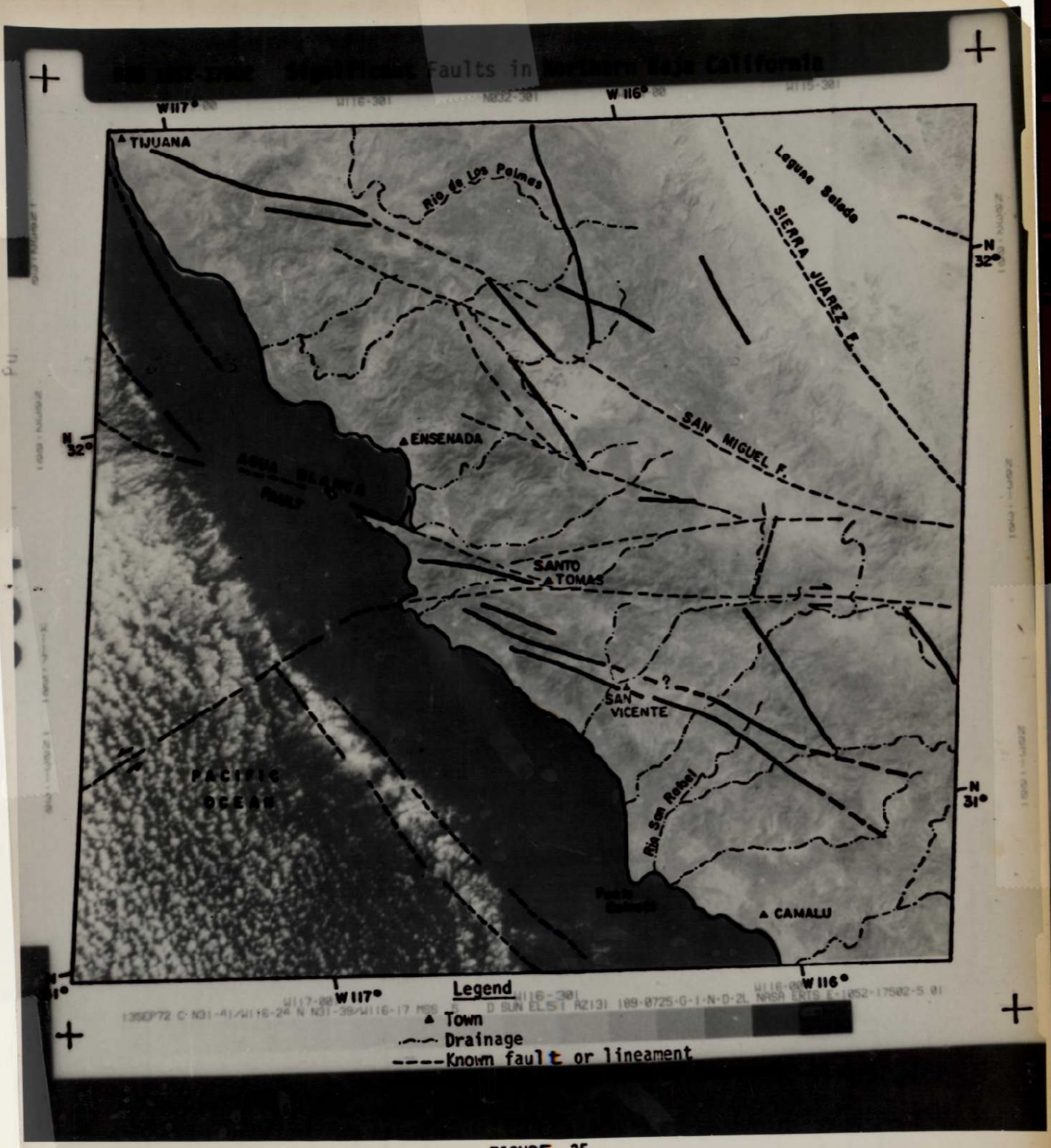

FIGURE 35

A-40

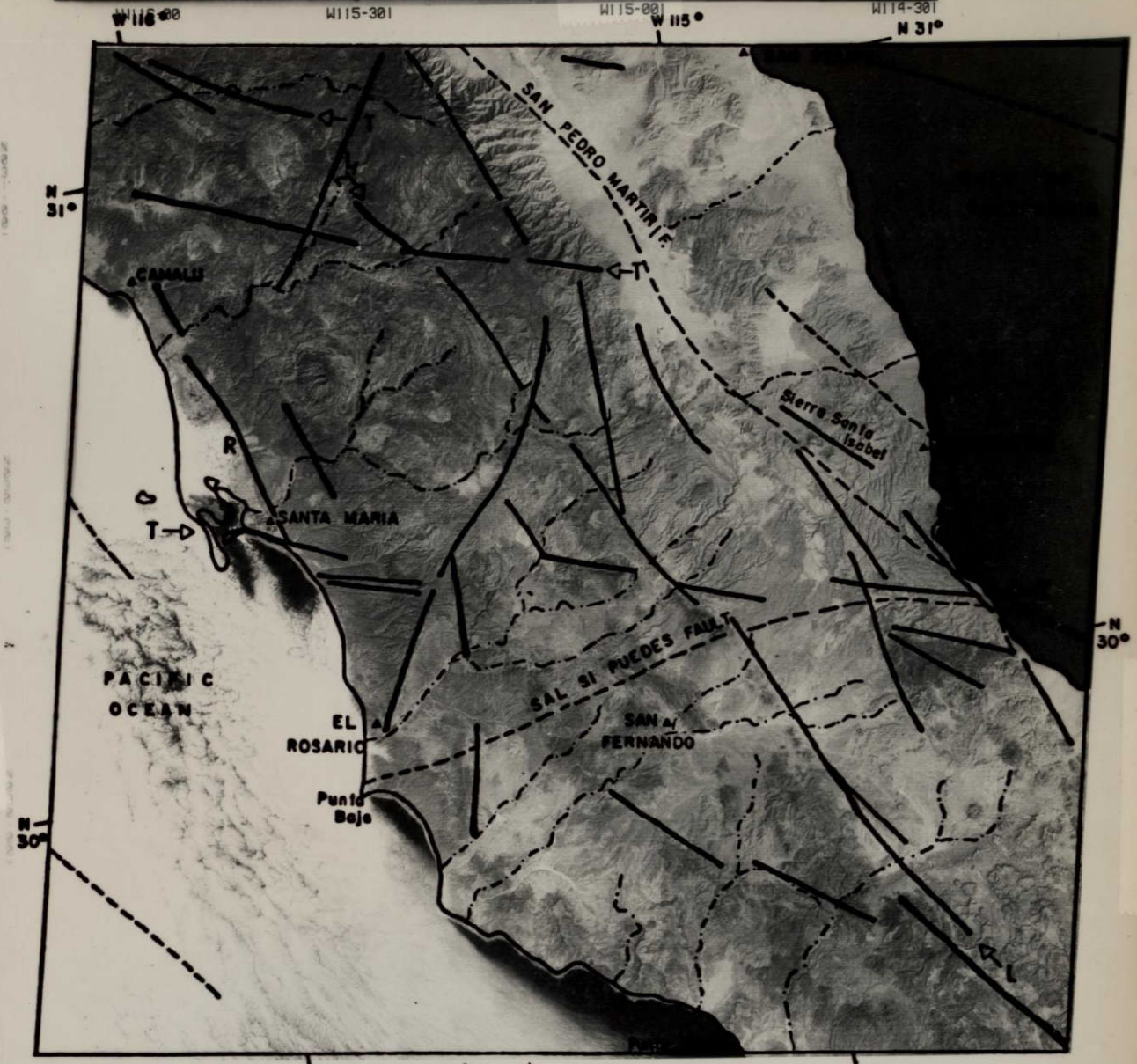

FIGURE 38

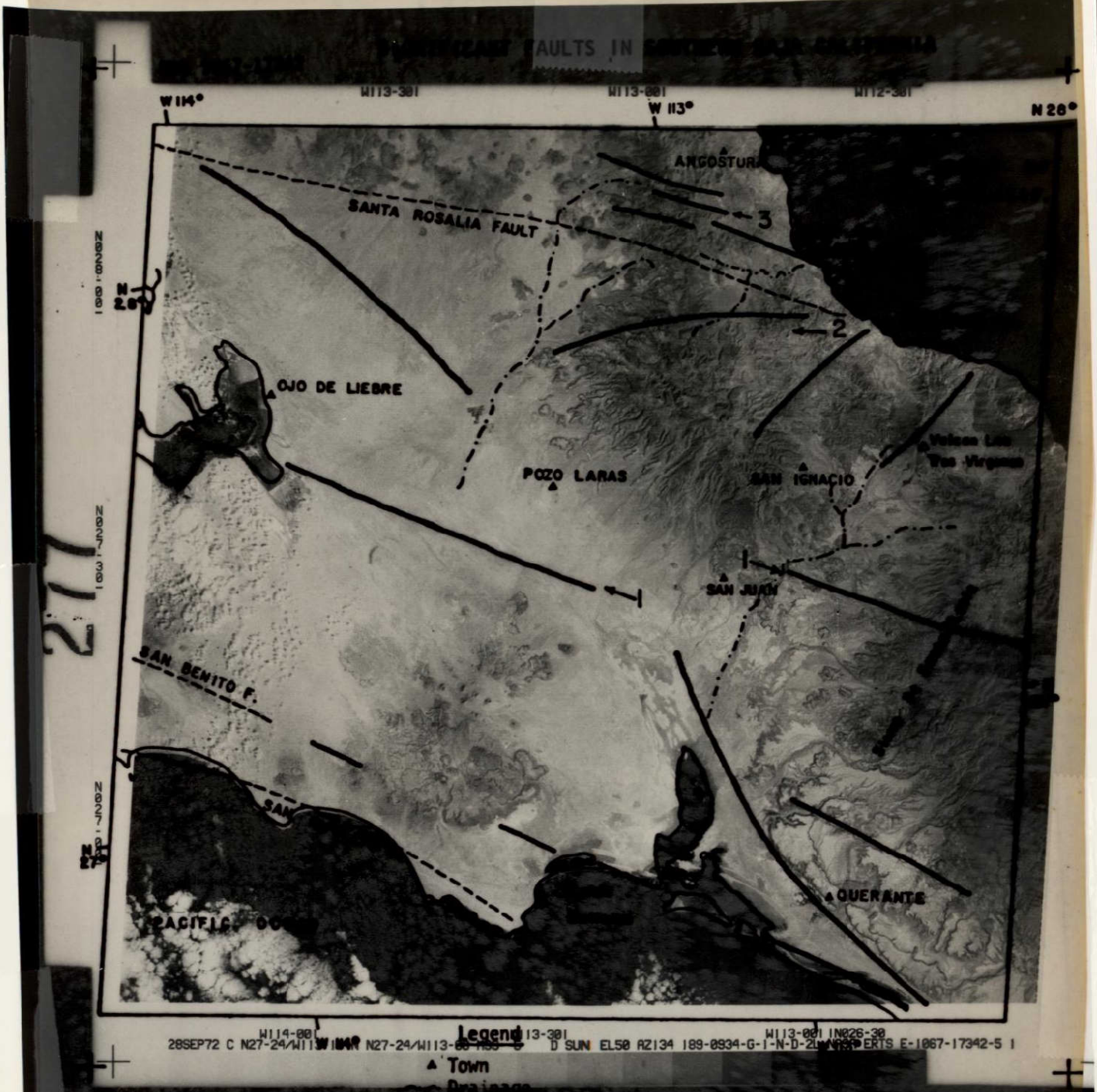

FIGURE 37

A-42

Faults and Seismic Activity of Southern Baja California

FIGURE 38

A-43

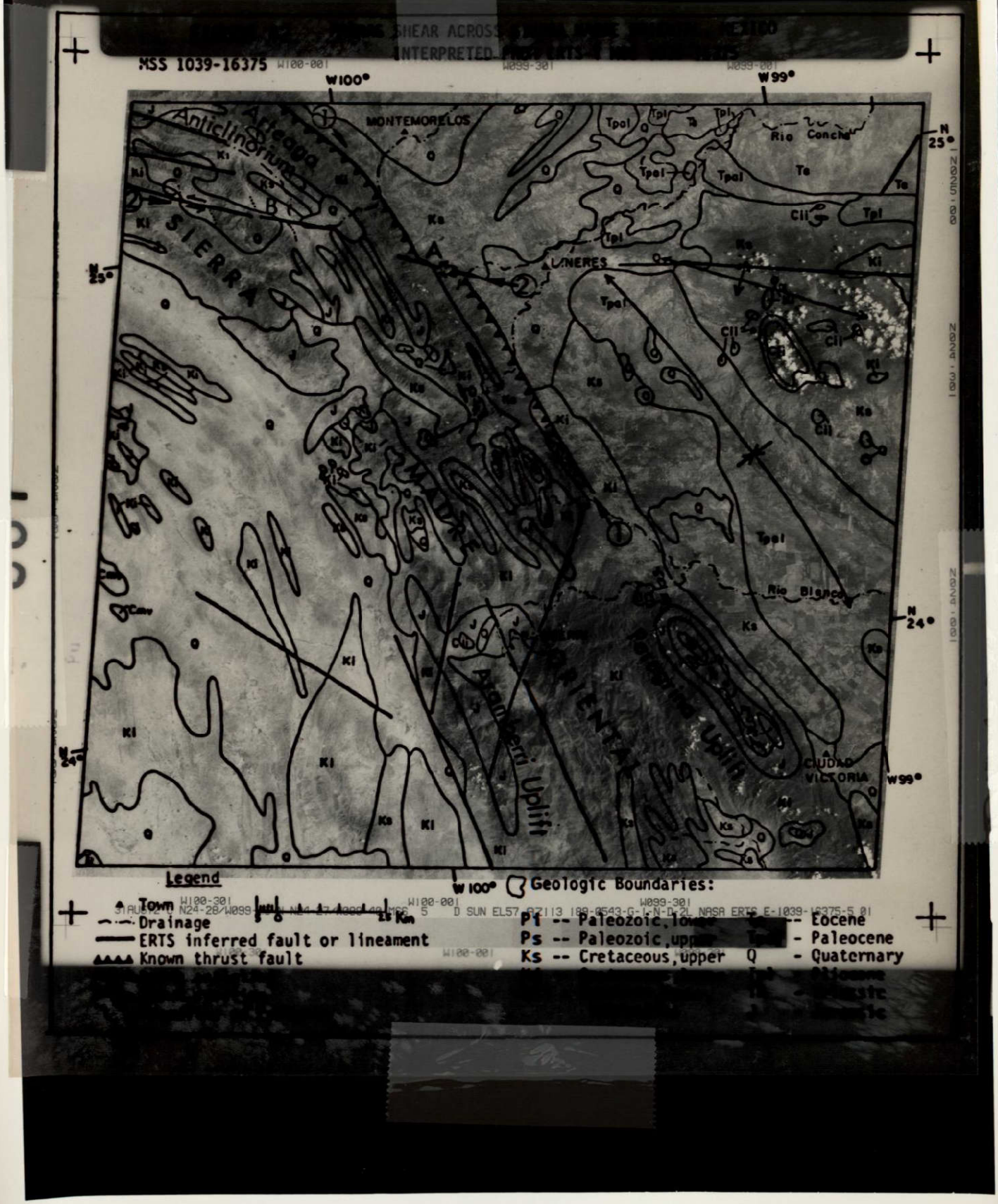
INTERPRETED
MSS 1039-16375
W100°
W99°
N25°
N24°
MONTEMORELOS
Anticlinorium
Arteaga
SIERRA
MADRE
ORIENTAL
Uplift
Aramberri Uplift
LINERES
Rio Conchas
Rio Blanco
CIUDAD VICTORIA
Legend
Town
Drainage
ERTS inferred fault or lineament
Known thrust fault
Geologic Boundaries:
Pl -- Paleozoic, lower
Ps -- Paleozoic, upper
Ks -- Cretaceous, upper
T -- Eocene
Tpal - Paleocene
Q - Quaternary

A-44

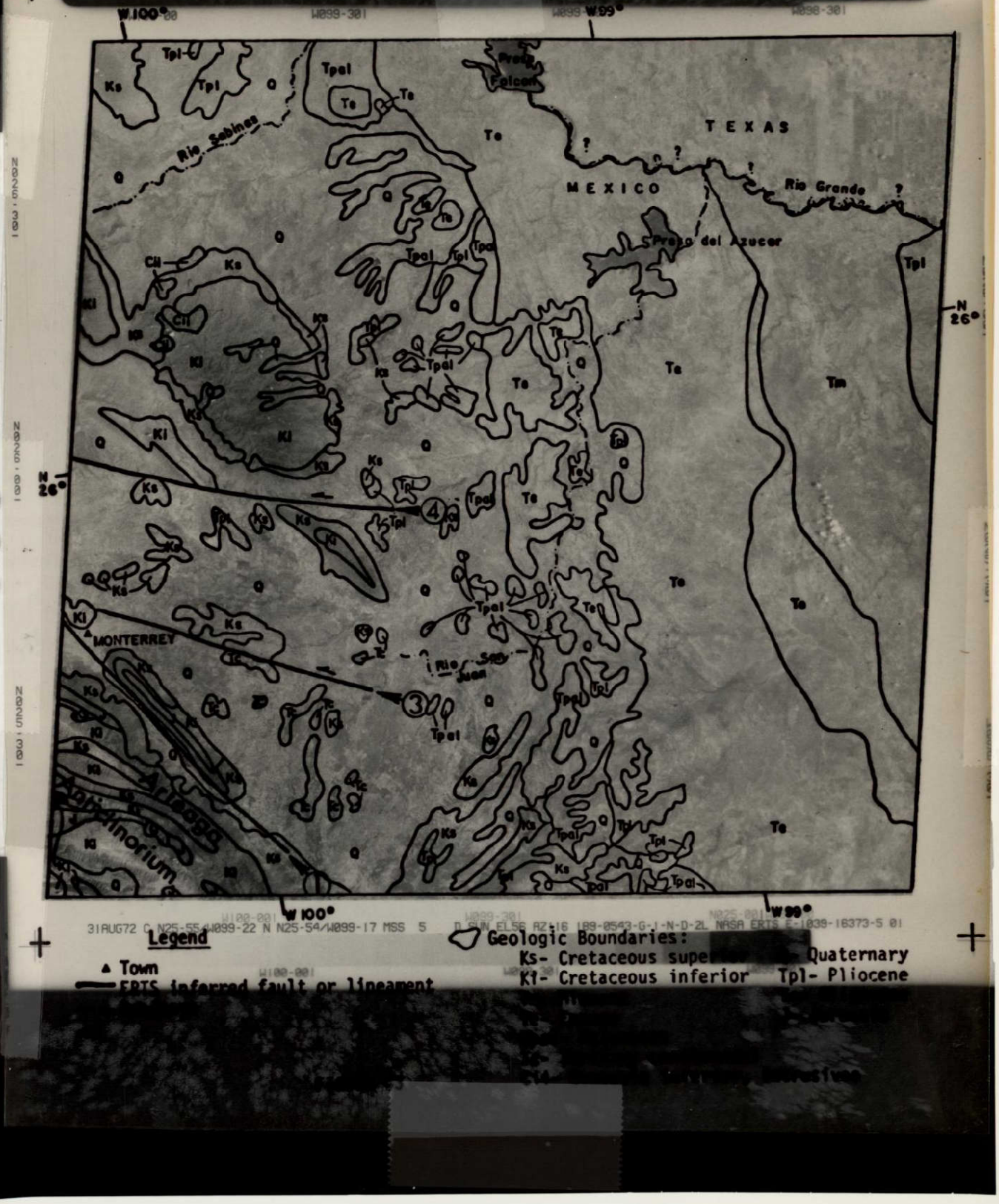
MSS 1839-16373 Section Study of Parras Shear Zone
W100°
W099°
N26°
TEXAS
MEXICO
Rio Grande
Rio Sabinas
Presa del Azucer
MONTERREY
Rio San Juan
Ks
Ki
Tpal
Tpl
Te
Tm
Q
Cli
Arteaga
Sinorium
31AUG72 C N25-55/W099-22 N N25-54/W099-17 MSS 5
Legend
Town
ERTS inferred fault or lineament
Geologic Boundaries:
Ks- Cretaceous super
Ki- Cretaceous inferior
Quaternary
Tpl- Pliocene

A 45

FIGURE 44 PARRAS SHEAR BELT ALONG PARRAS BASIN, MEXICO
INTERPRETED FROM ERTS-1 MSS 1077-16490

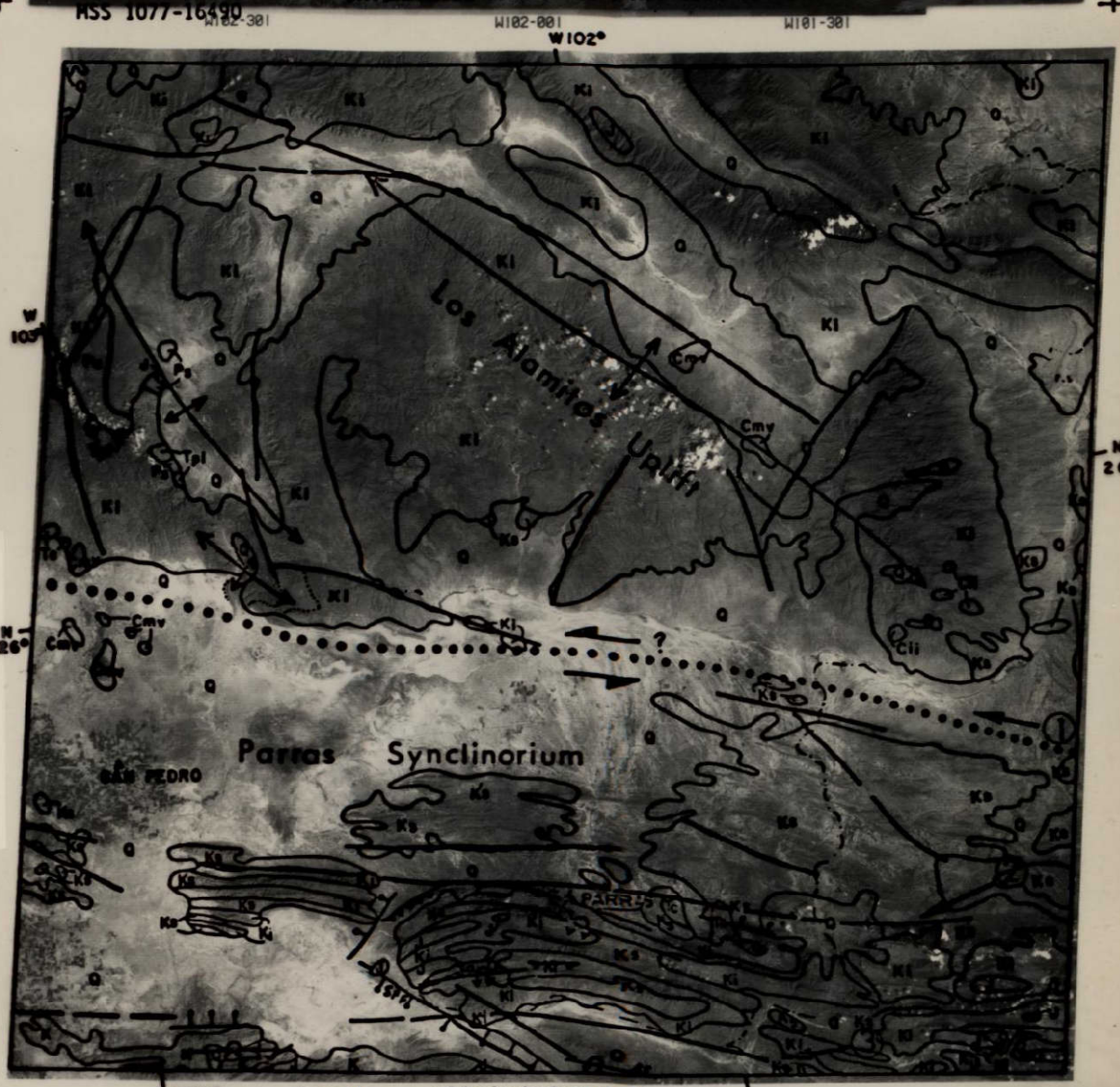

A-46

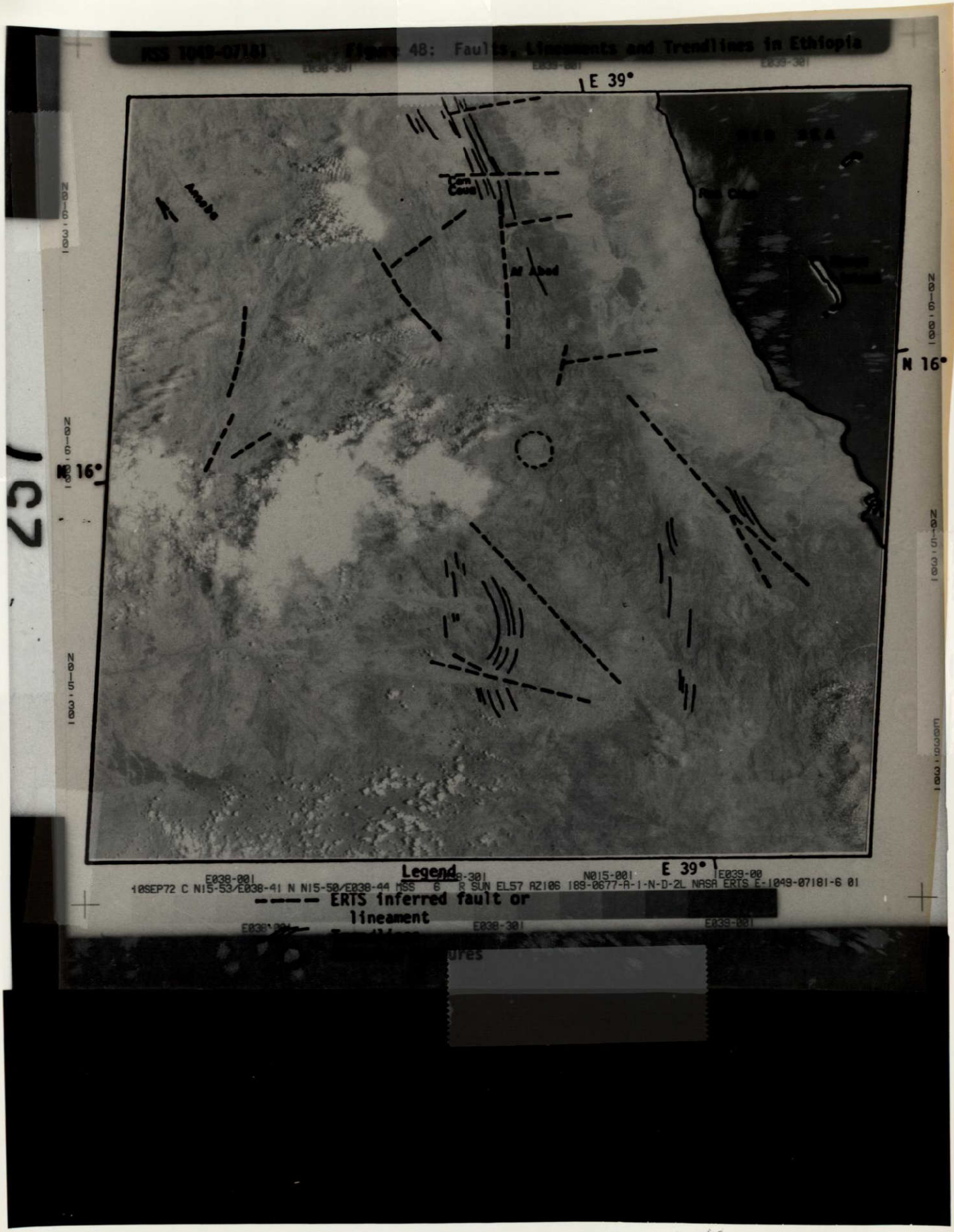

Figure 48: Faults, Lineaments and Trendlines in Ethiopia

A-48

Figure 49: Faults, Lineaments and Trendlines of Al Hamd Shear Zone

264

A-49

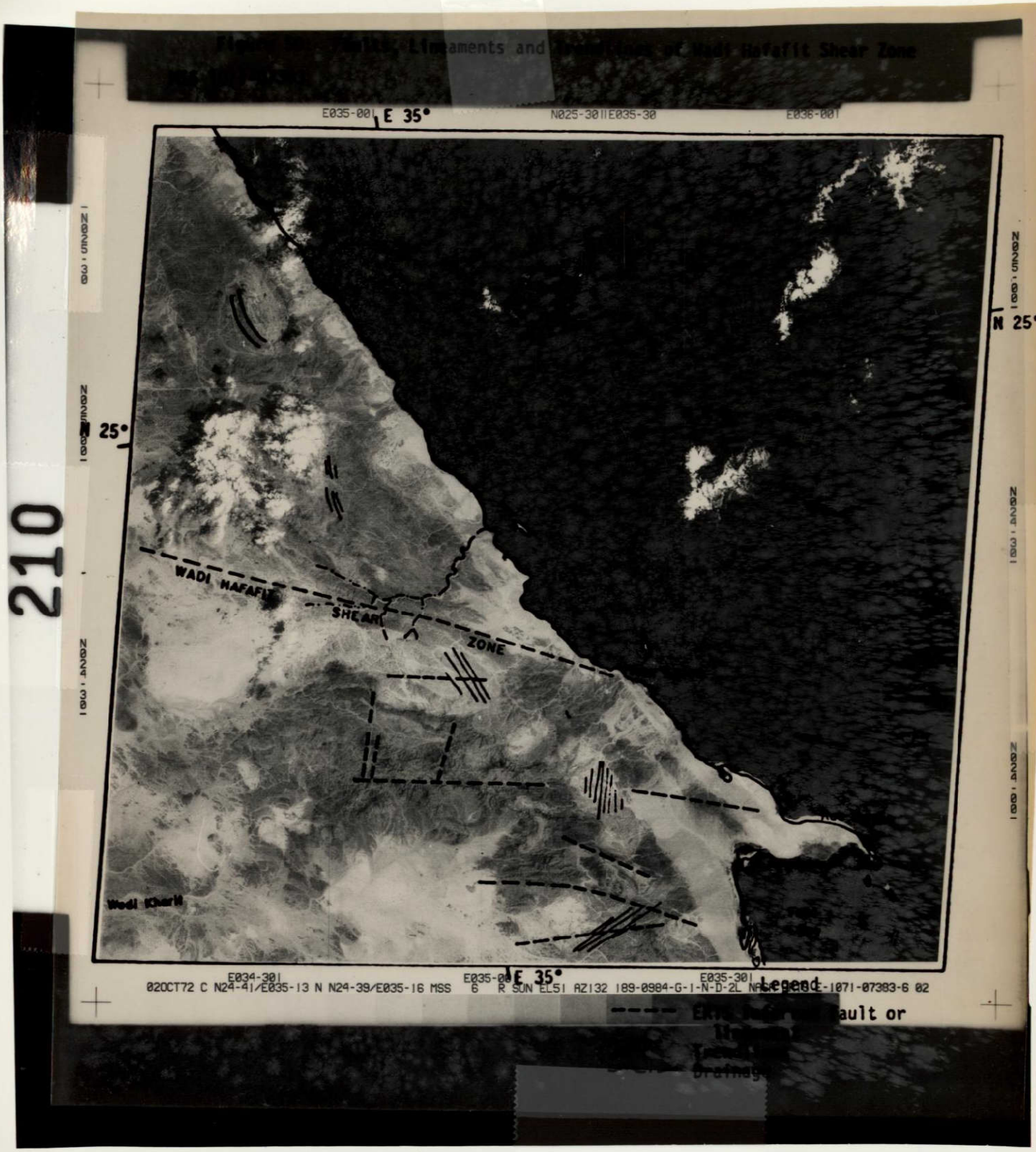
E035-00| E 35° N025-30|E035-30 E036-00|
N 25°
25°
WADI HAFAFIT SHEAR ZONE
Wadi Kharit
E034-30| E035-00 E 35° E035-30|
020CT72 C N24-41/E035-13 N N24-39/E035-16 MSS 6 R SUN EL51 AZ132 189-0984-G-1-N-D-2L
Legend
Fault or

210

A-50

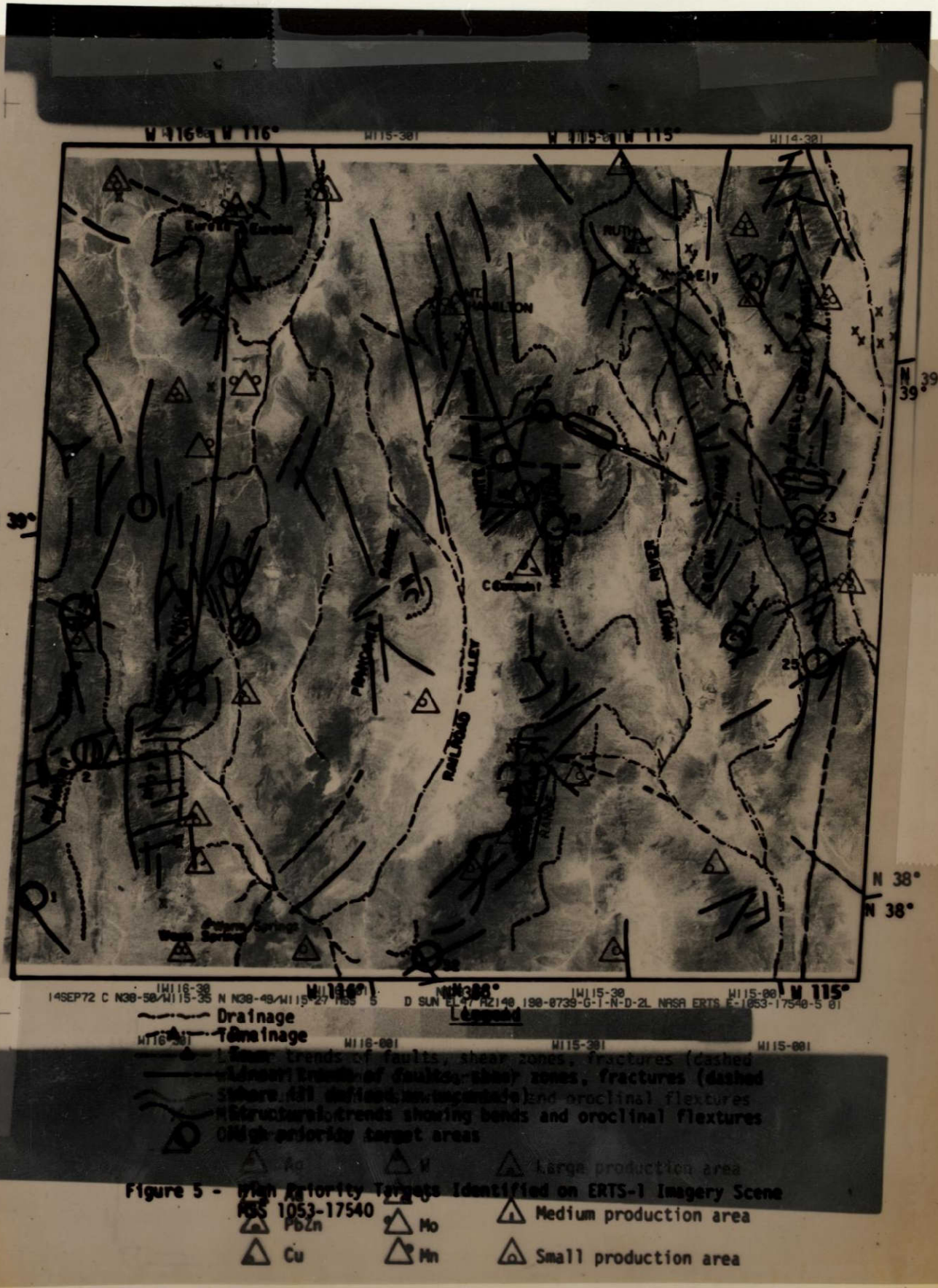

Figure 5 - High Priority Targets Identified on ERTS-1 Imagery Scene
E-1053-17540

Figure 2 - Structures Inferred from ERTS-1 Imagery and Mineral Districts

A-51